



**KINETIC MODELING, THERMODYNAMIC STUDIES AND SIMULATION OF  
REACTIONS WITH AND WITHOUT BOILING USING TEMPERATURE-TIME  
INFORMATION**

**NANA YAW ASIEDU**

A thesis submitted to the Faculty of Engineering and Built Environment, University of the Witwatersrand, Johannesburg South Africa, in the fulfillment of the requirement for the degree of Doctor of Philosophy in Engineering.

Johannesburg, South Africa

03 November 2015

## **DECLARATION**

I declare that this thesis is my own unaided work. It is being submitted for the degree of Doctor of Philosophy in the University of the Witwatersrand, Johannesburg. It has not been submitted for any degree or examination in any other university.



.....

*NANA YAW ASIEDU*

*NOVEMBER 2015*

## **DEDICATION**

This thesis is dedicated to my parents Mr. Daniel Koranteng Asiedu (late), and Mrs. Mary Asiedu, my dear wife Mrs. Yaa Adoma Asiedu and my children Kwabena Koranteng Asiedu, Kwadwo Ofosu-Appiah Asiedu (Jo) and Hilary Akuba Asiedu.

## ABSTRACT

This thesis discusses the Reaction Kinetics modeling of hydrolysis and esterification reactions of acetic anhydride at higher temperatures up to 336K. The thesis also proposes a new method of determining the heat of reaction and Equilibrium constant of reversible Exothermic processes of esterification reactions of acetic acid-Ethanol and acetic acid- propanol reactions. Furthermore this thesis discusses the modeling and Simulation of temperature profiles of reactive distillation process of acetic anhydride methanol reactions. The Experimental techniques consist of temperature – time measurements of the above reactions in an adiabatic batch reactor ( thermos-flask) connected to an electrical System which is linked to a computer with a data capturing component. This system enabled the reactions profiles displayed a real time profiles of the processes. This technique is a modified version of the technique developed by Glasser et al. The voltage-time changes during the Experiments were captured and converted to temperature time data and were used in all the analysis discussed in this thesis. Other Experiment consists of the calibration of the thermistor used for the experiments, the calibration of the reactor and the determinations of the heat transfer coefficients of the system (reactor and content) for each process studied. The results of the hydrolysis processes were used in the kinetic modeling of the Excess water-acetic anhydride reactions at higher temperatures. The results thus showed that at temperatures up to 366K the process still follows first order kinetics and this has not been reported in the literature. The heat of reaction for this process was consistent with what is reported in the literature. However the excess acetic anhydride – water process results showed a different reaction behavior with kinetics suggesting a second order process. The heat of the reaction and the activation energy of this process has been analyzed and reported in this thesis. This finding was surprising and is yet to be reported in the literature. The kinetics of acetic anhydride methanol process was studied by this technique and the results were consistent with what is reported in the literature. The kinetic modeling of this process has never being modeled by this method. The reversible exothermic processes studied were used to develop a thermodynamic method for the determination of heat of reaction and Equilibrium constant. This is a new thermodynamic model.

The measurements made for the acetic anhydride- methanol process was used in modeling and simulation of temperature profiles in a batch reactive distillation system. The simulated temperature profiles in conjunction with thermodynamic considerations will be useful in the monitoring of concentration profiles in the reactive batch distillation systems.

## ACKNOWLEDGEMENTS

This work was done when I was given a study-leave with sponsorship from Kwame Nkrumah University of Science and Technology (KNUST) Kumasi- Ghana. I am very grateful to the University for giving me this opportunity to study. I am thankful to my supervisors and mentors Professor Diane Hildebrandt and Professor David Glasser (Prof G) for giving me the opportunity to work with their research center, Center of Materials and process synthesis, COMPS, the most innovative research group known to me. I am grateful for your financial support, patience, guidance and encouragement to develop me into an independent researcher. There is one thing I will always remember- my first day at Joburg, where Prof. Glasser took me to his residence and cared for me. Prof. Thank you very much. On the other hand the encouragement from Prof Hildebrandt during tough moments is something I will never forget, thank you Prof. Hildebrandt. This work would not have been completed if mention is not made of the then Chief Technician of the Chemistry School of the University of the Witwatersrand, Mr. Basil Chassoulas, your expertise in Electronic Engineering enabled me automated my system and obtained real-time information of all my processes. I say thank you very much. My thanks also go to Jamaine Ntumka, David Ming, Dr. Ronald Abbas, Craig Griffiths, Dr. Celestine Baraka, Prof. Bilal Patel and all research students at COMPS for your support, encouragement and advice. I am grateful to Prof. S. K. Kwofie, (Witsie), Head, Department of Material Science and Engineering –KNUST Kumasi-Ghana for your advice of encouraging me to study at University of the Witwatersrand, Johannesburg South Africa. Prof, I really enjoyed my stay at Wits and I have gotten my share of the edge. My hearty appreciation also goes to Dr. G. Afrane, former Principal- Koforidua Polytechnic and Dr. A. A. Adjaottor, formerly Head of Department of Material Science and Engineering- KNUST Kumasi, Prof. S. K. Y. Gawu (Witsie), Head Department of Geodetic Engineering –KNUST Kumasi and Dr. Anthony Andrews (Wisie), Department of Materials Engineering, KNUST for all the advice, support and encouragement. Thank you very much. My hearty appreciation goes to me elder brother Dr. Daniel K. Asiedu, MD, PhD (USA) for your wonderful support during the time I was leaving for Joburg (SA). I owe a great debt of gratitude to my wife and best friend Mrs Yaa Adoma Asiedu and our kids Koranteng, Ofosu-Appiah (Jo) and Akuba for accompanying me to Johannesburg South Africa to pursue this doctoral studies, you have always been my source of happiness and joy for you this thesis is affectionately dedicated.

## PUBLICATIONS AND CONFERENCE PRESENTATIONS

This thesis is based on the following papers:

Estimating Thermodynamic and Equilibrium Quantities of Exothermic Reversible Processes-published by *American Chemical Society (ASC) Journal - Industrial and Engineering Chemistry Research* June 2013 52 (23) 7630-7639.  
**DOI: 10.1021/ie301944u**

Modeling and Simulation of Temperature Profiles in a Reactive Distillation System for Esterification of Acetic Anhydride with Methanol- published by:  
*International Institute for Science, Technology and Education (IISTE)(USA) Journal of Chemical Process Engineering Research* June 2013  
**ISSN-2225-0913(online) 2013 vol. 10 51-94**

Kinetic Modeling of the Hydrolysis of Acetic Anhydride at Higher Temperatures using Adiabatic Batch Reactor (Thermos-flask)-Article in press: *Journal of Chemical and Process Technology* 2013 4:176.  
**DOI: 10.4172/2157-7048.1000176**

### Conference proceedings:

**Asiedu, N.**, Hildebrandt, D., Glasser, D., Hausberger, B.

Batch distillation targets for minimum energy consumption: ICSST 2007, Beijing, China 14 -16 October 2007.

**Asiedu, N. Y.**, Hildebrandt, D., Glasser, D., Hausberger, B.

Opportunities for reduction of energy consumption of Batch distillation processes- presented at Annual meeting AIChE Salt Lake City, USA 2007.

## **TABLE OF CONTENTS**

### **CHAPTER ONE**

1.1 Introduction	1
1.2 Objectives of the Research	1
1.3 Thesis outline	2
1.4 References	4

### **CHAPTER TWO**

Review of the theoretical description of Temperature-time profiles	5
2.1 Introduction	5
2.2 Adiabatic measurements	5
2.3 Differential Thermal Analysis	6
2.4 Non- Adiabatic Thermal Analysis	7
2.5 Mathematical Analysis of Adiabatic Heating Curve	10
2.6 The heat balance	11
2.6.1 The heat balance Equation for adiabatic batch reactor	11
2.6.2 Comparing Concentration-time profiles and temperature-time profiles	12
2.6.3 First order processes	14
2.6.4 Second order processes	15
2.6.5 Linear dependence of temperature and Extent of reaction	16
2.6.6 First order Irreversible processes	18
2.6.7 Second order Irreversible Processes	19
2.6.8 Second Order Reversible Process	19
2.6.9 Calculating additional Information	21

2.7 References	21
2.8 List of Symbols	23
<b>CHAPTER THREE</b>	<b>25</b>
3.0 Experimental descriptions and procedures	25
3.1 Experimental Apparatus and procedures	25
3.2 Experimental Apparatus	25
3.2.1 The electrical circuit for measuring the resistance of the thermister	26
3.2.2 The circuit theory	27
3.2.3 Calibration of the Thermistor	28
3.2.4 Description of the reaction vessel	33
3.2.5 Calibration of the reaction vessel	34
3.2.6 Experimental determination of heat transfer coefficient of the process	38
3.2.7 The block diagram of the experimental set-up	46
3.3 Experimental procedure and results	48
3.3.1 The Esterification Reactions	48
3.3.1.1 Acetic Acid- Ethanol Reactions	48
3.3.1.2 Experimental Descriptions	48
3.3.1.3 Experimental Results	49
3.3.2 Acetic Acid- Propanol Reactions	53
3.3.2.1 Experimental Descriptions	53
3.3.2.2 Experimental results	54
3.3.3 Acetic Anhydride-Methanol Reactions	57
3.3.3.1 Experimental Description	57
3.3.3.2 Experimental Results	58
3.3.4 The Hydrolysis Reactions	61
3.3.4.1 The Acetic Anhydride-Excess water Reactions	61
3.3.4.2 Experimental descriptions	61
3.3.4.3 Experimental Results	62
3.5 Discussion of Experimental Results	68
3.6 List of Symbols	69

## CHAPTER FOUR

A paper published by the America Chemical Society Journal of Industrial and Engineering

Chemistry Research 2013 52 7630-7639. DOI: 10.1021/ie301944u

### Estimating Thermodynamic and Equilibrium Quantities of Exothermic Reversible Processes

Abstract	70
4.1 Introduction	71
4.2 Theoretical Development	72
4.2.1 Equilibrium Information from thermos-flask	72
4.2.2 Energy balance of the thermos-flask	73
4.3 The Experimental Set-up	74
4.4 The Thermistor Calibration	76
4.4.1 The electrical circuit of the system	77
4.4.2 The circuit theory	78
4.4.3 The Thermister calibration	77
4.4.4 Relationship between thermistor resistance and temperature	81
4.5 The Reactor (Thermos-flask) Calibration	83
4.5.1 Experimental determination of heat transfer Coefficient of the process	87
4.5.2 Determination of UA/mCp for the reaction mixture	96
4.6 Experimental procedures and results	97
4.6.1 Acetic Acid-Ethanol Reactions	97
4.6.2. Experimental Results	98
4.7 Acetic Acid-Propanol Reactions	101
4.7.1 Experimental Results	102
4.8 Analysis of Experimental Results	105
4.8.1 Model Solution	104
4.9 Conclusions	109
4.10 Acknowledgements	109
4.11 List of Symbols	109
4.12 References	112

## CHAPTER FIVE

**A paper published by International Institute of Science and Technology (IISTE) USA,  
Journal of Chemical and process Engineering Research. ISSN-2225-0913 June 2013 vol. 10  
51-95**

5.1 Modeling and Simulation of Temperature profiles in a reactive distillation system for the esterification of Acetic Anhydride with methanol	113
5.2 Abstract	114
5.3 Introduction	114
5.4 The mathematical model of the reacting System	115
5.5 The Experimental Set-up	117
5.6 The Thermistor Calibration	118
5.6.1 The Electrical Circuit of the System	119
The Circuit Theory	
5.6.2 The Calibration	120
5.6.3 Relationship between thermistor Resistance and Temperature	123
5.7 The Reactor Calibration	125
5.8 Determination of $UA/mC_p$ for the reaction mixture	128
5.9 Variation of rate of reaction with concentration change	144
5.10 Kinetics and Thermodynamic analysis of the Experiments	150
5.11 Modeling Approach	154
5.12 Model Validation	155
5.12.1 Results and Discussion	156

5.14 Conclusions	170
5.15 Acknowledgement	170
5.16 List of Symbols	170
5.17 References	172

## CHAPTER SIX

**This article has been accepted for publication by- Journal of Chemical Engineering and Process Technology 2013 4:176. DOI: 10.4172/2157-7048.1000176**

6.1 Kinetic Modeling of the Hydrolysis of Acetic Anhydride at Higher Temperatures using Adiabatic Batch Reactor (Thermos-Flask)	174
6.2 Abstract	175
6.3 Introduction	175
6.4 Theory of homogeneous reactions	177
6.5 The mathematical model of the reacting system	178
6.6 The experimental set-up	180
6.7 The thermistor calibration	182
6.7.1 The electrical circuit of the system	183
6.7.2 The thermistor calibration	184
6.7.3 Relationship between thermistor resistance and temperature	186
6.8 The reactor (Thermos-Flask) calibration	189
6.9 Experimental procedures and results	191
6.9.1 Excess Water-Acetic Anhydride reactions	191
6.9.2 Experimental determination of heat transfer coefficient of the process	191

6.9.3 Determination of UA/mC <sub>p</sub> for the reaction mixture	198
6.9.4 Variation of rate of reaction with concentration change	207
6.9.5 Kinetics and thermodynamic analysis of the experiments	211
6.10 Experimental procedures and results	215
6.10.1 Excess Acetic Anhydride-water reactions	215
6.10.2 Determination of UA/mC <sub>p</sub> for the reaction mixture	215
6.10.3 Variation of rate of reaction with concentration change	226
6.10.4 Kinetics and thermodynamic analysis of the experiments	229
6.11 Experimental procedures and results	233
6.11.1 Acetic Anhydride-Methanol reactions	233
6.11.2 Determination of UA/mC <sub>p</sub> for the reaction mixture	233
6.11.3 Variation of rate of reaction with concentration change	241
6.11.4 Kinetics and thermodynamic analysis of the experiments	244
6.12 Discussion of Results.	249
6.13 Conclusions	251
6.14 Acknowledgements	252
6.15 List of Symbols	252
6.16 References	254

## **CHAPTER SEVEN**

7 Concluding Remarks	256
----------------------	-----

## LIST OF TABLE

3.1 Summary of characteristics of figures (3.6) - (3.8)	45
4.1 Summary of characteristics of figures(4.8) – (4.10)	94
4.2 Some constants of reacting species	96
4.3 Parameters for Ethyl acetate process	107
4.4 Parameters for propyl acetate process	107
4.5 Heat of reaction for ethyl acetate process	107
4.6 Heat of reaction for propyl acetate process	108
4.7 Equilibrium constants for ethyl acetate process	108
4.8 Equilibrium constants for propyl acetate process	108
4.9 Mean value $\Delta H_r$ and $K^0$ eq.	108
5.1 Summary of characteristics of figures (5.8) – (5.10)	135
5.2 Some constants of reacting species	136
5.3 Summary of the characteristics of the above temperature - time plots	140
5.4 Variation of rate and concentration at T= 320K.	144
5.5 Variation of rate and concentration at T= 325K.	146
5.6 Variation of rate and concentration at T= 335K.	148
5.7 Thermodynamic information of the Experiments	153
6.1 Summary of characteristics of figures (6.8 – 6.10)	196
6.2 Some constants of reacting species	197
6.3 Summary of characteristics of figures (6.12 – 6.14)	201
6.4 Variation of rate and concentration at 345K.	205
6.5 Variation of rate and concentration at 350K	207

6.6	Variation of rate and concentration at 355K	208
6.7	Thermodynamic information of the Experiments	212
6.8	UA/MCP of the Experiments (4) – (6)	214
6.9	Summary of characteristics of Experiments (4) – (6)	220
6.10	Variation of rate and concentration at $T = 320\text{K}$	224
6.11	Variation of rate and concentration at $T = 335\text{K}$	225
6.12	Variation of rate and concentration at $T = 340\text{K}$	226
6.13	Thermodynamic information of the Experiments (4) – (6)	230
6.14	Some constants of reacting species	231
6.15	Summary of characteristics of figures (6.35 – 6.37)	235
6.16	Variation of rate and concentration at 320K	239
6.17	Variation of rate and concentration at 325K	240
6.18	Variation of rate and concentration at 335K	241
6.19	Thermodynamic information of the Experiments (7, 8, and 9)	246

## LIST OF FIGURES

3.1 The electrical Circuit of the system	26
3.2 The thermistor voltage – time profile	29
3.3 The thermistor temperature – time profile	30
3.4 Regression line of $m (R_{th})$ against $1/T$	32
3.5 The reaction vessel	33
3.6 Thermos-flask cooling curve at $T_o = 316K$	35
3.7 Regression line of heat transfer coefficient of reactor	37
3.6 (a) Adiabatic Reactor (Thermos-flask) cooling curve at $T_o = 343.08K$	39
3.6 (b) Regression line of heat transfer coefficient of reactor at $343.03K$	40
3.7 (a) Adiabatic Reactor (Thermos-flask) cooling curve at $T_o = 347.77K$	41
3.7 (b) Regression line of heat transfer coefficient of reactor at $347.77K$	42
3.8 (a) Adiabatic Reactor (Thermos-flask) cooling curve at $T_o = 347.80K$	43
3.8 (b) Regression line of heat transfer coefficient of reactor at $347.80K$	44
3.9 A plot of mass of water ( $m$ ) against $(mC_p /UA)$	45
3.10 Block diagram of Experimental Set –up	47
3.11 Acetic Acid – Ethanol Reaction: Temperature – time profile at $283K$	50
3.12 Acetic Acid – Ethanol Reaction: Temperature – time profile at $289K$	51
3.13 Acetic Acid – Ethanol Reaction: Temperature – time profile at $295K$	52
3.14 Acetic Acid – Propanol Reaction: Temperature – time profile at $285.1K$	54

3.15	Acetic Acid – Propanol Reaction: Temperature – time profile at 290.4K	55
3.16	Acetic Acid – Propanol Reaction: Temperature – time profile at 297.8K	56
3.17	Acetic Anhydride –Methanol process: Temperature – time profile at 290K	58
3.18	Acetic Anhydride/Methanol process: Temperature – time profile at 294K	59
3.19	Acetic Anhydride/Methanol process: Temperature – time profile at 299K	60
3.20	Hydrolysis Process : Temperature – time profile at 305K	62
3.21	Hydrolysis Process : Temperature – time profile at 310K	63
3.22	Hydrolysis Process : Temperature – time profile at 329K	64
3.23	Hydrolysis Process : Temperature – time profile at 286K	65
3.24	Hydrolysis Process : Temperature – time profile at 294K	66
3.25	Hydrolysis Process : Temperature – time profile at 305K	67
4.1	Block diagram of Experimental set-up	76
4.2	The electrical circuit of the system	77
4.3	The thermistor voltage – time profile	79
4.4	The thermistor temperature – time profile	80
4.5	Regression line of ( $R_{TH}$ ) against $1/T$	82
4.6	Thermos-flask cooling curve at = 361K	84
4.7	Regression line of heat transfer coefficient of reactor.	86
4.8a	Thermos-flask cooling curve – $M_W = 200g$	88
4.8b	Regression line of heat transfer coefficient of reactor.	89
4.9 (a)	Reactor cooling – $M_W = 300g$	90
4.9 (b)	Regression line of heat transfer coefficient of reactor.	91

4.10 (a) Reactor cooling curve $M_W = 400g$	92
4.10 (b) Regression line of heat transfer coefficient of reactor.	93
4.11A plot of mass of water ( $M_W$ ) against ( $mC_p/UA$ )	95
4.12Acetic Acid – Ethanol Reaction profile at $T_o = 283K$	98
4.13Acetic Acid – Ethanol Reaction profile at $T_o = 289K$	99
4.14Acetic Acid – Ethanol Reaction profile at $T_o = 296K$	100
4.15Acetic Acid – Propanol Reaction profile at $T_o = 285K$	102
4.16Acetic Acid – Propanol Reaction profile at $T_o = 290K$	103
4.17Acetic Acid – Propanol Reaction profile at $T_o = 297K$	104
5.1 The block diagram of the Experimental set-up	117
5.2 The electrical circuit of the system	119
5.3 The thermistor voltage – time profile	121
5.4 The thermistor temperature – time profile	122
5.5 Regression line of ( $R_{TH}$ ) against $1/T$ .	124
5.6 Thermos-flask cooling curve at $T_o = 361K$	126
5.7 Regression line of heat transfer coefficient of reactor.	127
5.8 (a) Reactor cooling curve – $M_W = 200g$	129
5.8 (b) Regression line of heat transfer coefficient of reactor.	130
5.9 (a) Reactor cooling curve – $M_W = 300g$	131
5.9 (b) Regression line of heat transfer coefficient of reactor.	132
5.10 (a) Reactor cooling curve – $M_W = 400g$	133

5.10 (b) Regression line of heat transfer coefficient of reactor.	134
5.11 A plot of mass of water (m) against ( $mC_p/ UA$ )	135
5.12 Acetic Anhydride – Methanol Reaction profile at 290K	137
5.13 Acetic Anhydride – Methanol Reaction profile at 294K	138
5.14 Acetic Anhydride – Methanol Reaction profile at 299K	139
5.15 Concentration – time plot of acetic Anhydride experiment (1)	141
5.16 Concentration – time plot of acetic Anhydride experiment (2)	142
5.17 Concentration – time plot of acetic Anhydride experiment (3)	143
5.18 Concentration – rate plot at 320K	145
5.19 Concentration – rate plot at 325K	147
5.20 Concentration – rate plot at 335K	149
5.21 Arrhenius plot of Experiment – 1	150
5.22 Arrhenius plot of Experiment – 2	151
5.23 Arrhenius plot of Experiment – 3	152
5.24 (a) Profile of model – predicted and Experimentally measured temperatures Experiment(1)	156
5.24 (b) Parity plots of model - predicted and Experimentally measured temperatures – Experiment(1)	157
5.24 (c) Percentage deviation plot – Experiment(1)	158
5.24 (d) Correction factor plot – Experiment(1)	159

5.25 (a) Profile of model – predicted and Experimentally	
measured temperatures – Experiment(2)	160
5.25 (b) Parity plots of model - predicted and Experimentally	
Measured temperatures – Experiment(2)	161
5.25 (c ) Percentage deviation plot – Experiment(2)	162
5.25 (d) Correction factor plot – Experiment(2)	163
5.26 (a) Profile of model – predicted and Experimentally	
Measured temperatures – Experiment (3)	164
5.26 (b) Parity plots of model - predicted and Experimentally	
Measured temperatures – Experiment (3)	165
5.26 (c ) Percentage deviation plot – Experiment(3)	166
5.26 (d) Correction factor plot – Experiment(3)	167
6.1 The block diagram of the Experimental set-up	180
6.1 The electrical circuit of the system	181
6.2 The thermistor voltage – time profile	183
6.3 The thermistor temperature – time profile	184
6.4 The regression line of $\ln(R_{TH})$ against $1/T$ .	186
6.5 Reactor cooling curve – $M_W = 400g$	187
6.6 Regression line of heat transfer coefficient of reactor.	188

6.7 (a) Reactor cooling curve – $M_w = 200g$	190
6.8 (b) Regression line of heat transfer coefficient of reactor.	191
6.9 (a) Reactor cooling curve – $M_w = 300g$	192
6.9 (b) Regression line of heat transfer coefficient of reactor.	193
6.10 (a) Reactor cooling curve- $M_w = 400g$	194
6.8 (b) Regression line of heat transfer coefficient of reactor.	195
6.11 A plot of mass of water against (MCP/UA)	196
6.12 Temperature – time plots – Excess water reaction at 305K	198
6.13 Temperature – time plots – Excess water reaction at 310K	199
6.14 Temperature – time plots – Excess water reaction at 328K	200
6.15 Concentration – time plots of acetic anhydride at 305K	202
6.16 Concentration – time plots of acetic anhydride at 310K	203
6.17 Concentration – time plots of acetic anhydride at 328K	204
6.18 Concentration – rate plot at 345K	206
6.19 Concentration – rate plot at 350K	207
6.20 Concentration – rate plot at 355K	208
6.21 Arrhenius plot of Experiment (1)	209
6.22 Arrhenius plot of Experiment (2)	210
6.23 Arrhenius plot of Experiment (3)	211
6.24 (a) Regression line for UA/MCP of Experiment (4)	214
6.24 (b) Experimental and Adiabatic curves of Experiment (4)	215

6.25 (a) Regression line for UA/MCP of Experiment (5)	216
6.25 (b) Experimental and Adiabatic curves of Experiment (5)	217
6.26 (a) Regression line for UA/MCP of Experiment (6)	218
6.26b) Experimental and Adiabatic curves of Experiment (6)	219
6.27 Concentration – time plots of Experiment (4)	221
6.28 Concentration – time plots of Experiment (5)	222
6.29 Concentration – time plots of Experiment (6)	223
6.30 Concentration – rate plot at 320K	224
6.31 Concentration – rate plot at 335K	225
6.32 Concentration – rate plot at 340K	226
6.33 Arrhenius plot of Experiment (4)	227
6.34 Arrhenius plot of Experiment (5)	228
6.35 Arrhenius plot of Experiment (6)	229
6.36 Experimental and Adiabatic curves of Experiment (7)	232
6.37 Experimental and Adiabatic curves of Experiment (8)	233
6.38 Experimental and Adiabatic curves of Experiment (9)	234
6.39 Concentration – time plots of Experiment (7)	236
6.40 Concentration – time plots of Experiment (8)	237
6.41 Concentration – time plots of Experiment (9)	238
6.42 Concentration – rate plot at 320K	239
6.43 Concentration – rate plot at 335K	240
6.44 Concentration – rate plot at 340K	241

6.44 Arrhenius plot of Experiment (7)	243
6.46 Arrhenius plot of Experiment (8)	244
6.47 Arrhenius plot of Experiment (9)	244

## APPENDIX-DATA ON ATTACHED COMPACT DISC

APPENDIX A: Time, Voltage, Temperature, Resistance data

APPENDIX B: Data for thermos –flask calibration

APPENDIX C1: Flask cooling curve –  $m_{\text{water}} = 200\text{g}$

APPENDIX C2: Flask cooling curve –  $m_{\text{water}} = 300\text{g}$

APPENDIX C3: Flask cooling curve –  $m_{\text{water}} = 400\text{g}$

APPENDIX D1: Temperature - time data :Acetic Acid – Ethanol Reaction  $T_o = 283\text{K}$

APPENDIX D2: Temperature - time data : Acetic Acid – Ethanol Reaction  $T_o = 289\text{K}$

APPENDIX D3: Temperature - time data: Acetic Acid – Ethanol Reaction  $T_o = 296\text{K}$

APPENDIX E1: Temperature -time data :Acetic Acid – Propanol Reaction  $T_o = 285\text{K}$

APPENDIX E2: Temperature - time data :Acetic Acid –Propanol Reaction  $T_o = 290\text{K}$

APPENDIX E3: Temperature - time data :Acetic Acid –Propanol Reaction  $T_o = 298\text{K}$

APPENDIX F1: Temperature - time data: Acetic Anhydride – Methanol  $T_o = 290\text{K}$

APPENDIX F2: Temperature - time data: Acetic Anhydride – Methanol  $T_o = 294\text{K}$

APPENDIX F3: Temperature - time data: Acetic Anhydride – Methanol  $T_o = 299\text{K}$

APPENDIX G1: Temperature –Time data: Acetic Anhydride –Excess Water at  $305\text{K}$

APPENDIX G2: Temperature - Time data: Acetic Anhydride –Excess Water at  $310\text{K}$

APPENDIX G3: Temperature -Time data :Acetic Anhydride –Excess Water at 325K

APPENDIX H1: Temperature - Time data: Excess Acetic Anhydride – Water at 286K

APPENDIX H2: Temperature - Time data: Excess Acetic Anhydride – Water at 294K

APPENDIX H3: Temperature - Time data: Excess Acetic Anhydride – Water at 305K

# **CHAPTER 1**

## **INTRODUCTION**

### **1.1 INTRODUCTION**

Temperature versus time profiles or history of a chemical reaction in a controlled temperature environment contains a vast amount of information about the nature of the chemical reaction. A lot of techniques or methods have been developed to extract both kinetics and thermodynamic information of the reaction from temperature-time profiles. Techniques commonly used have been extensively discussed in the proceeding chapter. Over the last forty years a number of methods have been developed for the measurement of kinetics of liquid-phase reactions just by following the temperature-time profiles of the contents of a batch reactor. The advantages of these methods have been reviewed by King and Glasser (1965) and Glasser and Williams (1971). Recently Scott, Williams and Glasser (1974) have developed an experimentally and computationally simple but accurate technique for obtaining both kinetic and thermodynamic information from temperature-time curves. All other approaches involve either complicated experimental apparatus or the evaluation of the kinetic and thermodynamic parameters from a limited number of experimental data points on the temperature-time curve. It is not the intension of this work to repeat the arguments of the best method or better computational accuracies but to highlight certain trends. In addition this work will show why such an intrinsically simple method has not achieved the popularity which it deserves. Finally, this work shows the method in a form from which will have both the inherent simplicity of temperature measurement and the ease of analysis of concentration-time data.

### **1.2 OBJECTIVES OF THE RESEARCH**

This research focuses on experimental measurements of temperature-time profiles of selected liquid-phase exothermic reactions which occurred in an adiabatic batch reactor. The research thus discusses the analysis of the temperature-time profiles with the objectives listed below:

- ❖ To demonstrate how the information from temperature-time profiles can be used in the development of a new technique to obtain to thermodynamic and equilibrium information of reversible exothermic processes.

- ❖ To develop a simulation model for experimentally measured temperature-time profiles for temperature and composition predictions for single stage batch reactive distillation systems.
- ❖ To develop kinetic models using information from temperature-time measurements of some chemical processes which have not been analyzed by this technique in the literature.

### **1.3 THESIS OUTLINE**

#### **CHAPTER 2**

Temperature-time measurements techniques are reviewed. Here the emphasis is on the methodologies and theoretical developments and analysis of the temperature-time profiles in obtaining kinetic and thermodynamic information of exothermic liquid-phase chemical reactions.

#### **CHAPTER 3**

This chapter describes the various experimental details employed in this work. This section is about experimental apparatus and methods used. The theory of the electrical circuit designed for this work is discussed. The thermistor resistance and temperature measurements are also discussed. It also shows the mathematical developments governing the temperature-time profiles of an adiabatic batch reactor. The chapter also discusses the analysis for obtaining kinetic and thermodynamic parameters. Here experimental descriptions of various chemical processes studied are also discussed and their temperature-time profiles are also presented.

#### **CHAPTER 4**

This chapter is an article published by the **American Chemical Society (ASC) Journal-Industrial and Engineering Chemistry Research 2013 52 (23) pp7630-7639. DOI: 10.1021/ie301944u**. It discusses the development of a new technique for the determination of equilibrium and thermodynamic information using temperature-time measurements of equilibrium controlled reversible exothermic processes.

## **CHAPTER 5**

This chapter has also been published by *International Institute for Science, Technology and Education (IISTE)- Journal of Chemical Process Engineering Research June 2013 Volume 10. ISSN-2225-0913 (online) vol.10 2013 p51-p94*. It discusses the development of a simulation model for temperature-time profiles for the prediction of temperature and composition in a single stage batch reactive distillation systems.

## **CHAPTER 6**

This chapter is an article which has been accepted for publication by the - **Journal of Chemical Engineering and Process Technology 2013 4:176. DOI: 10.4172/2157-7048.1000176**. It discusses the development of kinetic models of excess acetic anhydride-water, acetic anhydride-excess water and acetic anhydride-methanol processes at higher temperatures.

## **CHAPTER 7**

This is the final chapter of this thesis. It states the overall conclusion of the thesis. The contribution of this thesis to knowledge is clearly stated here and the relevance of the thesis title is verified by confirming that the objectives have been achieved. In this section areas of future research that are related to this thesis are also spelt out.

#### **1.4 REFERENCES**

King, R. P. and Glasser, D. (1965). The use of the adiabatic calorimeter for the reaction rate studies. S. Afr. Ind. Chem., **19**, 12.

Glasser, D. and Williams, D. F. (1971). The study of liquid phase kinetics using temperature as a measured variable. I&EC Fundam., **10**, 516.

Scott, P. D., Williams, D. F. and Glasser, D. (1974). S. Afr. J. Sci., **70**, 10.

## CHAPTER 2

### REVIEW OF THE THEORETICAL RELATIONSHIPS UNDERLYING TEMPERATURE-TIME PROFILES IN ADIABATIC AND NON ADIBATIC REACTIONS

#### 2.1 INTRODUCTION

This section reviews some pertinent background work of temperature –time profiles for kinetic and some thermodynamics information of chemical reactions processes. It also discusses the detailed theory behind temperature- time profiles. For some years, reaction kinetic parameters have been extracted by various techniques from temperature –time profiles of adiabatic processes. Calorimetric techniques of rate measurement have become popular in recent times because of its non-specificity and it's easy to of application the technique to heterogeneous reaction systems, non-aqueous systems and biological processes.

#### 2.2 ADIABATIC MEASUREMENT

Most of the early techniques of obtaining rate information of processes by temperature monitoring/measurement were developed for adiabatic systems. This is because there is a direct proportionality between temperature changes and the extent of reaction. Livingston et al (1953) stated that Duclaux (1908) and Chilintzev (1912) were amongst the first workers to propose the use of adiabatic temperature changes to study reaction kinetics. A lot of processes were considered adiabatic process if the rate of heat transfer during reaction was negligible when compared with the reaction rate. Hartridge and Roughton (1925) studied acid-sodium hydroxide neutralization reaction by measuring temperature profile of the reaction in a flow reactor to estimate the time to reach completion. La Mer and Read (1930) used a similar technique in studying the neutralization reaction between dichromate ions and sodium hydroxide.

In both studies heat losses were assumed to be negligible and the temperature profile along the length of each reactor was assumed to be a direct measure of the degree of reaction. With the assumptions stated above the heats of neutralization allowed the calculation of the rate constant

of the reactions. Chipperfield (1966) modified Hartridge and Roughton's flow apparatus such that smaller amounts of reactants could be used to obtain rate information. A similar modified system was developed by Kernohan and Roughton (1968) to obtain kinetic information of the very fast carbon dioxide-hemoglobin reactions. Sturtevant (1941) built an adiabatic calorimeter to measure the rates of chemical reactions. His system was very complicated and could only be used to study processes with half-lives more than 10 minutes. The rate constant was determined from temperature changes with time from a technique developed by Roseveare (1931). Recently the use of adiabatic calorimeters in rate measurement studies have focused on restricting heat transfer from the reaction vessel(s). Dyne, King and Glasser (1966) built an adiabatic reactor in which a direct heating current was automatically fed to the wall of the reactor in order to maintain the reactor wall at the same temperature as the reaction mixture. It is clearly seen that the use of adiabatic thermometric methods for rate measurements is complicated by the elaborate experimental apparatus to ensure that no effective heat transfer occurs between the adiabatic system and its surroundings during the reaction. This complicated apparatus shifted researchers' attention to look for methods and techniques to study rates of reactions.

### **2.3 DIFFERENTIAL THERMAL ANALYSIS**

Borchard and Daniel (1957) first applied the technique of differential thermal analysis (DTA) in the studies of reactions N,N-dimethylaniline and ethyl iodine as well as the decomposition process of benzenediazonium chloride by monitoring continuously the temperature difference between two identical reaction vessels, one in which reaction was occurring and the other in which no reaction was taking place. Both reactors were held in a bath and the temperature of the surroundings was increased linearly with time. Blumberg (1959) extended the DTA method to heterogeneous solid-liquid phase reaction between vitreous silica and hydrofluoric acid.

Both methods discussed required the evaluation of the slopes of temperature difference versus time which gave inaccurate results. Berger et al (1968) built a complex differential micro calorimetric apparatus to study biological processes.

A computer simulated model of the heat balances of the apparatus yielded the required rate data. Feher, Rohmer and Lutz (1971) proposed a technique of obtaining kinetic data from the temperature-time profile for the first order reaction occurring in a differential heat flow calorimeter. By applying integration, corrections were made to the heat transfer which allowed

for calculations of the rate constant. The maximum of the temperature difference versus time yielded a value for the heat of reaction- a thermodynamic quantity. The advantage of the DTA technique is that it provides kinetic and thermodynamic information of the process from only one experiment. Thus rate constant, activation energy and heat of reaction can be obtained in a single experiment. However a drawback of this technique is the complicated apparatus required and the fact that both reaction vessels have similar heat transfer properties.

## **2.4 NON-ADIABATIC THERMAL RATE MEASUREMENT**

The problems associated with carrying out reactions in adiabatic environment pushes researchers to allow heat transfer during reaction rate measurements. With this technique the temperature-time profile of reactions in most cases produced a non-linear relationship with the extent of the reaction. By correcting for heat transfer can the approximate adiabatic temperature –time profile be reconstructed. The manner in which the heat transfer corrections are made has also been a subject of much work. The methods used have yielded inaccurate kinetic results and have been experimentally or computationally complicated. It appears the first attempt to allow for heat transfer in the analysis of reaction temperature-time profiles was due to Westheimer and Kharesch (1946). These researchers used the method of Sturtevant to measure the rate of nitration of nitro-aromatic compounds. In their experiment, the adiabatic temperature rise was estimated by correcting the total experimental temperature rise for heat transfer between the reactor and the surroundings. Their results yielded only approximate rate data and it was not generally applicable. Rand and Hammett (1950) measured the steady-state temperature rise in a flow reactor, during the course of fairly fast reactions. By correcting such a steady-state reading for temperature changes due to dilution, mixing and heat transfer, straight line plots were generated and the rate constants and enthalpy of the reaction was obtain for first order kinetics.

Not only was the method subject to errors from the estimates of heat dilution and mixing and the resulting uncertainty in steady-state temperature rise, but also in the case of second order reaction kinetics, straight line plots could only be generated for equivalent reactant concentrations. Mars(1961) estimated the rate constant for the conversion of carbon monoxide to carbon dioxide from the axial temperatures of a water gas shift reactor. The temperature profiles differed at radial positions in the reactor, the mean value of the slopes of the tangents at the bending points of the various axial temperature profiles was used for each rate constant

calculations. The technique was not designed for general laboratory applications and it was of doubtful accuracy. Bell and Clunie (1952) obtained rate constants for reaction with half-lives of 3s to 3min, by the use of a flow reactor and by comparing the total temperature rise under isothermal conditions to that expected under adiabatic conditions. If a value for the enthalpy of reaction is not available, this method requires some other other experiments to measure the kinetic parameters:

- the determination of the total temperature experimental change under adiabatic conditions
- the determination of the heat transfer coefficient of the reactor

Corrections also need to be made for heats of dilution and mixing. Although rate constant are simply evaluated from the requisite data, only one temperature reading from each temperature-time profile is used while the significant information in the rest of the curve is ignored. Schmidt, Mickley and Grotch (1964) used a complicated heat balance model of the axial temperature-time profile in a gas flow reactor to measure the kinetics of cumene cracking in a fixed bed of catalyst pellets. Numerical differentiation of the axial temperature-time profile yielded first and second derivatives which were then used to calculate the rate of the reaction. They claimed that the technique was generally applicable, the numerical calculations of the first and second derivatives of the temperature profile is of questionable accuracy and also all the information in the temperature profile was not utilized. Over the last 15-20 years various methods have been developed to obtain accurate data from experimental temperature-time information (data) of the reaction occurring in the batch reactors. Becker et al (1960,1965,1966,1967) researched on the use of analogue computers to extract kinetic variables from temperature-time data.

Becker and Walisch (1965) used Peltier cooling to remove the heat generated by a reaction. A signal represented the Peltier cooling was amplified and integrated electronically to obtain a signal corresponding to the cooling energy supplied in any time since the start of the reaction. The integrated signal was used to generate a straight line plot of cooling rate against total cooling in any given time. The slope of this line yielded the rate constant for a first order kinetics. Later Becker and Maelicke (1967) employed a similar integration technique which in the absence of Peltier cooling was applied directly to temperature-time curve of the reaction in order to generate a straight line graph of the rate of heat generation against total heat generation. Again the slope yielded the rate constant of the reaction. Glasser and Williams (1971) recorded the temperature – time profiles of reactions occurring in a non-adiabatic batch reactor placed in an isolated

environment. By performing non-linear regression analysis of the heat and mass balances describing the system, values of the rate constant and enthalpy of the process was calculated. The essential difference between in this technique and that of Becker et al was that in the former case the analysis of the experimental data is achieved by the use of complicated experimental apparatus, whereas in the later case the simpler apparatus was used at the expense of great computational complexity. Both methods requires separate determination of heat transfer coefficient of the reactor, although both methods are independent of heat of mixing and heat of dilution. Just about the same time Glasser and Williams published their technique of obtaining kinetic and thermodynamic parameters of reactions, Dammers et al (1971) apply an approach identical to that of Glasser and Williams to some numerical calculation of the temperature-time graphs of a non-adiabatic process as a function of the extent of reaction. West and Svirebely (1971) have allowed for heat transfer in the equation applied by Sturtevant to supposedly adiabatic temperature-time profiles of some reactions. The approach is less vigorous and simpler than that of Glasser and Williams. The techniques of West and Svirebely differ from a modification of Glasser and Williams method. Both methods require the use of non-linear regression analysis to obtain kinetic and thermodynamic parameters, unless the rate constant of the reaction is much smaller than the heat transfer constant of the reaction vessel. In the latter case the tail of the temperature-time profile at infinite time yields the rate constant from the slope of a plot of logarithm of temperature difference against time. Zahra, Lagarde and Romanetti (1973) approximated the temperature-time profile of a reaction occurring under non-adiabatic conditions by the first two terms of an expansion of the rate expression. Within this approximation non-linear regression methods were applied to calculate the rate parameters. Fredlien and Launder (1969) reconstructed the adiabatic curve by correcting the temperature-time profile of the non-adiabatic reaction for the effect of heat transfer. The correction requires the evaluation of the area under the non-adiabatic temperature-time curve for each reading taken from the curve. Moiseev, Avetisyn, and Astrushka-Vich (1971) applied a similar method to reconstruct the adiabatic temperature-time curve of a reaction from the measurements from non-adiabatic process. It is seen from the outline of the various techniques that obtaining kinetic and thermodynamic information from temperature-time profiles of reactions involves either complicated experimental apparatus or sophisticated data processing techniques. The technique used in reconstructing the adiabatic profiles from non-adiabatic processes discussed in this thesis

is based partly on techniques of Glasser and Williams in terms of simplicity of apparatus and partly on Fredlien and Launder's techniques of the reconstruction of the adiabatic curve from non-adiabatic profile.

## **2.5 MATHEMATICAL ANALYSIS OF ADIABATIC HEATING CURVE**

The fundamental law governing the temperature-time profile of an adiabatic reaction is discussed. When a reaction proceeds adiabatically the temperature varies with time owing to the reaction heat liberated and one obtains the 'so called' heating curves.

The differential equation appropriate to such curves is discussed on the basis of the following assumptions stated below:

1. The law of mass action holds.
2. The law of Arrhenius relating specific rate constant with temperature holds.
3. The heat change is due practically exclusively to a single reaction.
4. The heat of reaction is independent of temperature.
5. The specific heat of the system is independent of temperature and composition.

The temperature of a single reaction system under adiabatic conditions is uniquely related to the extent of the reaction. This allows a direct substitution of the energy balance equation into the material balance equation resulting in a differential equation (DE) for the temperature-time variation in an adiabatic reacting system.

## **2.6 THE ENERGY BALANCE**

This section serves to develop the theory required in order to determine the kinetic and thermodynamic parameters for first and second order homogeneous liquid phase reactions that may be extracted from temperature-time profiles of each process that will be considered during the experimental work.

### **2.6.1 THE ENERGY BALANCE EQUATION FOR A NON- ADIABATIC BATCH REACTOR**

For a constant-volume batch reactor:

$$-r_A = -\frac{1}{V} \frac{dN_A}{dt} = -\frac{dC_A}{dt} \quad (2.1)$$

where

$r_A$  is the rate of formation of A (mol/s)

V is the volume of batch reactor ( $m^3$ )

$N_A$  is number of moles of A in the reactor at some time t (mol)

$C_A$  is the concentration of A in the reactor (mol/L)

The energy or the heat balance for the reaction occurring in a batch reactor over a time dt can be written as:

Heat generated by reaction + Heat generated by stirrer speed = Heat absorbed by reactor contents + heat transferred through reactor walls (2.2)

$$(-\Delta H_{rxn})(-r_A)V dt + Q_s dt = mC_p dT + UA(\Delta T)dt \quad (2.3)$$

where

$\Delta H_{rxn}$  is the heat of reaction (kJ/mol)

$Q_s$  is the heat generated by the stirrer (J/s)

U is the overall heat transfer coefficient between the contents of the reactor and the surroundings ( $J/m^2.s.K$ )

A is the area for heat transfer ( $m^2$ )

m is the mass of the reactor and its contents (kg)

$C_p$  is the specific heat of the reactor and its contents (J/mol.K)

$\Delta T$  is the temperature difference between the contents of the reactor T and the surroundings  $T_o(K)$

$Q_s dt = 0$  since its effect is negligible, hence equation (2.3) becomes:

$$(-\Delta H_{rxn})(-r_A)V dt = mC_p dT + UA(\Delta T)dt \quad (2.4)$$

Consider:

$$(-r_A)V = \frac{d\varepsilon}{dt} = \text{rate of reaction} \quad (2.5)$$

Plug equation (2.5) into equation (2.4) and integrate to give equation (2.6) below:

$$(T - T_o) + \frac{UA}{mC_p} \int_0^\infty (T - T_o)dt = \frac{(-\Delta H_{rxn})}{mC_p} \Delta\varepsilon \quad (2.6)$$

## 2.6.2 COMPARING CONCENTRATION-TIME PROFILES AND TEMPERATURE- TIME PROFILES

Consider a series of consecutive or parallel chemical reactions in a liquid phase stirred tank (batch) reactor, the temperature of the reactor content as a function of time may be described as:

$$mC_p \frac{dT}{dt} = \sum_{i=1}^n H_i \frac{d\varepsilon_i}{dt} - U_A (T - T_{amb}) + Q_s \quad (2.7)$$

Equation (2.7) is only valid if the temperature of the reactor contents at any time is uniform. This requirement is met in liquid phase systems by ensuring that the reactor is well stirred.

In the absence of any chemical reaction equation (2.7) becomes:

$$mC_p \frac{dT_1}{dt} = -U_A (T_1 - T_{amb}) + Q_s \quad (2.8)$$

If conditions are such that  $U_A$  is much smaller than the rates of the chemical reactions in equation (2.7) and the temperature range in the reacting and non-reacting experiments is similar and the rate of heat transfer between the reactor and the surroundings is similar over the entire time in which the reaction(s) and cooling with non-reaction occurs. to be a constant over the entire time in which the reaction(s) occurs, if the heat generated by the reaction does not change significantly equations (2.7) and (2.8) becomes:

$$mC_p \frac{dT_2}{dt} = \sum_{i=1}^n H_i \frac{d\varepsilon_i}{dt} - C \quad (2.9)$$

$$mC_p \frac{dT_1}{dT} = -C \quad (2.10)$$

Subtracting (2.9) from (2.10) it can be shown that:

$$mC_p \frac{d(\Delta T)}{dt} = \sum_{i=1}^n H_i \frac{d\varepsilon_i}{dt} \quad (2.11)$$

where:

$$\Delta T = T_1 - T_2 \quad (2.12)$$

$$\frac{d\varepsilon_i}{dt} = f_i (\varepsilon_i, k) \quad (2.13)$$

Where  $\Delta T$  is the approximation to the adiabatic temperature rise in the reactor. Each rate constant  $k_i$  is assumed to be a function of temperature as expressed by the Arrhenius form. It is established that over a small temperature range the rate constant do not vary significantly. If during the reaction the temperature change is sufficiently small, the temperature dependent of the rate constant may be ignored.

Under this condition equation (2.11) becomes independent of equation (2.13) and the former may be integrated to yield:

$$mC_p (\Delta T_o - \Delta T) = \sum_{i=1}^n H_i \varepsilon_i \quad (2.14)$$

$\Delta T_o$  is initial temperature difference.

Thus for a single reaction ( $n=1$ ), measurement of  $(\Delta T_o - \Delta T)$  is equivalent to the measurement of the concentration-time history of the reaction. Thus plots devised for the concentration – time may be applied to the temperature-time data obtain from equation (2.10).

### **2.6.3 FIRST ORDER PROCESSES**

Consider a single first order reaction ( $n=1$ ) in equations (2.13) and (2.14) and let

$k = k_1$ , then we can write :

$$mC_p (\Delta T_o - \Delta T) = H_1 \varepsilon_1 \quad (2.15)$$

and

$$\frac{d\varepsilon_1}{dt} = f_1 (\varepsilon_1, k_1) \quad (2.16)$$

To use equation (2.15) to measure  $k_1$  one need to determine  $\Delta T_o$ , the temperature difference at zero time when the extent of reaction is zero. In practice the temperature-time curve at zero time is complicated by the temperature changes resulting from mixing of reactants. In order to avoid this difficulty,  $T_1$  are chosen as the straight function of time corresponding to the constant rate of cooling after reaction is essentially complete.

$T_2$  is the temperature-time trace corresponding to the reaction,  $e_{1F}$  is defined to be the extent of the reaction at point  $T_F$  where  $T_2$  asymptotes to  $T_1$ . The definition of  $T_1$ ,  $T_2$  and  $e_{1F}$  are illustrated by Scott 1974.

Equation (2.16) is integrated to yield:

$$e_1 = e_{1F} (1 - \exp(-k_1 t)) \quad (2.17)$$

Combination equations (2.15) and (2.17) yields equation (2.18):

$$\frac{mC_p}{H_1} (\Delta T - \Delta T_F) = e_{1F} - e_1 \quad (2.18)$$

By definition  $\Delta T_F = 0$ , and equation (2.18) becomes :

$$\frac{mC_p}{H_1} (\Delta T) = e_{1F} - e_1 \quad (2.19)$$

From equation (2.19) a plot of  $\ln(e_{1F} - e_1)$  versus time (t) will be linear with slope  $k_1$ . Hence the initial temperature difference is not required to calculate  $k_1$ . The difference ( $\Delta T_o$ ),  $T_1$  and  $T_2$  curves at zero time correspond to the total adiabatic rise due to the reaction plus the temperature effect of mixing. The latter term is made up of both the heat of mixing of reactants (physical heat of mixing) and the heating due to the difference in temperature between the added reactants and content of the flask (vessel) (sensible heat of mixing). The sensible heat of mixing may be calculated from the knowledge of the masses, temperatures and heat capacities of both reactants.

#### **2.6.4 SECOND ORDER PROCESSES**

A process in which it is first order with respect to each of the two reactants (A) and (B), equations (2.13) and (2.14) becomes:

$$\frac{de}{dt} = k (A_o - \varepsilon)(B_o - \varepsilon) \quad (2.20)$$

$$mC_p (\Delta T_o - \Delta T) = H_e \cdot \varepsilon \quad (2.21)$$

For  $A_o \neq B_o$ , integration of (2.20) yield:

$$kt = \frac{1}{B_o - A_o} \ln \left[ \frac{A_o (B_o - \varepsilon)}{B_o (A_o - \varepsilon)} \right] \quad (2.22)$$

If  $T_1$  and  $T_2$  are chosen in the same manner as for first order reactions, equation (2.11) yields, for  $n = 1$ ,  $H_1 = H_e$ , and  $e_1 = e$ , then we can write:

$$\frac{d\Delta T}{dt} = \frac{H_e}{mC_p} \cdot \frac{d\varepsilon}{dt} \quad (2.23)$$

and hence

$$\Delta T = \frac{H_e}{mC_p} (A_o - \varepsilon) \quad (2.24)$$

Combining equations (2.22) and (2.24) we have:

$$kt = -\frac{1}{B_o - A_o} \ln \left( \frac{B_o}{A_o} \right) + \frac{1}{B_o - A_o} \ln \beta \quad (2.25)$$

where

$$\beta = 1 + \frac{B_o - A_o}{\frac{mC_p}{H_e} \Delta T}$$

A plot of  $\log \beta$  versus time (t) will give a straight line of slope  $(B_o - A_o)k$ . Here it is necessary to determine  $H_e$  before k.  $H_e$  may be calculated by extrapolation of Temperature –time curve to zero time, ( $e = 0$  in equation (2.24)) thereby eliminating the initial mixing effects from the value of  $\Delta T_o$ . This is only effective when there is a clear demarcation between heats of mixing and heats of reaction, thus when the initial rate of reaction is slow compared to the rate of mixing. If this condition is not satisfied, the total temperature rise may be corrected to give the temperature rise due to the reaction  $\Delta T_{He}$  by approximating the measurement of the physical and sensible heats of mixing. It is also possible to calculate  $H_e$  from a run of equal initial concentrations of reactants. If  $A_o = B_o$  equation (2.20) is integrated to give:

$$\frac{1}{A_o - \epsilon} - \frac{1}{A_o} = kt \quad (2.26)$$

and the equivalent of equation (2.25) is given by:

$$\frac{1}{\Delta T} = \frac{mC_p}{A_o H_e} + \frac{kmC_p}{H_e} \cdot t \quad (2.27)$$

A straight line is obtained by plotting inverse of  $\Delta T$  against time (t), this allows the determination of  $H_e$  from the intercept and k from the slope.

### **2.6.5 LINEAR DEPENDENCE OF TEMPERATURE AND EXTENT OF REACTION**

Consider a multiple reactions in a system of R independent chemical reactions with S molecular species reacting.

This system can be described mathematically as follows:

$$\sum_{j=1}^s \alpha_{ij} A_j = 0, \quad i = 1, 2, \dots \dots R \quad (2.28)$$

$\alpha_{ij}$  – Stiochiometric coefficient of species  $A_{ij}$  in  $i$ .

The mole of  $A_j$  present in the reaction mixture at any time is given by:

$$N_j = N_j^o + \sum_{i=1}^R \alpha_{ij} \epsilon_i, \quad j = 1, 2 \dots \dots \dots S \quad (2.29)$$

In terms of moles/mass we can write:

$$g_j = g_j^o + \sum_{i=1}^R \frac{\alpha_{ij} \epsilon_i}{M}, \quad j = 1, 2 \dots \dots \dots S \quad (2.30)$$

Differentiating equation (2.30) with respect time we obtain:

$$\frac{dg_j}{dt} = \sum_{i=1}^R \frac{\alpha_{ij}}{M} \cdot \frac{d\epsilon_i}{dt}, \quad j = 1, 2 \dots \dots \dots S \quad (2.31)$$

Enthalpy by definition is a function of temperature (T), pressure (P) and mass concentration of each species ( $g_i$ ) where  $i=1,2,3,\dots,n$ , thus we can write:

$$\mathbf{H} = \mathbf{f}(\mathbf{T}, \mathbf{P}, \mathbf{g}_i) \quad (2.32)$$

By differentiating equation (2.32) and considering the fact that for a constant pressure process we can write;

$$\frac{\partial H}{\partial T} = C_p \quad (2.33)$$

Hence it can be shown that:

$$\frac{dH}{dt} = C_p \cdot \frac{dT}{dt} + \sum_{i=1}^R \frac{\Delta H_i}{M} \cdot \left( \frac{d\epsilon_i}{dt} \right) \quad (2.34)$$

For an adiabatic operation:

$$\frac{dH}{dt} = 0 \quad (2.35)$$

Then equation (2.34) becomes:

$$C_p \cdot \frac{dT}{dt} + \sum_{i=1}^R \frac{\Delta H_i}{M} \cdot \left( \frac{d\epsilon_i}{dt} \right) = 0 \quad (2.36)$$

If  $\Delta H_i$  and  $C_p$  are strong functions temperature, then their ratio is can be considered to be constant, thus integrating equation (2.34) we obtained:

$$T - T_o = \sum_{i=1}^R \frac{(-\Delta H_i)}{mC_p} \cdot \epsilon_i \quad (2.37)$$

Hence for a single chemical reaction equation (2.37) becomes:

$$T = T_o + \frac{(-\Delta H)}{mC_p} \cdot \varepsilon \quad (2.38)$$

Equation (2.37) thus shows the linear dependency of temperature and extent of reaction at anytime in an adiabatic batch reactor.

In terms of conversion of the limiting reagent equation (2.38) can be modified, as shown in equation (2.39):

$$T = T_o + \frac{(-\Delta H)}{mC_p} X_A \quad (2.39)$$

By definition complete conversion of A,  $X_A = 1$  in equation (2.39), the term  $\Delta T_{ad}$  is the adiabatic temperature rise of the reactor

$$\frac{(-\Delta H)}{mC_p} = \Delta T_{ad} \quad (2.40)$$

### **2.6.6 FIRST ORDER IRREVERSIBLE PROCESS**

Consider the process  $A \rightarrow P$ .

The total temperature change is related to the reactants originally present:

$$(T_f - T_o) = \frac{N_{Ao}(-\Delta H(T_o))}{mC_p} \quad (2.41)$$

By combining equations (2.38) and (2.41) and eliminating  $T_o$  gives:

$$\varepsilon = \frac{mC_p}{(-\Delta H(T_o))} (T - T_f) + N_{Ao} \quad (2.42)$$

Differentiating equation (2.42) with respect to temperature as a variable gives:

$$\frac{d\varepsilon}{dT} = \frac{mC_p}{(-\Delta H(T_o))} \quad (2.43)$$

For a first order process, substitution from equation (2.29) gives

$$\frac{d\varepsilon}{dt} = k_o \exp\left(-\frac{E_a}{RT}\right) (N_{Ao} - \varepsilon) \quad (2.44)$$

Combining equations (2.41) and (2.42) with equation (2.44) yields:

$$\frac{dT}{dt} = k_o (T_f - T) \exp\left(-\frac{E_a}{RT}\right) \quad (2.45)$$

Equation (2.45) is thus the differential equation describing the temperature –time profile of a first order irreversible process.

### **2.6.7 SECOND ORDER IRREVERSIBLE PROCESS**

Consider the second order irreversible reaction below and assume the process is first order with respect to each reactant:



$$\frac{d\varepsilon}{dt} = k_x \exp\left(-\frac{E_a}{RT}\right) N_A N_B \quad (2.46)$$

By substituting equations (2.29), (2.42) and (2.43), we can show that,

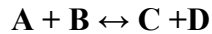
$$\frac{dT}{dt} = \frac{N_{A0} k_x (T_f - T)(T_{fo} - T)}{(T_f - T_o)} \exp\left(-\frac{E_a}{RT}\right) \quad (2.47)$$

$$T_{fo} = \frac{(N_{B0} - N_{A0})(T_f - T_o) + N_{A0} T_f}{N_{A0}} \quad (2.48)$$

Equations (2.47) and (2.48) are thus the differential equation describing the temperature –time profile of a second order irreversible process.

### **2.6.8 SECOND ORDER REVERSIBLE PROCESS**

Consider the reversible reaction below:



where the concentration of [C] and [D] are initially zero. Since the equilibrium constant is unknown, we define the concentrations as a departure from equilibrium as follows:

$$C_A = C_{AE} - \frac{\varepsilon}{V} \quad (2.49)$$

$$C_B = C_{BE} - \frac{\varepsilon}{V} \quad (2.50)$$

$$C_C = C_{CE} + \frac{\varepsilon}{V} \quad (2.51)$$

$$C_D = C_{DE} + \frac{\varepsilon}{V} \quad (2.52)$$

For a second order reversible reaction we can write

$$-\frac{dC_A}{dt} = k_1 C_A C_B - k_2 C_C C_D \quad (2.53)$$

Using the definitions of  $C_A, C_B, \dots, C_D$  as stated in equations (2.49) to (2.52) we can write equation (2.53) as follows:

$$\frac{1}{V} \frac{d\varepsilon}{dt} = k_1 \left( C_{AE} - \frac{\varepsilon}{V} \right) \left( C_{BE} - \frac{\varepsilon}{V} \right) - k_2 \left( C_{CE} + \frac{\varepsilon}{V} \right)^2 \quad (2.54)$$

$$\text{where } C_{AE} = C_{AO} - C_{CE} \quad (2.55)$$

$$C_{BE} = C_{BO} - C_{CE} \quad (2.56)$$

Substitution of equations (2.41) and (2.42) into (2.54) yields:

$$\frac{dT}{dt} = \frac{(-\Delta H)}{C_p} \cdot \frac{1}{\rho} \{ k_1 [ C_{AO} - C_{CE} - \omega ] [ C_{BO} - C_{CE} - \omega ] - k_2 [ C_{CE} + \omega ]^2 \} \quad (2.57)$$

where,

$$\omega = \frac{C_p}{(-\Delta H)} \rho (T - T_f)$$

$$k_1 = k_{10} \exp\left(-\frac{E_1}{RT}\right)$$

$$k_2 = k_{20} \exp\left(-\frac{E_2}{RT}\right)$$

$$\Delta H = E_2 - E_1$$

$$\rho = \frac{m}{V}$$

At equilibrium we can write:

$$\frac{k_2}{k_1} = \frac{C_{AE} \cdot C_{BE}}{C_{CE} \cdot C_{CE}} \quad (2.58)$$

Substituting equations (2.55) and (2.56) and solving for  $C_{CE}$  gives:

$$C_{CE} = \frac{k_1 (C_{AO} + C_{BO}) \pm \sqrt{k_1^2 (C_{AO} + C_{BO})^2 + 4k_1 k_2 C_{AO} C_{BO}}}{2 (k_1 - k_2)} \quad (2.59)$$

where  $0 \leq C_{CE} \leq C_{AO}$ , assuming component A is the limiting reactant. Hence equations (2.57) and (2.59) thus describe the temperature–time variation for a second order reversible reaction.

## **2.6.9 CALCULATING ADDITIONAL INFORMATION**

An overall heat balance for an irreversible reaction gives:

$$\frac{(-\Delta H)}{C_p} = \frac{m(T_f - T_i)}{N_{AO}} \quad (2.60)$$

If  $T_f$  and  $T_i$  are known from experiment,  $\Delta H/C_p$  can be calculated. The final temperature can be determined by allowing the reaction to go to completion. To obtain the temperature at zero time ( $T_i$ ) back extrapolation of the temperature – time plot is required, because in the initial stages of the experiment, the temperature –time curves are disturbed. These variations are probably due to heat of mixing and sensible heat supplied to the reactants to attain bulk phase temperature. However back extrapolation is inaccurate because the largest gradient is encountered in the initial region of the curve. Therefore an alternative method of estimating  $T_i$  is required. When the kinetic constants are known the differential equations describing the heating curves described above can be plotted as a linear function. This will allow the evaluation of  $T_i$  by a more accurate back extrapolation. In this work kinetic parameters were not known and were not considered in all of the analysis. Heat of mixing and sensible heats were assumed to be negligible compared with heat of reaction which was one of the parameters of interest. Initial temperature ( $T_i$ ) was accurately capture using a more sophisticated data acquisition software call Clarity.

## **2.7 REFERENCES**

- Becker, F. and Hoffman, H. (1966). Z. Physik. Chem. 50, 162
- Becker, F. and Maelicke, A.(1967).Thermokinetische Messungen Nach Derm Prinzip Der Wärmeflußkalorimetrie. Z. Physik. Chem. 55, 280
- Becker, F. and Spalink, F. (1960). Untersuchung Des Zeitlichen Ablaufes Chemischer Reaction Durch Kalorimetrisch Messungen. Z. Physik. Chem. 26, 1
- Becker, F. and Walisch, W. (1965). Isothermal calorimetry with automatically controlled Peltier-cooling and continouous interagrations of the compensation power. Z. Physik. Chem. 46, 279
- Bell, R. P. and Clunie, J. C. (1952). A thermal method of following fast reactions in solutions. Proc. Roy. Soc. A212, 16
- Berger, R. L., Yu Bing Fok Chick and Davids, N. (1968). “ Rev. Sci. Instruments” 39(3), 362

Borchardt, H. J. and Daniels, F. (1957). The application of differential thermal analysis of the study of reaction kinetics. *J. A. C. S.* 79, 41

Chelintzev, V. (1912). "J. Russ. Phys. Chem. Soc." 44, 465

Chipperfield, J. R. (1966). The kinetics of combination of carbon dioxide with the anions of glycine, glycyl-glycine and related amino acids. *Proc. Roy. Soc. Ser" B* 164, 401

Dammers, W.R. Frankvoort, W. and Tels, M. (1971). Temperature-time and temperature-concentration curves in reaction calorimetry. *Thermochin. Acta*, 3, 133

Duclaux, J. (1908). "Compt. Rend." 146, 120

Dyne, S., King, P. and Glasser, D. (1967). Automatically controlled adiabatic reactor for reaction rate studie. *Rev. Sci. Instrments* 38, 209

Feher, F., Rohmer, H. and Lutz, H. D. (1971). About differential Wärmeflußkalorimetrie for measuring heats of reaction, rate constants and slower reactions. *Z. Anorg. ALLG. Chem.* 383, 293

Fredlein, R. A. and Lauder, I. (1969). A thermal technique for studying moderately fast reactions in solutions. *Aust. J. Chem.* 22, 33

Glasser, D. and Williams, D. F. (1971). The study of liquid phase kinetics using temperature as a measured variable . *I & E. C. Fundam.* 10, 516

Hartridge, H. and Roughton, F. J. W. (1925). "Proc. Cambridge Phil. Soc." 22, 246

Kernohan, J.C. and Roughton, F.J. W. (1968). *J. Physiol. (London)*, 197, 345

La Mer, V. K. and Read, C. L. (1930). Rapid reactions. The velocity and heat effects involved in the neutralization of sodium dichromate by sodium hydroxide *J.A.C.S.* 52, 3098

Livingston, R. (1953). *Techniques of organic chemistry*. Vol. 8. ed. By Weissberger, A., Interscience, New York, pg 58

Mars, P.(1961). *Chem. Eng Sci.* Factors governing the behavior of the adiabatic water-gas shift reactor. 41, 375

Moiseev, V. D., Avetisyn, N. G. and Astrushkevich, A. A. (1971). *Kinetika I Kataliz* 12(5), 1315

Rand, M. J. and Hammett, L. P. (1950). Reaction rates in a stirred flow reactor. *J.A.C.S.* 72, 287

Roseveveare, W. E. (1931). Methods of calculating and averaging rate constant. *J.A.C. S.* 53, 1651

Schmidt, J. P., Mickley, H. S. and Grotch, S. L. (1964). Use of adiabatic experiments for kinetic studies in fixed catalyst beds. *A.I. Ch.E. J.* 10, 149

Sturtevant, J. M. (1941). Calorimetric investigations of organic reactions II A new Calorimeter. The mutarotation of  $\alpha$ - and  $\beta$ -D-Glucose. J. Phys. Chem. 45, 127

West, E.D. and Svirbely, W. J. (1971). Analysis of solution kinetics data coupled with thermal transients in an adiabatic calorimeter I. J. Phys. Chem. 75(26), 4029

Westheimer, F. H. and Karasch, M. S. (1946). The kinetics of nitration of aromatic nitro compounds in sulphuric acid. J.A.S.C. 68, 1871

Zahra, C., Lagarde, L. and Romanetti, R. (1973). Thermokinetic studies of slow reactions by heat conducting calorimetry. Thermochim. Acta, 6, 145

## **2.8 LIST OF SYMBOLS**

$r_A$  –rate of reaction of A

V –volume

$N_A$  –moles of A

t – time

$C_A$  –concentration of A

$\Delta H_{\text{rxn}}$  –enthalpy of reaction

$Q_s$  –quantity of heat

m –mass

$C_p$  –specific heat capacity

U –heat transfer coefficient

A –surface area

$f_i$  – function with respect to  $i$ th-order.

$\epsilon$  – extent of the  $i$ th chemical reaction

$H_i$  –enthalpy of  $i$

$T_{\text{amb}}$  –ambient temperature

$\Delta T$  –change in temperature

k –specific rate constant

$A_j$  – moles of specie  $j$  present in the mixture

$A_o$  –initial amount of A

$B_o$  –initial amount of B

$\alpha_{ij}$  –stoichiometric coefficient

$T_o$  –initial temperature

$N_A$ - moles of A

$E_a$  – activation energy

R –molar gas constant

## CHAPTER 3

### **EXPERIMENTAL APPARATUS, PROCEDURES AND EXPERIMENTAL DATA**

#### **3.1 INTRODUCTION**

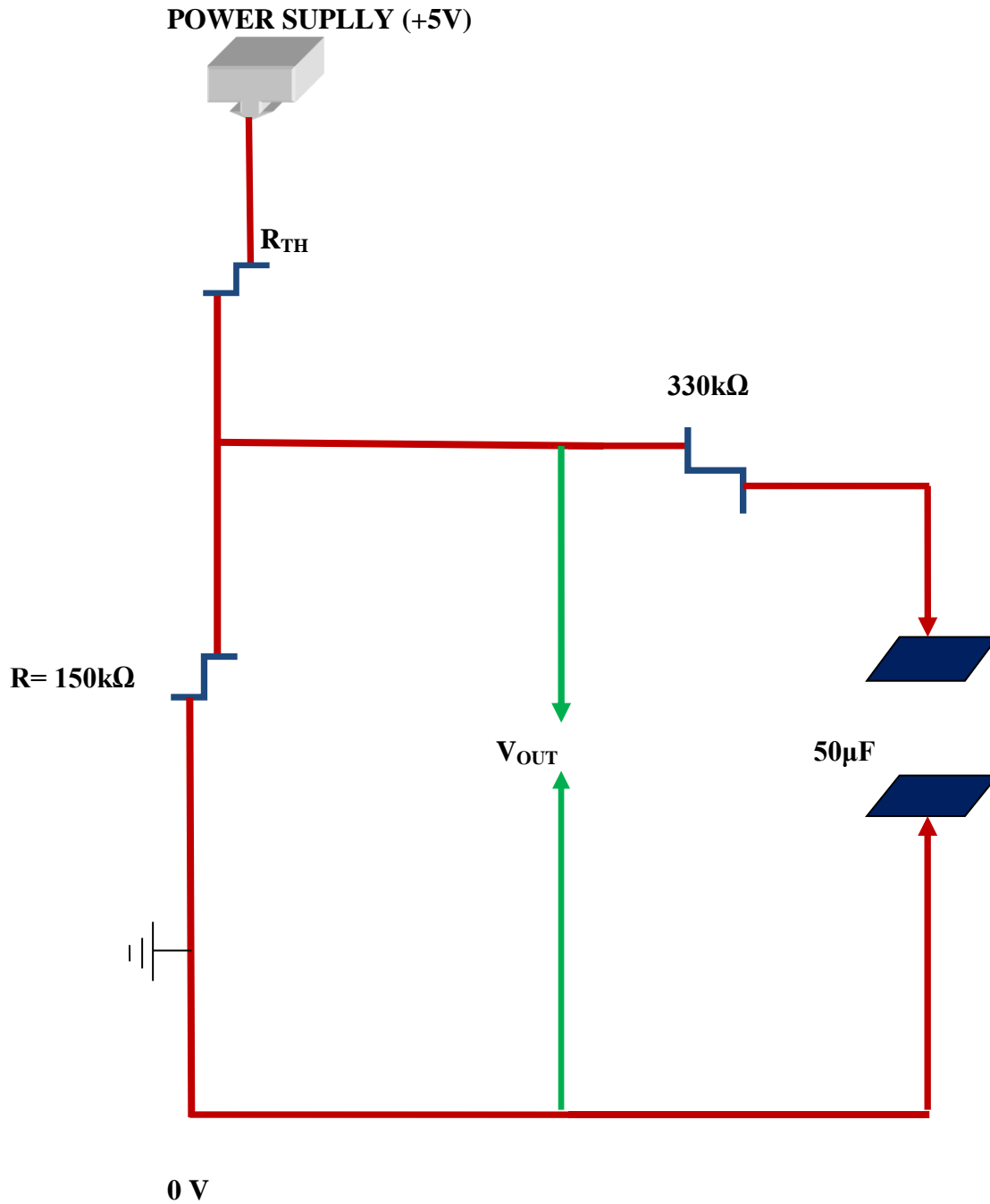
**This chapter describes the apparatus in section 3.2 to section 3.2.6. The experimental procedures and measured experimental data are given in sections 3.2.7 to 3.3.1.4.3**

#### **3.2 EXPERIMENTAL APPARATUS**

The experimental apparatus used is quite simple. It consist of a thermos flask, in which the reactions are done and a thermistor, with associated circuit, for measuring the temperature with time during reaction. The thermistor, electrical circuit used for the measurement of the resistance and the calibration of the thermistor are described in section 3.2.1 The reaction vessel, the thermos flask is described in section 3.2.4. The flask is fairly well insulated, but it is not truly adiabatic, hence the method of determining the heat loss from the flask (which we refer to as calibration of the reaction vessel) and correcting the measured temperature to the temperature that would have been in an adiabatic system is described in section two above.

Temperature changes are a common feature of almost all chemical reactions and can be easily measured by a variety of thermometric techniques. Following the temperature change during reaction is useful especially for fast chemical reactions where the reacting species are not easily analyzed chemically. In the past, the adiabatic method does not appear to have been used for kinetic studies. This was due to the fact that, construction of truly adiabatic reaction vessels is not possible and also obtaining kinetic parameters from experimental measurements were complex and required the use of numerical techniques. We described in section 2.4 how these difficulties were overcome.

### 3.2.1 THE ELECTRICAL CIRCUIT FOR MEASURING THE RESISTANCE OF THE THERMISTOR



Figure(3.1): The electrical circuit used to measure the resistance of the thermistor. The thermistor is represented by  $R_{TH}$  and the voltage that is measured used to calculate the resistance of the thermistor is  $V_{out}$ .

### **3.2.2 RELATIONSHIP BETWEEN MEASURED VOLTAGE $V_{out}$ AND THE THERMISTOR RESISTANCE $R_{TH}$**

From Kirchhoff law's we can write:

$$V_{out} + V_{TH} = 5V \quad (3.1)$$

$V_{out}$  – Voltage measured across the reference thermistor during the course of reaction.

$V_{TH}$  – Voltage across thermistor ( $R_{TH}$ ).

From (3.1):

$$V_{TH} = 5V - V_{out} \quad (3.2)$$

$$R_{TH} = \frac{V_{TH}}{I_{total}} = \frac{5V - V_{out}}{I_{total}} \quad (3.3)$$

From the circuit  $V_{TH}$  and  $I_{total}$  are unknowns.  $R_{TH}$  is resistance due to the thermistor, and  $I_{total}$  is the same through and  $R_{TH}$  can be determine from equation (3.4) as :

$$I_{total} = \frac{V_{out}}{R} \quad (3.4)$$

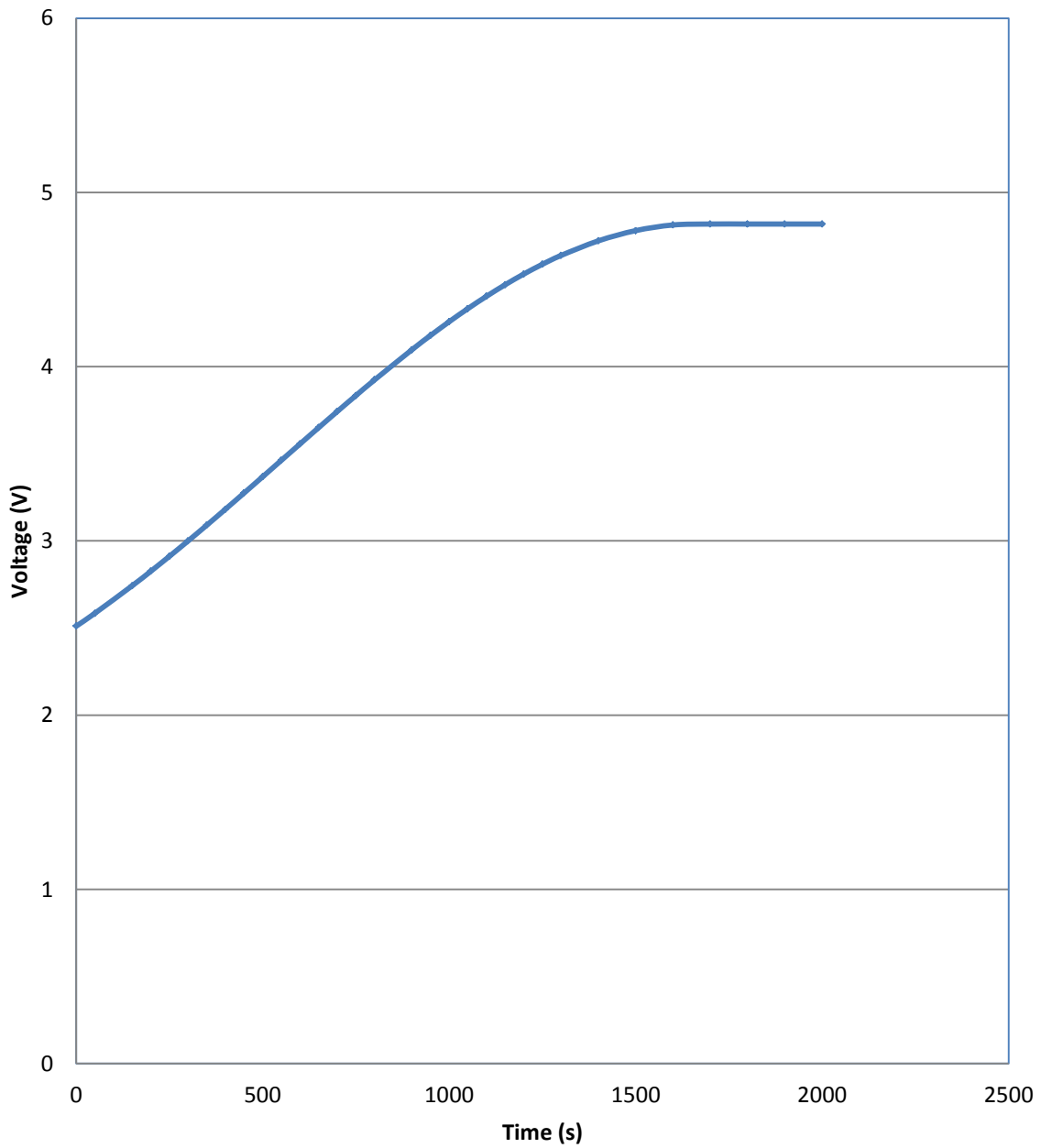
$V_{out}$  is known from experimental voltage –time profile and  $R$  (150k $\Omega$ ) is also known from the circuit. Thus when  $I_{total}$  is determined from (3.4),  $R_{TH}$  which is the thermistor's resistance and it is related to temperature at any time during the chemical reaction can be determine as:

$$R_{TH} = \left(\frac{5V}{V_{out}} - 1\right)R \quad (3.5)$$

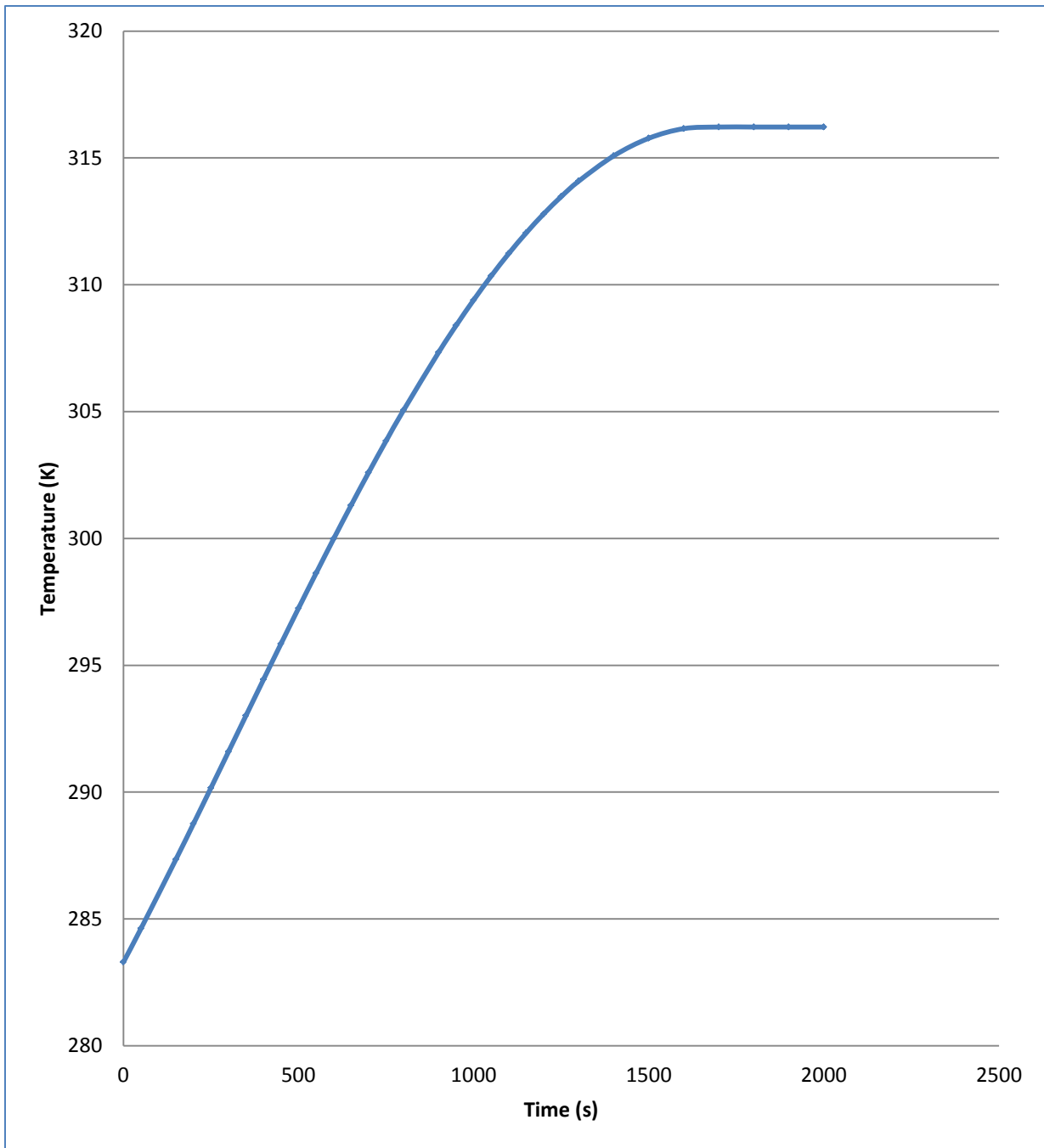
### **3.2.3 CALIBRATION OF THE THERMISTOR**

The thermistor used was a negative temperature coefficient (NTC) thermistor with unknown thermistor constants. The calibration of the thermistor involves the determination of the thermistor constants and can be used to establish the relationship between the resistance of the thermistor and temperature.

This was done by filling a vessel with water and putting the vessel in a water bath. The thermistor and an electronic digital temperature measuring device, which measured the actual temperature in the vessel, were both inserted in the vessel and the vessel was sealed. The voltage was monitored until the voltage reaches steady state. The thermistor was connected to a computer with a data acquisition software to record data of voltage versus time as shown in figure 3.2 below. This voltage/time plot was used to match the temperature/time data obtained from the electronic digital temperature device. The profiles are shown in figure (3.2) and (3.3) below.



**Figure(3.2): The thermistor voltage-time profile during the calibration run**



**Figure(3.3): The measured temperature-time profile during the calibration run**

Thermistor resistance ( $R_{TH}$ ) was determined by using eqn (3.5) above. The temperature dependence of an NTC is typically given by:

$$R_{TH} = \exp\left(\frac{B}{T} + C\right) \quad (3.6)$$

Where T is the temperature in Kelvin. This can be rearranged to give:

$$\ln(R_{TH}) = \frac{B}{T} + C \quad (3.7)$$

where the parameters (B) and (C) are the thermistor constants and were obtained from comparing the measured resistance to the measured temperature. The constants were determined by fitting the “best” least square straight line plot of  $\ln(R_{TH})$  against  $1/T$  of the measured temperature as shown in figure 3.4 giving the thermistor temperature dependence as:

$$\ln(R_{TH}) = -\frac{1773.8}{T} + 18.178 \quad (3.8)$$

Appendix (A) on the CD Rom shows the temperature-resistance data used for the regression analysis.

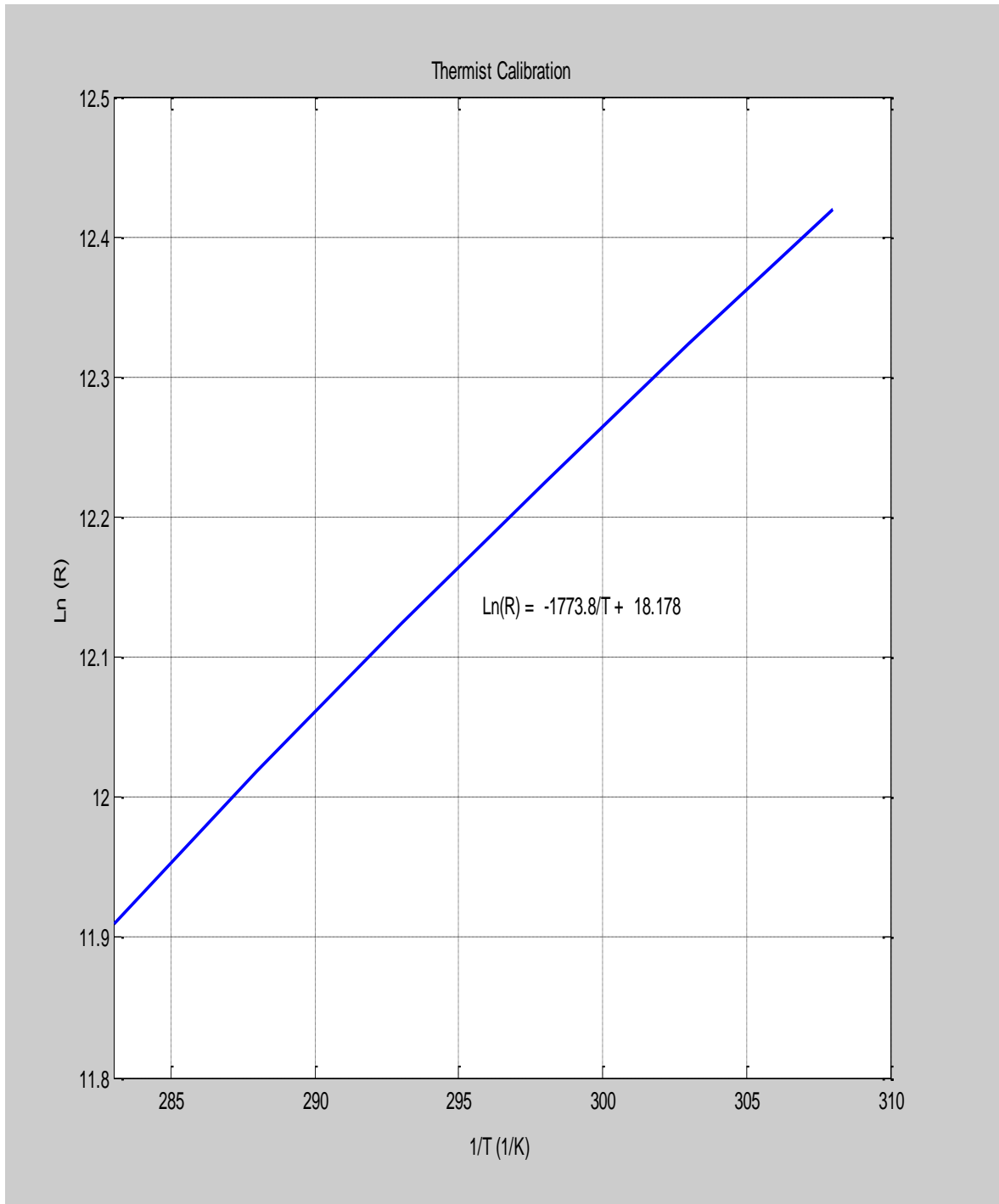


**Figure (3.4): Regression line of  $\ln(R_{TH})$  against  $1/T$  in order to determine the temperature dependence of the thermistor.**

### **3.2.4 DESCRIPTION OF THE REACTION VESSEL**

The reaction vessel used was the ordinary Dewar thermos flask with removable screw cap lid. The flask had a total volume of 500mL with internal diameter of 4.5cm and total length of 22.0cm. The reaction vessel (thermos flask) was stirred using a magnetic stirrer driven by a magnetic plate at a constant speeds. A figure of the reaction vessel appears in figure (3.5) below:



**Figure (3.5): The reaction vessel**

### **3.2.5 CALIBRATION OF THE REACTION VESSEL**

The reactor calibration involves determination of the heat transfer coefficient (UA) of the reactor (including the contents and the vessel) used in performing the experiment. This was done by filling the vessel with 400.0g of distilled water at 361K and the temperature of the water in the vessel was measured until the temperature-time profile reached steady state. Figure (3.6) shows the measured temperature-time profiles of the system during the calibration experiment.

If we assume that UA and the heat capacity of the flask and its contents are constant during this experiment, the change in temperature of the water in the vessel (T) with time (t) can be described by equation (3.9) below:

$$T - T_s = (T_o - T_s) \exp\left(-\frac{uA}{mC_p} t\right)_{system} \quad (3.9)$$

Where  $T_0$  is the initial temperature of the water in the vessel,  $T_s$  is the steady state or asymptotic temperature of the water,  $m$  is the mass of the flask and its content and  $C_p$  is the specific heat of flask and content.

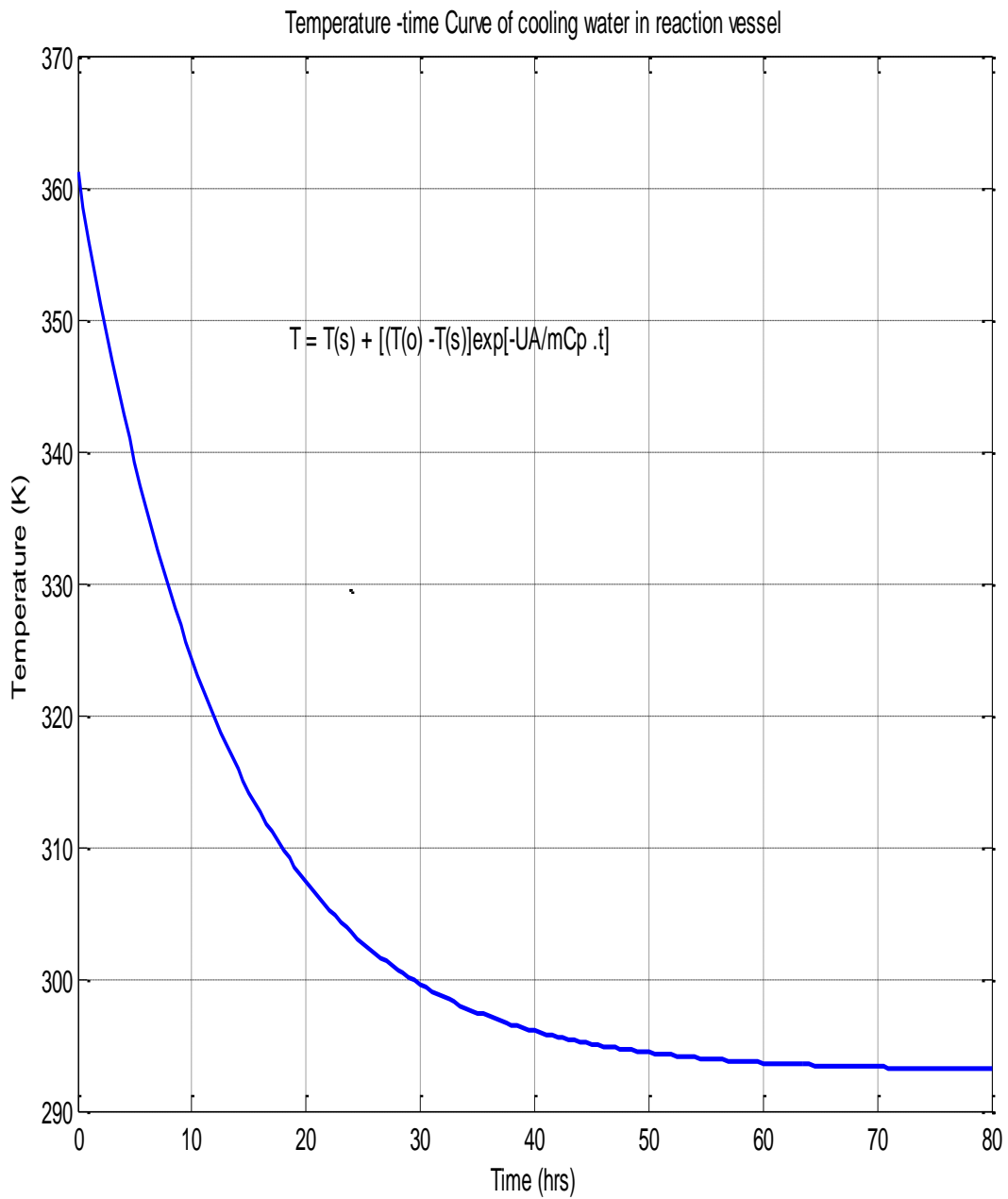


**Figure (3.6) :Measured temperature of water (T) versus time in the thermos flask during the cooling experiments used to calibrate the reaction vessel. The initial temperature  $T_{(o)} = 361K$**

From eq(3.9) the values of  $T_o$  and  $T_s$  were obtained from figure(3.6). Rearrangement of eq(3.9) gives;

$$\ln\left(\frac{T - T_s}{T_o - T_s}\right) = \ln(Y) = \left(-\frac{UA}{mC_p}t\right)_{system} \quad (3.10)$$

Since T and t values are known least square regression analysis was performed and a straight plot of  $\ln(Y)$  against time is shown in figure (3.7) below. Experimental data is shown in appendix (B) in the CD Rom attached.

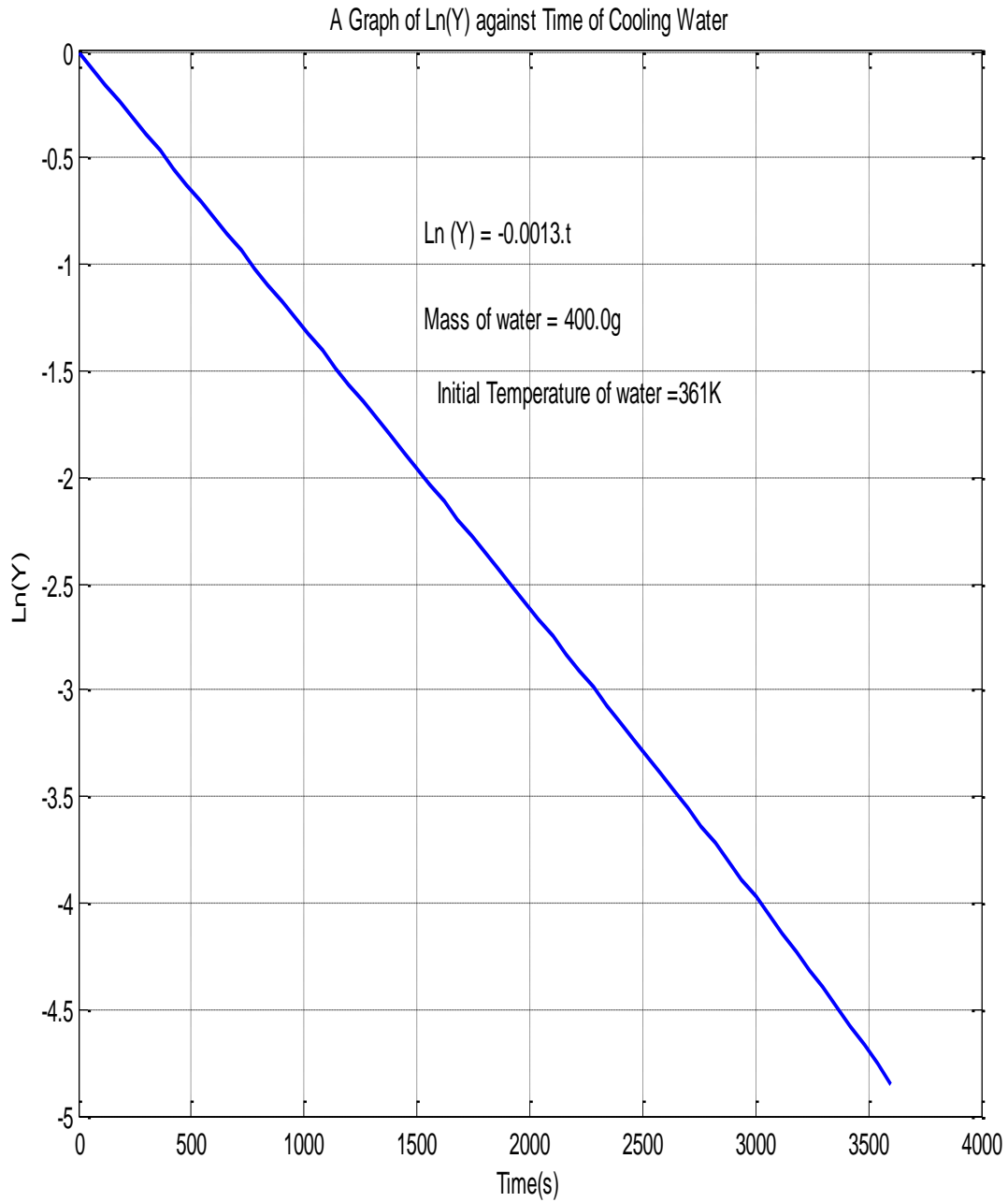


**Figure (3.7) :Regression line using equation (3.10) in order to determine the heat transfer coefficient of reactor system (flask and content)**

The slope of the straight line of figure(3.6) is given by  $0.0013\text{s}^{-1}$  which corresponds to the value of  $(UA/mC_P)_{\text{system}}$  of the flask and content.

### **3.2.6 DETERMINATION OF HEAT TRANSFER COEFFICIENTS OF THE FLASK AND CONTENTS OF FLASK**

The measured heat transfer coefficient contains both factors relating to the reaction vessel itself and the contents (ie water) of the vessel. The value  $UA/mC_p$  that were measured in the previous section is that for the system ie vessel and content. For a given system (reaction vessel and content) one can write:

$$\left(\frac{mC_p}{UA}\right)_{system} = \left(\frac{m C_p}{UA}\right)_{water} + \left(\frac{mC_p}{UA}\right)_{vessel} \quad (3.11)$$

In this experiment different amount of water ( $m_w$ ) (200g, 300g and 400g) was injected into the reaction flask at 343.08K, 347.77K and 347.85K and allowed to cool until the temperature reaches a steady-state temperature ( $T_s$ ). Figures (3.6a), (3.7a) and (3.8a) of the cooling processes are shown below. As the temperature of the contents of the flask cools, the cooling process can be described by equation (3.9) above. A nonlinear least-square regression analysis was performed on all the three experimental curves. Using equation(3.10), the value of  $(UA/mC_p)_{system}$  for each cooling curve was obtained. Figures (3.6b),(3.7b) and (3.8b) shows the regression lines. Data used for this experiment is shown in appendices (C1,C2 and C3) on the attached CD Rom.

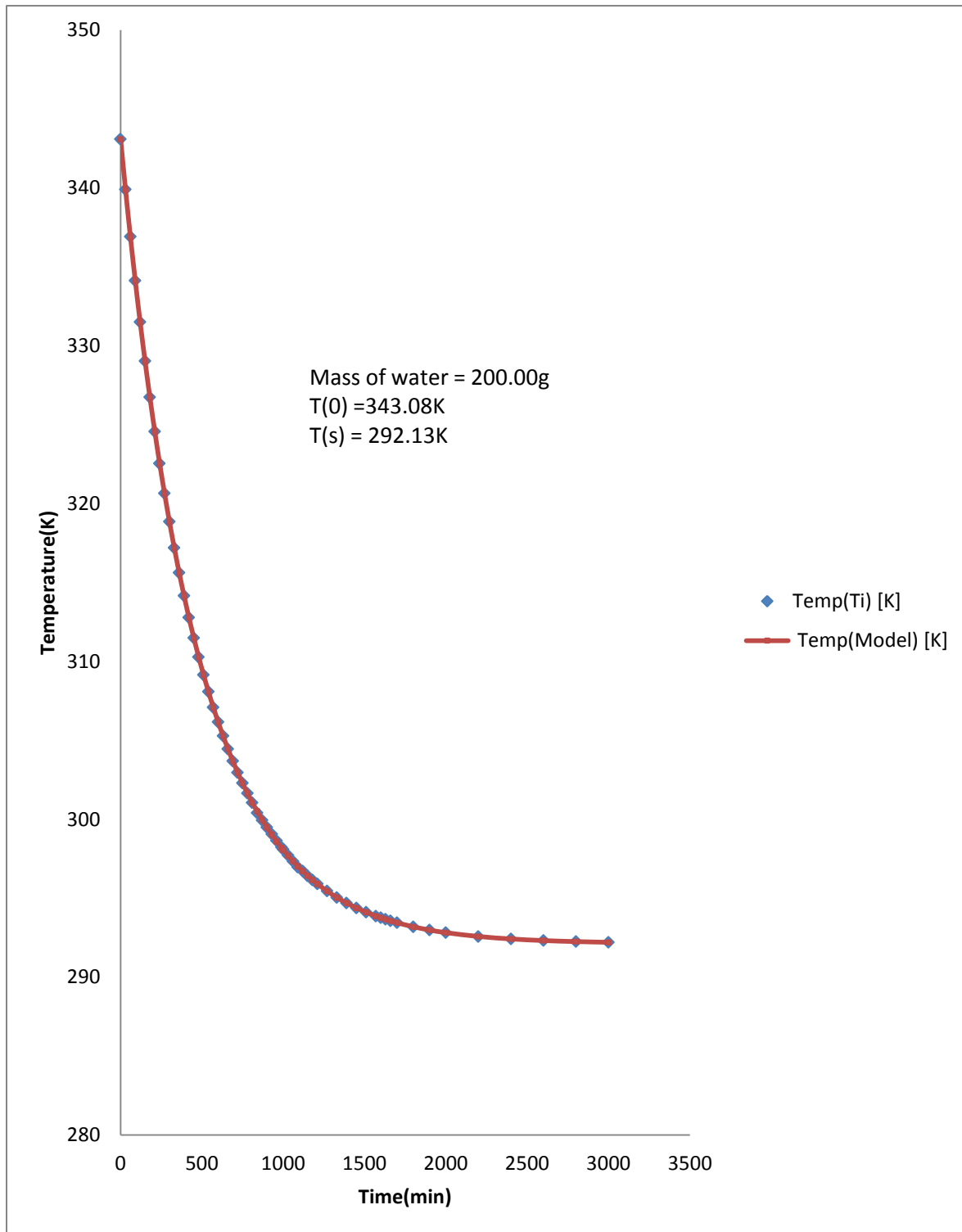


**Fig (3.6a):** Reactor (Thermos-flask) cooling curve with  $T_{(0)} = 343.08\text{K}$  with 200g of water

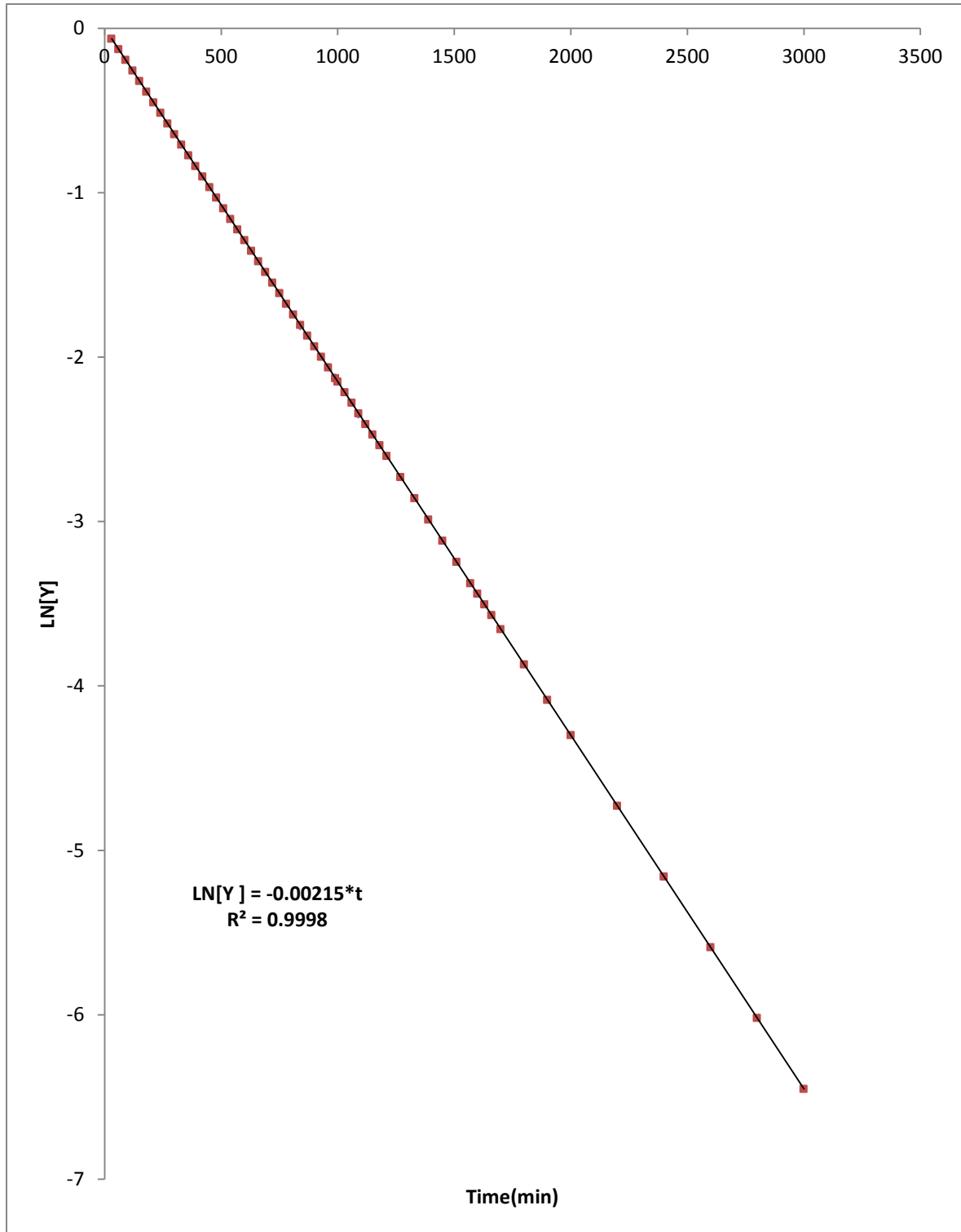


**Fig (3.6b):** Regression line using equation (3.10) and the data in figure (3.6a). The slope of the line is related to the heat transfer coefficient of the system (vessel and content)

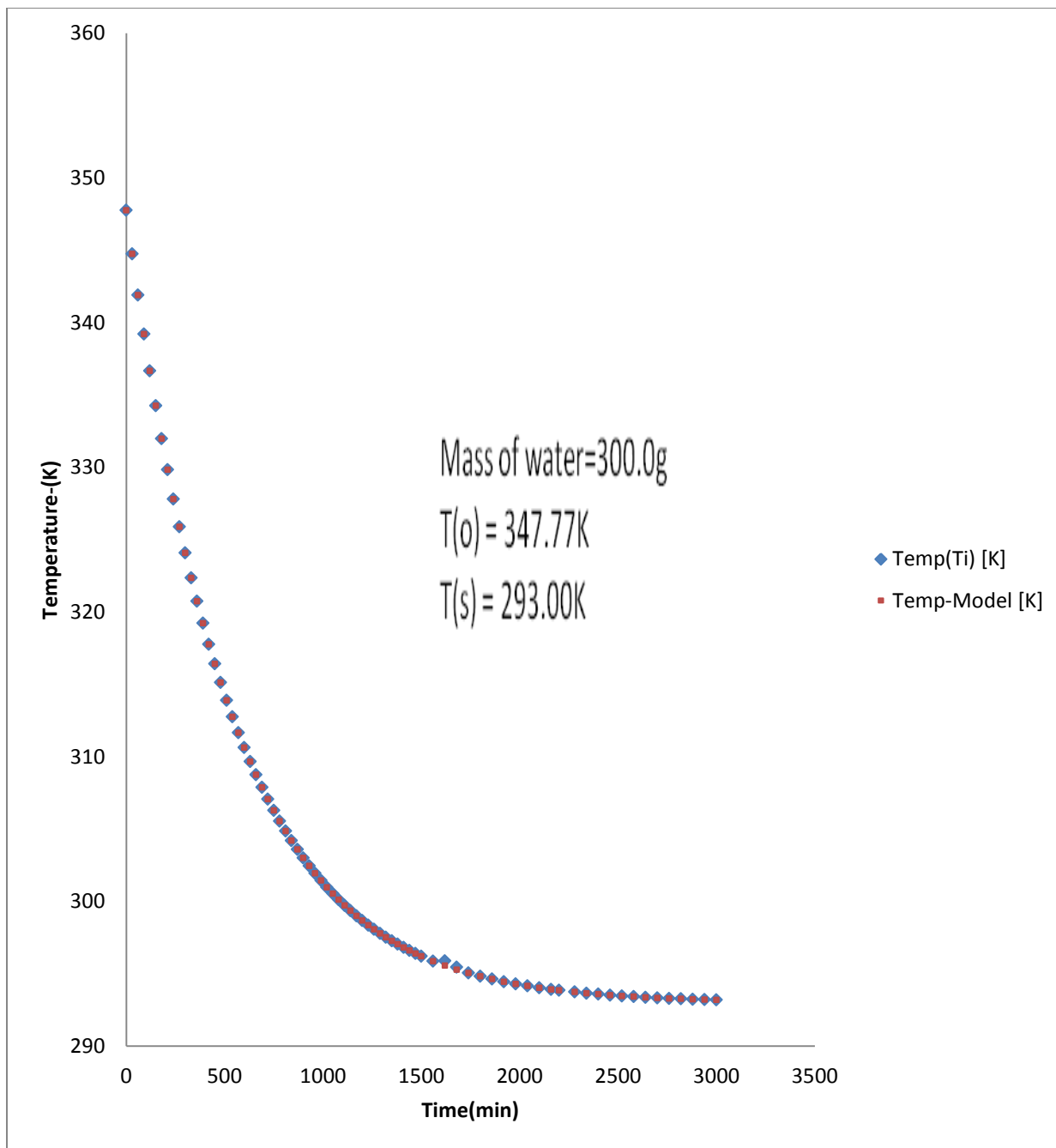


**Fig (3.7a): Reactor (Thermos-flask) cooling curve with  $T(o) = 347.77\text{K}$  with 300g of water**

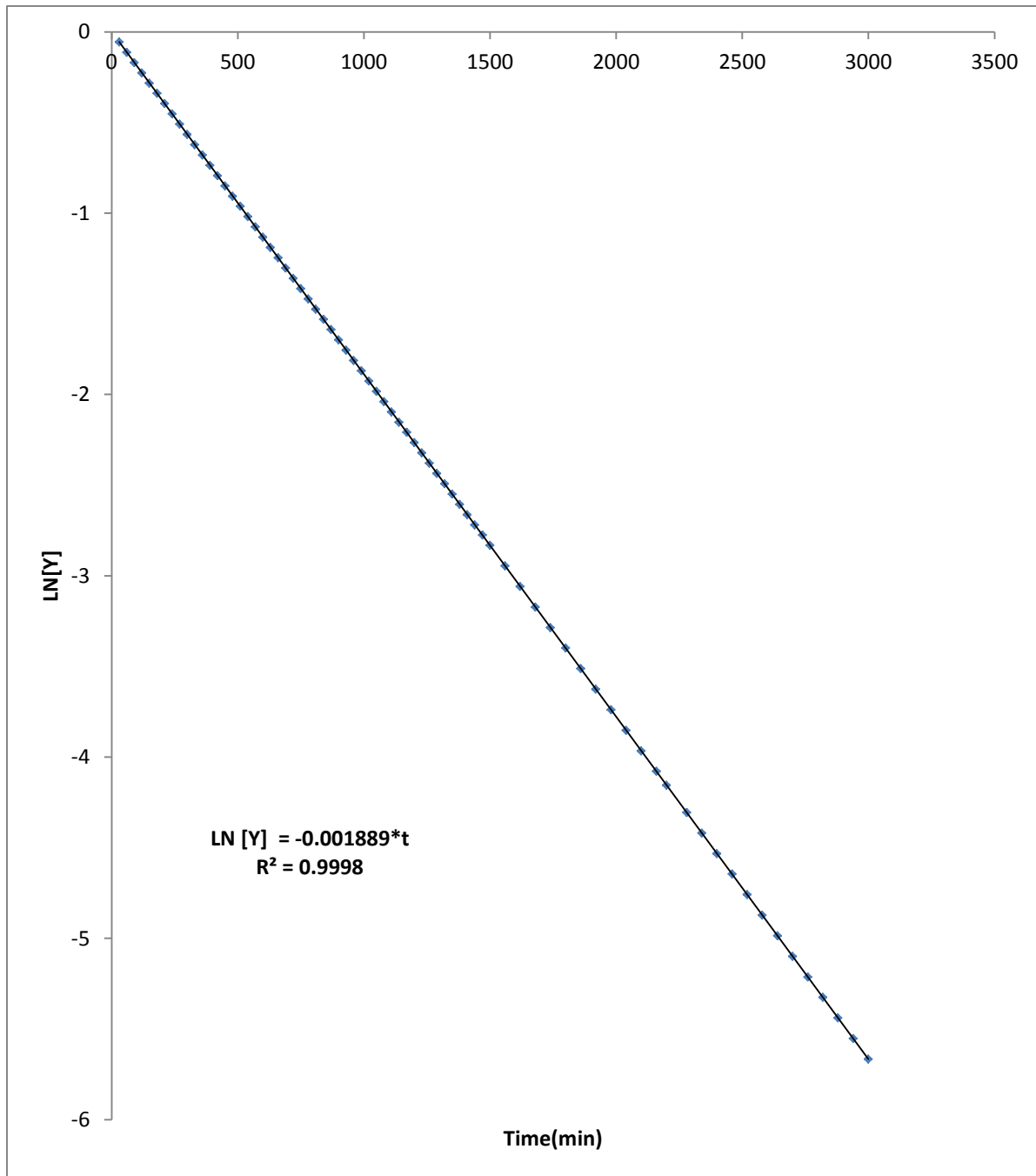


**Fig (3.7b):** Regression line using equation (3.10) and the data in figure (3.7a). The slope of the line is related to the heat transfer coefficient of the system (vessel and content)

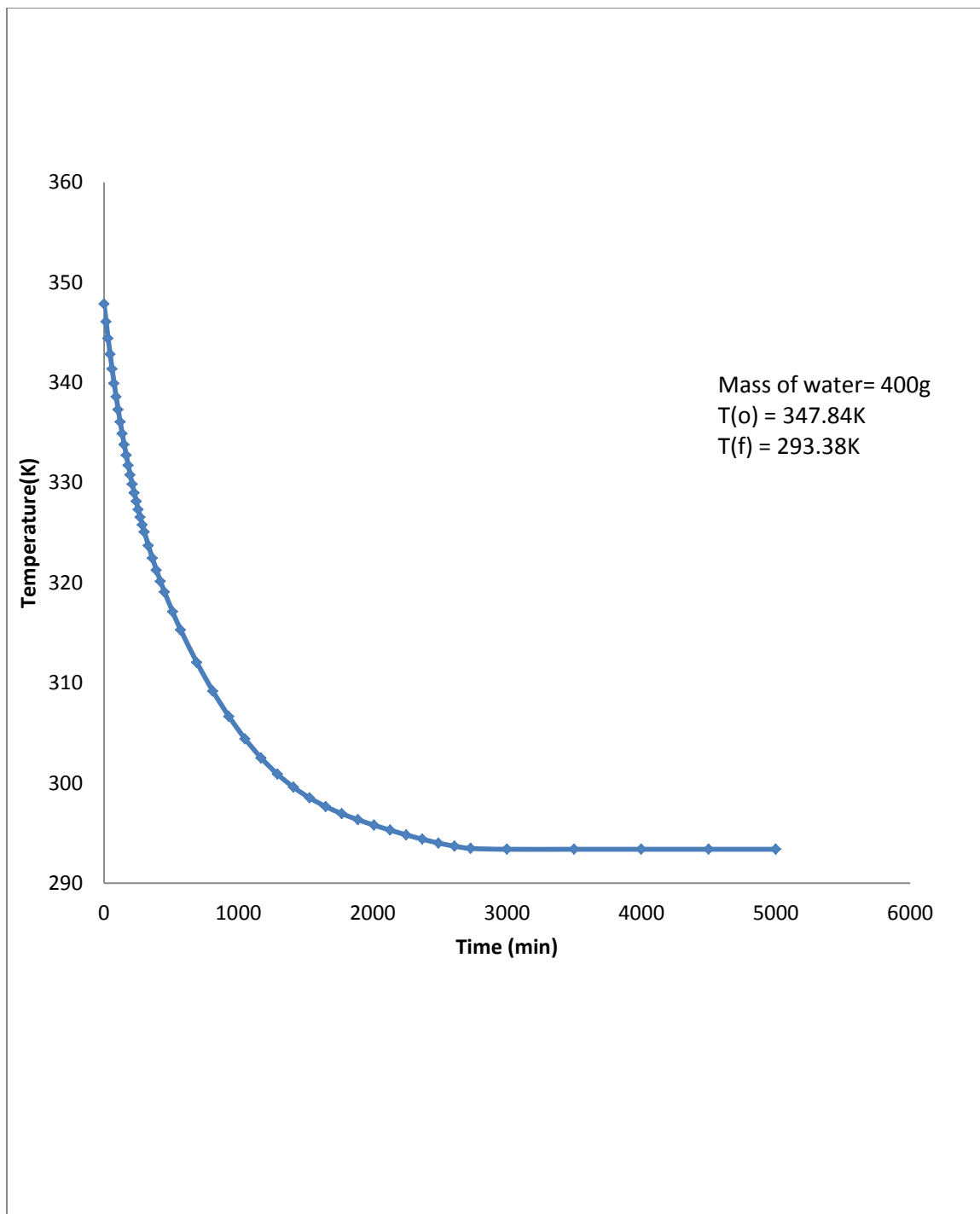


**Fig (3.8a): Reactor (Thermos-flask) cooling curve with  $T_{(o)} = 347.84K$  with 400g of water**

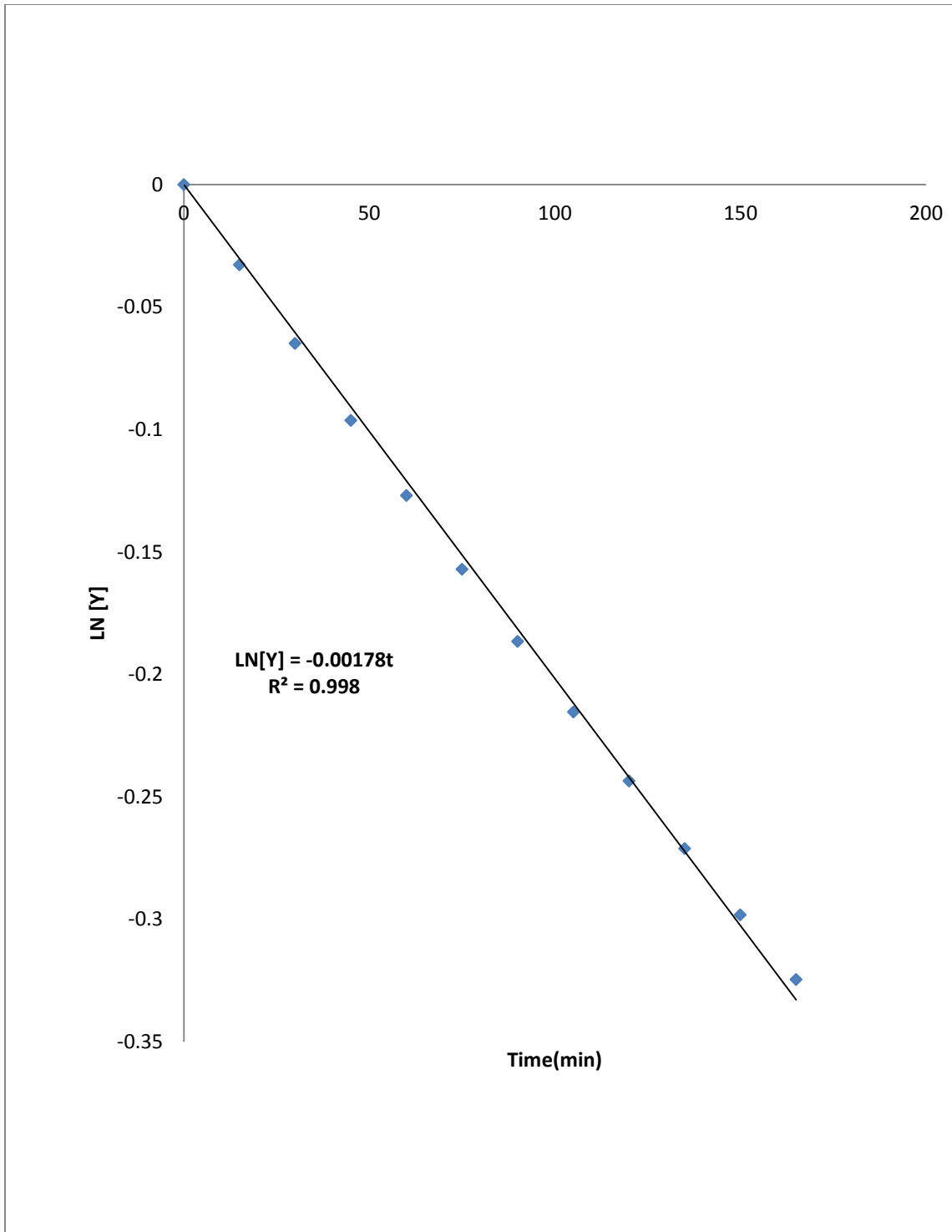


**Fig (3.8b): Regression line using equation (3.10) and the data in figure (3.8a). The slope of the line is related to the heat transfer coefficient of the system (vessel and content)**

Table (3.1): Summary of measured  $(UA/mC_p)_{system}$  taken from figures (3.6)-(3.8)

Mass of water(g)	Initial Temperature(K) ( $T_o$ )	Final Temperature(K) ( $T_s$ )	$(UA/mC_p)_{system}$ ( $min^{-1}$ )
200	343.08	292.13	0.00215
300	347.77	293.00	0.00189
400	347.84	293.38	0.00178

From table (3.1) and using equation 3.11, a plot of mass of water against  $(mC_p/UA)_{system}$  is shown in figure(3.9) below. From this we determined that  $(C_p/UA)_{water} = 0.468min/g$  while the Y-intercept is  $(mC_p/UA)_{system}$  is 372.74min. Knowing this allows us to determine the value of  $(UA/mC_p)_{system}$  for varying amounts of liquid in the flask.

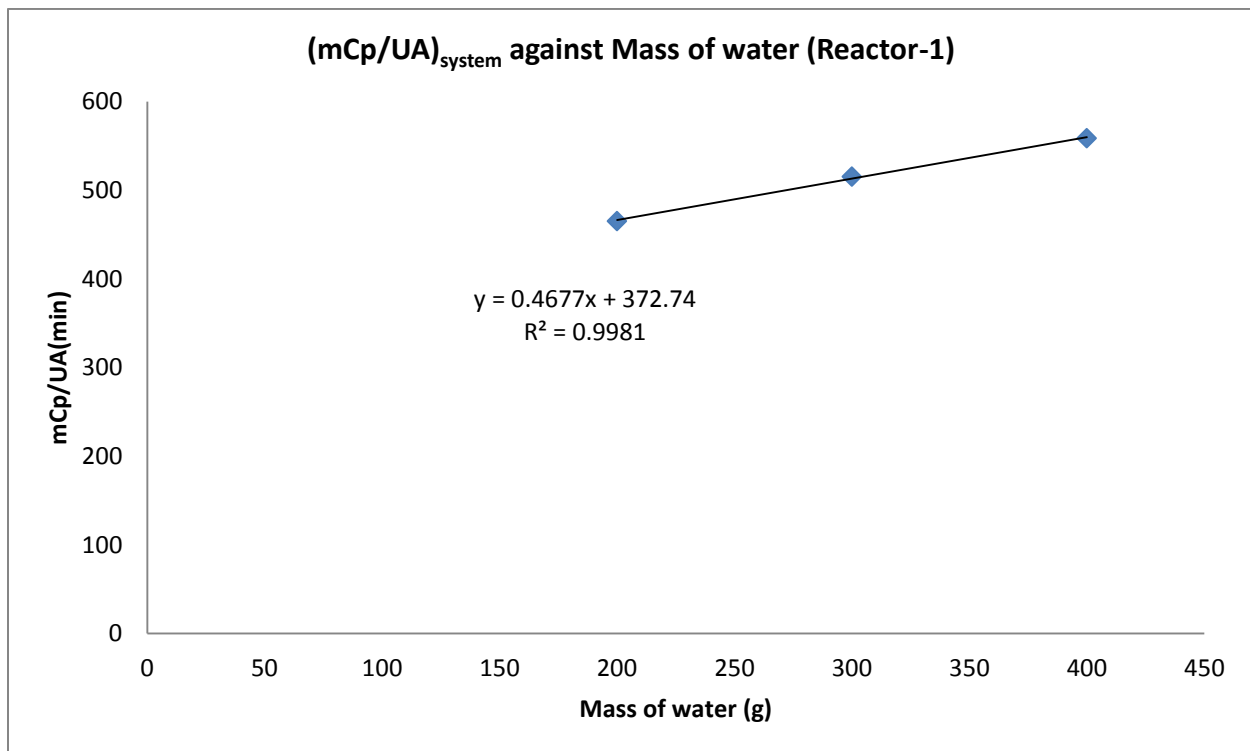


**Fig (3.9): A plot of mass of water against  $(mC_p/UA)_{system}$  based on equation 3.11. The intercept is  $(mC_p/UA)_{system}$  while the slope is  $(C_p/UA)_{water}$**

### **3.2.7 THE BLOCK DIAGRAM OF THE EXPERIMENTAL SET -UP**

The experimental set-up is shown in the block diagram of figure (3.10) below. The experimental set-up consists of the thermos-flask which was used as the reaction vessel and which was made up from 18/8 stainless steel and had a total volume of 500ml and which was stirred using a removable magnetic stirrer. The flask is provided with a negative temperature coefficient (NTC) thermistor connected on-line with a data-logging system. The signal from the sensor (thermistor) is sent to a measuring and a control unit amplifier and a power interface. The acquisition units are connected to a data processor. A process control engineering support was used for data management. The data acquisition system, Clarity has the following component: C50 Clarity Chromatography SW, single instrument, 3 x 55 Clarity Add-on instrument SW, 194 (INT9 quad channel A/D converter card). The hardware is INT9 PCI A/D 24 bit converter.

The properties of the equipment are: Input signal range 100mV -10V. Acquisition frequency 10 - 100Hz, Internal A/D converter ( INT9-1 to 4 channel PCI A/D converter). All physically available analog inputs and outputs as well as virtual channel are all automatically monitored and the process values are stored.

The process values were transmitted in such a way that the computer screen displays profiles of voltage versus time curves. Data acquisition software was used to convert the compressed data form of the history file on the hard disk into text file format. The text files were converted to excel spreadsheet and the data were then transported into Matlab 2010a for analysis.

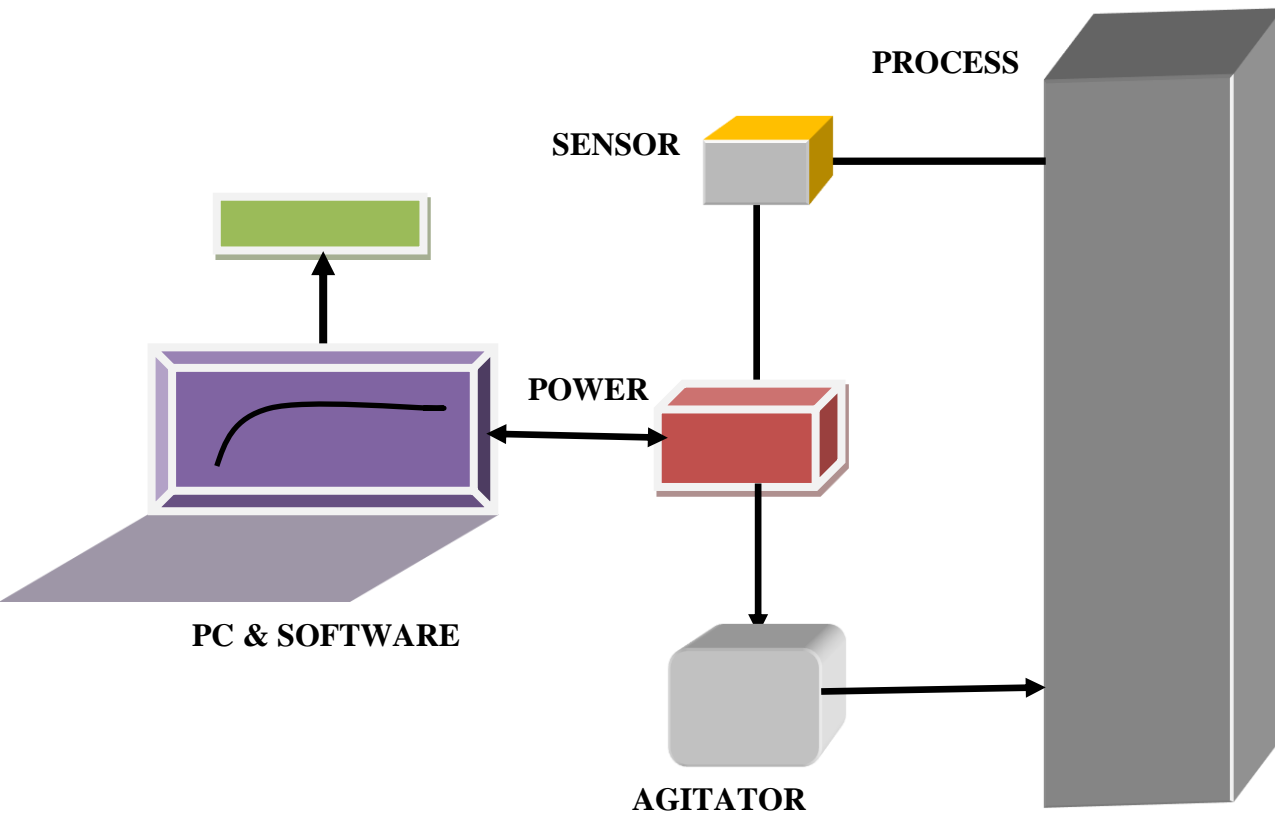


**Figure (3.10): Block diagram of experimental set-up**

### **3.3 EXPERIMENTAL RESULTS**

This section describes various reactions studied. The reactions include:

- ❖ Esterification processes
  - Acetic acid-Ethanol reactions
  - Acetic acid-Propanol reactions
  - Acetic anhydride-methanol reactions
- ❖ Hydrolysis processes
  - Acetic anhydride- Excess water reactions
  - Excess acetic anhydride-Water reactions

The various experimental conditions are described, the results of the measured temperature versus time during the reactions are given using various initial conditions.

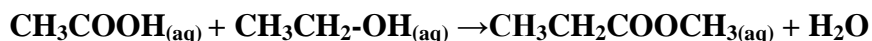
#### **3.3.1 ESTERIFICATION REACTIONS**

The esterification reactions considered includes the following:

- Acetic Acid-Ethanol Reactions
- Acetic Acid-Propanol Reactions
- Acetic Anhydride-Methanol Reactions

##### **3.3.1.1. ACETIC ACID –ETHANOL REACTIONS**

This liquid phase esterification reaction is described by:



$$\Delta H_{\text{rxn}}(298\text{K}) = -6.12\text{kJ/mol}$$

##### **3.3.1.2 EXPERIMENTAL DESCRIPTIONS**

Analytical reagent grade acetic acid was used in all the experiments. In all experiments about 1.0 mol of acetic acid was poured into the reaction vessel followed by 1.0mol of the ethanol. 10ml of concentrated sulphuric acid was added to the reactant mixture as a catalyst to initiate the reaction.

These volumes were used so that at least 60% of the length of the sensor (thermistor) would be submerged in the resulting mixture. In course of the reaction the stirrer speed was set at 1000rev/min and the resulting voltage-time profiles were captured as described above and the corresponding temperature-time curve was determined using the thermistor equation derive in equation (3.8) above. Runs were carried at the following initial temperatures: 283K, 288K and 296K. The measured temperature-time profiles of the above experiments are shown in figures (3.11),(3.12) and (3.13) below.

### **3.3.1.3 EXPERIMENTAL RESULTS**

The results of the above described hydrolysis experiment is presented graphically below. The experimental data points which were used are presented in the appendices (D1,D2,D3) on the attached CD Rom.

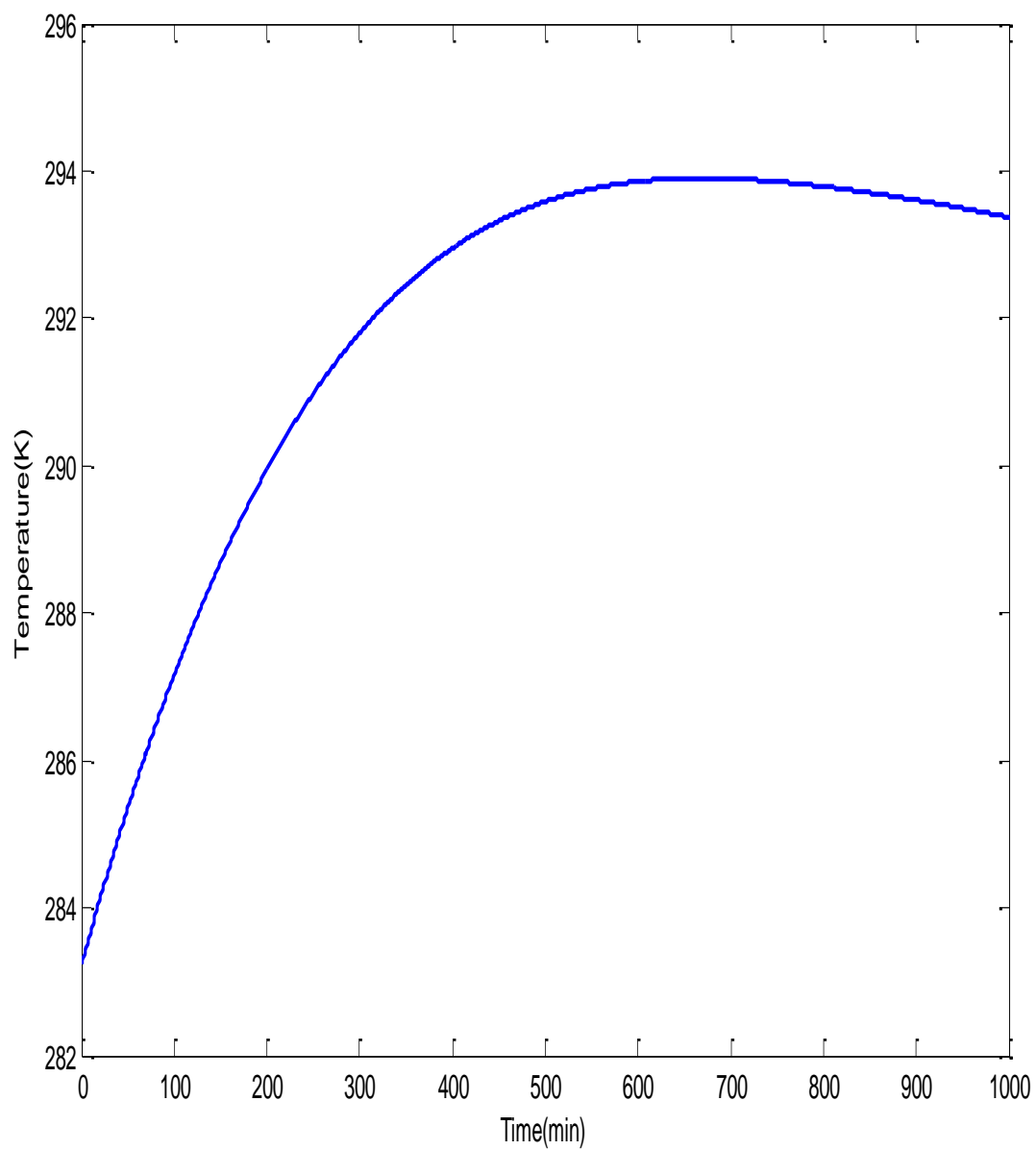


**Figure (3.11): Acetic Acid-Ethanol Reaction: Measured temperature-time profile at initial temperature of 283K**

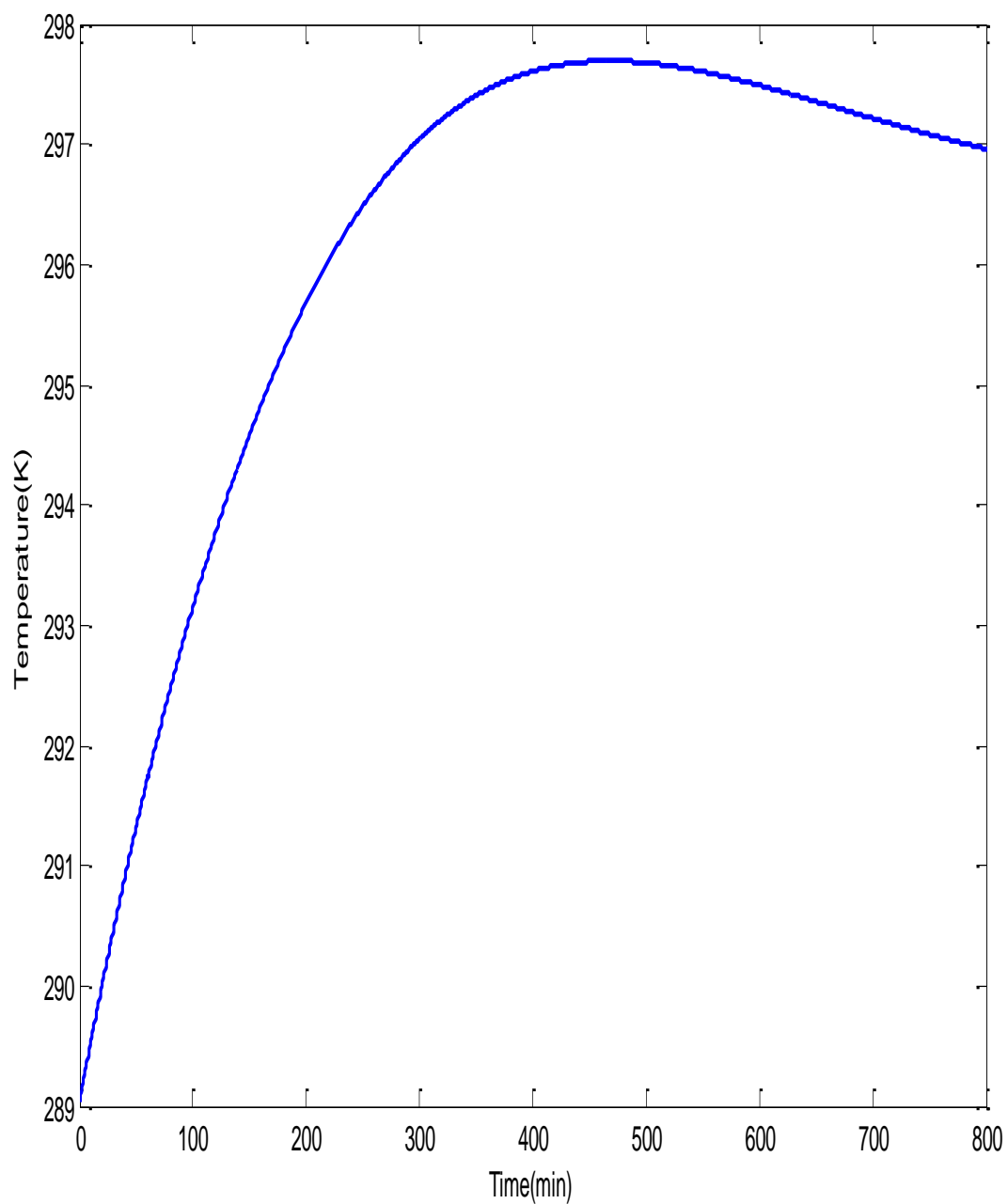


**Figure (3.12): Acetic Acid-Ethanol Reaction: Measured temperature-time profile at initial temperature of 289K**

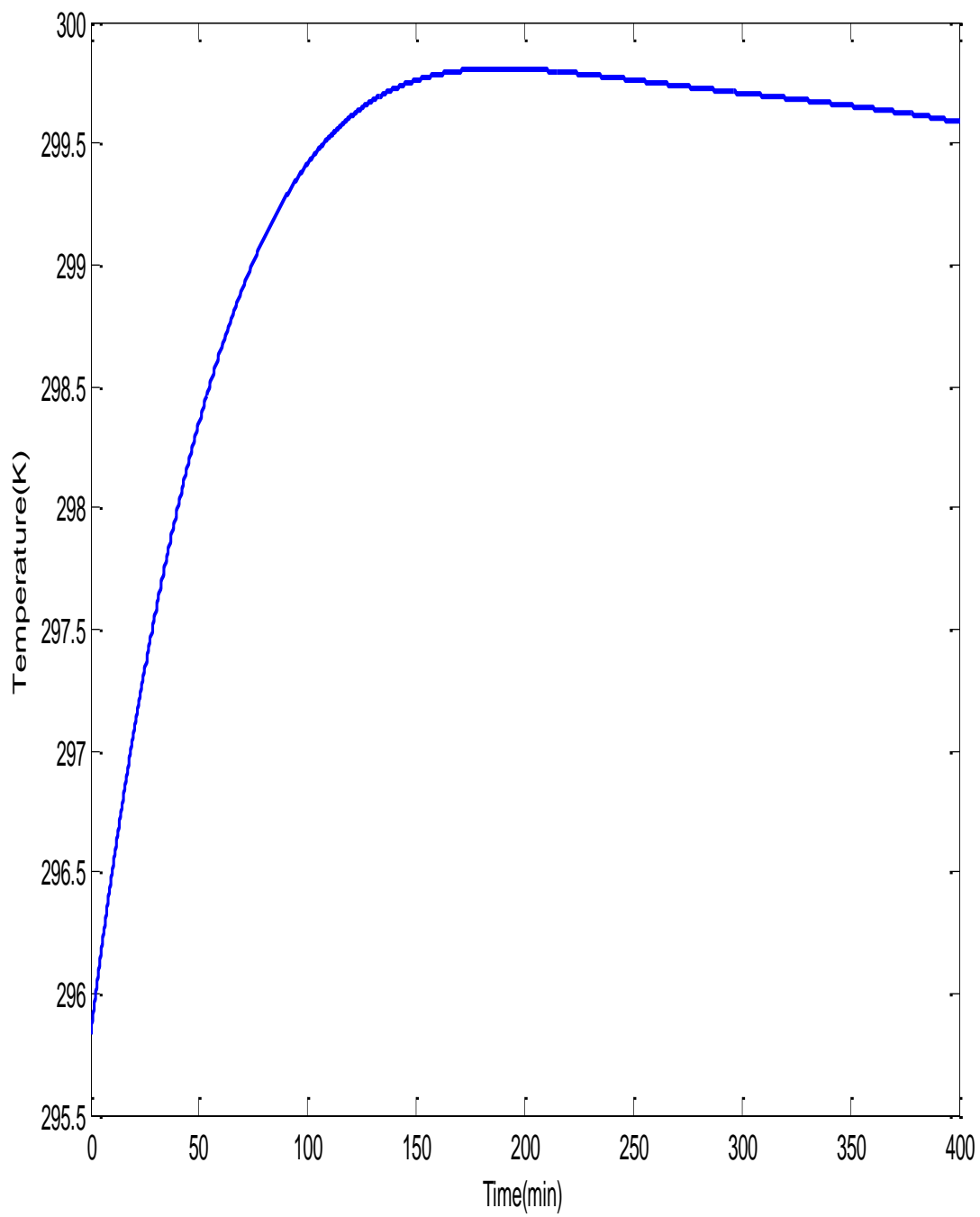
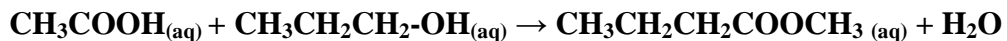


**Figure (3.13): Acetic Acid-Ethanol Reaction: Measured temperature-time profile at initial temperature of 295.8K**

### **3.3.2 ACETIC ACID –PROPANOL REACTIONS**

This liquid phase esterification reaction of acetic acid and propanol is described by:



$$\Delta H_{\text{rxn}}(298\text{K}) = -30.24\text{kJ/mol}$$

#### **3.3.2.1 EXPERIMENTAL DESCRIPTIONS**

Analytical reagent grade acetic acid was used in all the experiments. In all experiments about 1.0 mol of acetic acid was poured into the reaction vessel followed by 1.0mol of the propanol. 10ml of concentration sulphuric acid was added to the reactant mixture as a catalyst to initiate the reaction. These volumes were used so that at least 60% of the length of the sensor (thermistor) would be submerged in the resulting mixture. In course of the reaction the stirrer speed was set at 1000 rev/ min and the resulting voltage-time profiles were captured as described above and the corresponding temperature-time curve was determined using the thermistor equation derive in equation (3.8) above. Runs were carried out at the following initial temperatures: 285K, 290K and 298K. The temperature-time profiles of the above experiments are shown in figures (3.14),(3.15) and (3.16) below.

### 3.3.2.1 EXPERIMENTAL RESULTS

The results of the above described esterification experiment are presented graphically below. The experimental data points which were used are presented in the appendices (E1,E2,E3) on the attached CD Rom.

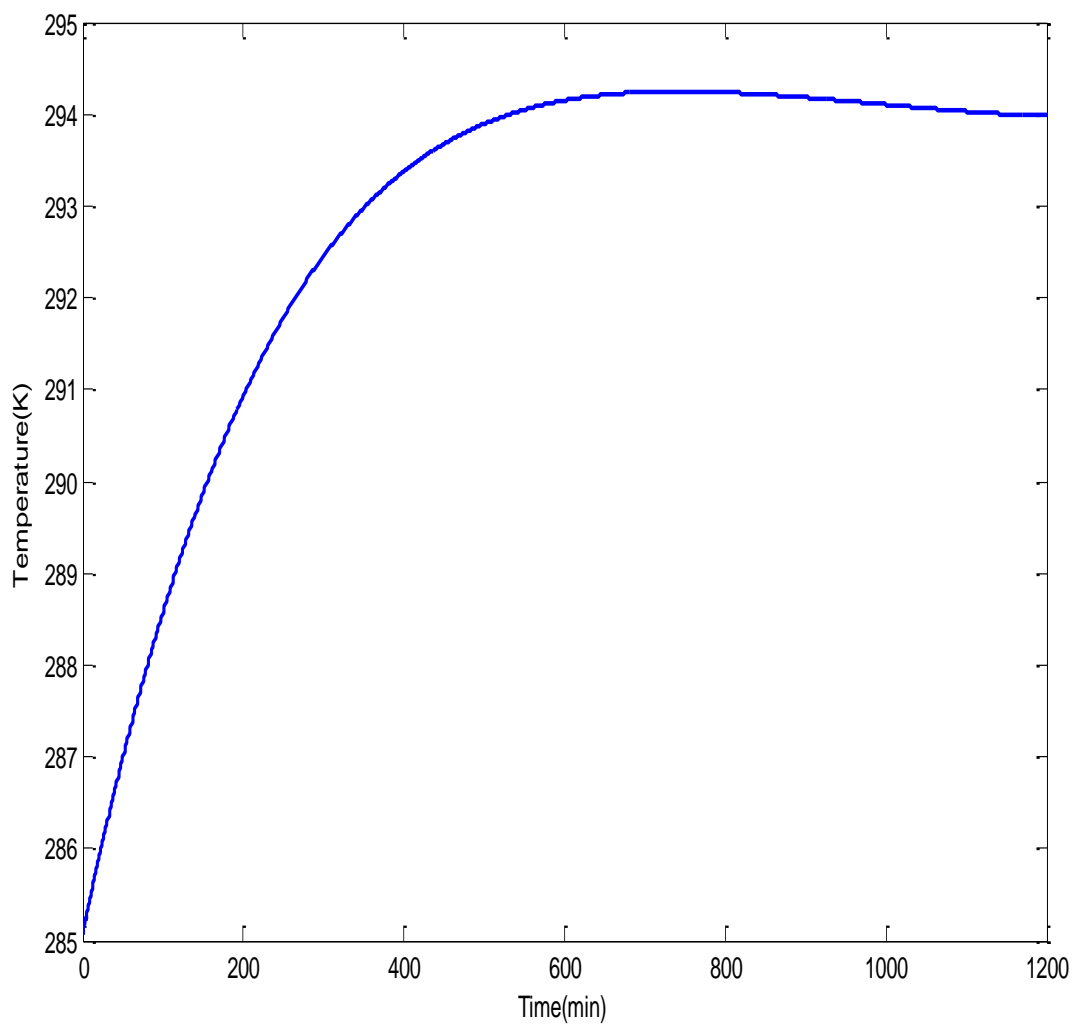


**Figure (3.14): Acetic Acid-Propanol Reaction: Measured temperature-time profile for an initial temperature of 285.1K**

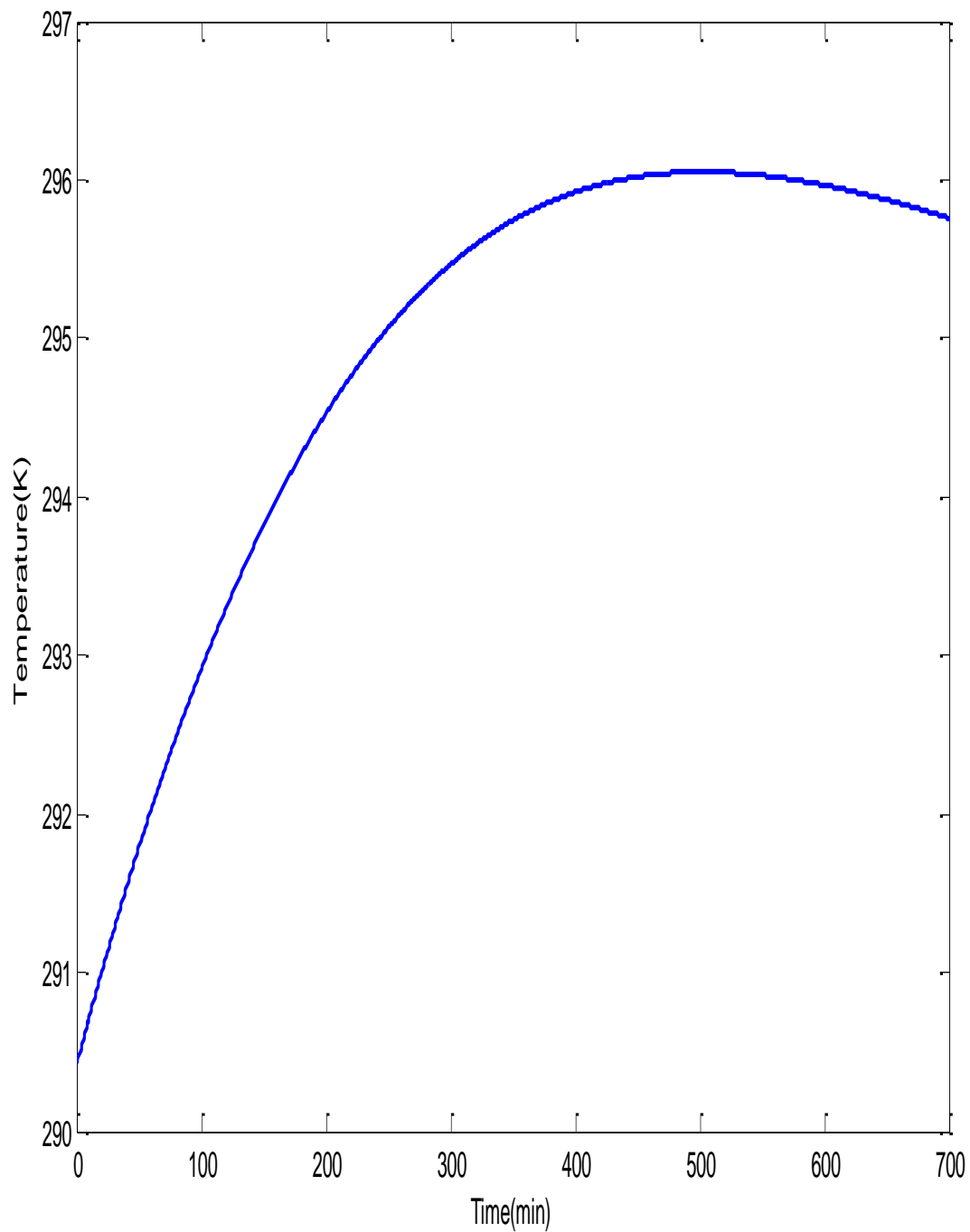


**Figure (3.15): Acetic Acid-Propanol Reaction: Measured temperature-time profile for an initial temperature of 290.4K**

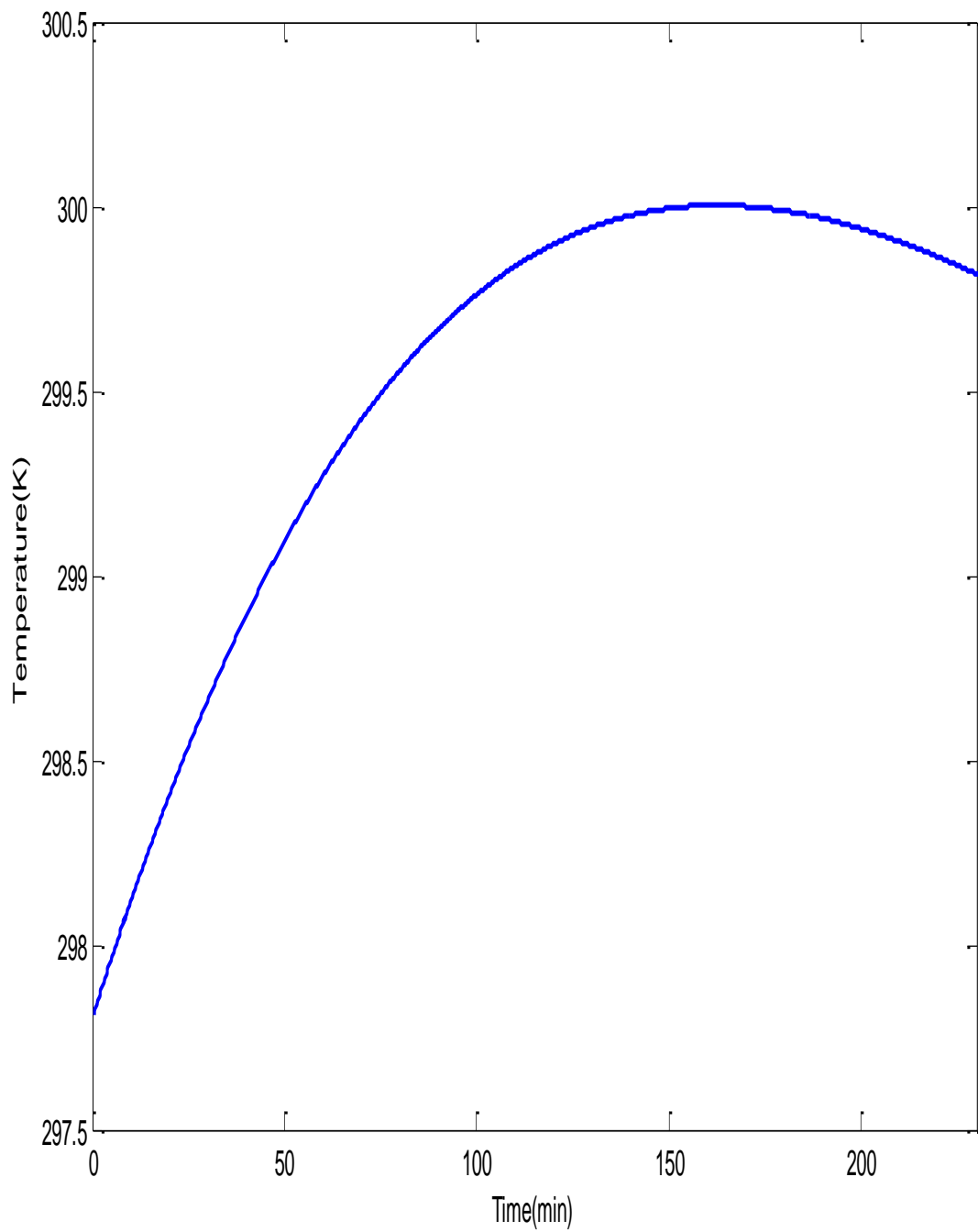
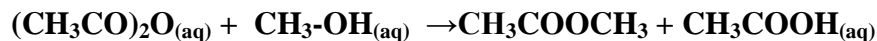


**Figure (3.16): Acetic Acid-Propanol Reaction: Measured temperature-time profile for an initial temperature of 297.8K**

### **3.3.3 ACETIC ANHYDRIDE –METHANOL REACTIONS**

This liquid phase esterification reaction between acetic anhydride and methanol is described by:



$$\Delta H_{\text{rxn}}(298\text{K}) = -66.00\text{kJ/mol}$$

#### **3.3.3.1 EXPERIMENTAL DESCRIPTIONS**

Analytical reagent grade acetic anhydride was used in all the experiments. In all experiments about 1.0 mol of acetic anhydride was poured into the reaction vessel followed by 3.0 mols of the methanol. Note that an excess of methanol is used in this case. In course of the reaction the stirrer speed was set at 1000rev/ min and the resulting voltage-time profiles were captured as described above and the corresponding temperature-time curve was determined using the thermistor equation derive in equation (3.8) above. Runs were carried out adiabatically at the following initial temperatures: 290K, 294K and 300K. The temperature-time profiles of the above experiments are shown in figures (3.17),(3.18) and (3.19) below.

### 3.3.3.2 EXPERIMENTAL RESULTS

Results of the esterification reaction between acetic anhydride and methanol are presented graphically below. The experimental data points which were used are presented in the appendices (F1,F2,F3) on the attached CD Rom.

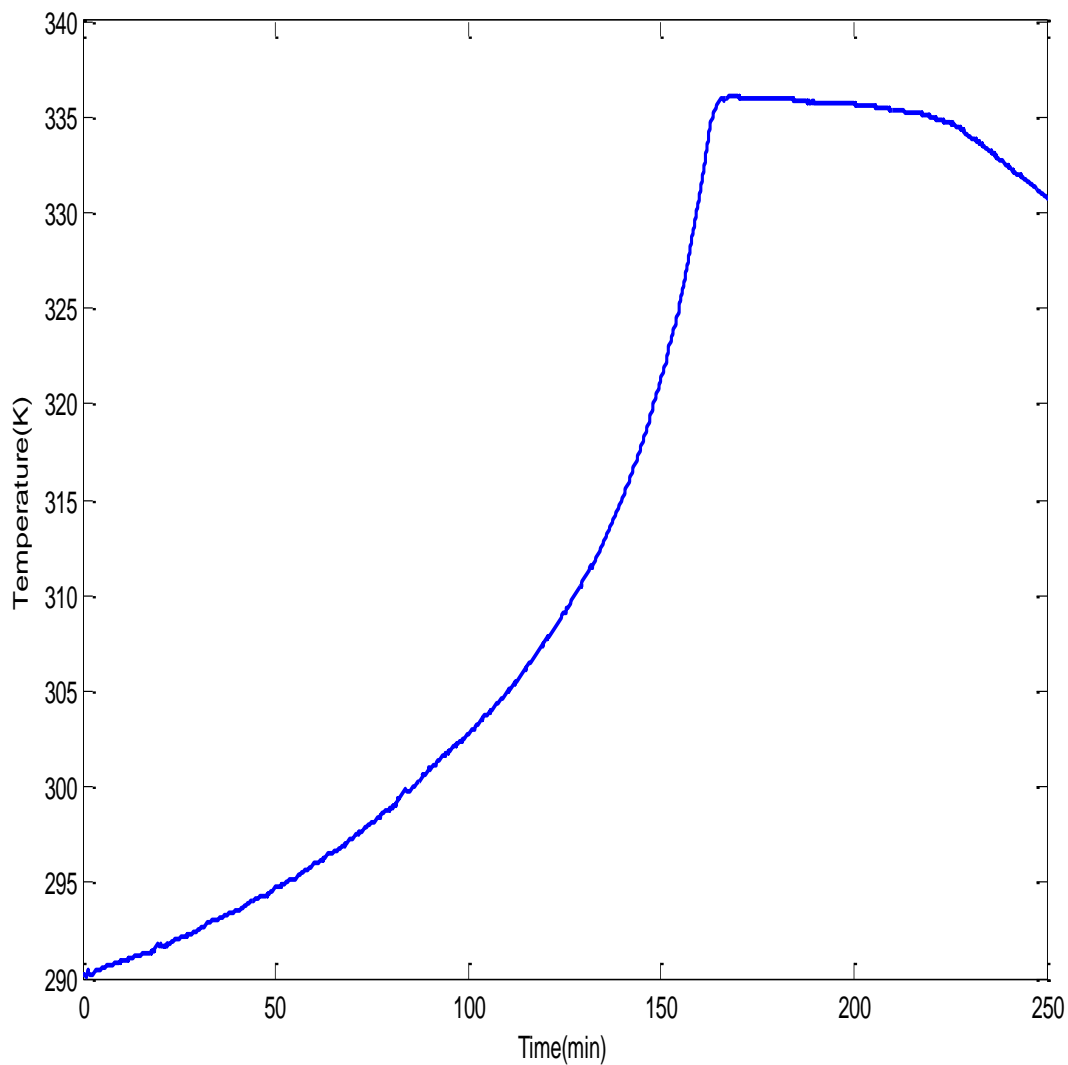


**Figure (3.17): Acetic Anhydride-methanol Reaction: Measured temperature-time profile for an initial temperature of 290K**

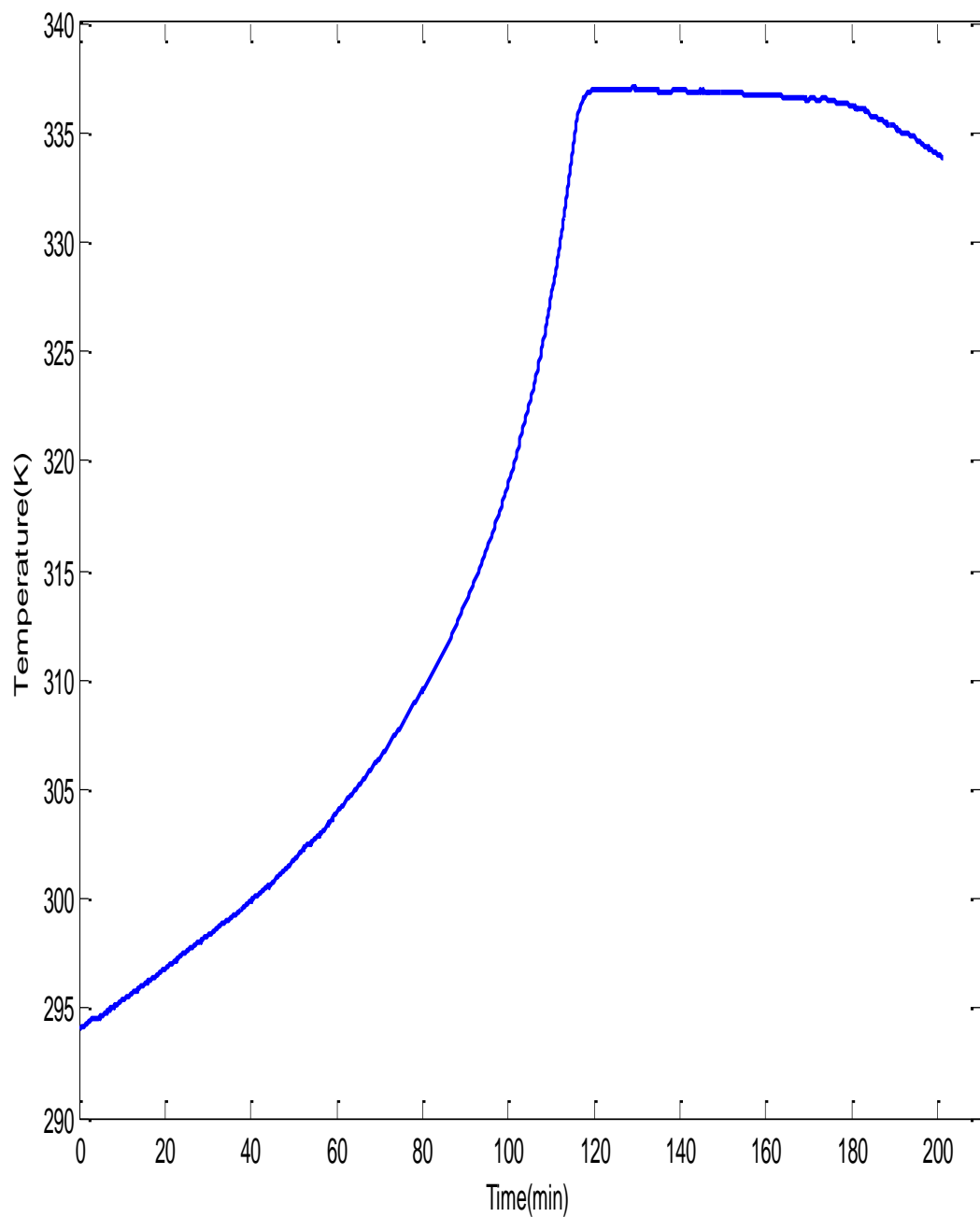


**Figure (3.18): Acetic Anhydride-methanol Reaction: Measured temperature-time profile for an initial temperature of 294K**

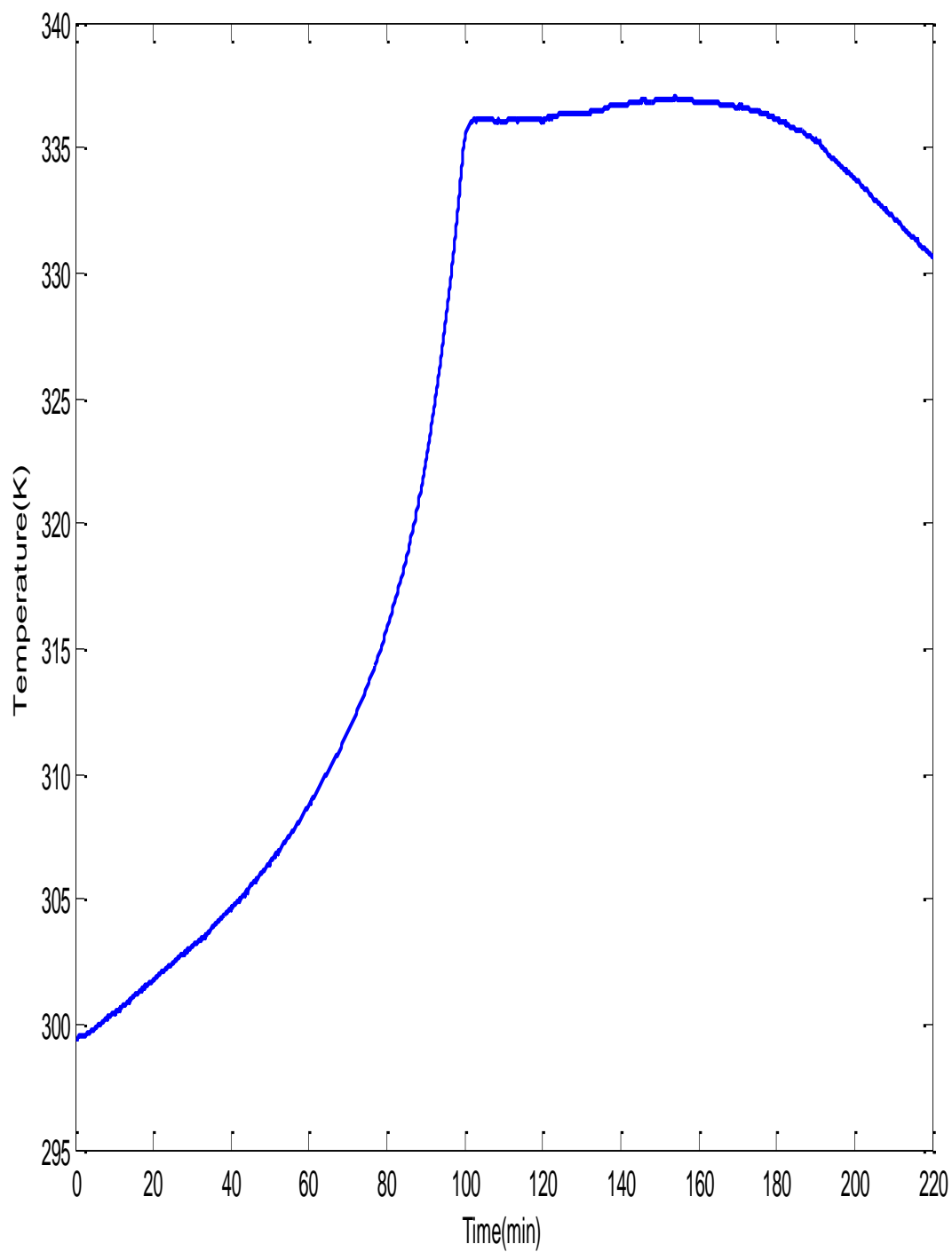


**Figure (3.19): Acetic Anhydride-Methanol Reaction: Measured temperature-time profile for an initial temperature of 299K**

### **3.3.4 HYDROLYSIS REACTIONS**

#### **THE FOLLOWING HYDROLYSIS REACTIONS WERE STUDIED**

- Acetic anhydride-water reactions using an excess of water
- Acetic anhydride-water reactions using an excess of acetic anhydride

#### **3.3.4.1 THE ACETIC ANHYDRIDE – WATER REACTION**

The stoichiometry of the reaction may be written as:



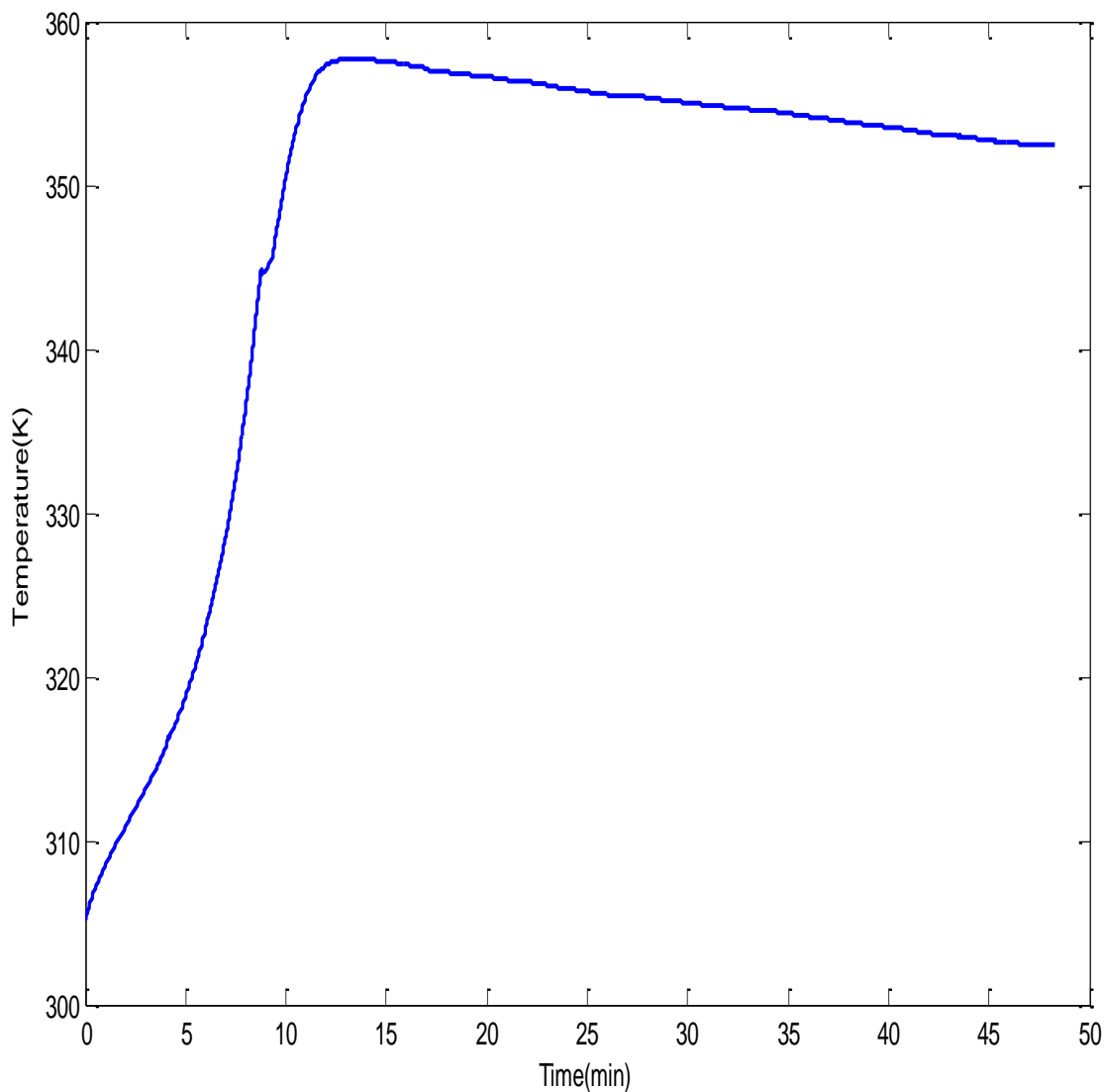
The first set of these experiments were run with excess water while the second set of reactions used excess acetic anhydride.

#### **3.3.4.2 EXPERIMENTAL DESCRIPTION**

Analytical reagent grade acetic anhydride was used in all the experiments and the water used was double distilled. In the first set of experiments (excess water) 1.0 mol of acetic anhydride was poured into the reaction vessel followed by 10.0 mols of the double distilled water. Note that there were 9 moles of water in excess in this experiment. Runs were carried out at the following initial temperatures: 305K, 310K and 328K. In the second set of experiments (excess acetic anhydride) 2.65 mols of acetic anhydride was poured into the reaction vessel followed by 0.55 mols of double distilled . In this case 2.1 mols of excess acetic anhydride were used. Runs were carried out at the following initial temperatures: 286K, 294K and 305K. In course of the reaction the stirrer speed was set at 1000rev/ min and the resulting voltage-time profiles were captured as described above and the corresponding temperature-time curve was determined using the thermistor equation derive in equation (3.8) above. The temperature-time profiles of the experiments with excess water are shown in figures are shown in figures (3.20),(3.21) and (3.22), whiles those using excess acetic anhydride are shown in figures (3.23), (3.24) and (3.25) below.

#### **3.3.4.3 EXPERIMENTAL RESULTS**

The results of the above described hydrolysis experiment is presented graphically below. The experimental data points which were used are presented in the appendix (G1,G2,G3 for excess water reactions and H1,H2 and H3 for excess anhydride reactions) on the attached CD Rom.



**Figure(3.20):Aceticanhydride-water reaction (excess water):Measured temperature-time profile for an initial temperature of 305K**

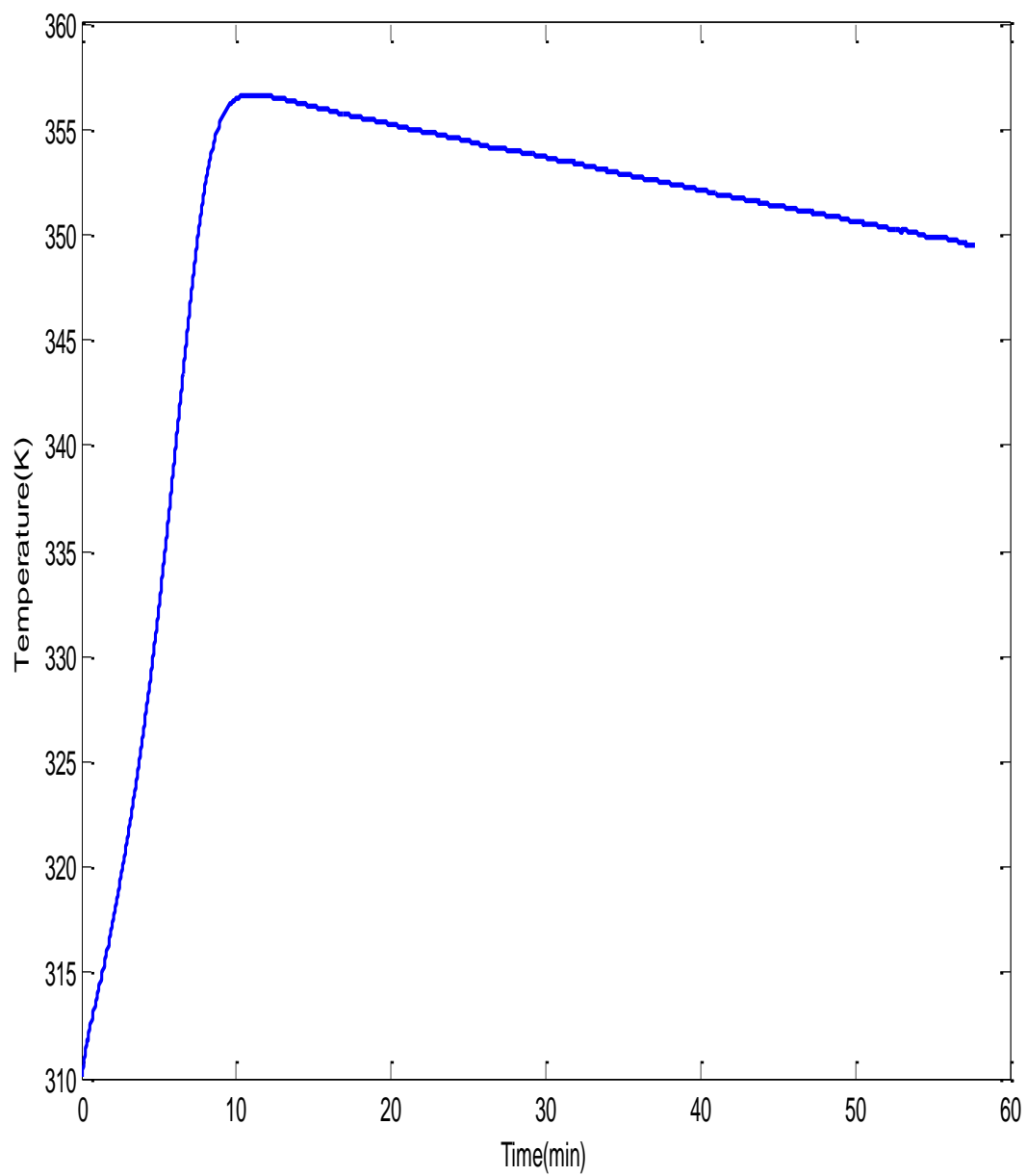


**Figure (3.21): Acetic anhydride-water reaction (excess water): Measured temperature-time profile for an initial temperature of 310K**

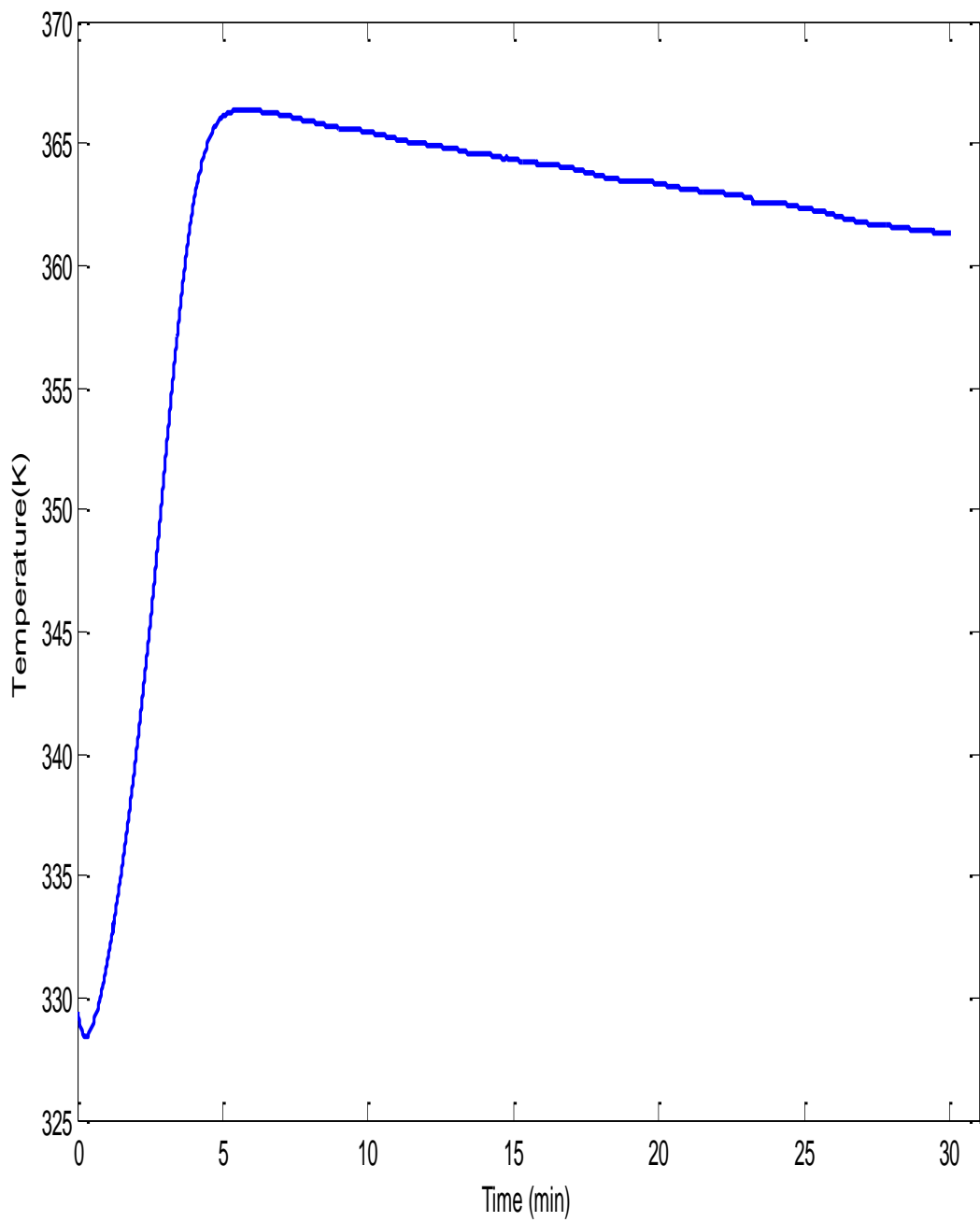


**Figure (3.22): Acetic anhydride-water reaction (excess water): Measured temperature-time profile for an initial temperature of 329K**

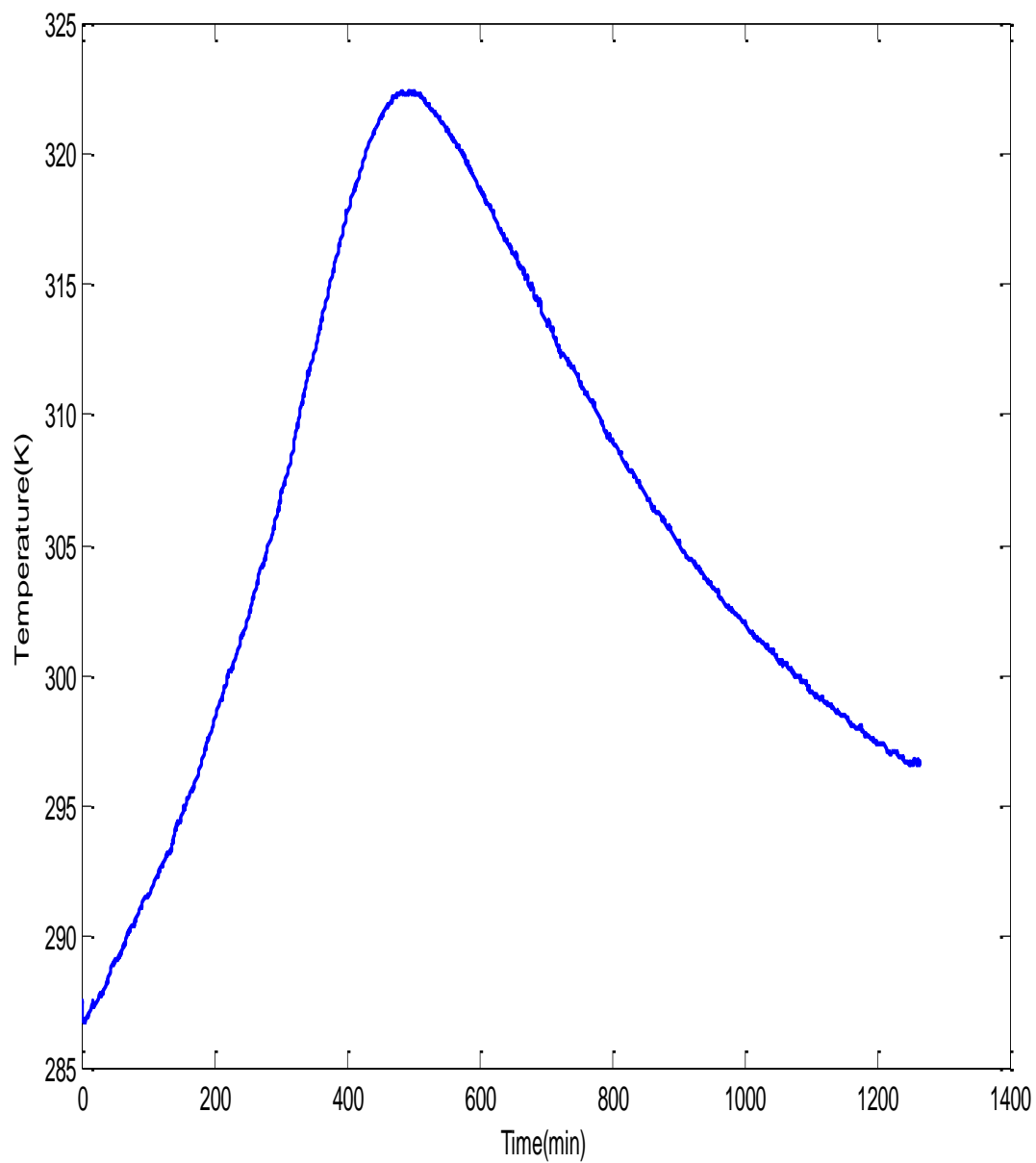


**Figure (3.23): Acetic anhydride-water reaction (excess anhydride): Measured temperature-time profile for an initial temperature of 287K**

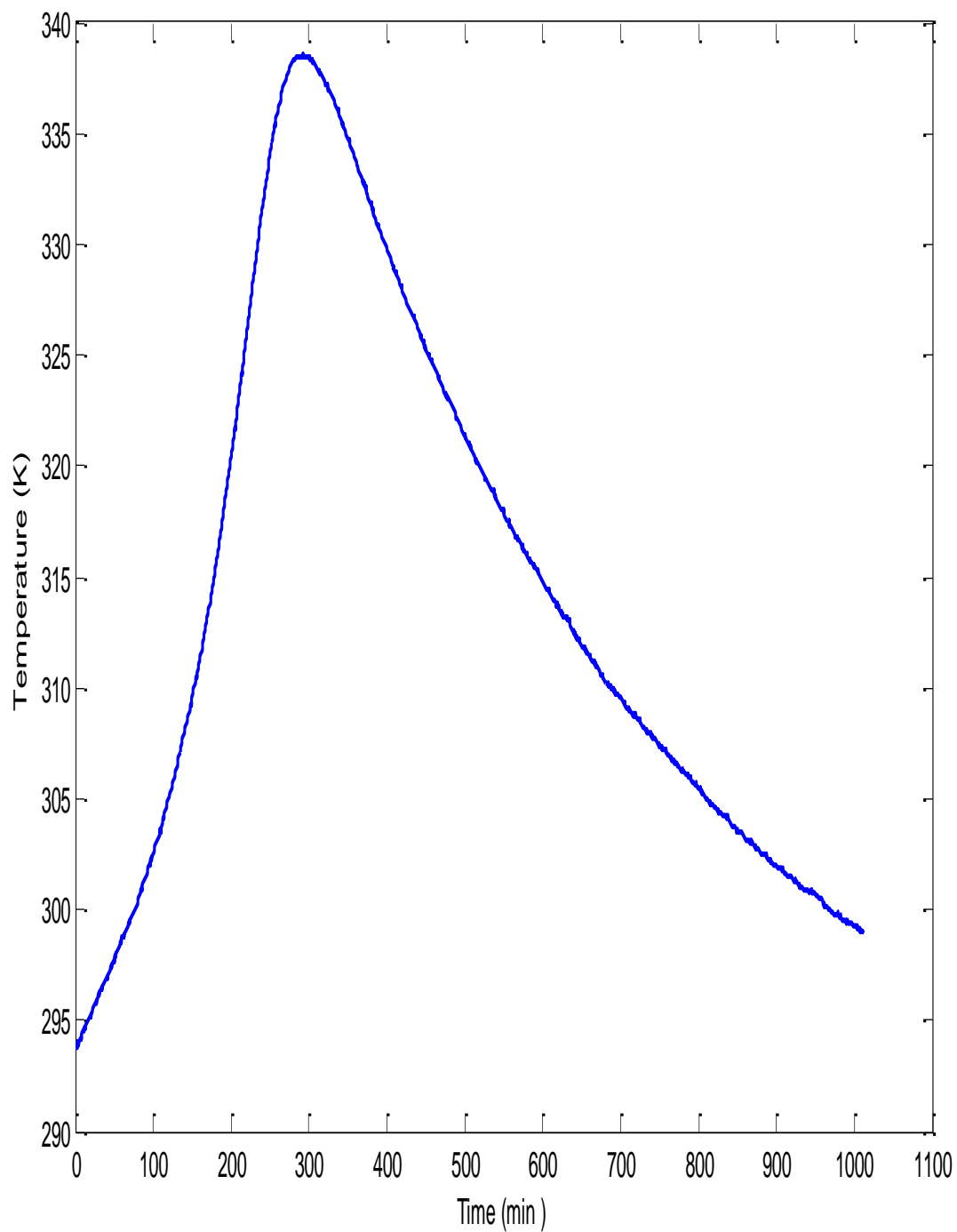


**Figure (3.24): Acetic anhydride-water reaction (excess anhydride): Measured temperature-time profile for an initial temperature of 294K**

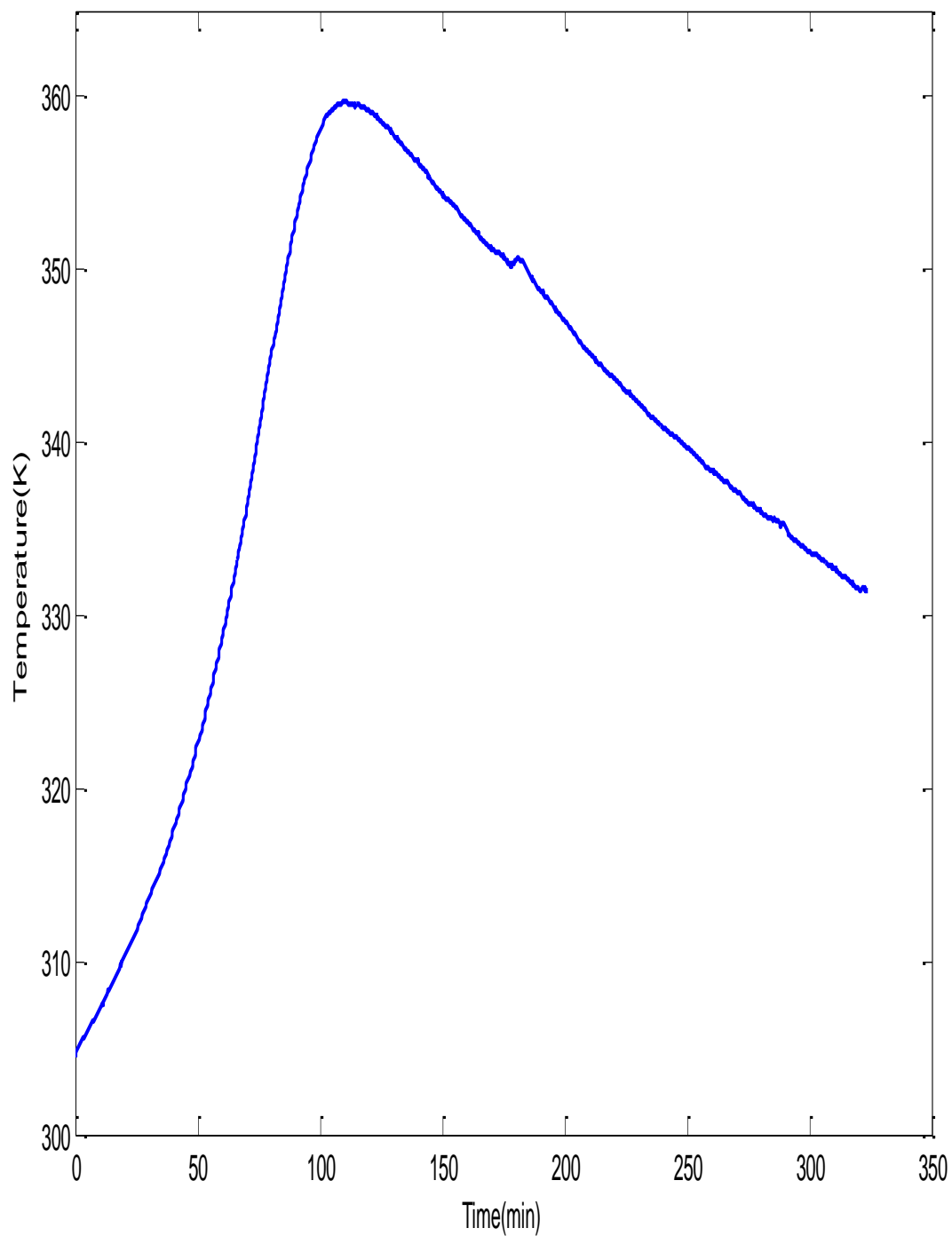


**Figure (3.25): Acetic anhydride-water reaction (excess anhydride): Measured temperature-time profile for an initial temperature of 305K**

### **3. 4 DISCUSSION OF RESULTS**

The cooling experiments show the cooling model fits accurately and it is not surprising. The simple model used to relate the measured heat transfer coefficient for the system, the contents of the flask and the flask also fits very well, allowing us to have confidence when estimating the heat transfer coefficient of the system with different amounts of liquid in the flask.

The drop in temperature as shown in the profile of Acetic anhydride-water reaction (excess water), with initial temperature of 329K in figure 3.22, is as a result of heat of mixing a cooler feed material with a heated contents of the vacuum flask. As the reactants was added very quickly and this mixing was very rapid, the initial temperature could be taken after the drop.

We have measured how the temperature of the contents of the flask changes with time for different reactions and different initial temperature. The reactions chosen cover a range of heats from -6.12kJ/mol for esterification of acetic acid and ethanol, to -66kJ/mol for the reaction between acetic anhydride and ethanol.

We find that the shape of the temperature-time curve changes with initial temperature with the maximum measured temperature increasing with increasing initial temperature, but with curvatures becoming sharper for higher temperatures and larger heats of reaction.

The shapes of the curves for the hydrolysis reactions with either water or acid anhydride in excess are very different.

The analysis of this data is the subject of the next three chapters.

### **3.5 LIST OF SYMBOLS**

A –surface area ( $m^2$ )

B,C – thermistor constants

$C_p$  –specific heat capacity(J/gk)

$\Delta H_{rxn}(298K)$  – Heat of reaction at 298K (J/mol)

$I_{total}$  – current flowing through the thermistor (Amps)

m –mass(g)

R – Reference resistance (ohms)

$R_{TH}$  – Resistance of thermistor (ohms)

t – Time(minutes)

T – temperature (Kelvin)

$T_o$  –initial temperature

$T_s$  –steady-state temperature

U –heat transfer coefficient ( $W/m^2.K$ )

$V_{out}$  – voltage measured in the electrical circuit containing thermistor (Volts)

$V_{TH}$  – voltage across thermistor (Volts)

#### **Subscripts**

System-refers to flask and content

Water-refers to water or contents of flask

Vessel-refers to the empty flask

## CHAPTER FOUR

*THIS PAPER HAS BEEN PUBLISHED BY THE INDUSTRIAL & ENGINEERING CHEMISTRY RESEARCH JUNE 2013 52 (23) pp 7630 -7639.*

### ESTIMATING THERMODYNAMIC AND EQUILIBRIUM INFORMATION OF ESTERIFICATION PROCESSES USING TEMPERATURE AS A MEASURED VARIABLE IN A THERMOS-FLASK

*N.Asiedu\**, *D.Hildebrandt\**, *D.Glasser\**

Centre of Material and Process Synthesis, School of Chemical and Metallurgical Engineering, University of Witwatersrand, Private mail Bag X3, Wits 2050, Johannesburg, South Africa.

\*Authors to whom correspondence may be addressed:

Emails : [nasiedusoe@yahoo.co.uk](mailto:nasiedusoe@yahoo.co.uk)

: [Diane.Hildebrandt@wits.ac.za](mailto:Diane.Hildebrandt@wits.ac.za)

: [David.Glasser@wits.ac.za](mailto:David.Glasser@wits.ac.za)

#### ABSTRACT

It is sometimes difficult to obtain physically meaningful parameters from experimental data for a chemical system when the mathematical model describing the system involves nonlinear functions. A simple method has been developed for the prediction of heat of reaction and equilibrium constants from experimental temperature-time data of exothermic reversible processes in adiabatic conditions. The success of this new technique is demonstrated by predicting the heat of reaction and equilibrium constant as a function of temperature for ethanol-acetic acid and propanol-acetic acid systems at temperatures between 283K-295K and 285K-297 respectively. This technique may be useful in the estimation of heat of reactions and equilibrium constants for exothermic reversible processes at higher temperatures.

**Keywords:** Heat of reaction, Equilibrium constant, Temperature, Adiabatic batchreactor

## 4.1 INTRODUCTION

The temperature-time history of a chemical process is of great importance for chemist and chemical engineers as it provide a great deal information about the nature of the process. A lot of methods have been developed to extract kinetic and thermodynamic information of processes from temperature-time history. Some of the techniques used are temperature measurements from flow reactors, Bell et al (1952), Rand et al (1950), Hartridge et al (1925), Peltier cooling method, Becker et al (1965), differential thermal analysis, Borchartt et al (1957), Blumberg (1959). These techniques either requires complicated experimental procedures or the evaluation of the kinetic information are obtained from a limited number of data points on the temperature –time curve. Simple experimentation at the expense of fairly complex data analysis has been achieved by Becker et al (1967) using an analogue computer and Williams and Glasser (1971) using digital computer. Scott, Williams and Glasser (1974) developed an experimentally and computationally simple but accurate technique for obtaining kinetic and thermodynamic parameters from temperature-time curves. In this work, the experimental techniques developed by Williams and Glasser and Scott, Williams and Glasser were adopted for the study of the esterification processes, to estimate heat of reactions and equilibrium as a function of temperature using the dewer thermos –flask as an adiabatic batch reactor. This is a new technique for determining equilibrium information of equilibrium limited processes using the thermos-flask.

## 4.2 THEORITICAL DEVELOPMENTS

### 4.2.1 EQUILIBRIUM INFORMATION FROM THERMOS-FLASK

Consider the Gibbs –Helmholtz equation:

$$\frac{d}{dT} \left( \frac{\Delta G}{T} \right) = \frac{(-\Delta H_r)}{T} \quad (1)$$

$$\text{But } \frac{\Delta G}{T} = -RT K_{eq} \quad (2)$$

Plugging eq(2) into eq(1) gives eq(3) as :

$$\frac{d}{dT} (\ln K_{eq}) = \frac{(\Delta H_r)}{RT^2} \quad (3)$$

Assuming  $\Delta H_r$  is independent of temperature or only varies a small amount of some range of temperature (T), integrating eq(3) gives:

$$\ln K_{eq} = \frac{(-\Delta H_r)}{T} + C \quad (4)$$

Given  $T = T_0$  at  $K_{eq} = K_{eq}^0$ , one can write eq(4) as:

$$\ln K_{eq}^0 = \frac{(-\Delta H_r)}{T_0} + C \quad (5)$$

Combining eq(4) and (5), the constant of integration (C) can be eliminated to give eq(6) as:

$$\ln \left( \frac{K_{eq}}{K_{eq}^0} \right) = \frac{(-\Delta H_r)}{R} \left( \frac{1}{T_0} - \frac{1}{T} \right) \quad (6)$$

Equation (6) can be rewritten as:

$$K_{eq} = K_{eq}^0 \exp \left\{ \frac{(-\Delta H_r)}{R} \left( \frac{1}{T_0} - \frac{1}{T} \right) \right\} \quad (7)$$

#### 4.2.2 ENERGY BALANCE OF THE THERMOS –FLASK

For a constant –volume batch reactor one can write:

$$-r_A = \frac{1}{V} \frac{dN_A}{dt} = -\frac{dC_A}{dt} \quad (8)$$

The energy balance equation can be established as:

$$\text{Heat generated} = \text{Heat absorbed by reactor contents} + \text{Heat transferred through reactor walls} \quad (9)$$

Eq(9) can be written as follows:

$$H = H_0 + (-\Delta H_r) x + UA \int_0^\infty (T - T_0) dt + mC_p (T - T_0) \quad (10)$$

$$\text{At } T_0, H_0 = mC_p (T - T_0) \quad (11)$$

Combining eq(10) and eq(11) one can write the total energy balance equation as follows:

$$mC_p (T - T_0) + mC_p (T - T_0) + UA \int_0^\infty (T - T_0) dt + (-\Delta H_r) x = 0 \quad (12)$$

Simplifying eq(12) gives eq(13):

$$mC_p (T - T_0) + UA \int_0^\infty (T - T_0) dt + (-\Delta H_r) x = 0 \quad (13)$$

Consider the esterification process given below:



For equimolar reactants we can write the equilibrium expression for eq(14) as follows:

$$K_{eq} = \frac{x^2}{(1-x)^2} \quad \text{or} \quad x = \frac{\sqrt{K_{eq}}}{1 + \sqrt{K_{eq}}} \quad (15)$$

Combining eq(7) and eq(15), x can be eliminated from eq(13) to give eq(16) below:

$$\frac{(-\Delta H_r) \cdot \sqrt{K_{eq}^0} \cdot \exp\left\{\frac{(-\Delta H_r)}{2R} \left(\frac{1}{T_0} - \frac{1}{T}\right)\right\}}{1 + \sqrt{K_{eq}^0} \cdot \exp\left\{\frac{(-\Delta H_r)}{2R} \left(\frac{1}{T_0} - \frac{1}{T}\right)\right\}} + mC_p (T - T_o) + UA \int_0^\infty (T - T_o) dt = 0 \quad (16)$$

$$\text{Let } (T - T_o) + \frac{UA}{mC_p} \int_0^\infty (T - T_o) dt = \alpha \text{ and } \frac{1}{2R} \left(\frac{1}{T_0} - \frac{1}{T}\right) = \beta \quad (17)$$

Eq(16) can be simplified as :

$$\frac{(-\Delta H_r) \cdot \sqrt{K_{eq}^0} \cdot \exp((-\Delta H_r)\beta)}{1 + \sqrt{K_{eq}^0} \cdot \exp(-\Delta H_r)} + mC_p \alpha = 0 \quad (18)$$

Equation (18) have 2 unknown quantities  $\Delta H_r$  and  $K_{eq}^0$  . If one can determine  $\alpha$  and  $\beta$ , from experiment then the 2 unknown quantities can be determined for the process and eq(7) can be establish for the esterification process.

### 4.3 THE EXPERIMENTAL SET-UP

The experimental set- up consist of adiabatic batch reactor (thermos-flask) made up of 18/8 stainless steel thermos-flask of total volume of 500mL equipped with a removable magnetic stirrer as shown in figure (4.1) The flask is provided with a negative temperature coefficient thermistor connected on-line with a data-logging system. The signal from the sensor (thermistor) is fed to a measuring and a control unit amplifier and a power interface. The acquisition units are connected to a data processor. A process control engineering support data management. The data acquisition system called Clarity has the following part numbers: C50 Clarity Chromatography SW, single instrument, 3 x 55 Clarity Add-on instrument SW, 194 (INT9 quad channel A/D converter card). The hardware is INT9 PCI A/D 24 bit converter. The properties: Input signal range 100mV -10V. Acquisition frequency 10 -100Hz, Internal A/D converter ( INT9-1 to 4 channel PCI A/D converter).

All physically available analog inputs and outputs as well as virtual channel are all automatically monitored and the process values are stored. The process values are transmitted in such a way that the computer screen displays profiles of voltage-time curves. Data acquisition software was used to convert the compressed data form of the history file on the hard disk into text file format. The text files are converted to excel spreadsheet and the data are then transported into matlab 2010a for analysis.

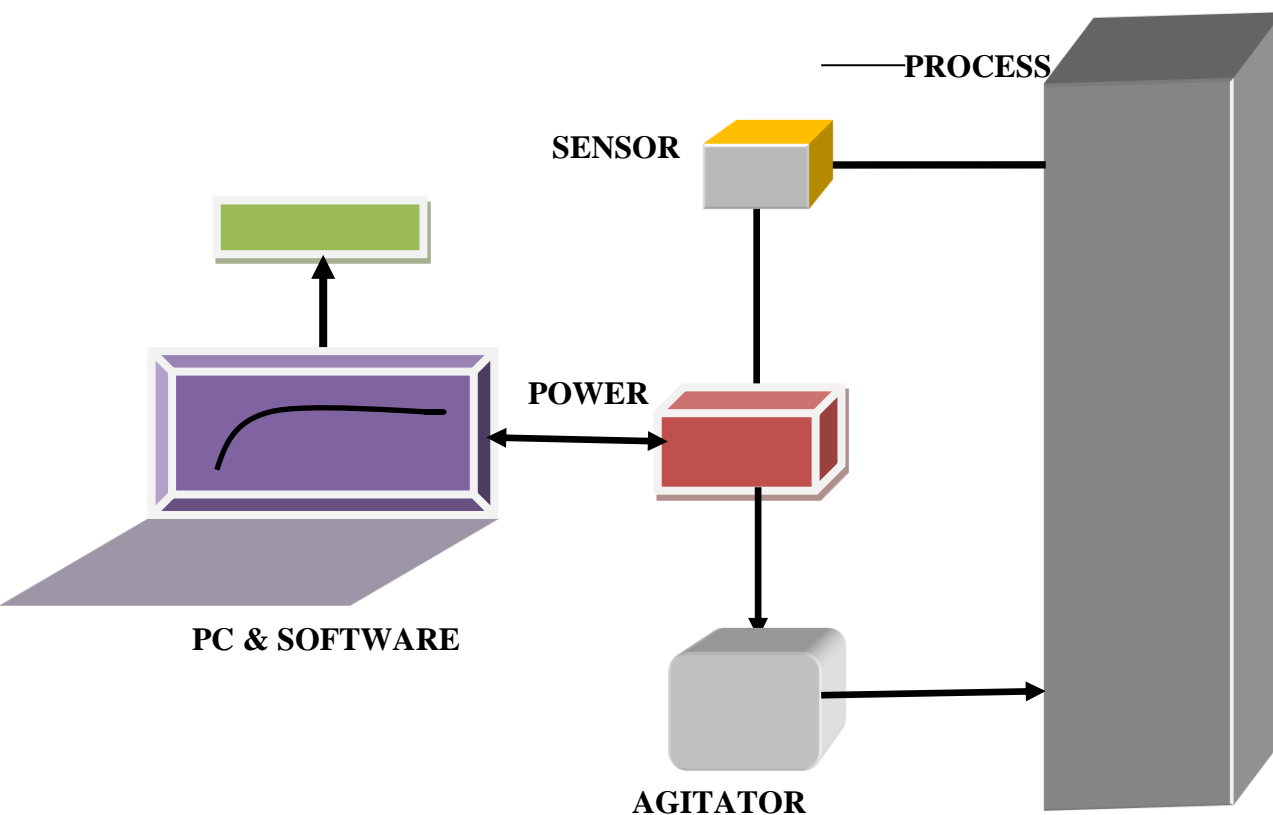
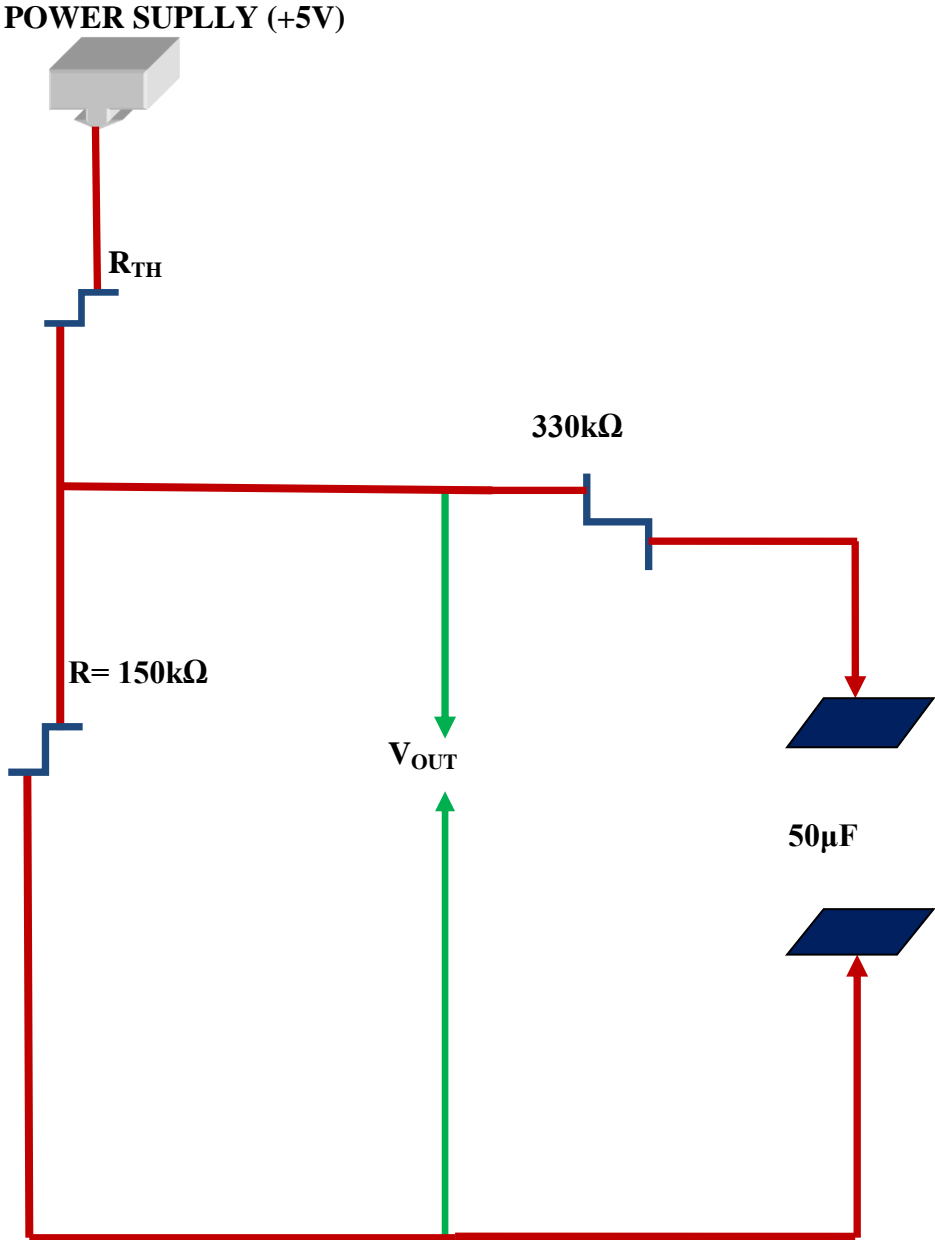


Figure (4.1): Block diagram of experimental set-up

#### 4.4 THE THERMISTOR CALIBRATION

This section describes the experimental details concerning the measurements of liquid phase reactions by temperature-time techniques. Temperature changes are a common feature of almost all chemical reactions and can be easily measured by a variety of thermometric techniques. Following the temperature changes is useful especially for fast chemical reactions where the reacting species are not easily analyzed chemically. This section thus describes the theory and the calibration of the thermistor used in the experiments described in this paper.

4.4.1 THE ELECTRICAL CIRCUIT OF THE SYSTEM



Figure(4.2): The electrical circuit of the system

#### 4.4.2 THE CIRCUIT THEORY

From Kirchhoff law's we can write:

$$V_{out} + V_{TH} = 5V \quad (19)$$

$V_{out}$  – Voltage measured by thermistor during the course of reaction.

$V_{TH}$  – Voltage across resistance ( $R_{TH}$ ).

From (19) one can write:

$$V_{TH} = 5V - V_{out} \quad (20)$$

$$R_{TH} = \frac{V_{TH}}{I_{total}} \quad (21)$$

From the circuit  $V_{TH}$  and  $I_{total}$  are unknowns.  $R_{TH}$  is resistance due to the thermistor, and  $I_{total}$  is the same through the circuit and can be determine as:

$$I_{total} = \frac{V_{out}}{R} \quad (22)$$

$V_{out}$  is known from experimental voltage –time profile and  $R$  (150k $\Omega$ ) is also known from the circuit. Thus when  $I_{total}$  is determined from eq(22),  $R_{TH}$  which is the thermistor's resistance and related to temperature at any time during the chemical reaction can be determine as:

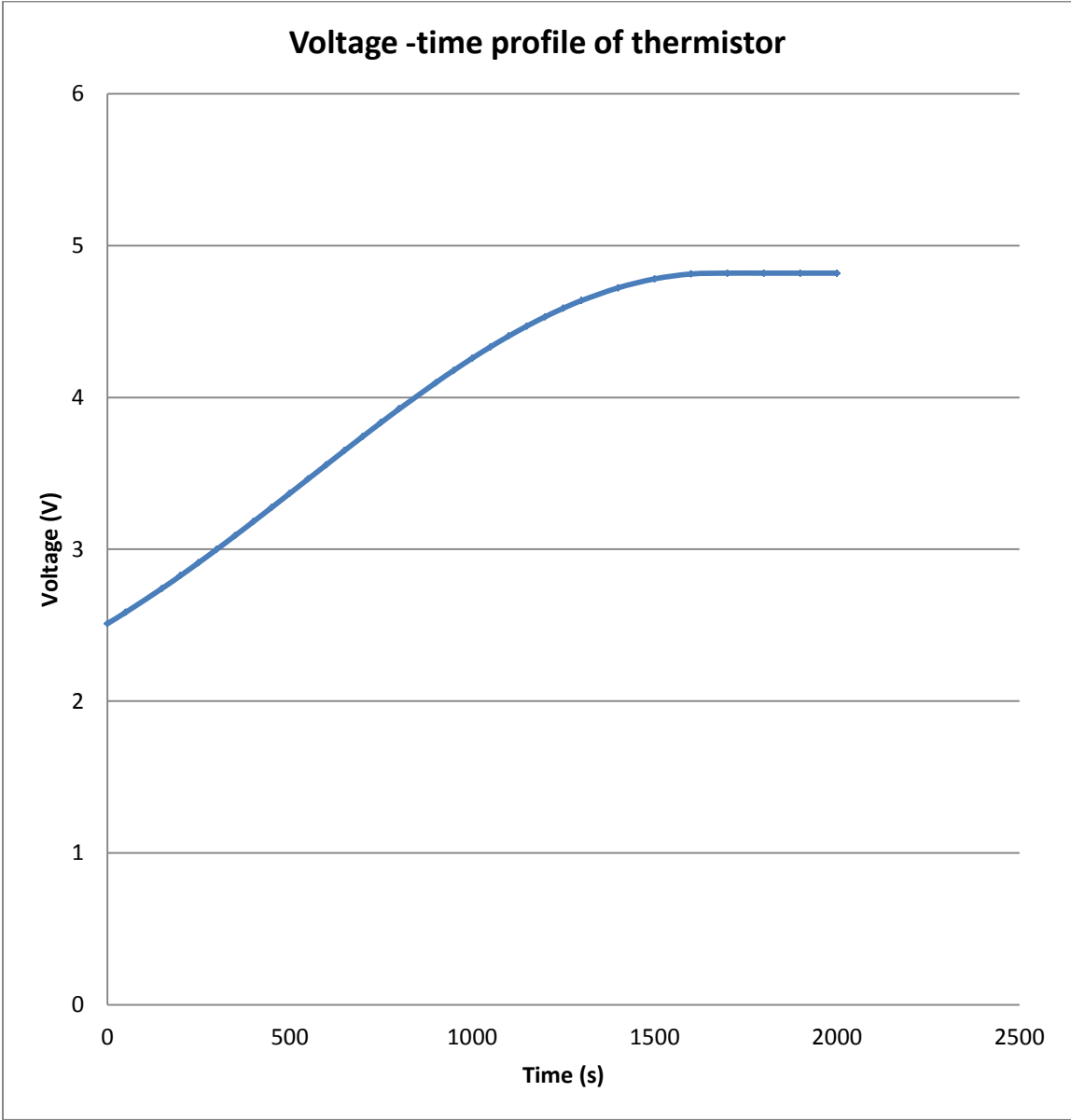
$$R_{TH} = \frac{V_{out}}{I_{total}} \quad (23)$$

#### 4.4.3 THE THERMISTOR CALIBRATION

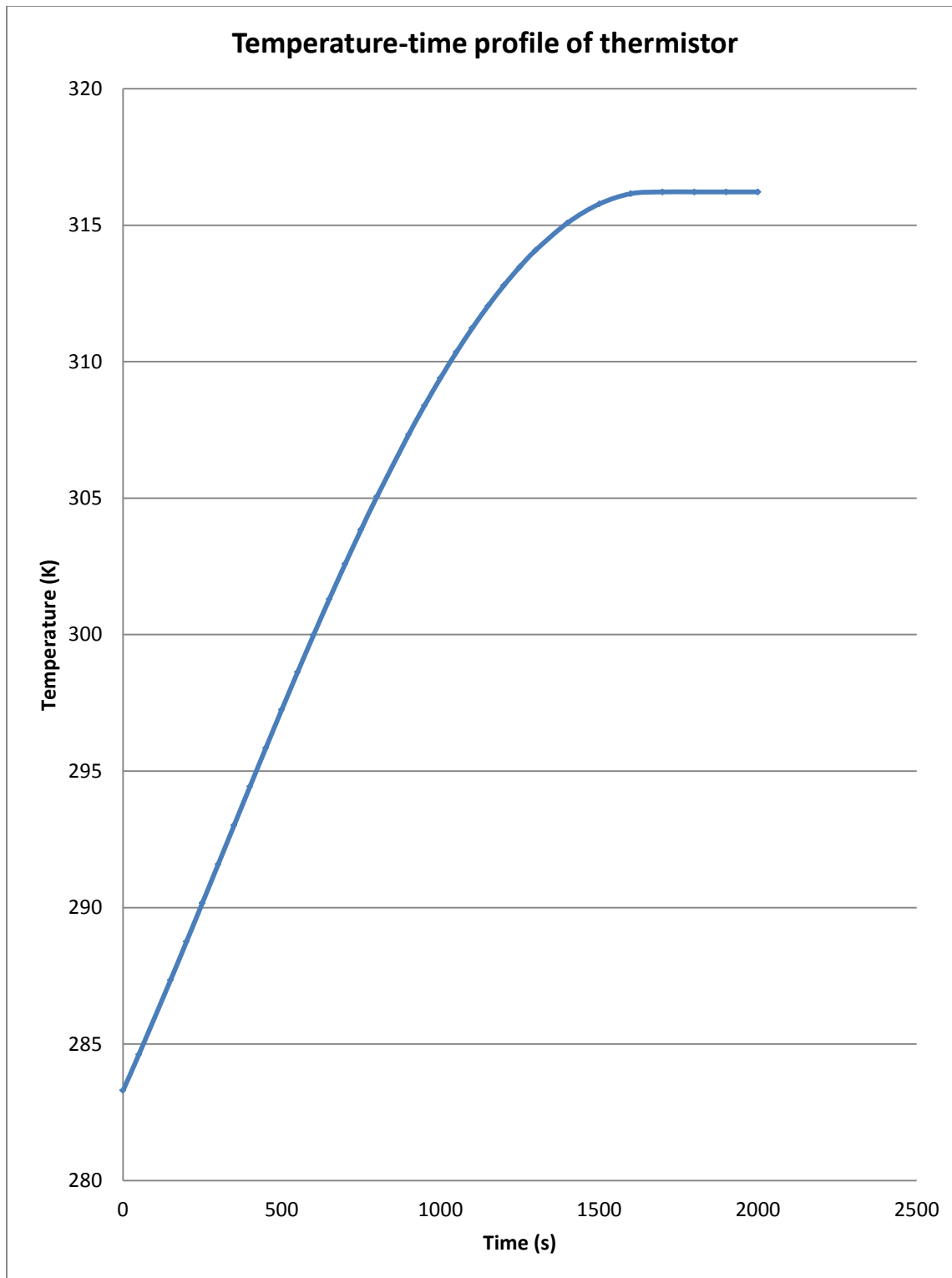
The thermistor used in the experiments was negative temperature coefficient with unknown thermistor constants. The calibrations involve the determination of the thermistor constants and establish the relationship between the thermistor's resistance and temperature.

This was done by fitting both the thermistor and an electronic digital temperature measuring device in a sealed vessel and the system was slowly warmed until the voltage reaches it

asymptotic state. The thermistor was connected to a computer with data acquisition software to provide data of voltage –time real-time plot as shown in figure (4.3) below. The voltage –time data was used to match the temperature-time data obtained from the electronic digital temperature device.



Figure(4.3): The thermistor voltage-time profile



Figure(4.4): The thermistor temperature-time profile

#### 4.4.4 RELATIONSHIP BETWEEN THERMISTOR RESISTANCE AND TEMPERATURE

Thermistor resistance ( $R_{TH}$ ) and Temperature (T) in Kelvin was modeled using the empirical equation given developed by Considine (1957)

$$R_{TH} = \exp\left(\frac{B}{T} + C\right) \quad (24)$$

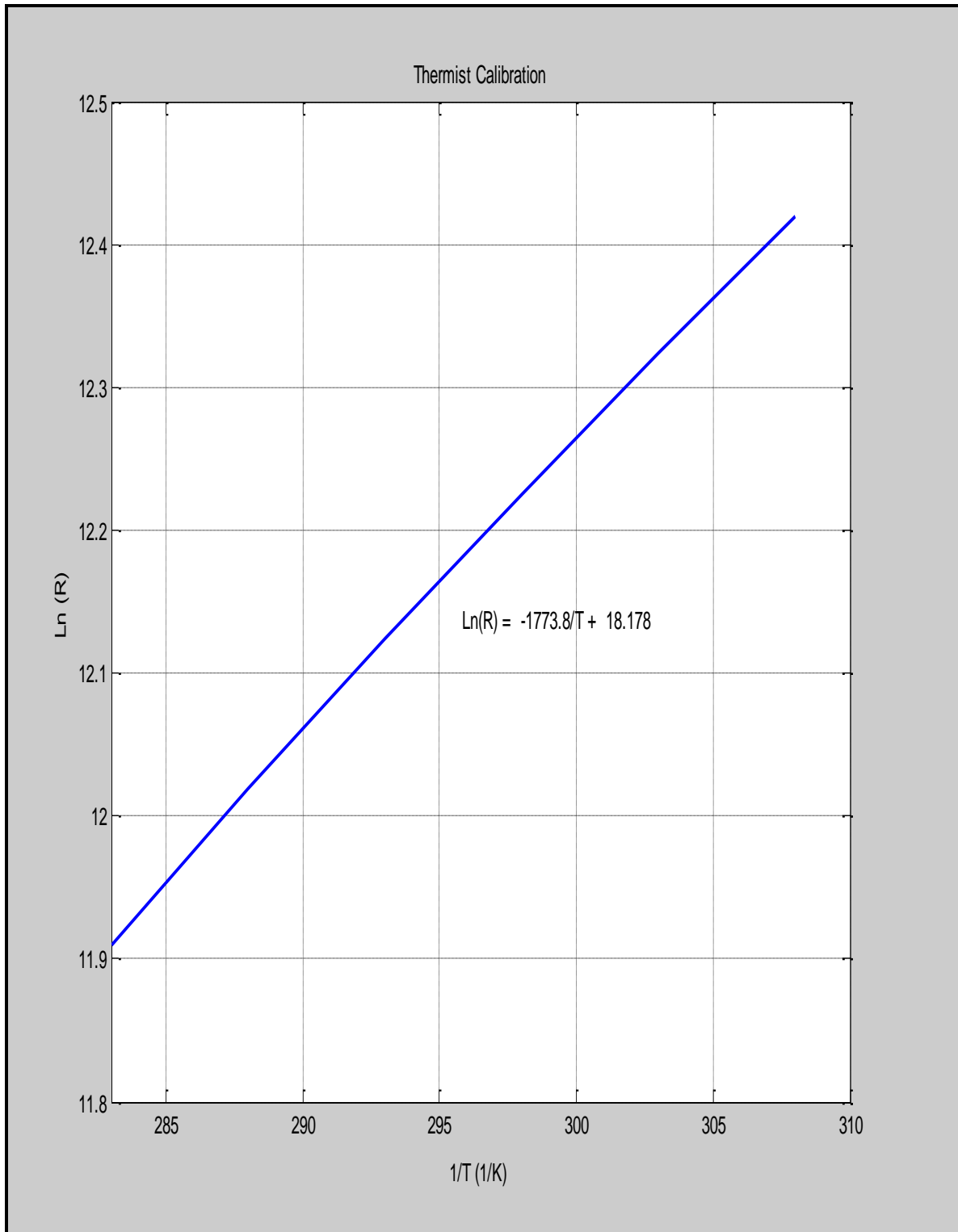
or

$$\ln(R_{TH}) = \frac{B}{T} + C \quad (25)$$

where the parameters (B) and (C) are the thermistor constants and were obtained from experimental calibration using warm water. The constants were determined by fitting the “best” least square straight line plot of  $\ln(R_{TH})$  against  $1/T$ , giving the thermistor equation as:

$$\ln(R_{TH}) = -\frac{1773.8}{T} + 18.178 \quad (26)$$

The calibration plot is shown in figure (4.5) below:



Figure(4.5): Regression line of  $\ln(R_{TH})$  against  $1/T$

#### 4.5 THE REACTOR (THERMOS-FLASK) CALIBRATION

The reaction vessel used was an ordinary dewer thermos-flask with removable screw cap lid. The flask has a total volume of 500mL. The calibration involves the determination of the heat transfer coefficient of the flask and fitting the experimental data to the model described in eq(20) below:

$$T = T_S + (T_O - T_S) \exp\left(-\frac{UA}{mC_p} t\right) \quad (27)$$

In this experiment 400.00g of distilled water at 361K ( $T_O$ ) was injected into the reaction vessel and left the system temperature to fall over a period of time until the temperature-time profile reaches its asymptotic state or the steady-state temperature ( $T_S$ ). The figure (4.6) below shows the temperature-time profile of the cooling process.

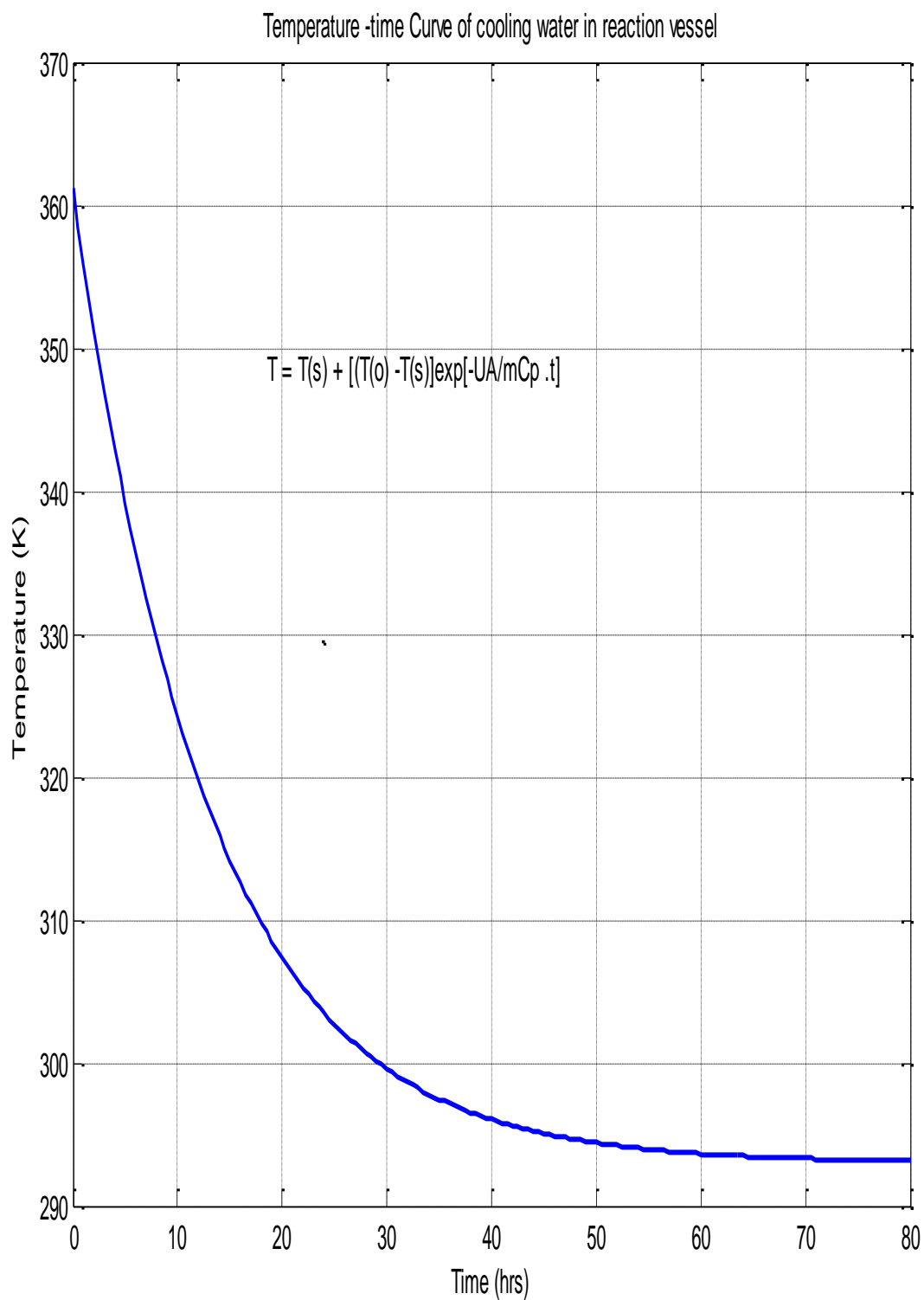


Fig (4.6) : Adiabatic Reactor (Thermos-flask) cooling curve@ T(0) =361K

From eq(20) the values of  $T_o$  and  $T_s$  were obtained from fig(5.6). Rearrangement of eq(20) gives;

$$\ln\left(\frac{T - T_s}{T_o - T_s}\right) = \ln(Y) = \left(-\frac{UA}{mC_p}t\right) \quad (28)$$

Since T and t values are known least square regression analysis was performed and a straight plot of  $\ln(Y)$  against time is shown in figure (4.7) below:

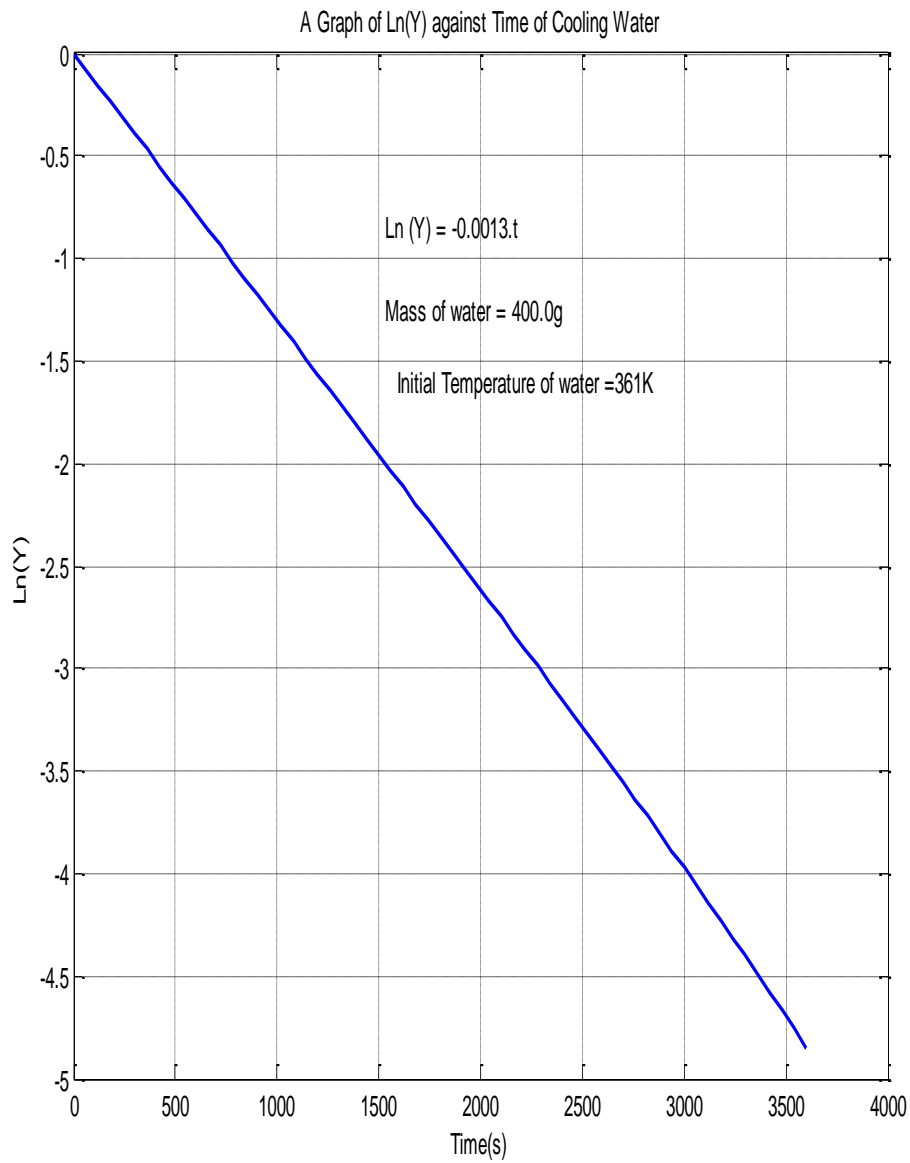


Fig (4.7) :Regression line of heat transfer coefficient of reactor

The slope of the straight line of fig(4.7) is given by  $0.0013\text{s}^{-1}$  which corresponds to the value of the heat transfer coefficient of the flask.

## 4.5.1 EXPERIMENTAL DETERMINATION OF HEAT TRANSFER

### COEFFICIENT OF THE PROCESS

For a given system (reaction vessel and content) one can write:

$$\left(\frac{mC_p}{UA}\right)_{system} = \left(\frac{m C_P}{UA}\right)_{water} + \left(\frac{mC_P}{UA}\right)_{vessel} \quad (29)$$

In this experiment different amount of water ( $m_w$ ) (200g, 300g and 400g) was injected into the reaction flask at 343.08K, 347.77K and 347.85K and allowed to cool until the temperature reaches a steady-state temperature ( $T_s$ ). Figures (4.8a), (4.9a) and (4.10a) of the cooling processes are shown below. The cooling process thus follows equation (27) above. A nonlinear least-square regression analysis was performed on all the three experimental curves. Using eq(28), the value of  $UA/mC_P$  for each cooling curve was obtained. Figures (4.8b),(4.9b) and (4.10b) shows the regression lines.

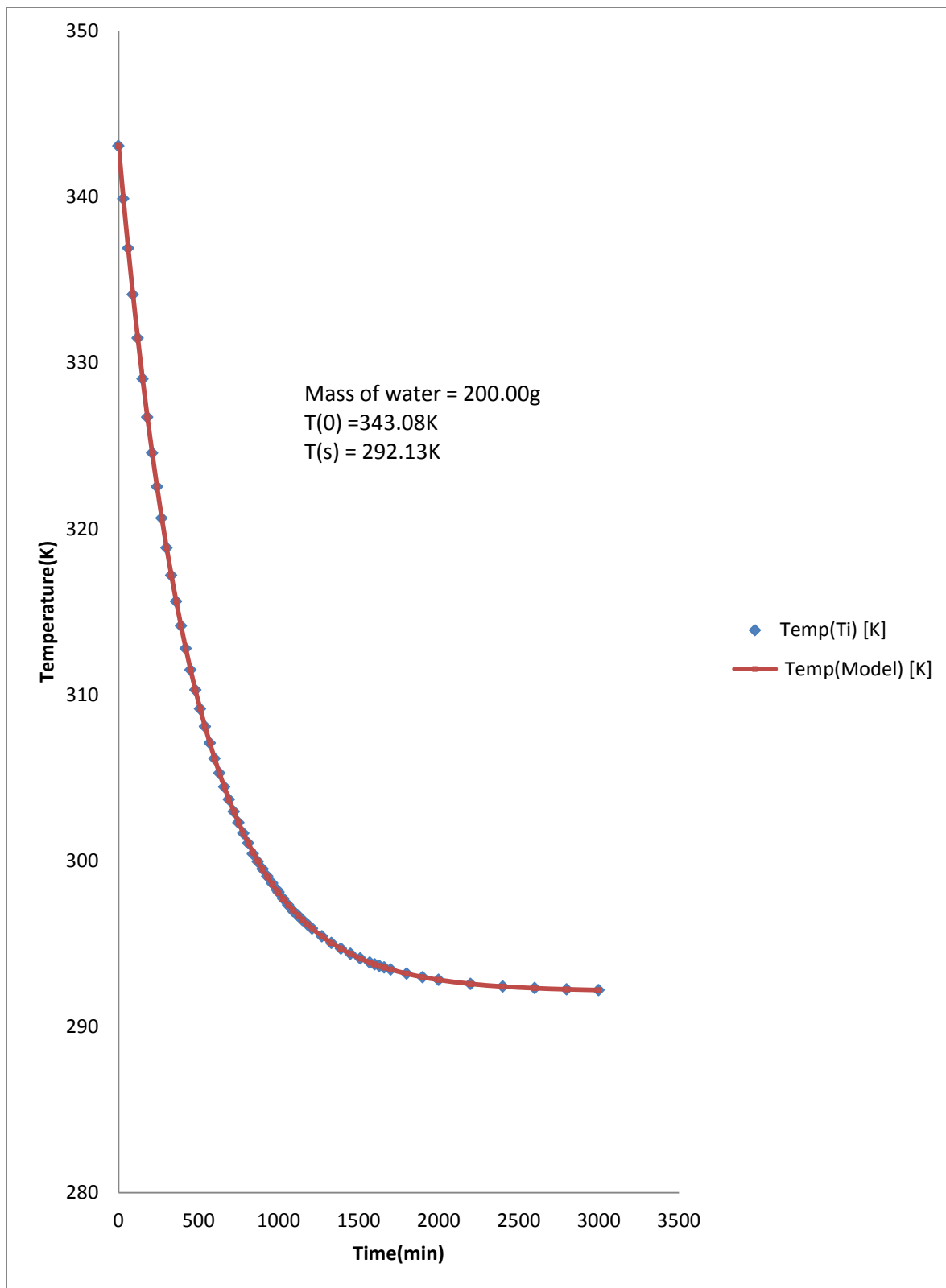


Fig (4.8a): Adiabatic Reactor (Thermos-flask) cooling curve @  $T(0) = 343.08\text{K}$

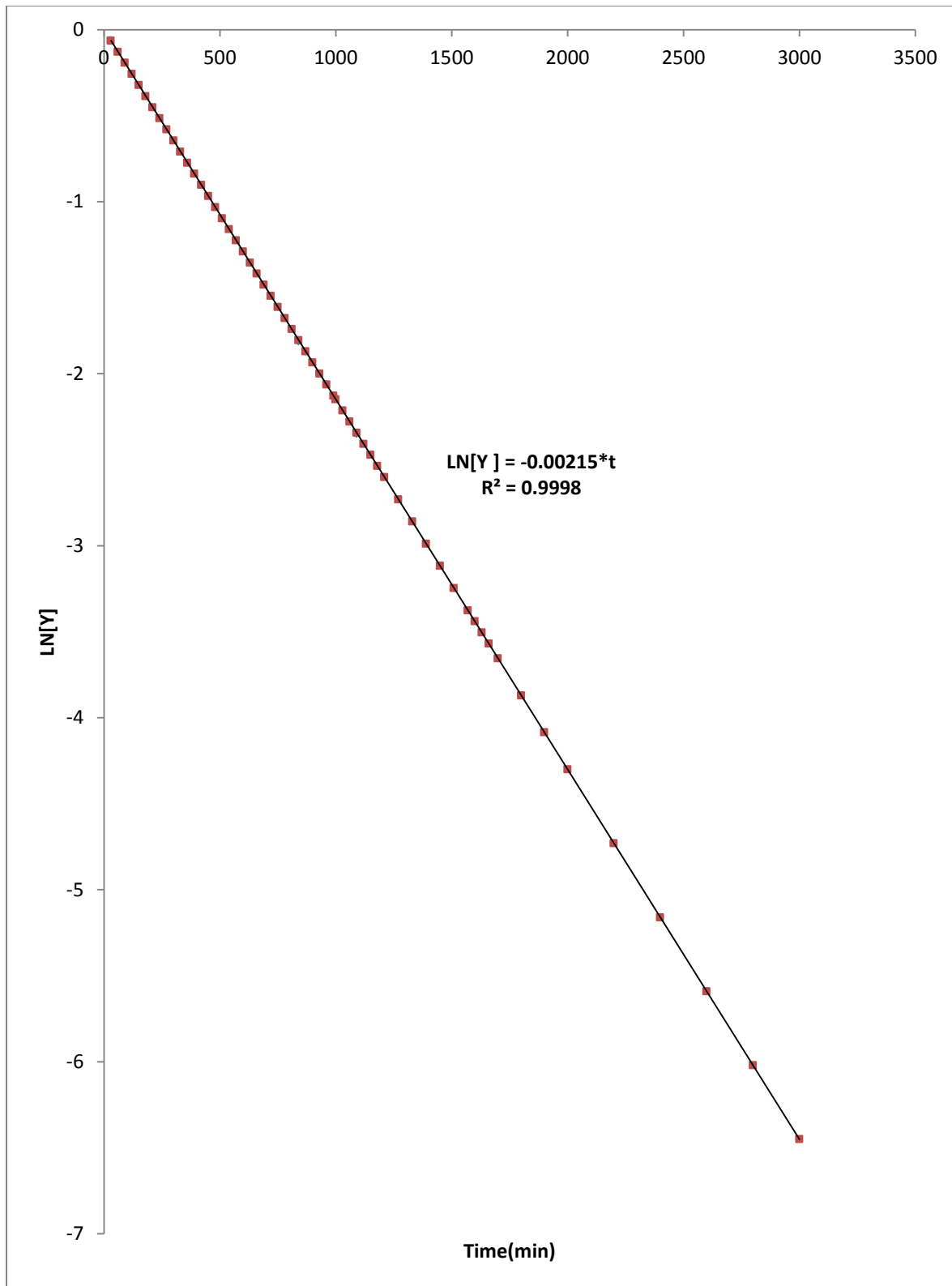


Fig (4.8b): Regression line of heat transfer coefficient of reactor

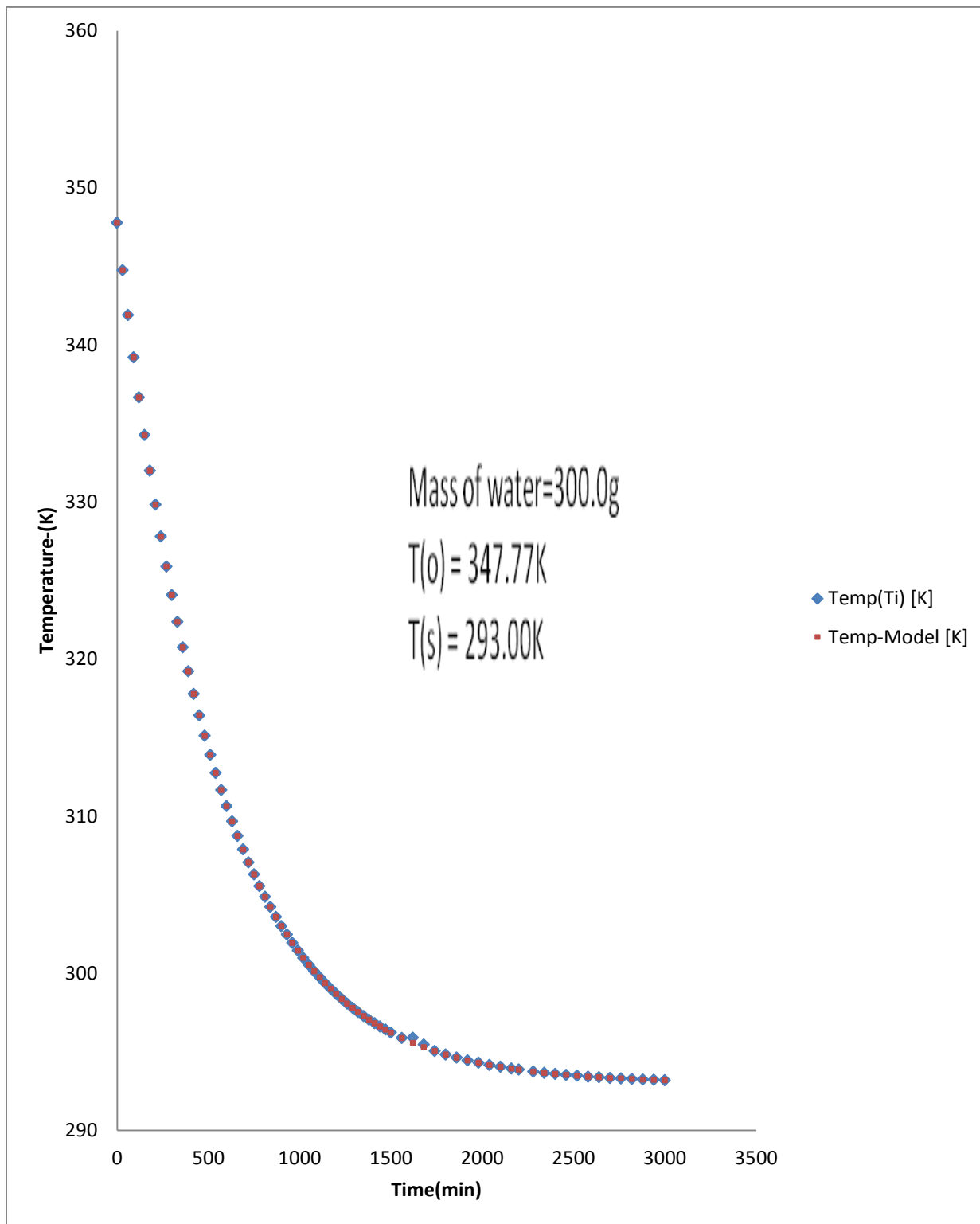


Fig (4.9a): Adiabatic Reactor (Thermos-flask) cooling curve @  $T(0) = 347.77\text{K}$

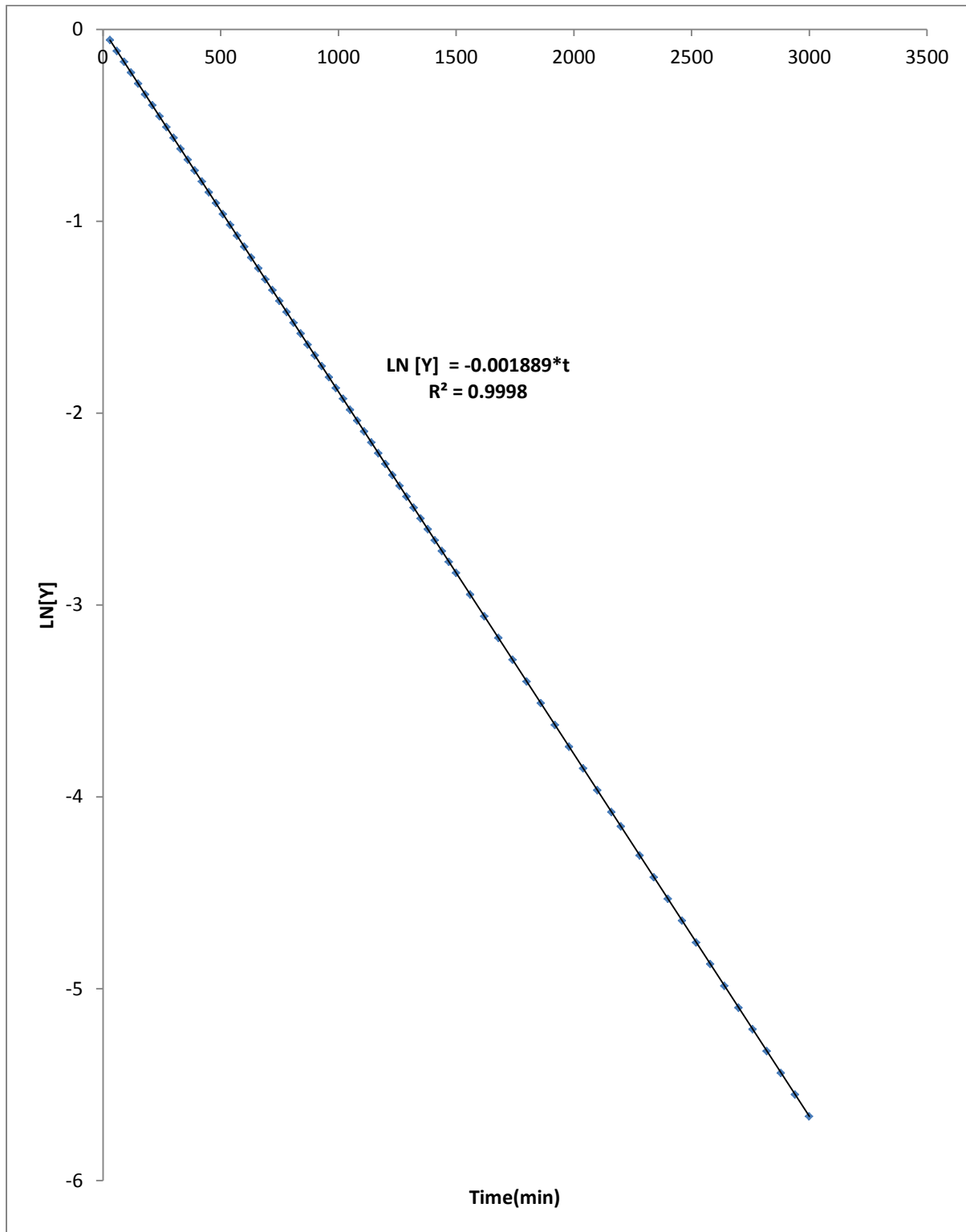


Fig (4.9b): Regression line of heat transfer coefficient of reactor

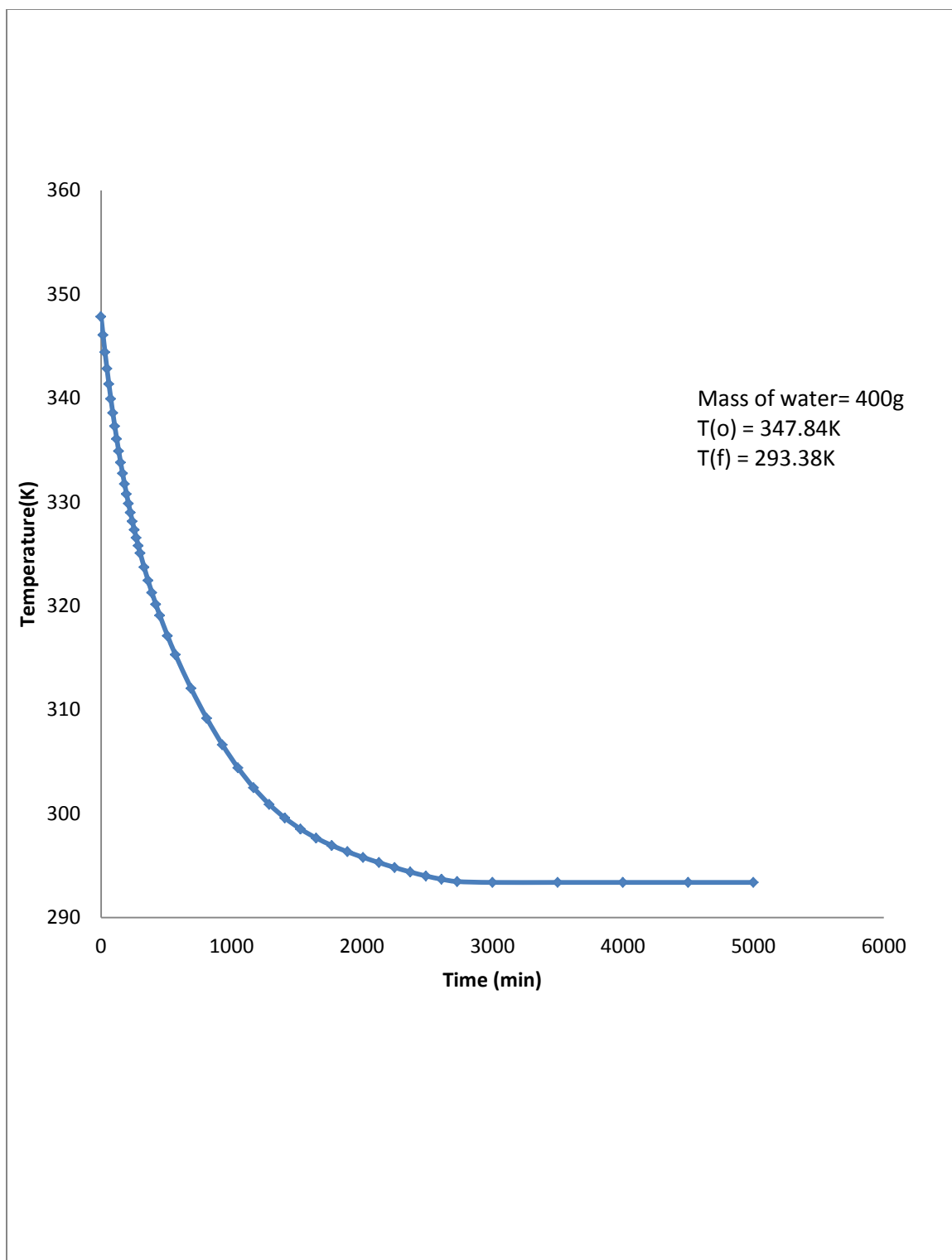


Fig (4.10a): Adiabatic Reactor (Thermos-flask) cooling curve @  $T(0) = 347.80\text{K}$

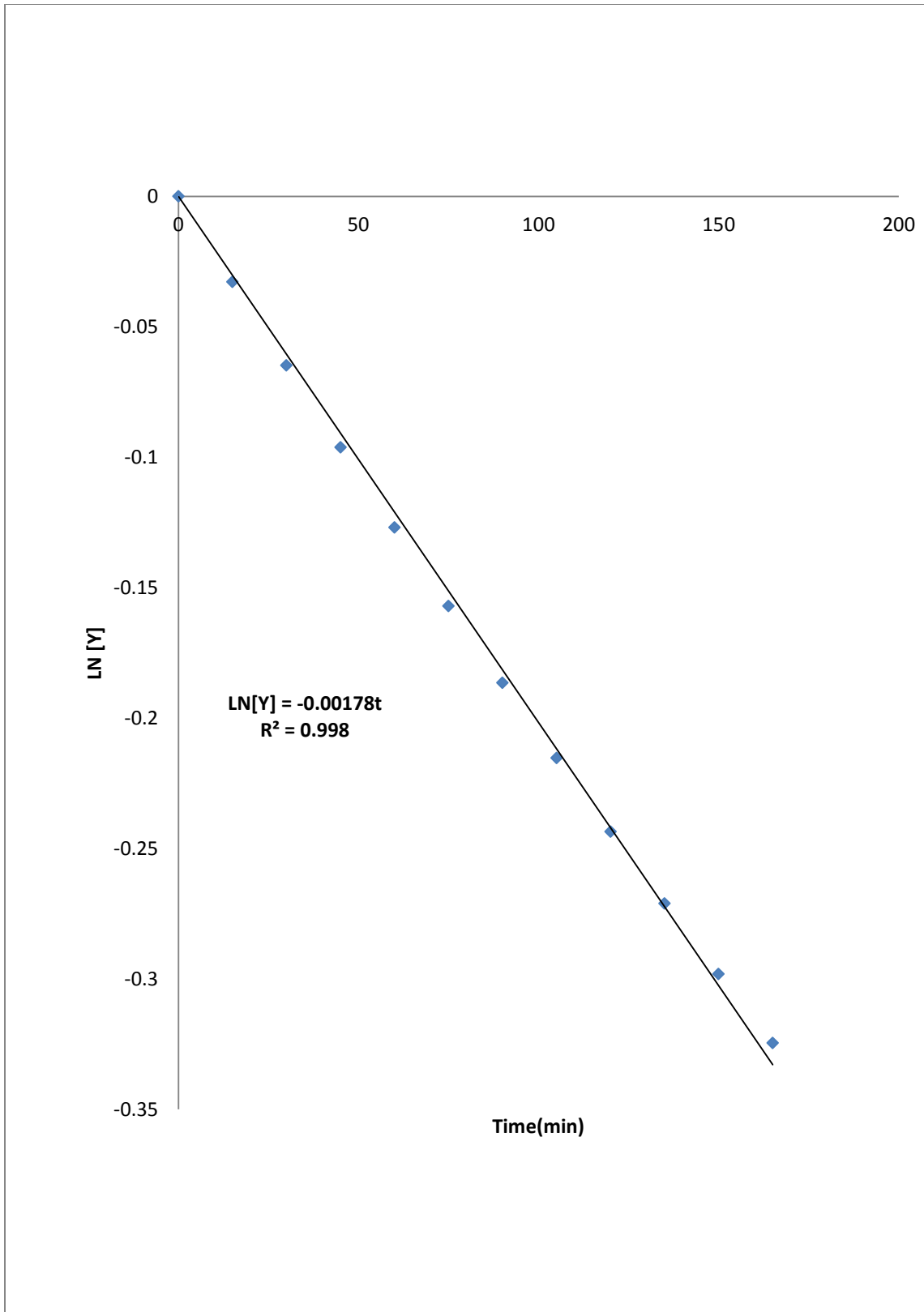


Fig (4.10b): Regression line of heat transfer coefficient of reactor

Table (4.1): Summary of characteristics of figures (8)-(10)

Mass of water(g)	Initial Temperature(K)	Final Temperature(K)	UA/mC <sub>p</sub> (min <sup>-1</sup> )
200	343.08	292.13	0.00215
300	347.77	293.00	0.00189
400	347.84	293.38	0.00178

From table (4.1) a plot of mass of water (m) against (mC<sub>p</sub>/UA) is shown in figure(11) below:

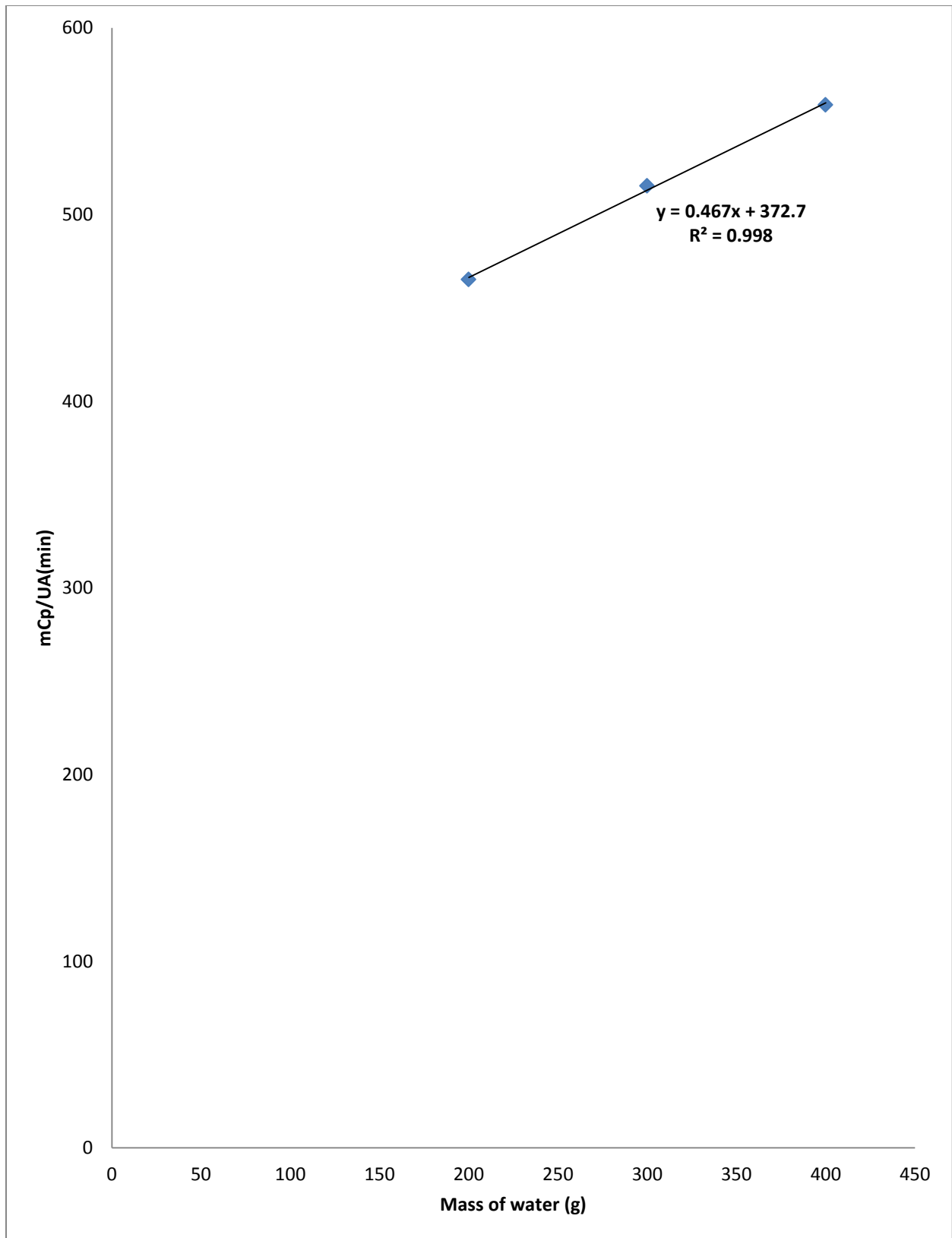


Fig (4.11): A plot of mass of water (m) against ( $mC_p/UA$ )

#### 4.5.2 DETERMINATION OF UA/mC<sub>p</sub> FOR THE REACTION MIXTURE

Table (4.2) below consist of some of the physical constants of the reacting species which was used in the determination of the quantity UA/mC<sub>p</sub>.

Table (4.2) : Some constants of reacting species:

Species	Moles	Molar mass(g/mol)	C <sub>p</sub> (kJ/kg.K)
Acetic acid	1.0	60.05	2.18
Ethanol	1.0	46.07	2.44
Propanol	1.0	60.10	2.40

Equation (30) was used to determine specific heat of the reacting mixture (C<sub>p,mix</sub>) and the quantity M<sub>T</sub>C<sub>p,mix</sub>.

$$C_{P,mix} = \frac{m_{AA}}{M_T} C_{P,AA} + \frac{m_{AL}}{M_T} C_{P,W} \quad (30)$$

M<sub>T</sub>, is the total mass of the reacting mixture and M<sub>T</sub>C<sub>p,mix</sub>. Since the reaction is not pure water we therefore determined its equivalent mass of water using equation (31) below.

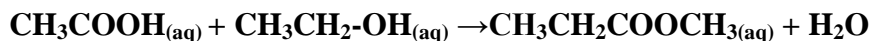
$$m_{eqv \text{ water}} = \frac{(M_T C_P)_{mix}}{C_{P,water}} \quad (31)$$

From figure (4.11) the value of the quantity (UA/mC<sub>p</sub>)<sub>mix</sub> was determined to be 0.0025/min.

## 4.6 EXPERIMENTAL PROCEDURES AND RESULTS

### 4.6.1 Acetic Acid –Ethanol Reactions

These liquid phase esterification reactions have general reaction model given by:



$$\Delta H_{\text{rxn}}(298\text{K}) = -6.12\text{kJ/mol}$$

Analytical reagent grade acetic acid was used in all the experiments. In all experiments about 1.0 mol of acetic acid was poured into the reaction vessel followed by 1.0mol of the ethanol. 10ml of concentration sulphuric acid was added to the reactant mixture as a catalyst to initiate the reaction. These volumes were used so that at least 60% of the length of the sensor (thermistor) would be submerged in the resulting mixture. Reactants were brought to a steady-state temperature before starting the stirrer. In course of the reaction the stirrer speed was set 1000rev/min and the resulting voltage-time profiles were captured as described above and the corresponding temperature-time curve was determined using the thermistor equation derive in equation (19) above. Runs were carried out adiabatically at the following initial temperatures: 283K, 288K and 296K. The temperature-time profiles of the above experiments are shown in figures (4.12),(4.13) and (4,14) below.

## 4.6.2 Experimental results

The results of the above described experiments are presented graphically below.

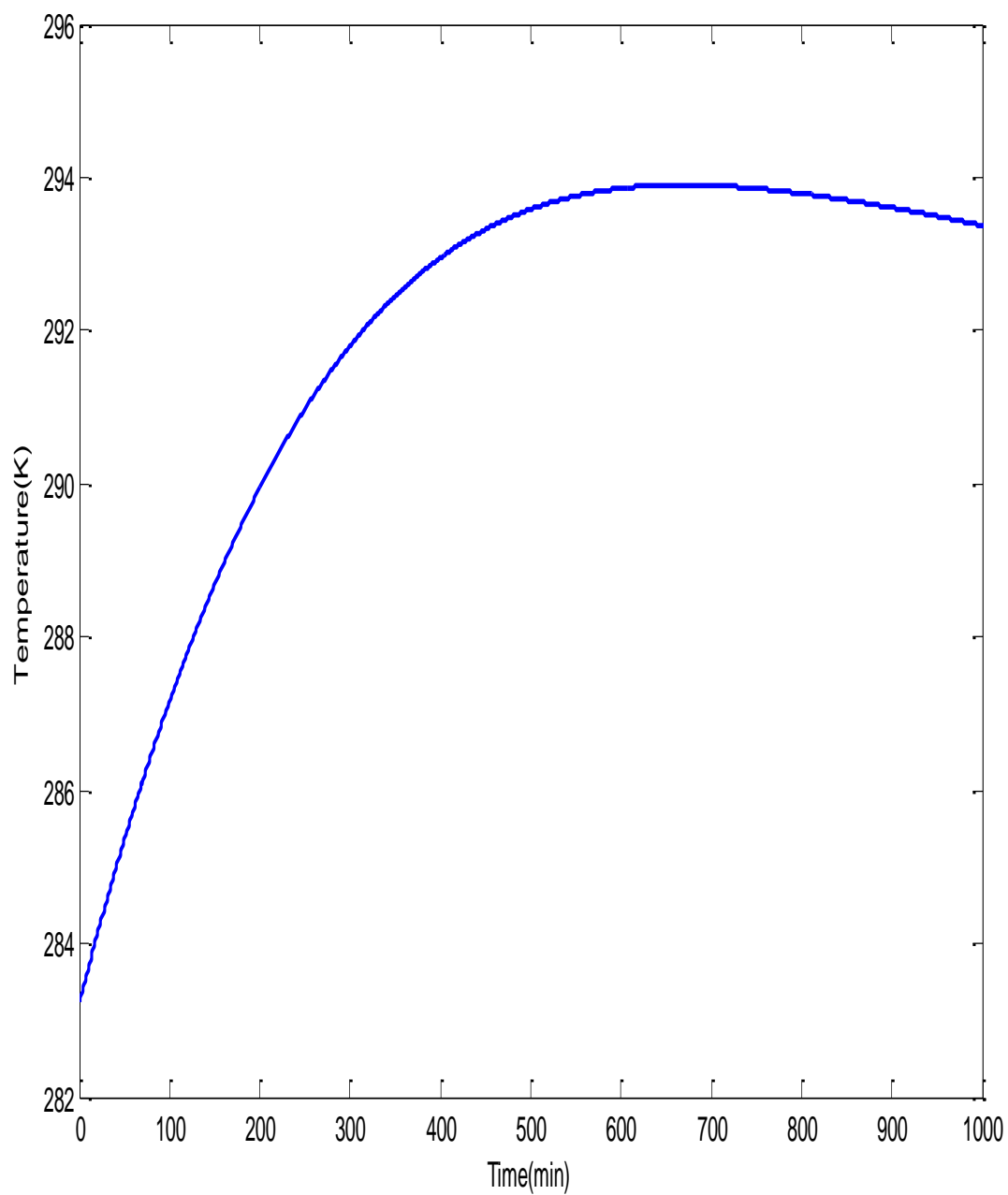


Figure (4.12): Acetic Acid-Ethanol Reaction: Temperature-time profile at 283K

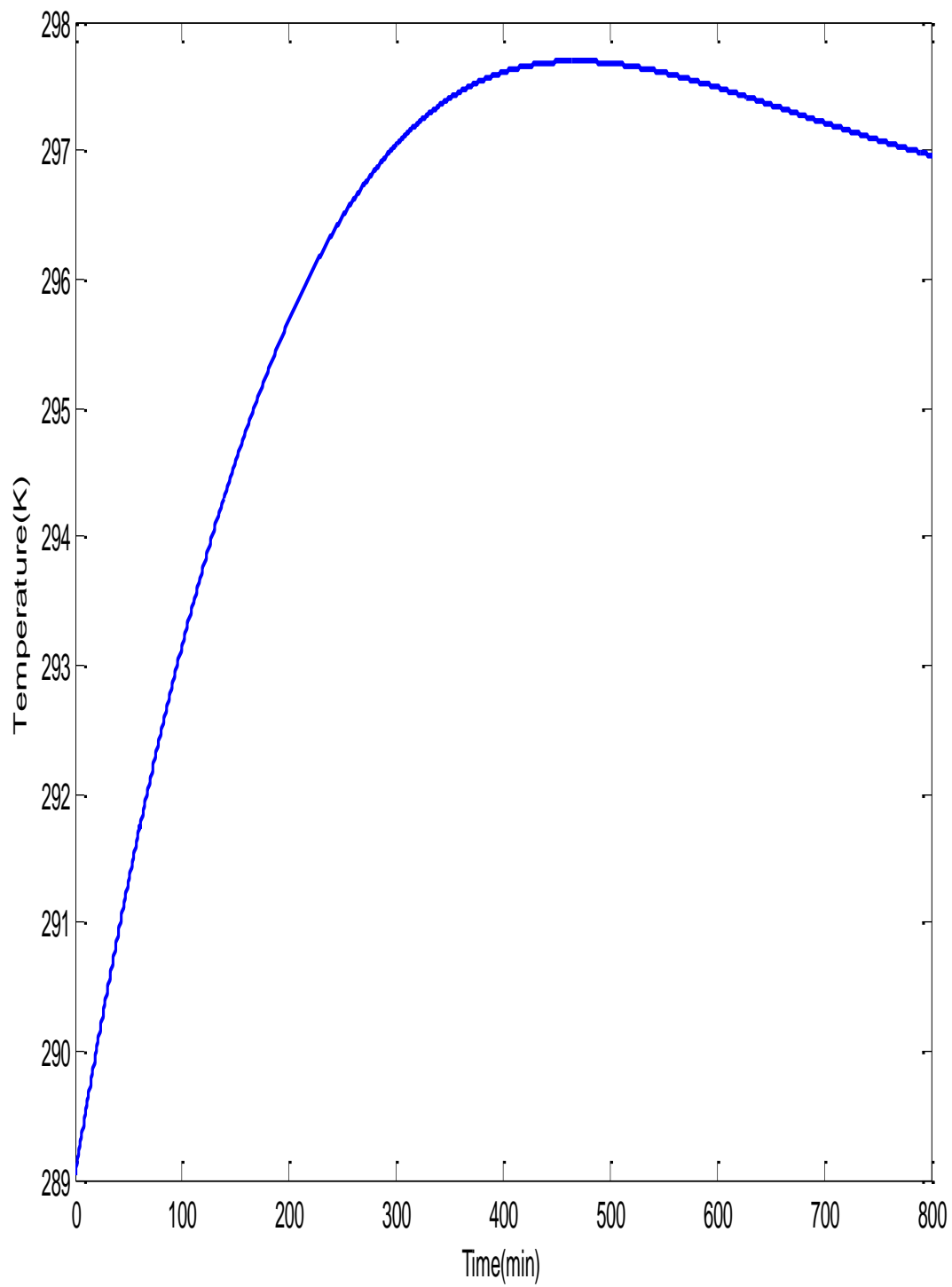


Figure (4.13): Acetic Acid-Ethanol Reaction: Temperature-time profile at 289K

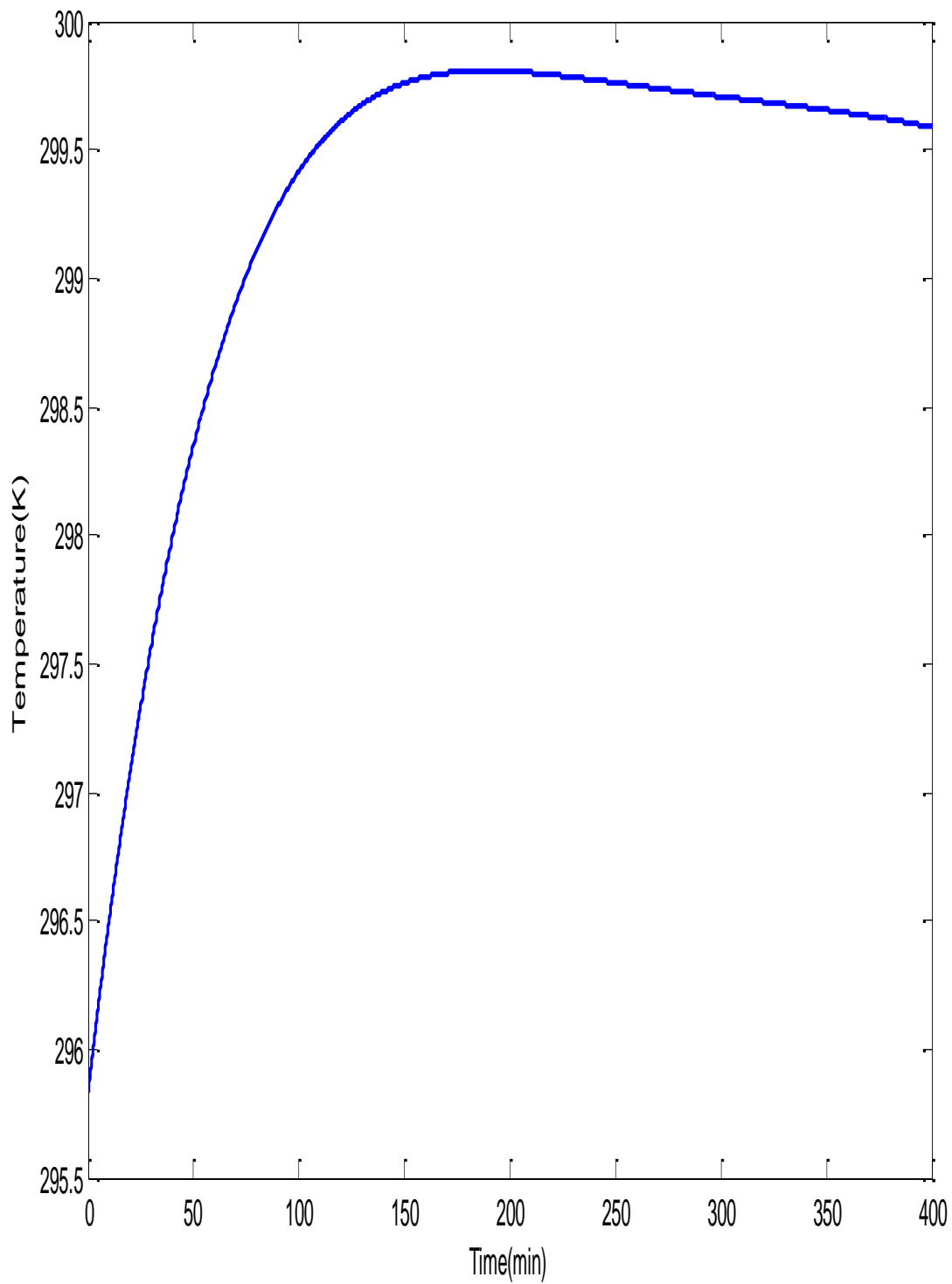
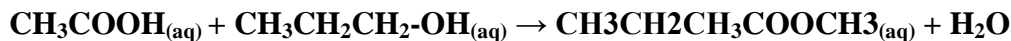


Figure (4.14): Acetic Acid-Ethanol Reaction: Temperature-time profile at 295.8K

#### 4.7 Acetic Acid –Propanol Reactions

These liquid phase esterification reactions have general reaction model given by:



$$\Delta H_{\text{rxn}}(298\text{K}) = -30.24\text{kJ/mol}$$

Analytical reagent grade acetic acid was used in all the experiments. In all experiments about 1.0 mol of acetic acid was poured into the reaction vessel followed by 1.0mol of the propanol. 10ml of concentration sulphuric acid was added to the reactant mixture as a catalyst to initiate the reaction. These volumes were used so that at least 60% of the length of the sensor (thermistor) would be submerged in the resulting mixture. Reactants were brought to a steady-state temperature before starting the stirrer. In course of the reaction the stirrer speed was set 1000rev/min and the resulting voltage-time profiles were captured as described above and the corresponding temperature-time curve was determined using the thermistor equation derive in equation above. Runs were carried out adiabatically at the following initial temperatures: 285K, 290K and 298K. The temperature-time profiles of the above experiments are shown in figures (4.15),(4.16) and (4.17) below.

### 4.7.1 EXPERIMENTAL RESULTS

The results of the above described hydrolysis experiment is presented graphically below.

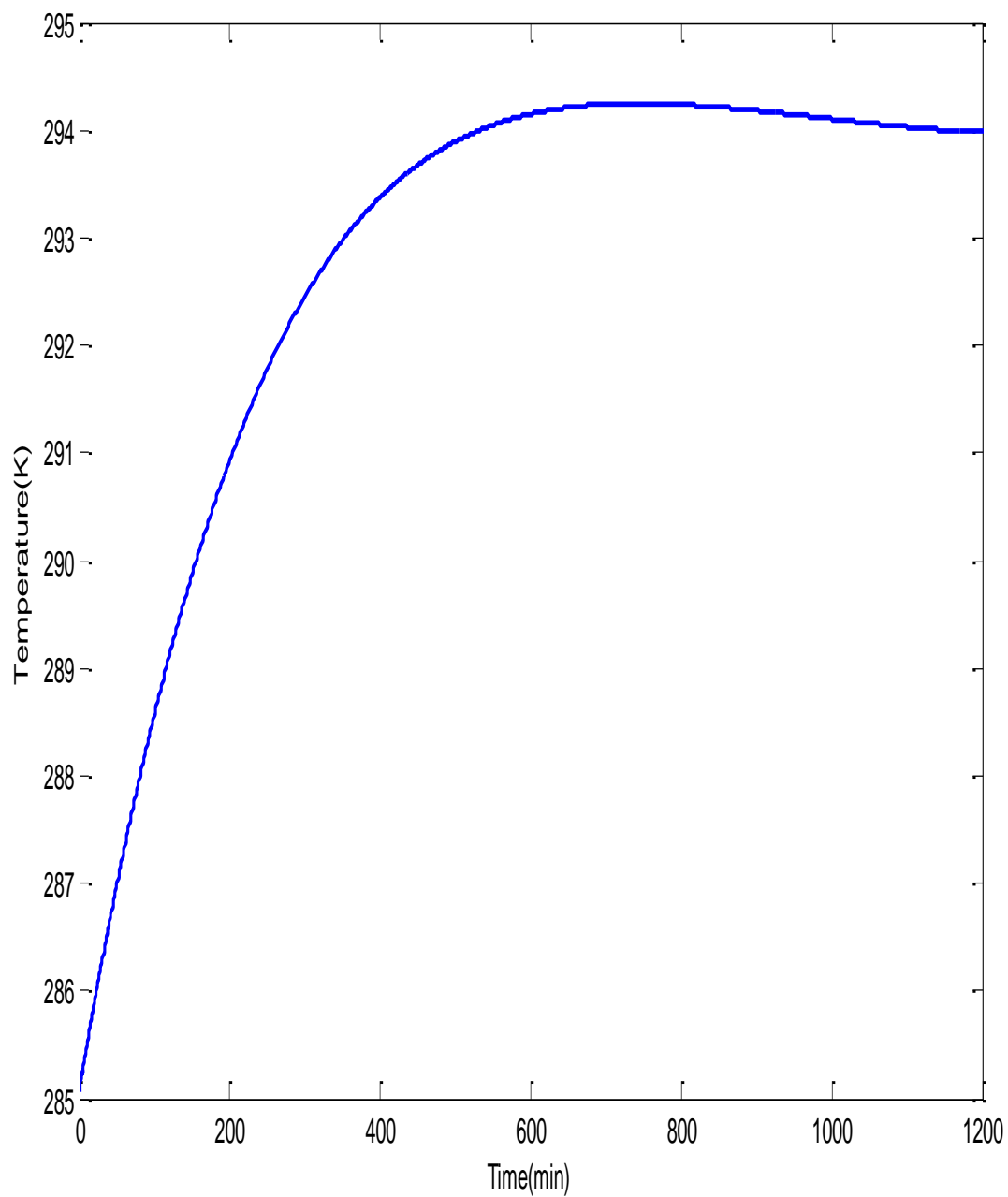


Figure (4.15): Acetic Acid-Propanol Reaction: Temperature-time profile at 285.1K

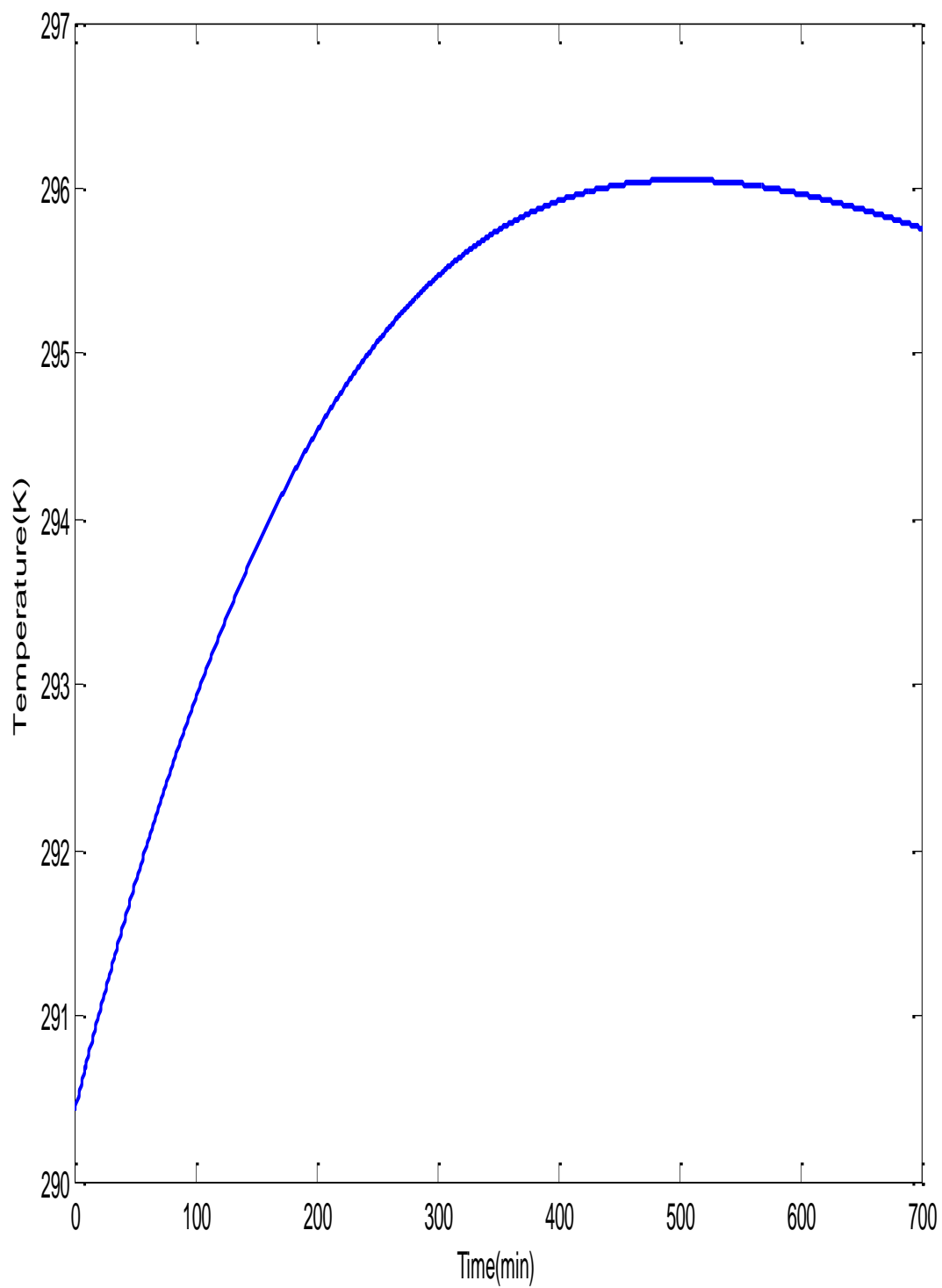


Figure (4.16): Acetic Acid-Propanol Reaction: Temperature-time profile at 290.4K

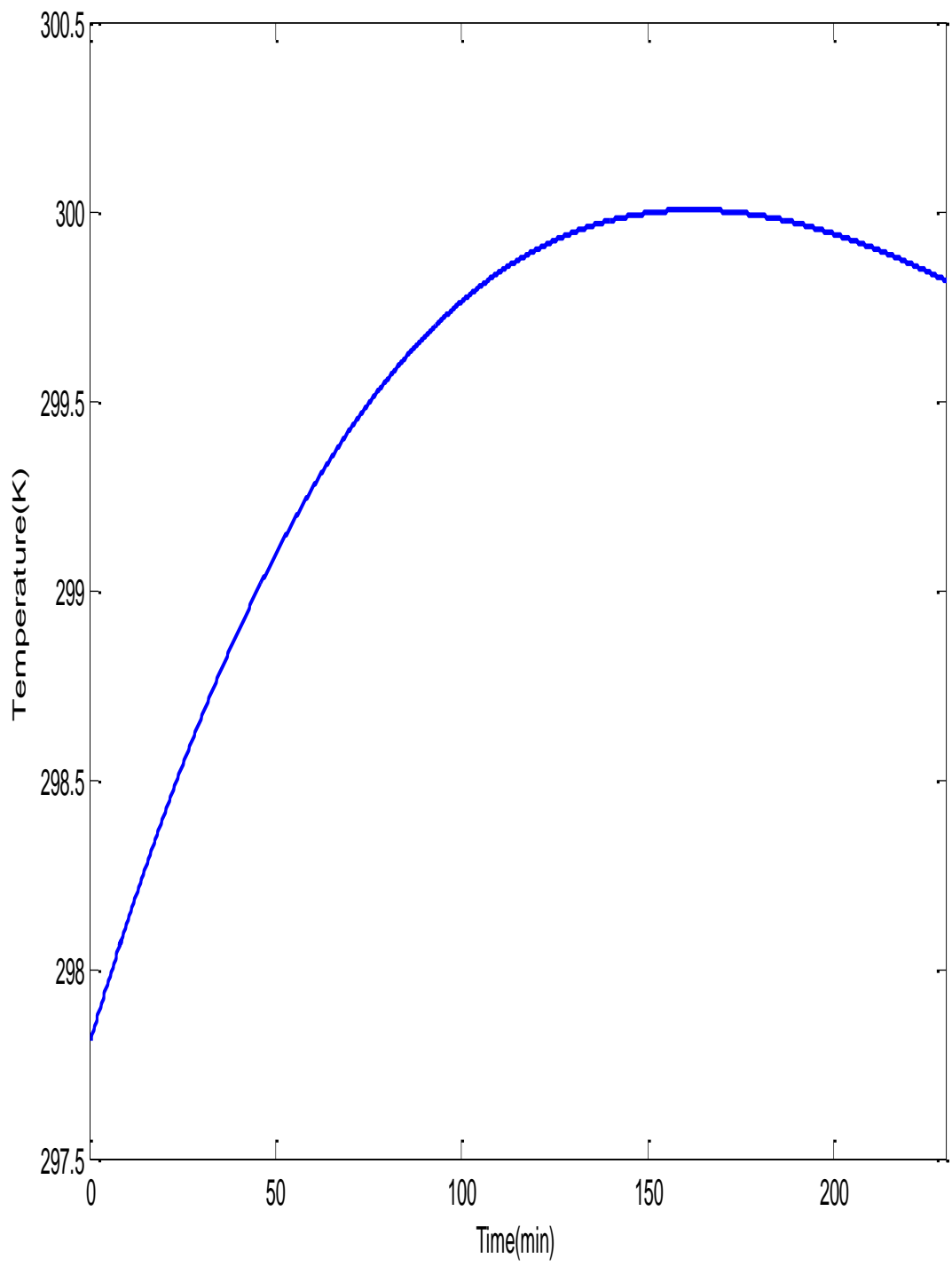


Figure (4.17): Acetic Acid-Propanol Reaction: Temperature-time profile at 297.8K

## 4.8 ANALYSIS OF EXPERIMENTAL RESULTS.

Consider model equations (16)-(18) as stated above:

$$\frac{(-\Delta H_r) \cdot \sqrt{K_{eq}^0} \cdot \exp\left\{\frac{(-\Delta H_r)}{2R} \left(\frac{1}{T_0} - \frac{1}{T}\right)\right\}}{1 + \sqrt{K_{eq}^0} \cdot \exp\left\{\frac{(-\Delta H_r)}{2R} \left(\frac{1}{T_0} - \frac{1}{T}\right)\right\}} + mC_p (T - T_0) + UA \int_0^\infty (T - T_0) dt = 0 \quad (32)$$

$$\text{Let } (T - T_0) + \frac{UA}{mC_p} \int_0^\infty (T - T_0) dt = \alpha \text{ and } \frac{1}{2R} \left(\frac{1}{T_0} - \frac{1}{T}\right) = \beta \quad (33)$$

Eq(16) can be simplified as :

$$\frac{(-\Delta H_r) \cdot \sqrt{K_{eq}^0} \cdot \exp((- \Delta H_r) \cdot \beta)}{1 + \sqrt{K_{eq}^0} \cdot \exp(-\Delta H_r \cdot \beta)} + \alpha mC_p = 0 \quad (34)$$

Equation (34) have 2 unknown quantities  $(-\Delta H_r)$  and  $K_{eq}^0$ . If one can determine  $\alpha$  and  $\beta$ , using the experimental results then the 2 unknown thermodynamic quantities can be determined for the process and eq(7) can be establish for the esterification process.

### 4.8.1 MODEL SOLUTION

At a given temperatures  $(T_1)$  and  $(T_2)$  from experimental results, corresponding  $(\alpha_1), (\beta_1)$ , and  $(\alpha_2), (\beta_2)$  can be determined form the experimental data for a given  $(T_0)$ . Then one can modify equation (18) as follows:

$$\begin{aligned} & (-\Delta H_r) \cdot \sqrt{K_{eq}^0} \cdot \exp((- \Delta H_r) \cdot \beta_1) + \alpha_1 mC_p + \sqrt{K_{eq}^0} \cdot \exp(-\Delta H_r \cdot \beta_1) \cdot \alpha_1 mC_p \\ & = 0 \end{aligned} \quad (35)$$

Similarly for a given  $(T_2)$ , one can write:

$$\begin{aligned}
& (-\Delta H_r) \cdot \sqrt{K_{eq}^0} \cdot \exp((-\Delta H_r) \cdot \beta_2) + \alpha_2 m C_p + \sqrt{K_{eq}^0} \cdot \exp(-\Delta H_r \cdot \beta_2) \cdot \alpha_2 m C_p \\
& = 0
\end{aligned} \tag{36}$$

For (T<sub>2</sub>) and (T<sub>2</sub>), at a given (T<sub>0</sub>), eliminating  $\sqrt{K_{eq}^0}$  using equations (19) and (20), one can write equation (21) as follows:

$$\begin{aligned}
& -\alpha_1(-\Delta H_r) \exp[(-\Delta H_r) \cdot \beta_2] \\
& \quad + \alpha_2(-\Delta H_r) \exp[(-\Delta H_r) \cdot \beta_1] \\
& \quad - \alpha_1 \alpha_2 m C_p \exp[(-\Delta H_r) \cdot \beta_2] + \alpha_1 \alpha_2 m C_p \exp[(-\Delta H_r) \cdot \beta_1] \\
& = 0
\end{aligned} \tag{37}$$

Similarly, for a given (T<sub>1</sub>) and (T<sub>3</sub>), at a given (T<sub>0</sub>), one can also write equation (22) as follows:

$$\begin{aligned}
& -\alpha_1(-\Delta H_r) \exp[(-\Delta H_r) \cdot \beta_3] \\
& \quad + \alpha_3(-\Delta H_r) \exp[(-\Delta H_r) \cdot \beta_1] \\
& \quad - \alpha_1 \alpha_3 m C_p \exp[(-\Delta H_r) \cdot \beta_3] + \alpha_1 \alpha_3 m C_p \exp[(-\Delta H_r) \cdot \beta_1] \\
& = 0
\end{aligned} \tag{38}$$

Hence, for a given (T<sub>2</sub>) and (T<sub>3</sub>), at a given (T<sub>0</sub>), one can also write equation (23) as follows:

$$\begin{aligned}
& -\alpha_2(-\Delta H_r) \exp[(-\Delta H_r) \cdot \beta_3] \\
& \quad + \alpha_3(-\Delta H_r) \exp[(-\Delta H_r) \cdot \beta_2] \\
& \quad - \alpha_2 \alpha_3 m C_p \exp[(-\Delta H_r) \cdot \beta_3] + \alpha_2 \alpha_3 m C_p \exp[(-\Delta H_r) \cdot \beta_2] \\
& = 0
\end{aligned} \tag{39}$$

By selecting temperatures (T<sub>1</sub>, T<sub>2</sub> and T<sub>3</sub>) as maximum temperatures for the processes table 4.3 and 4.4 below was developed which consists of parameters deduced from the experimental results which were used in solving for  $(-\Delta H_{rxn})$  in equations (37)- (39) for the two processes. The ( $\alpha$ ) and ( $\beta$ ) values were obtained using equation (17).

Table 4.3: Parameters for ethyl acetate process

Experiment (n)	T <sub>0</sub> (K)	T <sub>n</sub> (K)	α <sub>n</sub>	β <sub>n</sub>
1	283.3	293.7	14.639	0.000007731
2	288.7	297.7	13.559	0.000006107
3	295.6	299.8	9.836	0.00000285

Table 4.4: Parameters for propyl acetate process

Experiment (n)	T <sub>0</sub> (K)	T <sub>n</sub> (K)	α <sub>n</sub>	β <sub>n</sub>
1	285.1	294.2	15.940	0.000006524
2	290.4	296.0	15.510	0.000003917
3	297.8	300.0	9.764	0.00000148

Solving for (-ΔH<sub>rxn</sub>) using equations (37)-(39) combinations [T<sub>1</sub>-T<sub>2</sub>], [T<sub>1</sub>-T<sub>3</sub>] and [T<sub>2</sub>-T<sub>3</sub>], the following values obtained for the two processes are shown in tables (5.5) and (5.6) below.

Table 4.5: Heat of reactions for ethyl acetate process

Combinations	[T <sub>1</sub> -T <sub>2</sub> ]	[T <sub>1</sub> -T <sub>3</sub> ]	[T <sub>2</sub> -T <sub>3</sub> ]
Heat of reactions (J/mol)	4.01 * 10 <sup>4</sup>	8.15 * 10 <sup>4</sup>	9.85 * 10 <sup>4</sup>

Table 4.6: Heat of reactions for propyl acetate process

Combinations	[T <sub>1</sub> -T <sub>2</sub> ]	[T <sub>1</sub> -T <sub>3</sub> ]	[T <sub>2</sub> -T <sub>3</sub> ]
Heat of reactions(J/mol)	1.90 * 10 <sup>5</sup>	0.11 * 10 <sup>5</sup>	0.97 * 10 <sup>4</sup>

By modifying equations (35) or (36) the equilibrium constant ( $K^{\circ}$ ) values of the various temperature combinations were computed. Tables (4,7) and (4.8) show the equilibrium constant values for the two processes.

Table 4.7: Equilibrium constants ( $K^{\circ}$ ) for ethyl acetate process

Combinations	[T <sub>1</sub> -T <sub>2</sub> ]	[T <sub>1</sub> -T <sub>3</sub> ]	[T <sub>2</sub> -T <sub>3</sub> ]
Equilibrium constant( $K^{\circ}_{eq}$ )	1.209	0.0018	0.0010

Table 4.8: Equilibrium constants ( $K^{\circ}$ ) for propyl acetate process

Combinations	[T <sub>1</sub> -T <sub>2</sub> ]	[T <sub>1</sub> -T <sub>3</sub> ]	[T <sub>2</sub> -T <sub>3</sub> ]
Equilibrium constant ( $K^{\circ}_{eq}$ )	0.00033	0.1567	0.0024

Table 4.9: Mean values of the heat of reaction ( $\Delta H_r$ ) and the equilibrium constants ( $K^{\circ}_{eq}$ ) of the two processes.

PROCESS	$(-\Delta H_{rxn})_{mean}$	$(K^{\circ}_{eq})_{mean}$
<b>ETHYL ACETATE</b>	<b>7.343*10<sup>4</sup></b>	<b>0.404</b>
<b>PROPYL ACETATE</b>	<b>0.993 *10<sup>5</sup></b>	<b>0.053</b>

From the values in table 4.9 and with the help of eqn (7) above, the equilibrium values can then be estimated at temperature ranges within which  $(-\Delta H_{\text{rxn}})$  and  $K^0_{\text{eq}}$  values were evaluated.

#### 4.9 CONCLUSIONS

A new technique has been proposed and demonstrated for the determination of thermodynamic quantities (Heat of reaction and equilibrium constants) for exothermic reversible processes by utilizing experimental temperature-time information under adiabatic conditions. The proposed method used simple algebraic equations and do not involves derivatives of any function(s). Although the demonstration did not cover higher temperatures, the method is possible to be applied to estimate heat of reactions and equilibrium constants at higher temperatures.

#### 4.10 ACKNOWLEDGEMENTS

N. A would like to thank the National Research Fund (NRF) of South Africa, Directors of Centre of Material Processing and Synthesis (COMPS), Prof. David Glasser and Prof Diane Hildebrandt, University of Witwatersrand, Johannesburg, South Africa for financial support of this work.

#### 4.11 LIST OF SYMBOLS

$\Delta H_{\text{rxn}}$ -heat of reaction (KJ/mol)

H-Enthalpy

$H_0$ - Initial Enthalpy

$\Delta T$  (ad) –adiabatic temperature change (K)

$\Delta \epsilon$  –extent of reaction

A –preexponential factor

B,C – thermistor constants

$C_A$ -concentration of A (mol/L)

$C_p$  –specific heat capacity

$C_{P,AA}$  –specific heat capacity of acetic anhydride

$C_{P,mix}$  –constant heat capacity of reaction mixture (kJ/mol.K)

$C_{P,W}$  –specific heat capacity of water

$E_a$  – activation energy

$I_{total}$  – total current of the circuit

$K_{eqm}^o$  –Equilibrium constant

$m$  –mass

$M_{AA}$  –Mass of acetic anhydride

$M_{AL}$  –Mass of alcohol

$M_{eqv}$  –Equivalent amount of water

$M_T$  –mass of reaction mixture(Kg)

$N_A$  –mole of A (mol)

$Q$  –heat produced by stirrer

$R$  – molar gas constant

$R_2$  – known resistance in the circuit

$-r_A$  –rate of reaction of (A)

$R_{TH}$  – Thermistor resistance

$t$  – time

$T_{amb}$  –ambient temperature

$T_{max}$  –maximum temperature (K)

$T_o$  –initial temperature

T-reactor temperature (K)

$T_s$  – steady state temperature (K)

$T_s$  –steady-state temperature

U –heat transfer coefficient

U –heat transfer coefficient ( $J/m^2 \text{ s.K}$ )

v – total voltage of the circuit

V-Volume of vessel

$V_{out}$  – voltage measured by thermistor

$V_{TH}$  – voltage across thermistor resistance

x-Equilibrium conversion

$\alpha, \beta$ - constants

#### 4.12 REFERENCES

Becker, F. and Maelicke, A. (1967). "Z. Physik. Chem." 55, 280

Bell, R. P. and Clunie, J. C. (1952). "Proc. Roy. Soc." A212, 16

Borchardt, H. J. and Daniels, F. (1957). "J. A. C. S." 79, 41

Glasser, D. and Williams, D. F. (1971). "I & E. C. Fundam" 10, 516

Hartridge, H. and Roughton, F. J. W. (1925). "Proc. Cambridge Phil. Soc." 22, 246

Rand, M. J. and Hammett, L. P. (1950). "J.A.C.S." 72, 287

Bell, R. P. and Clunie, J. C. (1952). "Proc. Roy. Soc." A212, 16

Considine, D. M., (1957) "Process Instruments and Controls Hand book", McGraw-Hill Book Co., Inc., New York, pp. 2 -60.

Scott, P. D., Williams, D. F., and Glasser, D.(1974)." S. Afr. J. Sci.," 70, 10.

## CHAPTER FIVE

*THIS PAPER HAS BEEN PUBLISHED BY INTERNATIONAL INSTITUTE OF SCIENCE, TECHNOLOGY AND EDUCATION (IISTE)USA- JOURNAL OF CHEMICAL AND PROCESS ENGINEERING RESEARCH JUNE 2013, VOL. 10 pp55-94.*

**MODELING AND SIMULATION OF TEMPERATURE PROFILES IN A REACTIVE DISTILLATION SYSTEM FOR ESTERIFICATION OF ACETIC ANHYDRIDE WITH METHANOL**

*N.Asiedu<sup>\*</sup>, D.Hildebrandt<sup>\*</sup>, D.Glasser<sup>\*</sup>*

Centre of Material and Process Synthesis, School of Chemical and Metallurgical Engineering, University of Witwatersrand, Private mail Bag X3, Wits 2050, Johannesburg, South Africa.

\*Authors to whom correspondence may be addressed:

Emails: [nasiedusoe@yahoo.co.uk](mailto:nasiedusoe@yahoo.co.uk)

: [Diane.Hildebrandt@wits.ac.za](mailto:Diane.Hildebrandt@wits.ac.za)

: [David.Glasser@wits.ac.za](mailto:David.Glasser@wits.ac.za)

## ABSTRACT

This paper pertains to an experimental and theoretical study of temperature profiles in a one-stage adiabatic batch distillation/reactor for the production of methyl acetate and acetic acid from the esterification of acetic anhydride with methanol. Basically it deals with the development of a mathematical model for temperature predictions in the reactor. The reaction kinetics of the process was modeled using information obtained from experimental temperature-time data during the esterification processes. The simulation results were then compared with the experimental data. The maximum deviation of the model-predicted temperature from the corresponding experimentally measured was less than 4% which is quite within the acceptable range of experimental results.

**Keywords:** Modeling, Simulation, Reactive distillation, Temperature, Esterification, Acetic anhydride, Methanol

## 5.1 INTRODUCTION

The concept of reactive distillation was introduced in the 1920s to esterification processes, Key (1932). Reactive distillation has thus become an interesting alternative to conventional processes. Recently this technology has been recommended for processes of close boiling mixtures for separation. In the last years investigations of kinetics, thermodynamics for different processes have been made, Bock et al (1997), Teo and Saha (2004), Kenig et al (2000). Reactive distillation is also applied in process production of fuel ether, Mohl et al (1997). Popken (2001) studied the synthesis and hydrolysis of methyl acetate using reactive distillation technique using structured catalytic packing. The synthesis of methyl acetate has also been studied by Agreda et al (1990) and Kerul et al (1998). In this paper, the process considered the reactions of acetic anhydride-methanol for the production of methyl acetate and acetic acid. Most of the works done on the synthesis of methyl acetate through reactive distillation considered acetic acid and methanol reactions. This paper looks at the modeling of the kinetics of the methanol-acetic anhydride process and develops a simulation model for the temperature-time of the reaction as the process proceeds in an adiabatic batch reactor (one stage batch distillation process).

## 5.2 THE MATHEMATICAL MODEL OF THE REACTING SYSTEM

Given an adiabatic batch reactor the mathematical model is made up of a set of differential equations resulting from the mass and energy balances referred only to the reaction mixture because there is no heat transfer.

The stoichiometry of the reaction studied is given below:



$$\Delta H(298\text{K}) = -66\text{kJ/mol} \quad (1)$$

For a constant –volume batch reactor one can write:

$$-r_A = \frac{1}{V} \frac{dN_A}{dt} = -\frac{dC_A}{dt} \quad (2)$$

The energy balance equation can be established as:

Heat generated = Heat absorbed by reactor contents +

$$\text{Heat transferred through reactor walls} \quad (3)$$

$$(-\Delta H)(-r_A)Vdt + Q_{\text{stirrer}}dt = mC_p dT + UA (\Delta T)dt \quad (4)$$

$$\text{Given } (-r_A) = \frac{d\varepsilon}{dt} \quad (5)$$

where ( $\varepsilon$ ) is the extent of reaction, we can rearrange eq(6) to give eq(8) below:

$$UA (\Delta T)dt + mC_p = (-\Delta H) \frac{d\varepsilon}{dt} \quad (6)$$

Assume that heat given by stirrer speed ( $Q_{\text{stirrer}}$ ) is negligible. Integrating eq(4) gives

$$(T - T_o) + \frac{UA}{mC_p} \int_0^\infty (T - T_o)dt = \frac{(-\Delta H)}{mC_p} \Delta\varepsilon \quad (7)$$

The LSH of eq(7) can be used to correct experimental data to adiabatic conditions.

It is assumed that the reaction is independent of temperature, hence correcting the experimental data the adiabatic temperature rise parameter ( $\Delta T_{ad}$ ) can be obtained from the experimental result for the process. This adiabatic temperature rise is equal to the RHS of eq(9) or we can write;

$$\Delta T_{ad} = \frac{(-\Delta H)\epsilon}{mC_p} \quad (8)$$

From eq(8) one can easily show that the energy balance equation of an adiabatic batch reactor reduces to a linear form given by eq(9) as:

$$T = T_o + \Delta T_{ad} \epsilon \quad (9)$$

Theoretically the adiabatic temperature rise is by definition obtained when extent of reaction ( $\epsilon$ ) =1 or conversion ( $x$ ) = 1, with respect to the reactant of interest and its value can be computed in advance from the initial conditions (temperature and heat capacities) of the reacting species. Equation (9) also allows one to find extent of reaction and or conversion at any instant under adiabatic conditions by using only one measure of temperature. Then from the initial concentrations of the reactants the concentrations products can be monitored at any instant in the reactor.

### 5.3 THE EXPERIMENTAL SET-UP

The experimental set- up consist of adiabatic batch reactor (thermos-flask) made up of 18/8 stainless steel thermos-flask of total volume of 500mL equipped with a removable magnetic stirrer as shown in figure (5.1) The flask is provided with a negative temperature coefficient thermistor connected on-line with a data-logging system. The signal from the sensor (thermistor) is fed to a measuring and a control unit amplifier and a power interface. The acquisition units are connected to a data processor. A process control engineering support data management. The data acquisition system called Clarity has the following part numbers: C50 Clarity Chromatography SW, single instrument, 3 x 55 Clarity Add-on instrument SW, 194 (INT9 quad channel A/D converter card). The hardware is INT9 PCI A/D 24 bit converter. The properties: Input signal range 100mV -10V.

Acquisition frequency 10 -100Hz, Internal A/D converter ( INT9-1 to 4 channel PCI A/D converter). All physically available analog inputs and outputs as well as virtual channel are all

automatically monitored and the process values are stored. The process values are transmitted in such a way that the computer screen displays profiles of voltage-time curves. Data acquisition software was used to convert the compressed data form of the history file on the hard disk into text file format. The text files are converted to excel spreadsheet and the data are then transported into matlab 2010a for analysis.

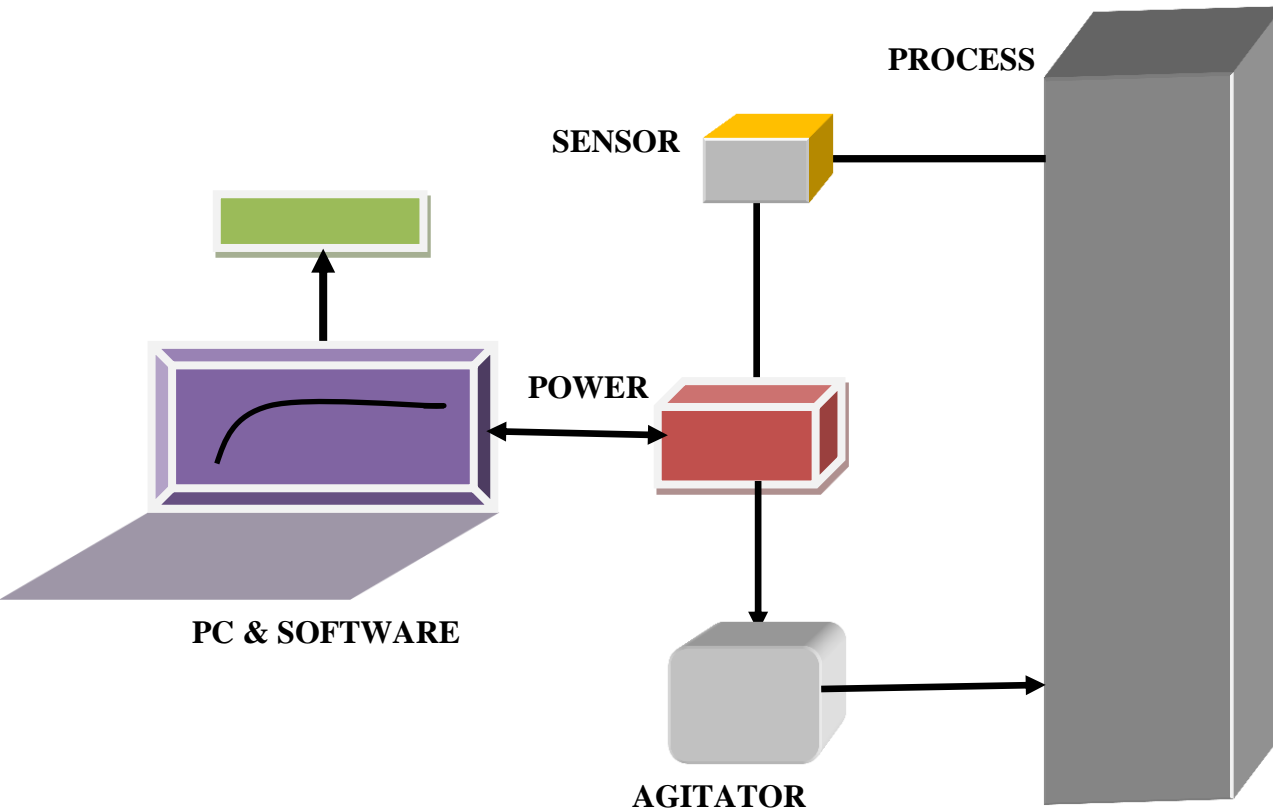
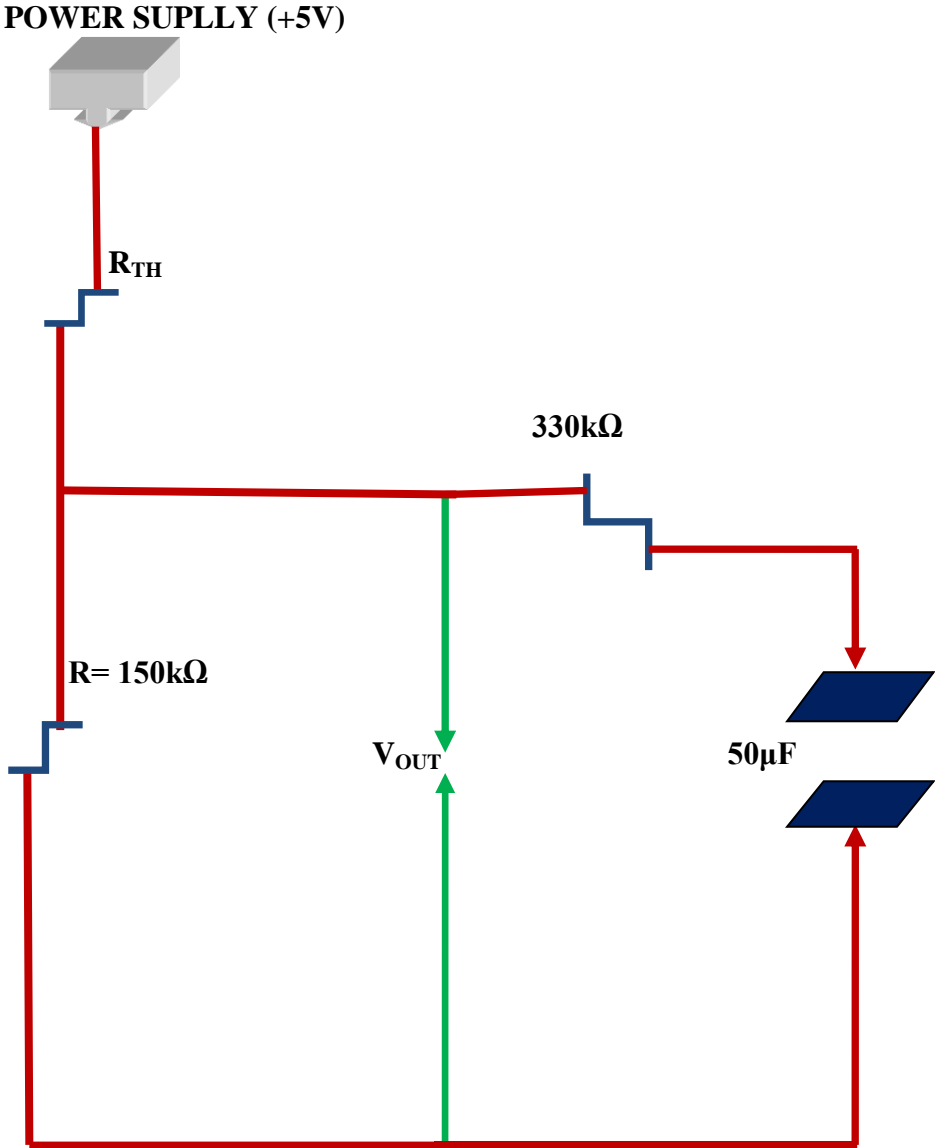


Figure (5.1): Block diagram of experimental set-up

#### 5.4 THE THERMISTOR CALIBRATION

This section describes the experimental details concerning the measurements of liquid phase reactions by temperature-time techniques. Temperature changes are a common feature of almost all chemical reactions and can be easily measured by a variety of thermometric techniques. Following the temperature changes is useful especially for fast chemical reactions where the reacting species are not easily analyzed chemically. This section thus describes the theory and the calibration of the thermistor used in the experiments described in this paper.

5.4.1 THE ELECTRICAL CIRCUIT OF THE SYSTEM



Figure(5.2): The electrical circuit of the system

### 5.4.2. THE CIRCUIT THEORY

From Kirchhoff law's we can write:

$$V_{out} + V_{TH} = 5V \quad (10)$$

$V_{out}$  – Voltage measured by thermistor during the course of reaction.

$V_{TH}$  – Voltage across resistance ( $R_{TH}$ ).

From (10) one can write:

$$V_{TH} = 5V - V_{out} \quad (11)$$

$$R_{TH} = \frac{V_{TH}}{I_{total}} \quad (12)$$

From the circuit  $V_{TH}$  and  $I_{total}$  are unknowns.  $R_{TH}$  is resistance due to the thermistor, and  $I_{total}$  is the same through the circuit and can be determine as :

$$I_{total} = \frac{V_{out}}{R} \quad (13)$$

$V_{out}$  is known from experimental voltage –time profile and R (150k $\Omega$ ) is also known from the circuit. Thus when  $I_{total}$  is determined from eq(13),  $R_{TH}$  which is the thermistor's resistance and related to temperature at any time during the chemical reaction can be determine as:

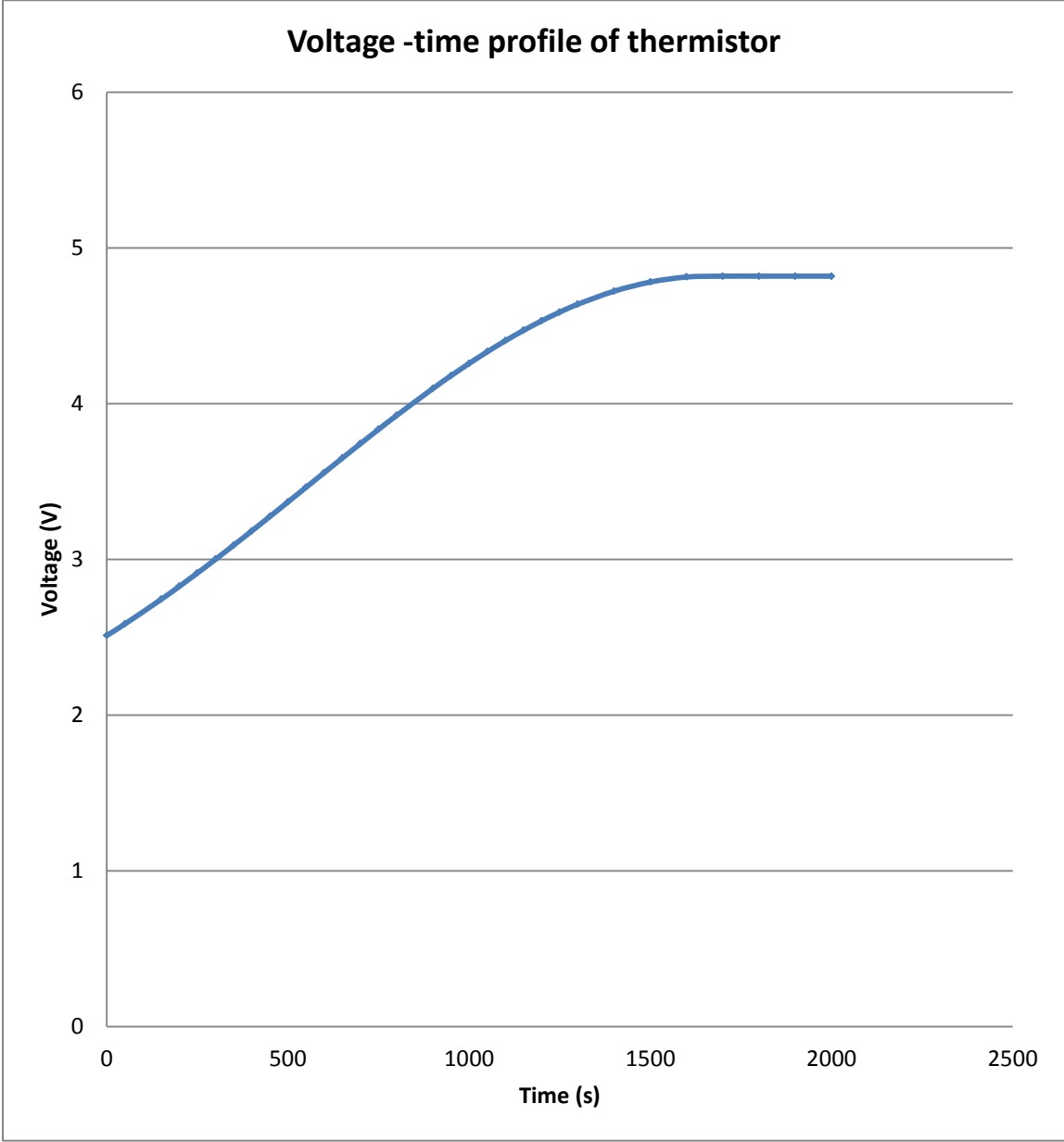
$$R_{TH} = \frac{V_{out}}{I_{total}} \quad (14)$$

### 5.4.3 THE THERMISTOR CALIBRATION

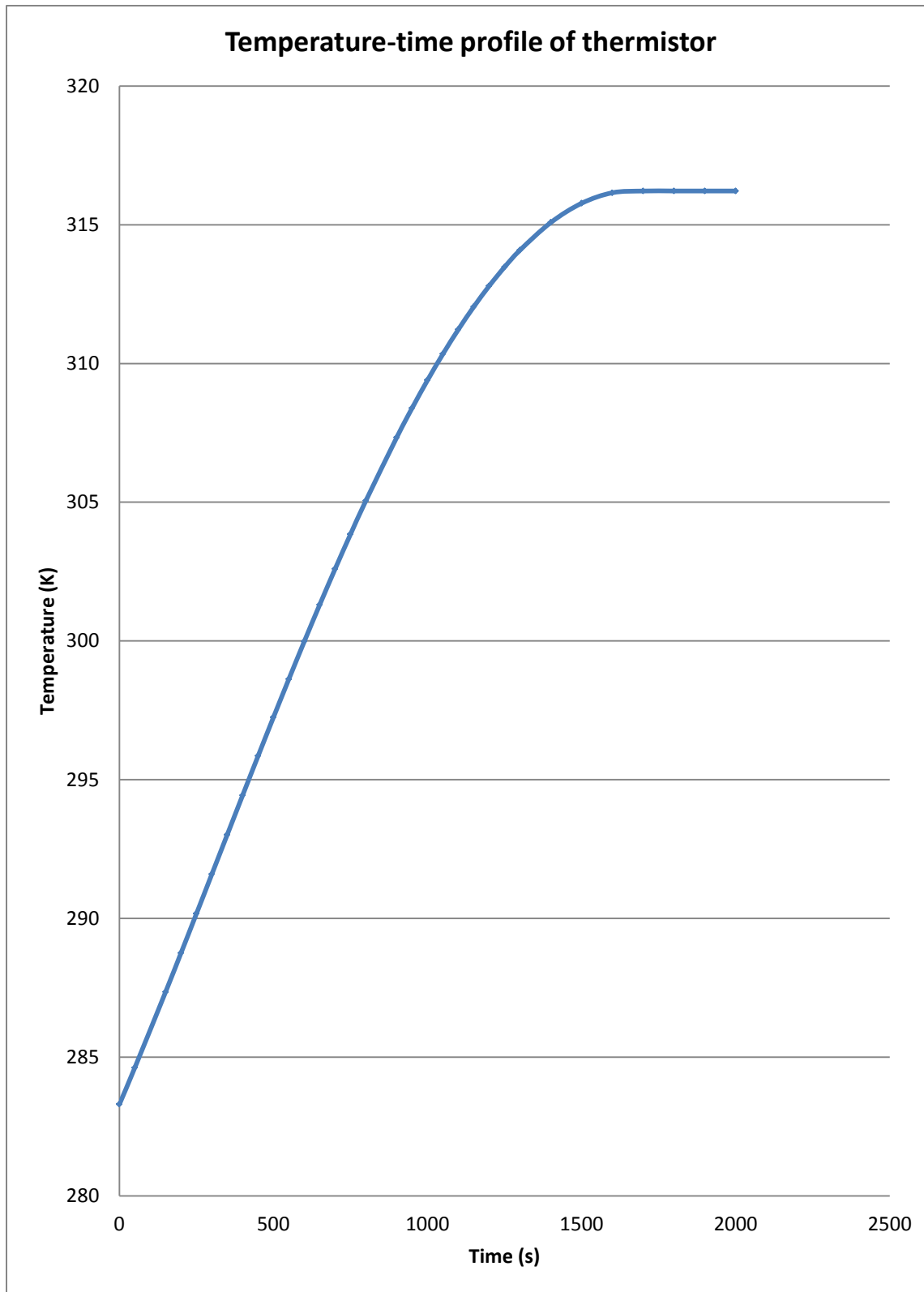
The thermistor used in the experiments was negative temperature coefficient with unknown thermistor constants. The calibrations involve the determination of the thermistor constants and establish the relationship between the thermistor's resistance and temperature.

This was done by fitting both the thermistor and an electronic digital temperature measuring device in a sealed vessel and the system ws slowly warmed until the voltage reaches it asymptotic state.The thermistor was connected to a computer with data acquisition software to

provide data of voltage –time real-time plot as shown in figure (3) below. The voltage –time data was used to match the temperature-time data obtained from the electronic digital temperature device.



Figure(5.3): The thermistor voltage-time profile



Figure(5.4): The thermistor temperature-time profile

#### 5.4.4 RELATIONSHIP BETWEEN THERMISTOR RESISTANCE AND TEMPERATURE

Thermistor resistance ( $R_{TH}$ ) and Temperature (T) in Kelvin was modeled using the empirical equation given developed by Considine (1957)

$$R_{TH} = \exp\left(\frac{B}{T} + C\right) \quad (15)$$

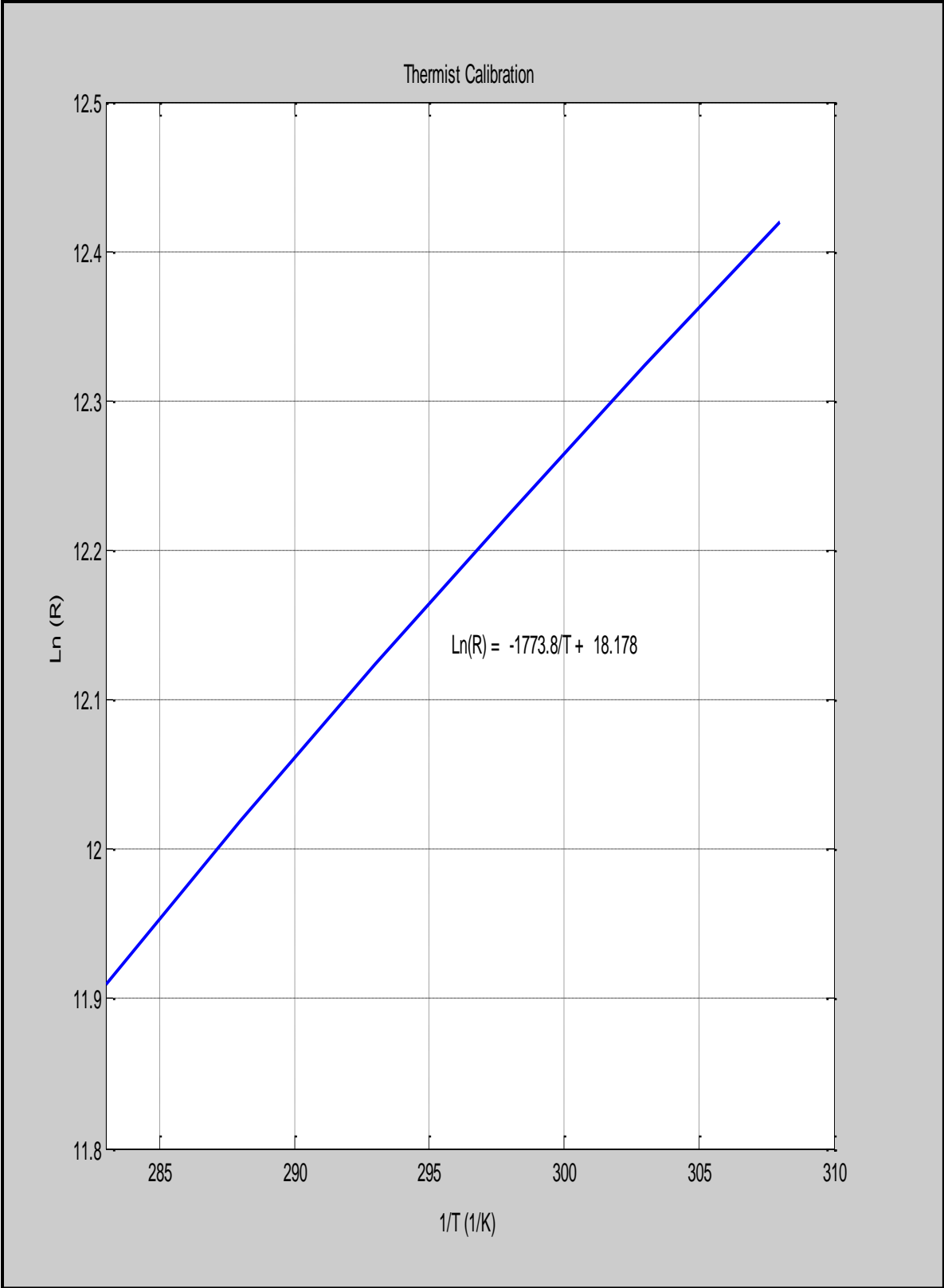
or

$$\ln(R_{TH}) = \frac{B}{T} + C \quad (16)$$

where the parameters (B) and (C) are the thermistor constants and were obtained from experimental calibration using warm water. The constants were determined by fitting the “best” least square straight line plot of  $\ln(R_{TH})$  against  $1/T$ , giving the thermistor equation as:

$$\ln(R_{TH}) = -\frac{1773.8}{T} + 18.178 \quad (17)$$

The calibration plot is shown in figure (5.5) below:



Figure(5.5): Regression line of  $\ln(R_{TH})$  against  $1/T$

## 5.5 THE REACTOR (THERMOS-FLASK) CALIBRATION

The reaction vessel used was an ordinary dewer thermos-flask with removable screw cap lid. The flask has a total volume of 500mL. The calibration involves the determination of the heat transfer coefficient of the flask and fitting the experimental data to the model described in eq(18) below:

$$T = T_S + (T_O - T_S) \exp\left(-\frac{UA}{mC_p} t\right) \quad (18)$$

In this experiment 400.00g of distilled water at 361K ( $T_O$ ) was injected into the reaction vessel and left the system temperature to fall over a period of time until the temperature-time profile reaches its asymptotic state or the steady-state temperature ( $T_S$ ). The figure (5.6) below shows the temperature-time profile of the cooling process.

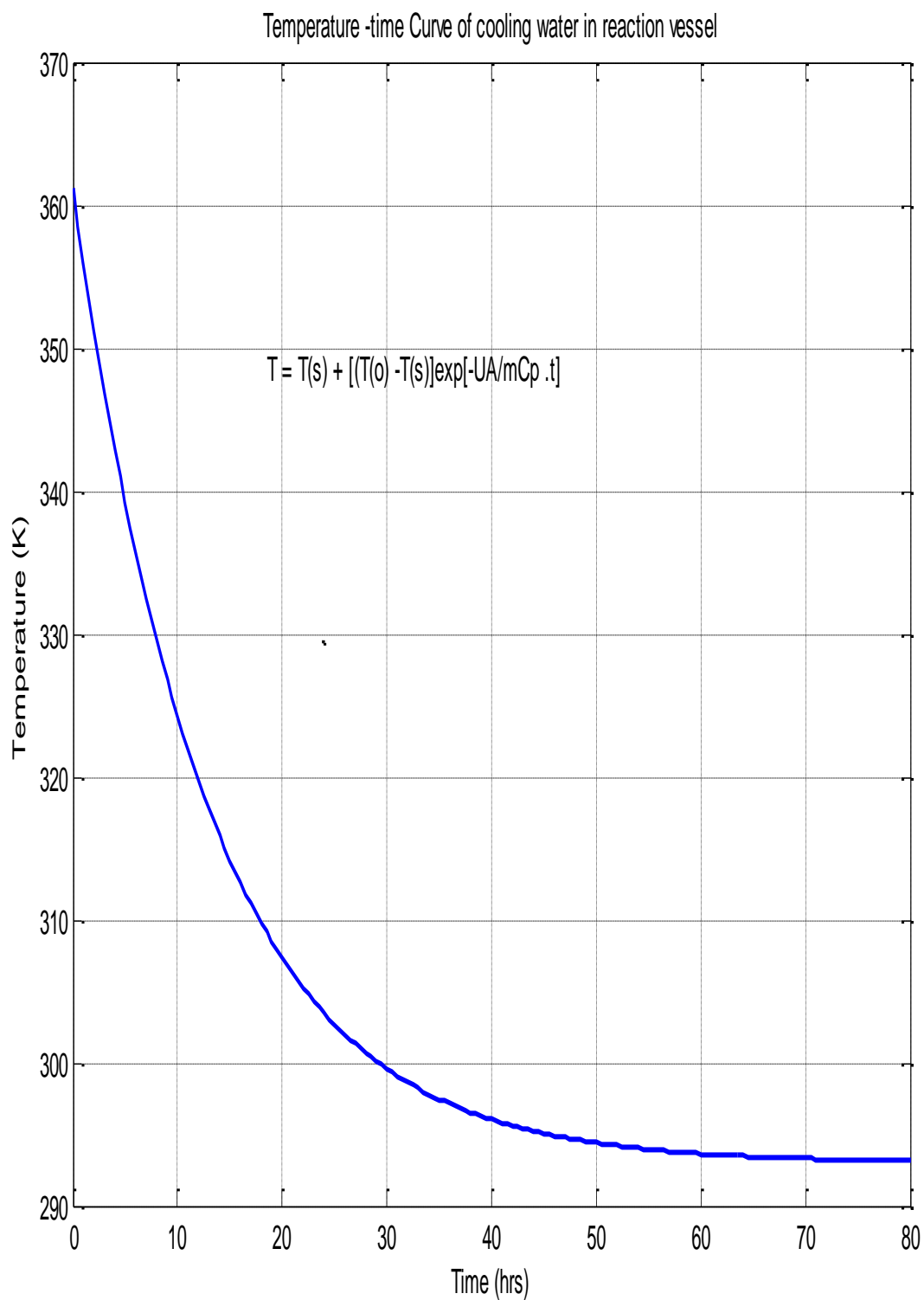


Fig (5.6) : Adiabatic Reactor (Thermos-flask) cooling curve@ T(0) =361K

From eq(18) the values of  $T_o$  and  $T_s$  were obtained from fig(5.6). Rearrangement of eq(18) gives;

$$\ln\left(\frac{T - T_s}{T_o - T_s}\right) = \ln(Y) = \left(-\frac{UA}{mC_p}t\right) \quad (19)$$

Since T and t values are known least square regression analysis was performed and a straight plot of  $\ln(Y)$  against time is shown in figure (5.7) below:

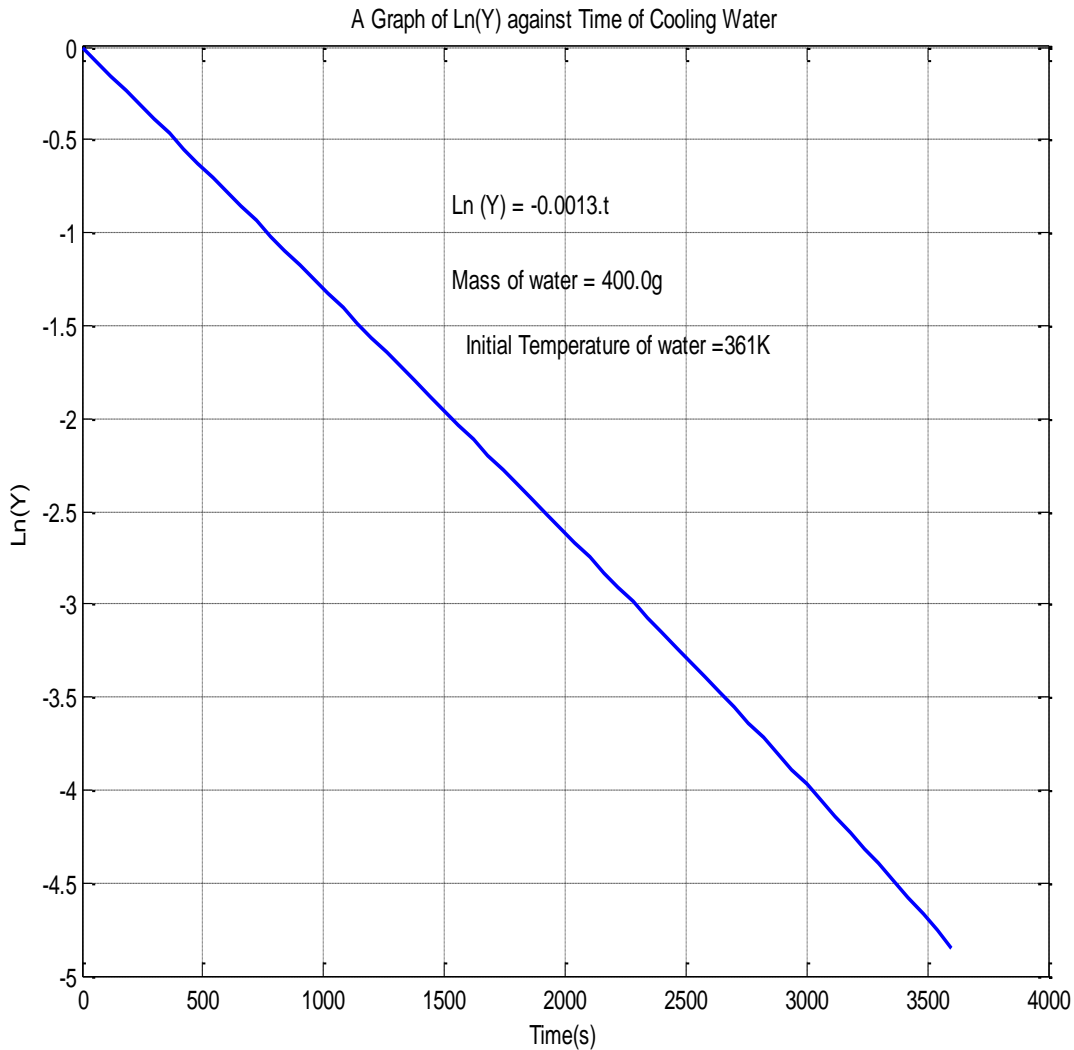


Fig (5.7) :Regression line of heat transfer coefficient of reactor

The slope of the straight line of fig(5.7) is given by  $0.0013s^{-1}$  which corresponds to the value of the heat transfer coefficient of the flask.

## 5.6 EXPERIMENTAL PROCEDURES AND RESULTS

Analytical reagent grade acetic anhydride was used in all the experiments. In all experiments about 1.0 mol of acetic anhydride was poured into the reaction vessel followed by 3.0mols of the methanol. These volumes were used so that at least 60% of the length of the sensor (thermistor) would be submerged in the resulting mixture. Reactants were brought to a steady-state temperature before starting the stirrer. In course of the reaction the stirrer speed was set 1000rev/min and the resulting voltage-time profiles were captured as described above and the corresponding temperature-time curve was determined using the thermistor equation derive in equation (17) above. Runs were carried out adiabatically at the following initial temperatures: 290K, 294K and 300K.

### 5.6.1 DETERMINATION OF $UA/mC_p$ FOR THE REACTION MIXTURE

For a given system (reaction vessel and content) one can write:

$$\left(\frac{mC_p}{UA}\right)_{system} = \left(\frac{m C_p}{UA}\right)_{water} + \left(\frac{mC_p}{UA}\right)_{vessel} \quad (20)$$

In this experiment different amount of water ( $m_w$ ) (200g, 300g and 400g) was injected into the reaction flask at 343.08K, 347.77K and 347.85K and allowed to cool until the temperature reaches a steady-state temperature ( $T_s$ ). Figures (5.8a), (5.9a) and (5.10a) of the cooling processes are shown below. The cooling process thus follows equation (18) above. A nonlinear least-square regression analysis was performed on all the three experimental curves. Using eq(19), the value of  $UA/mC_p$  for each cooling curve was obtained. Figures (5.8b),(5.9b) and (5.10b) shows the regression lines.

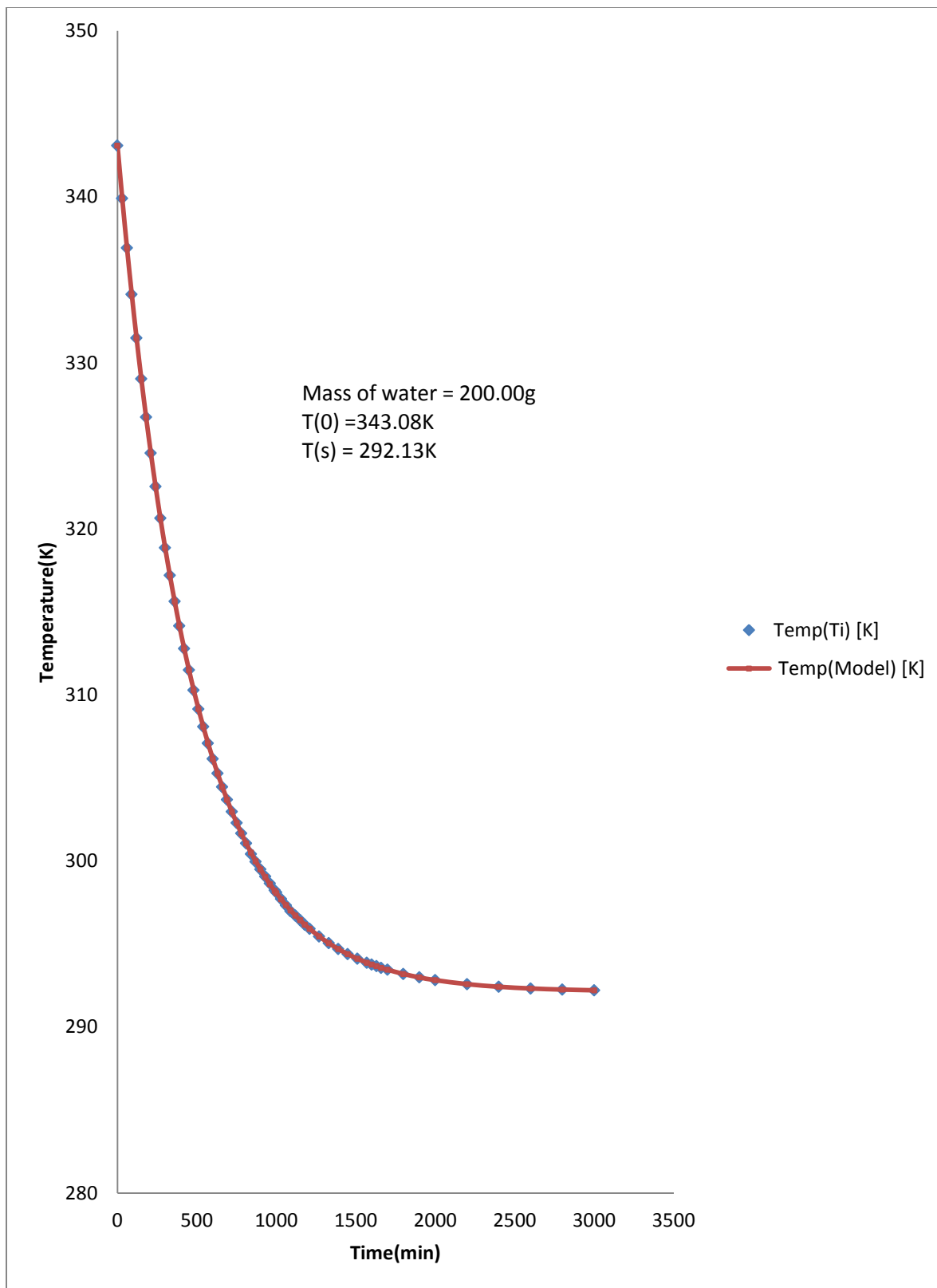


Fig (5.8a): Adiabatic Reactor (Thermos-flask) cooling curve @  $T(0) = 343.08\text{K}$

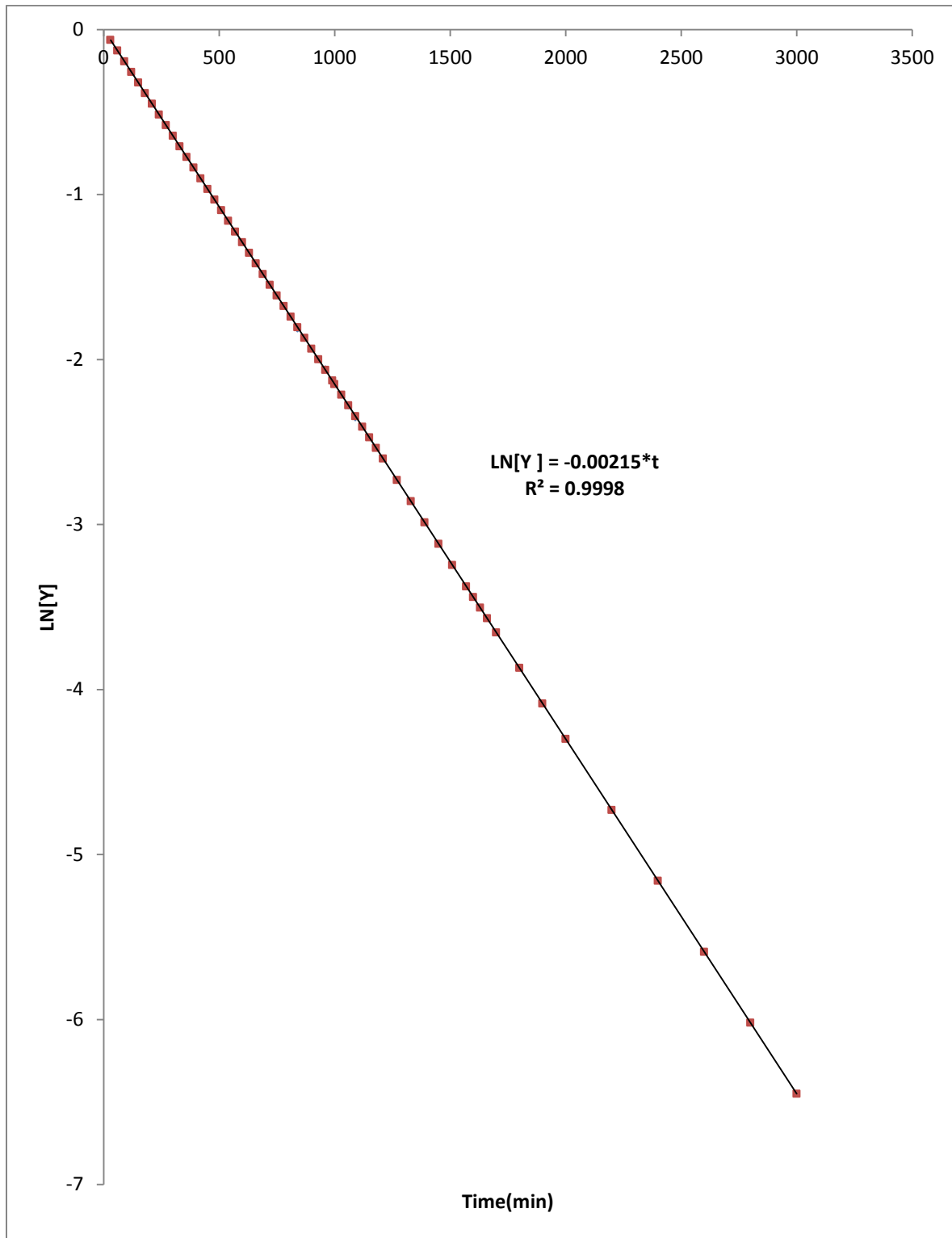


Fig (5.8b): Regression line of heat transfer coefficient of reactor

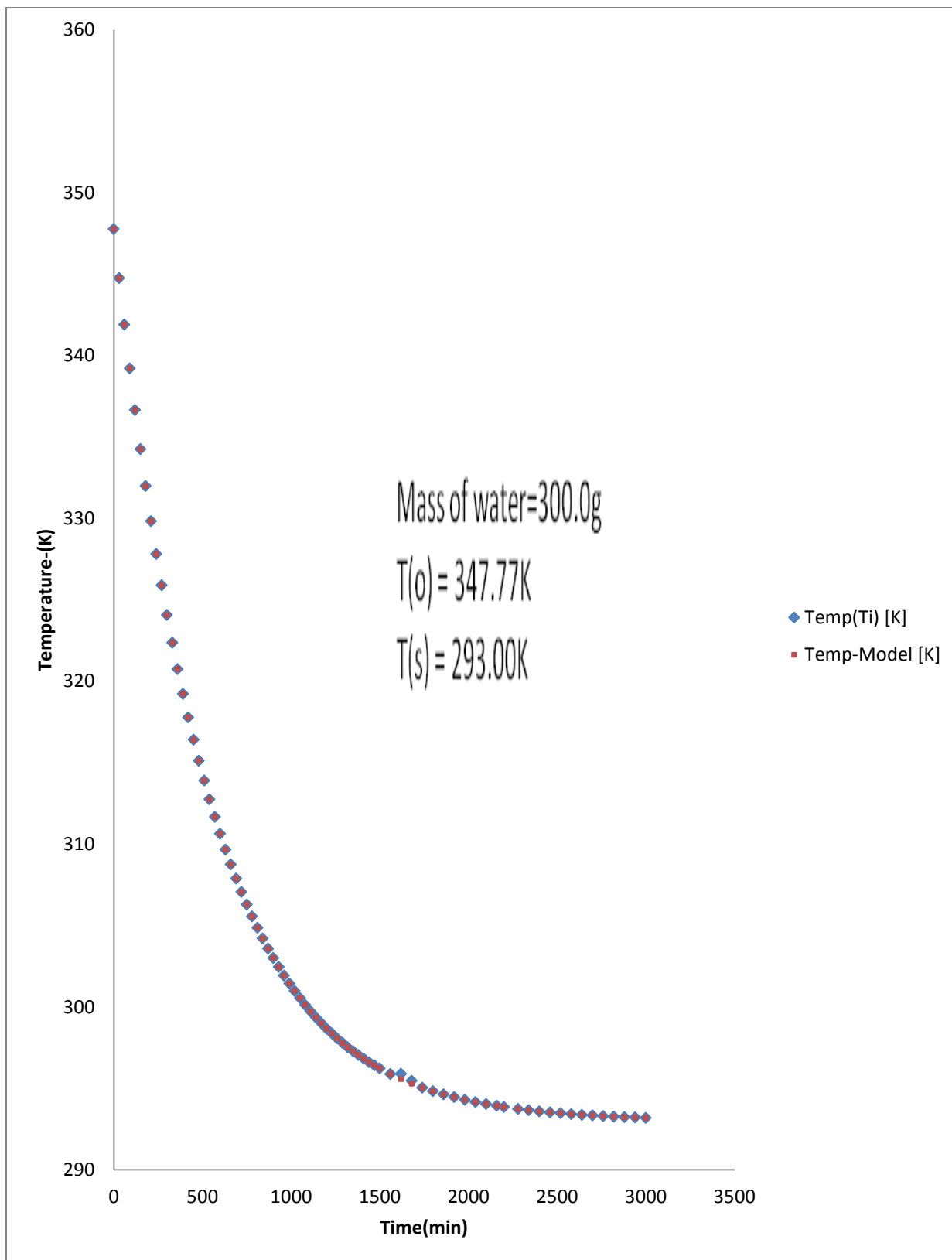


Fig (5.9a): Adiabatic Reactor (Thermos-flask) cooling curve @  $T(0) = 347.77\text{K}$

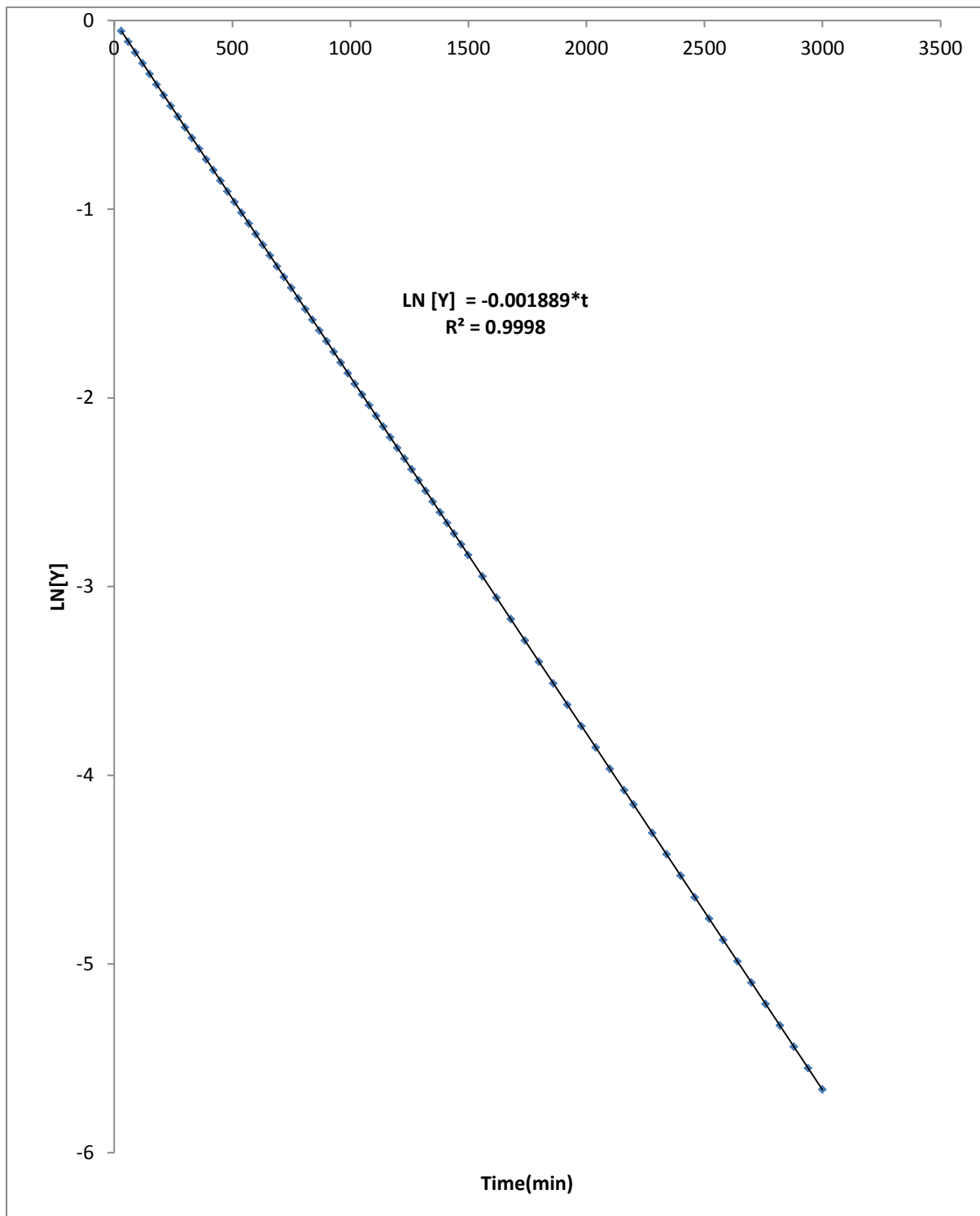


Fig (5.9b): Regression line of heat transfer coefficient of reactor

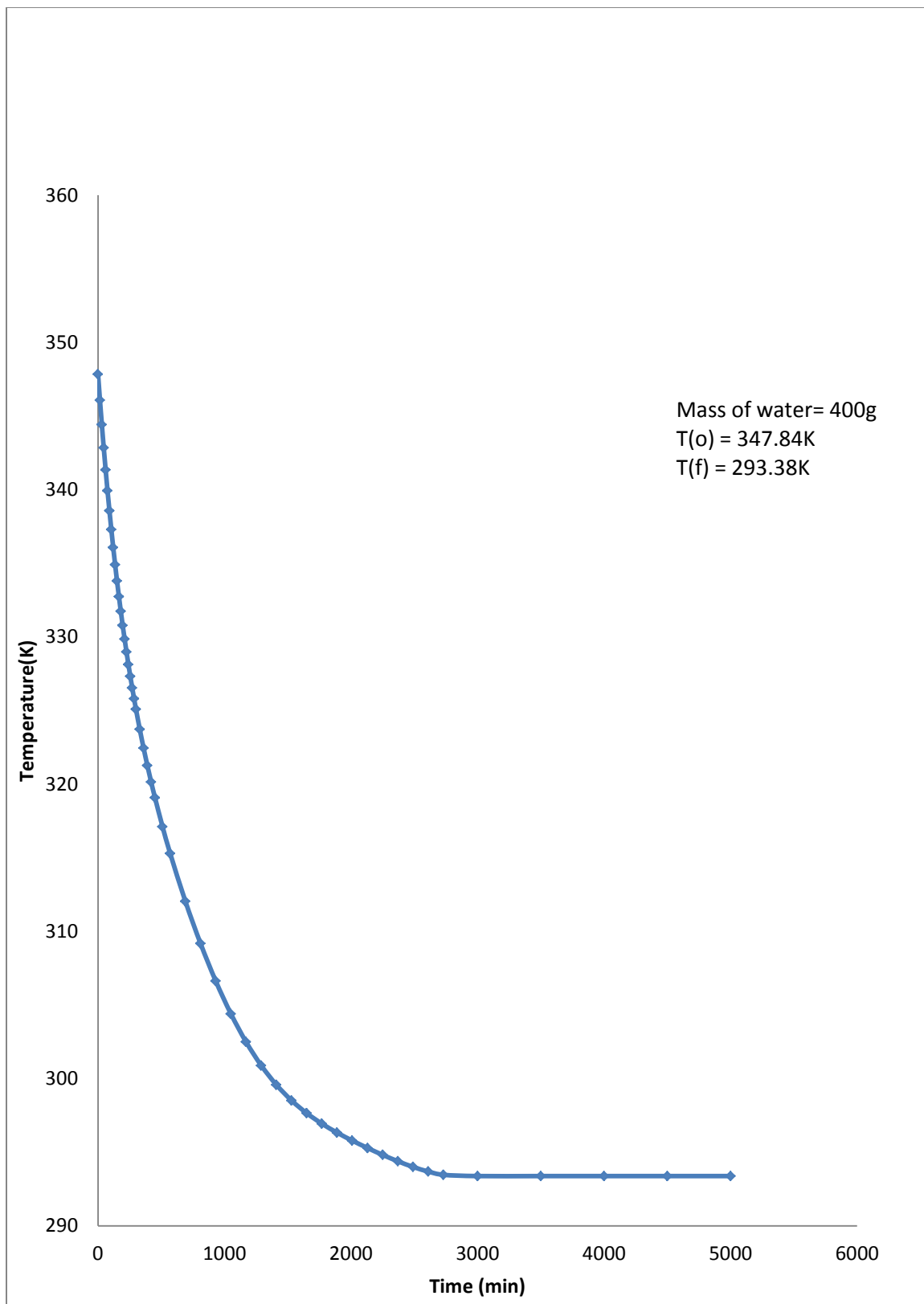


Fig (5.10a): Adiabatic Reactor (Thermos-flask) cooling curve @  $T(0) = 347.80\text{K}$

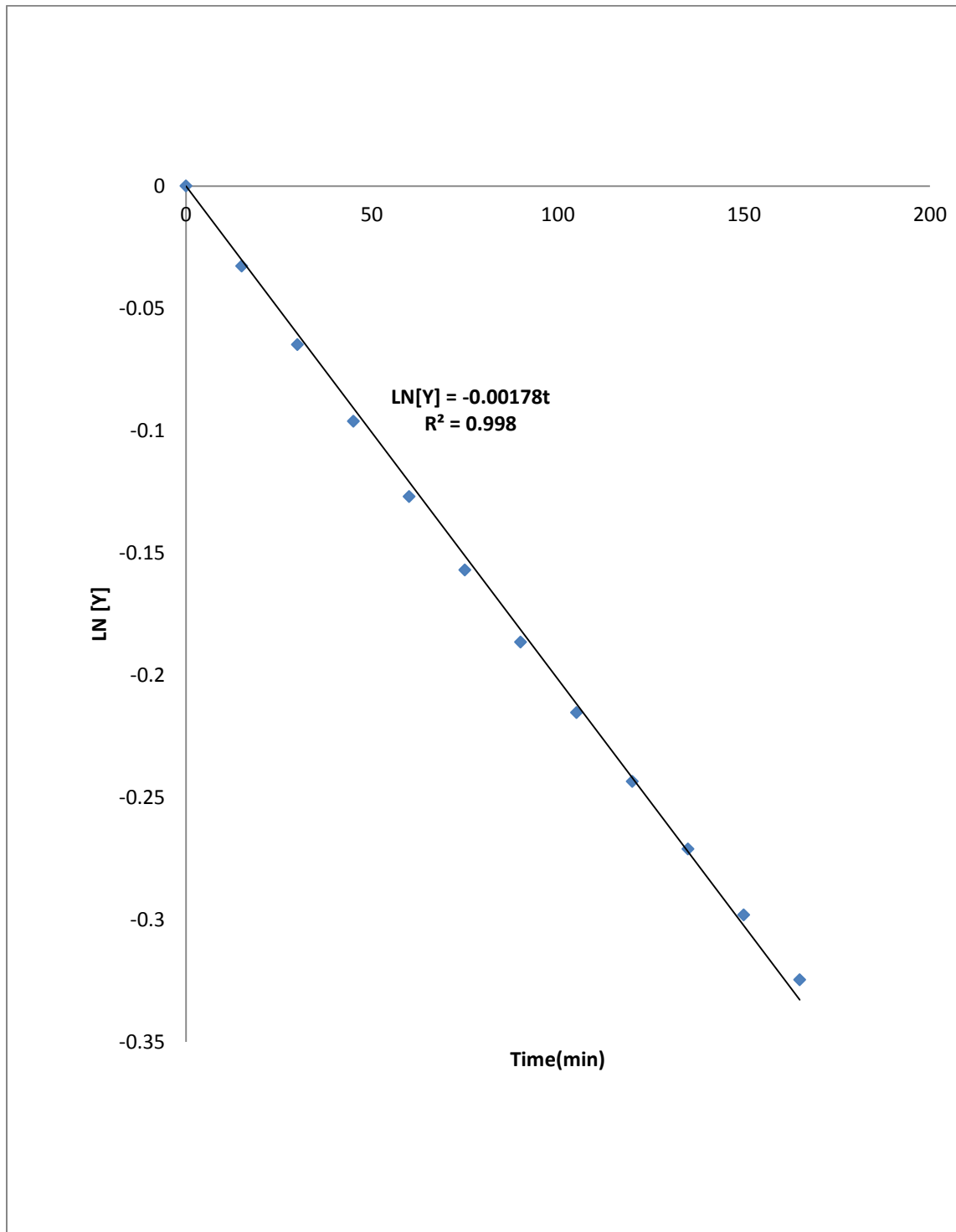


Fig (5.10b): Regression line of heat transfer coefficient of reactor

Table (5.1): Summary of characteristics of figures (5.8)-(5.10)

Mass of water(g)	Initial Temperature(K)	Final Temperature(K)	UA/mCp (min <sup>-1</sup> )
200	343.08	292.13	0.00215
300	347.77	293.00	0.00189
400	347.84	293.38	0.00178

From table (1) a plot of mass of water (m) against (mC<sub>p</sub>/UA) is shown in figure(5.9) below:

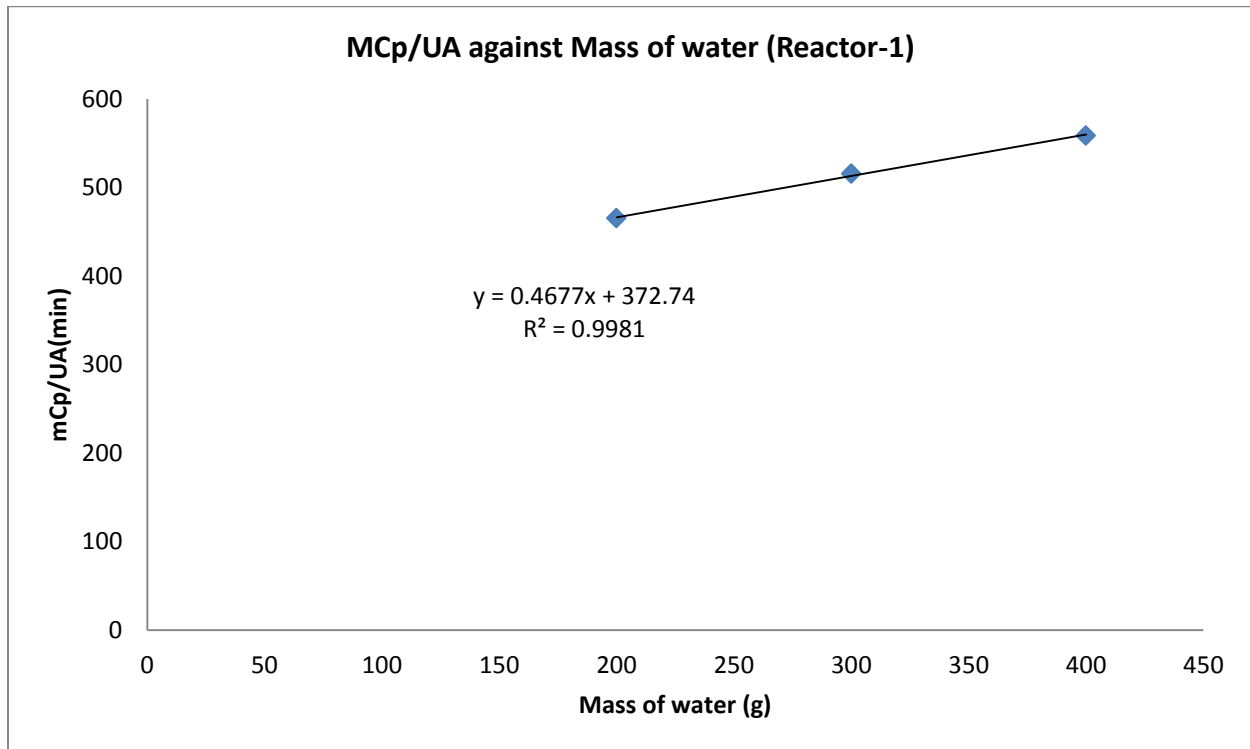


Fig (5.11): A plot of mass of water (m) against (mC<sub>p</sub>/UA)

Table (5.2) below consist of some of the physical constants of the reacting species which was used in the determination of the quantity UA/mC<sub>p</sub>.

Table (5.2) : Some constants of reacting species:

Species	Moles	Molar mass(g/mol)	$C_p$ (J/mol.K)
Acetic anhydride	1.0	102.9	189.7
methanol	3.0	32.04	79.5

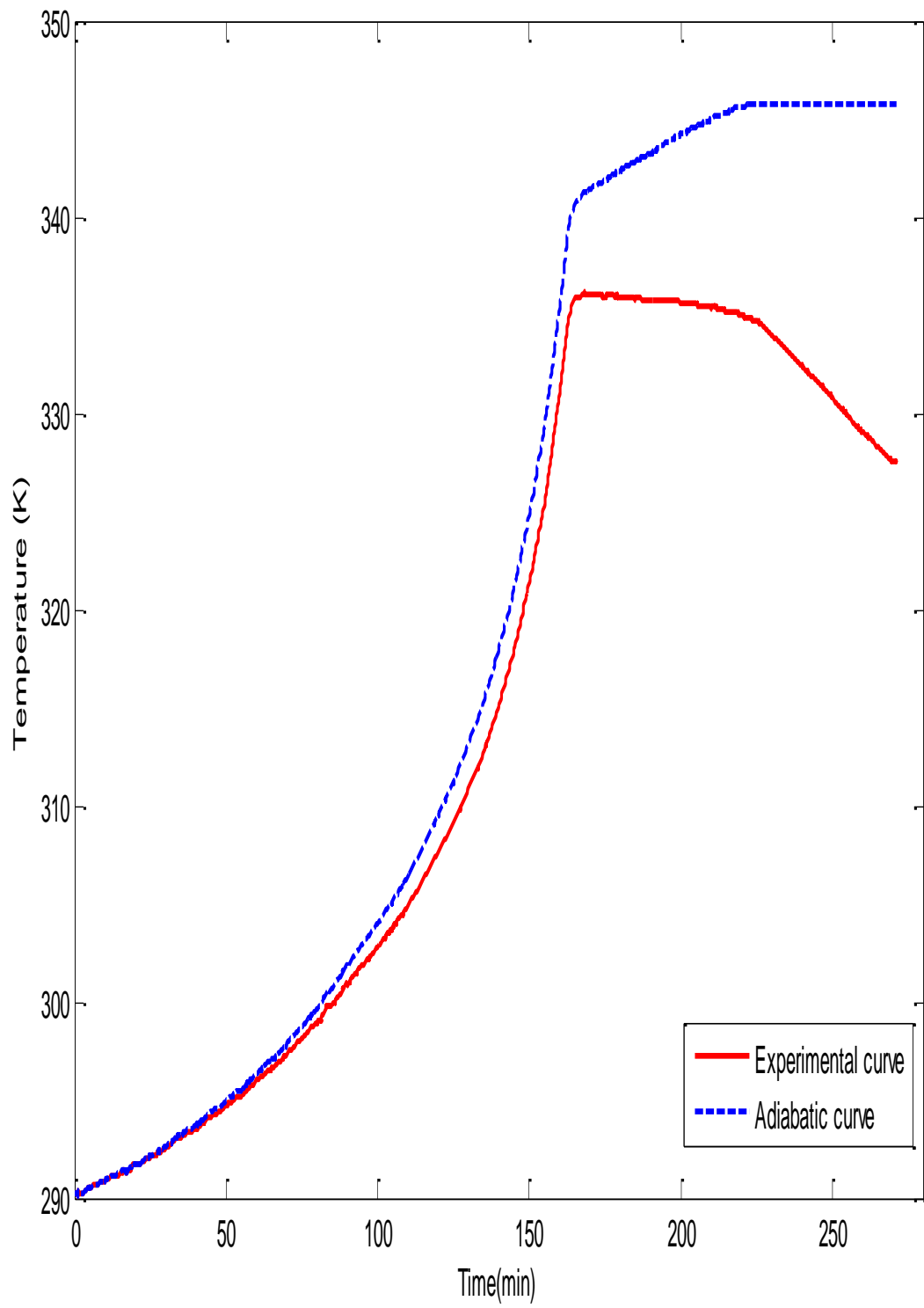
Equation (21) was used to determine specific heat of the mixture ( $C_{P,mix}$ ) and the quantity  $M_T C_{P,mix}$ .

$$C_{P,mix} = \frac{m_{AA}}{M_T} C_{P,AA} + \frac{m_m}{M_T} C_{P,m} \quad (21)$$

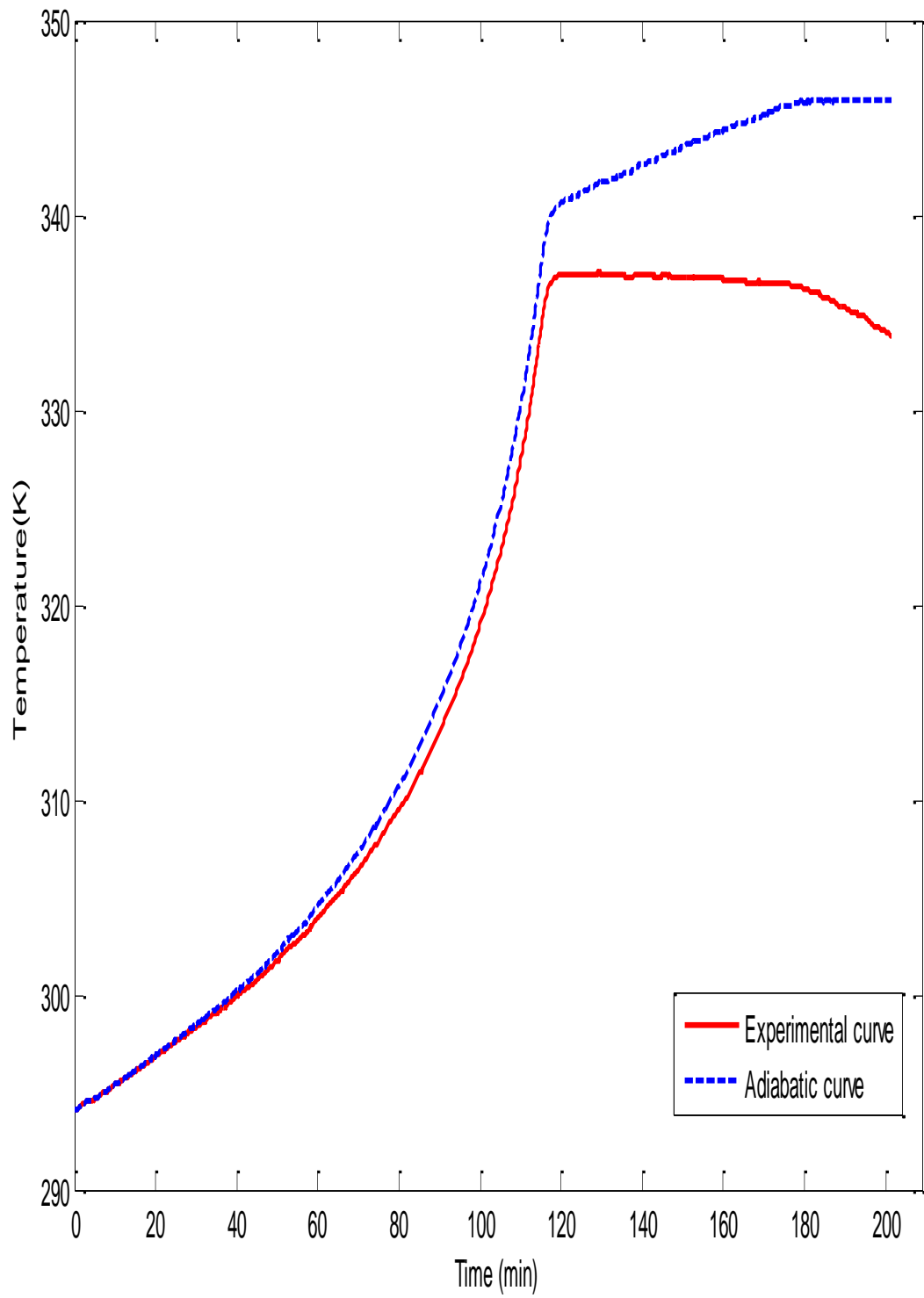
$M_T C_{P,mix}$  was calculated to be 545.19 J/mol. K Since the reaction mixture is not pure water we therefore determined its equivalent mass of water by dividing 545.19 J/mol. K by the specific heat of water;

$$m_{eqv \text{ water}} = \frac{(M_T C_P)_{mix}}{C_{P,water}} = 130.38 \text{ g water} \quad (22)$$

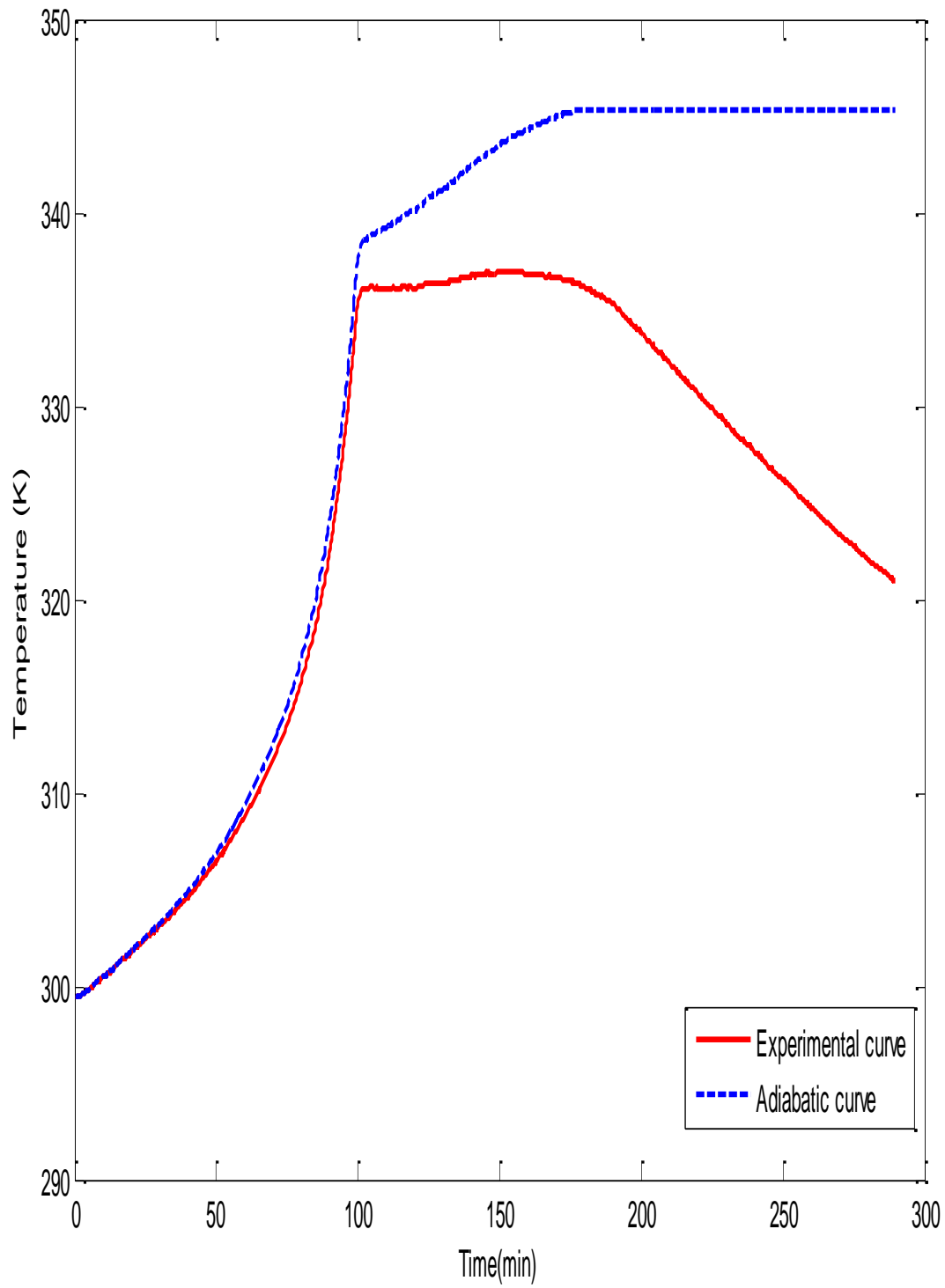
From the equation of the line in figure (9) the value of the quantity  $(UA/mC_p)_{mix}$  was determined to be 0.002307/min. This value was plugged in eq(7) above and the corrections of the experimental results to adiabatic conditions was performed. The figures (5.10),(5.11) and (5.12) below shows the experimental and the corrected temperature profiles for all the three experiments.



Fig(5.12): Experimental and Adiabatic curves of experiment-1



Fig(5.13): Experimental and Adiabatic curves of experiment-2



Fig(5.14): Experimental and Adiabatic curves of experiment-3

Table (5.3) : Summary of the characteristics of the above temperature-time plot:

Experiment	T <sub>0</sub> (K)	T <sub>max(adiabatic)</sub> (K)	ΔT <sub>exp(adiabatic)</sub> (K)
1	290.01	345.80	55.69
2	294.00	345.60	51.9
3	299.20	345.30	46.13

From eq(9) the variation of acetic anhydride concentration with temperature/time was deduces as:

$$C_{AA} = C_{AO} - \beta (T - T_o) \quad (23)$$

The constant (β) in eq(23) was calculated using the initial concentration of the acetic anhydride 4.364 mol/L and the adiabatic theoretical temperature change (ΔT)<sub>adiabatic</sub>. The figures (5.13),(5.14) and (5.15) show how acetic anhydride concentration varies with time for the three experiments.

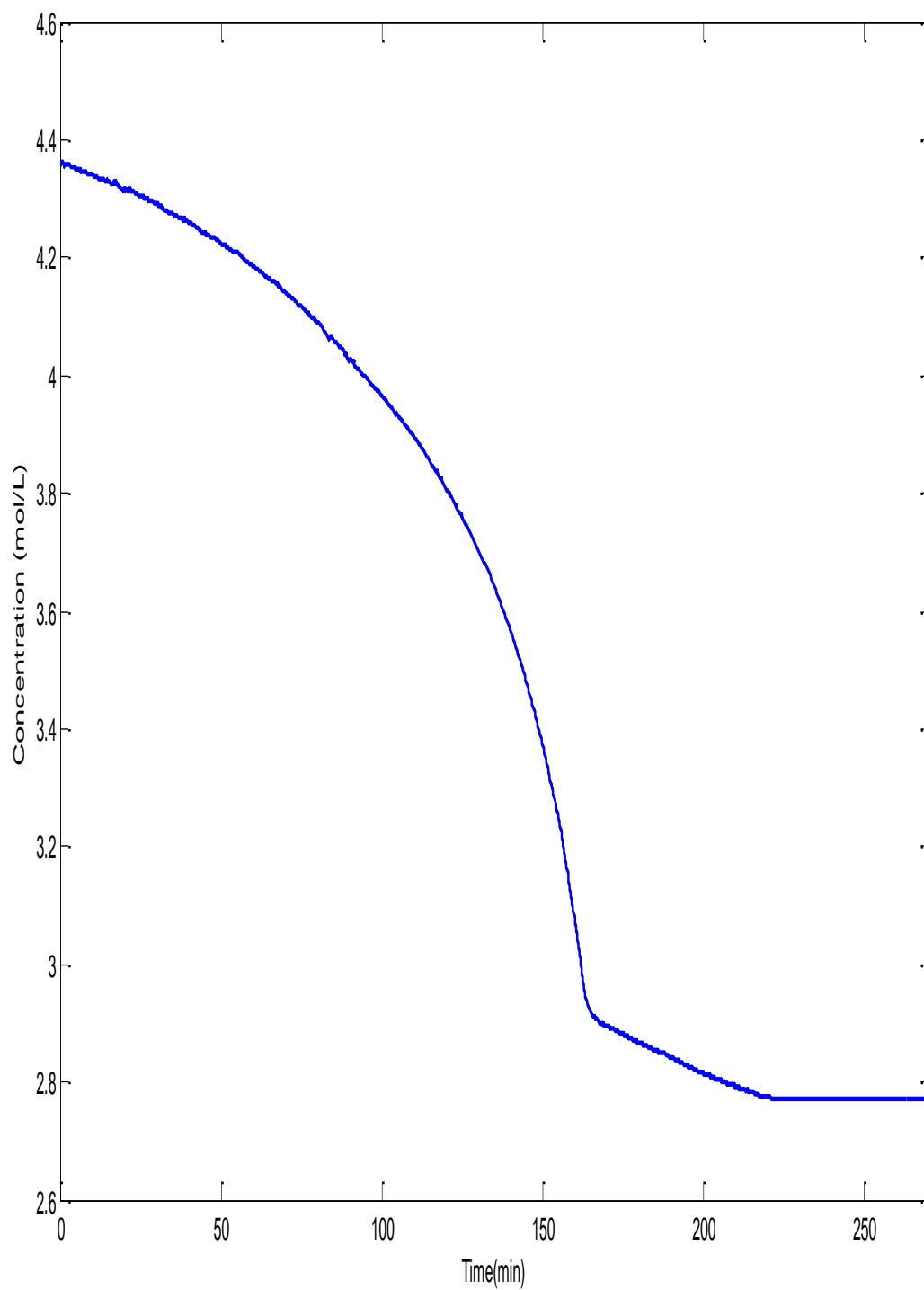


Fig (5.15): Concentration-time plot of acetic anhydride-reaction reaction-Experiment (1)

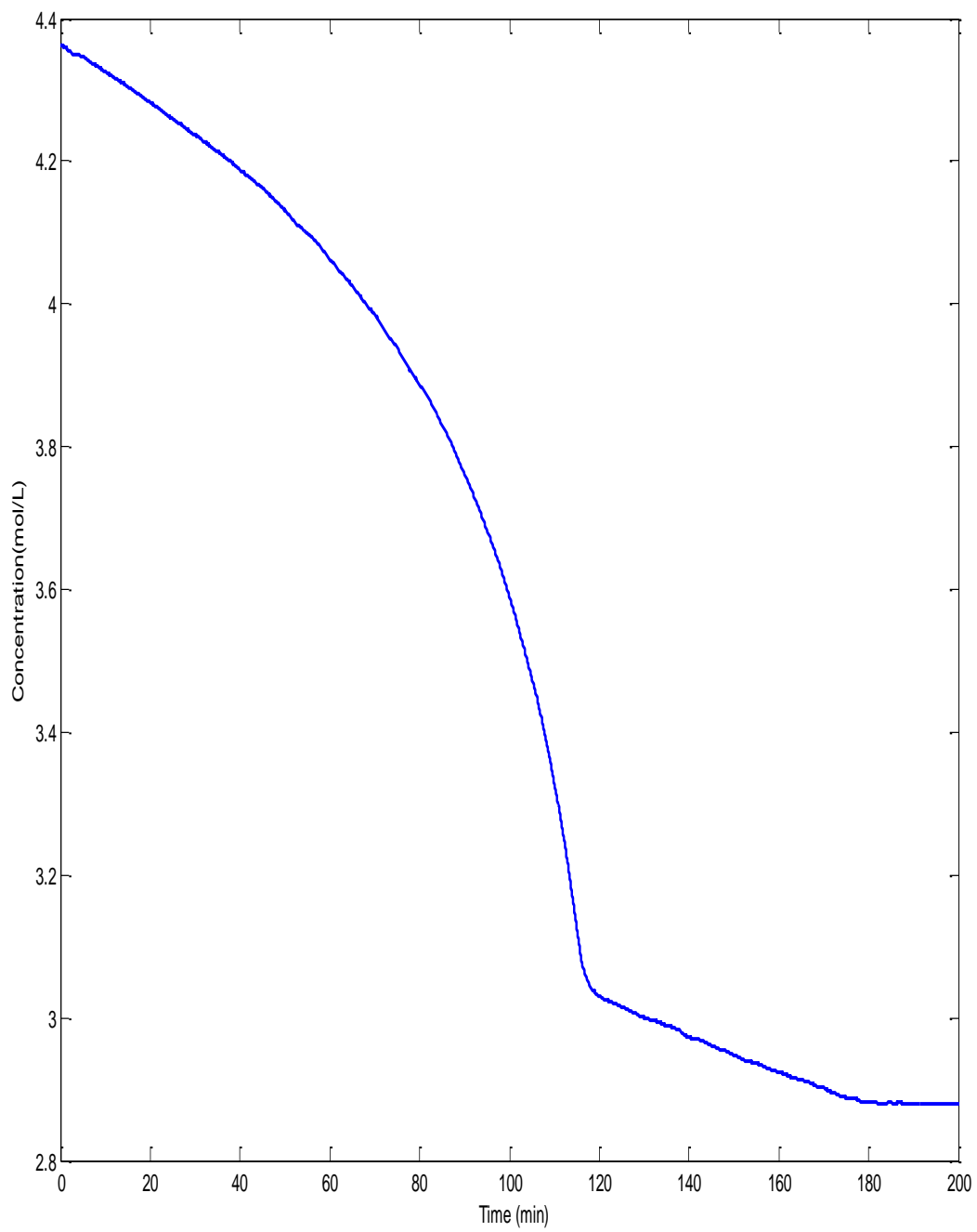


Fig (5.16): Concentration-time plot of acetic anhydride-reaction reaction-Experiment (2)

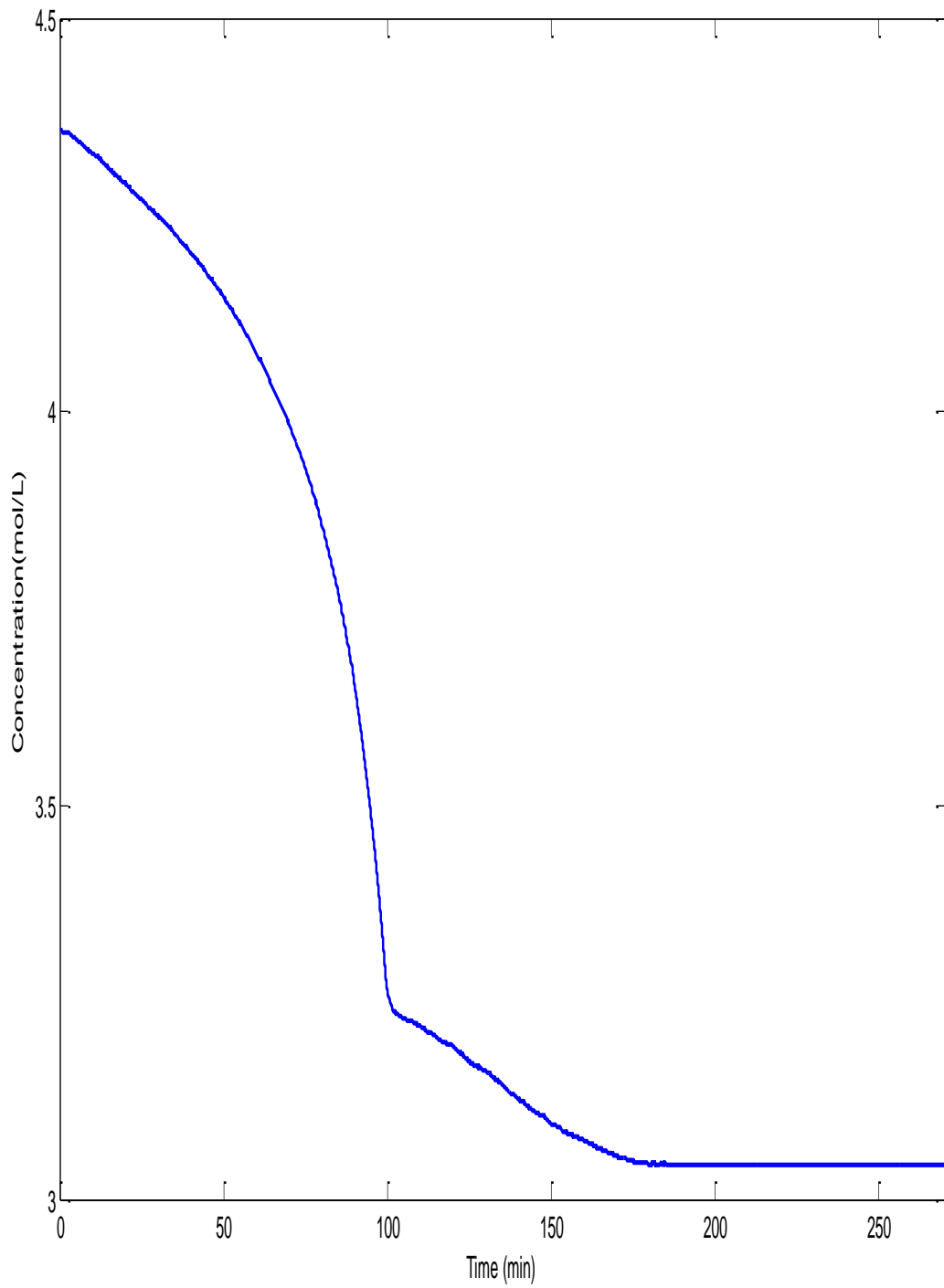


Fig (5.17): Concentration-time plot of acetic anhydride-reaction reaction-Experiment (3)

## 5.7 VARIATION OF RATE OF REACTION WITH CONCENTRATION

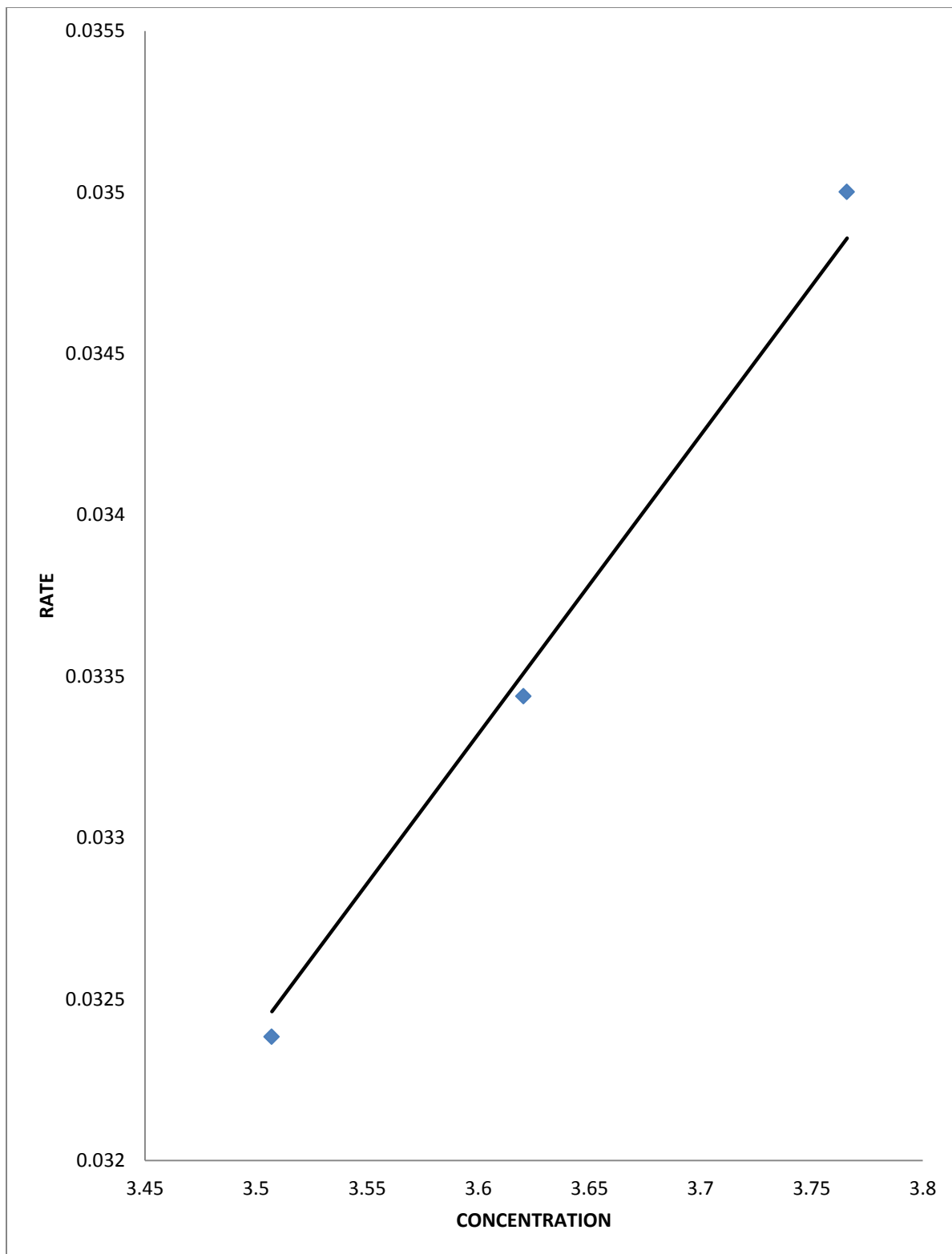
### CHANGE

Table (5.4) : Variations of temperature, rate and concentration at T =320K

T=320K			
Experiment	Concentration	Rate	Rate constant (k)
1	3.507025023	0.03238313	0.00936158
2	3.620338071	0.033438511	0.00923629
3	3.765872632	0.03500009	0.00929425

Average (k) = 0.00936

Standard deviation (k) =  $6.27 \times 10^{-5}$



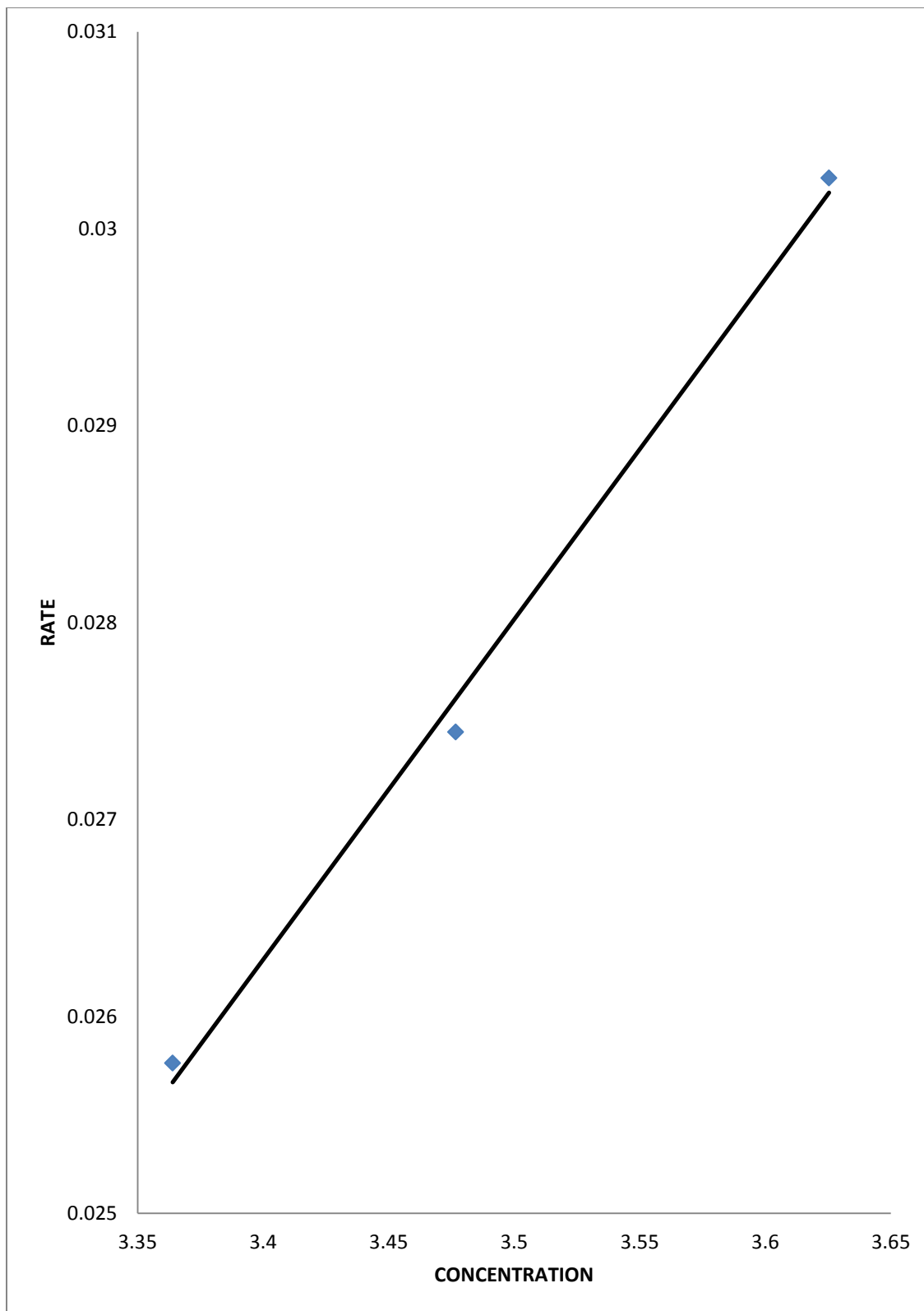
Figure(5.18): Concentration-rate plot @ 320K

Table (5.5) : Variations of temperature, rate and concentration at T =325K

T=325K			
Experiment	Concentration	Rate	Rate constant (k)
1	3.363932095	0.025762791	0.007658535
2	3.476755343	0.027443908	0.00789354
3	3.625365284	0.030256856	0.008345878

Average (k) =0.007966

Standard deviation (k) =0.00035



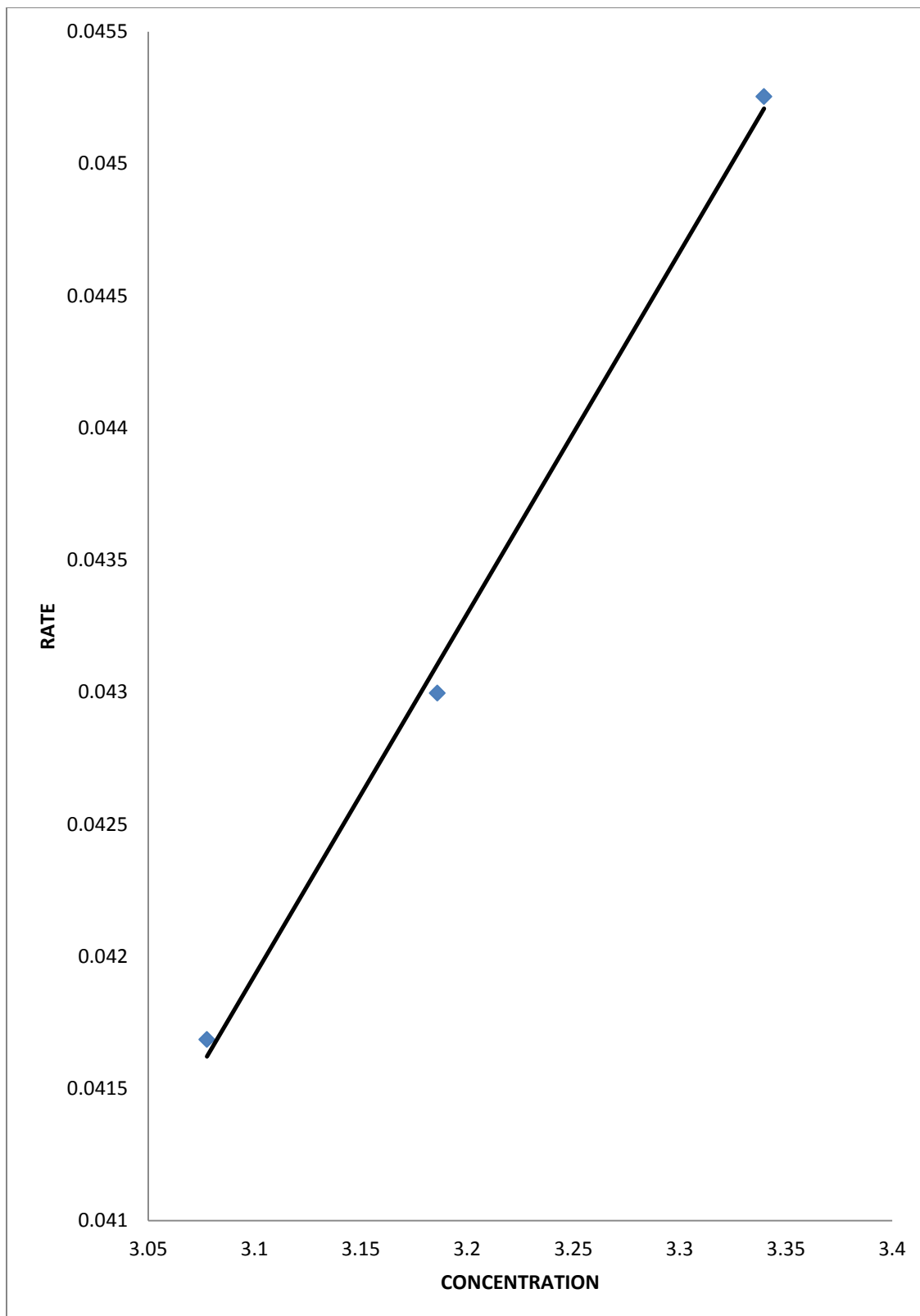
Figure(5.19): Concentration-rate plot @ 325

Table (5.6) : Variations of temperature, rate and concentration at T =335K

T=335K			
Experiment	Concentration	Rate	Rate constant (k)
1	3.077605537	0.041685326	0.013544727
2	3.186062023	0.04299617	0.013495082
3	3.339671258	0.045253824	0.013550382

Average (k) =0.01353

Standard deviation (k) = $3.04 \times 10^{-5}$



Figure(5.20): Concentration-rate plot @ 335K

## 5.8 KINETICS AND THERMODYNAMIC ANALYSIS OF THE EXPERIMENTS

The rate information obtained from the concentration-time plot enabled one to calculate specific rate constant  $k(T)$  of the processes at any time ( $t$ ) and temperature ( $T$ ). Arrhenius plots were thus generated from which kinetic parameters of the runs were extracted. The figures (5.18), (5.19) and (5.20) below show the Arrhenius plots for all the three experiments.

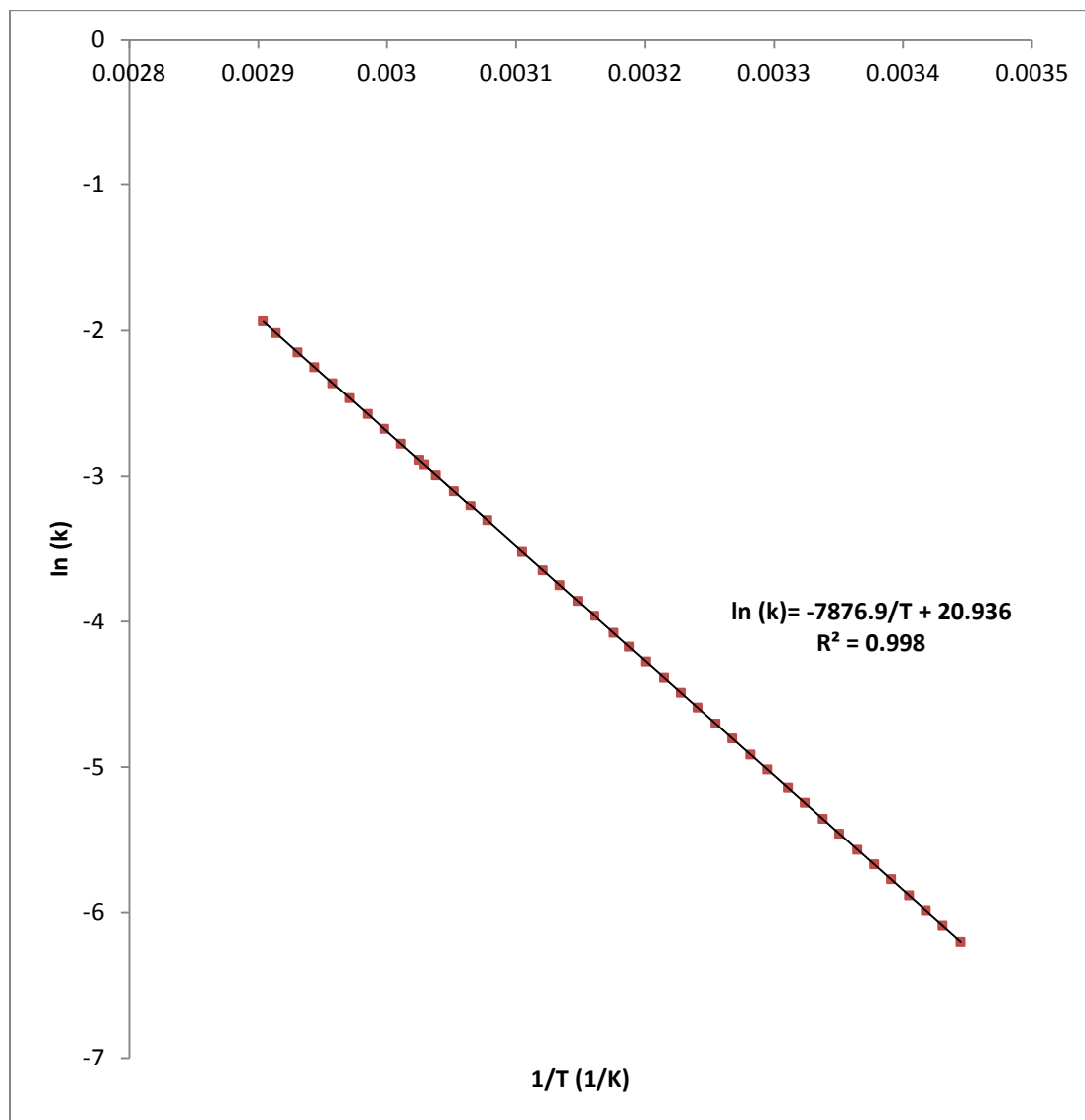


Figure (5.21): Arrhenius plot of experiment-1

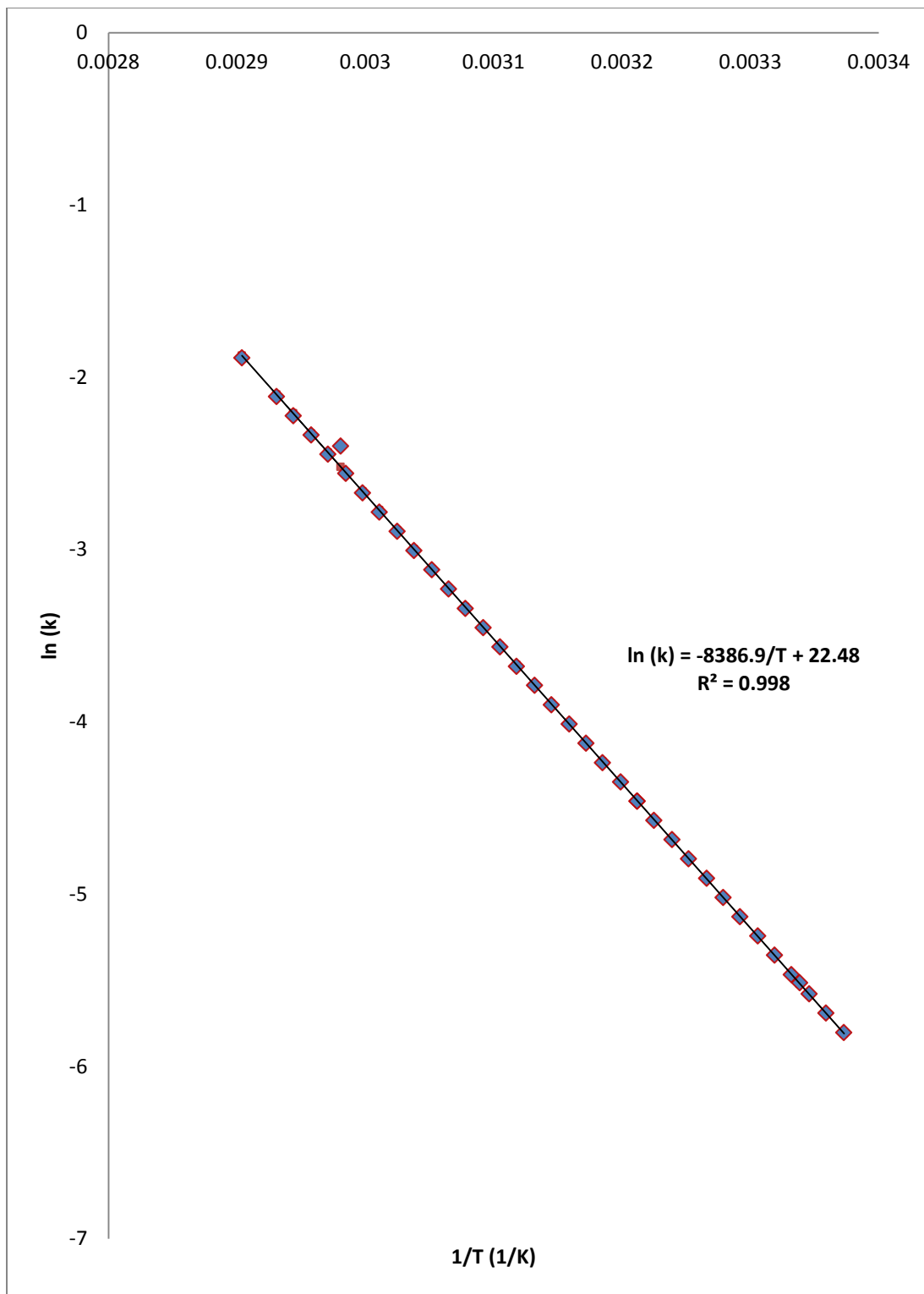


Figure (5.22): Arrhenius plot of experiment-2

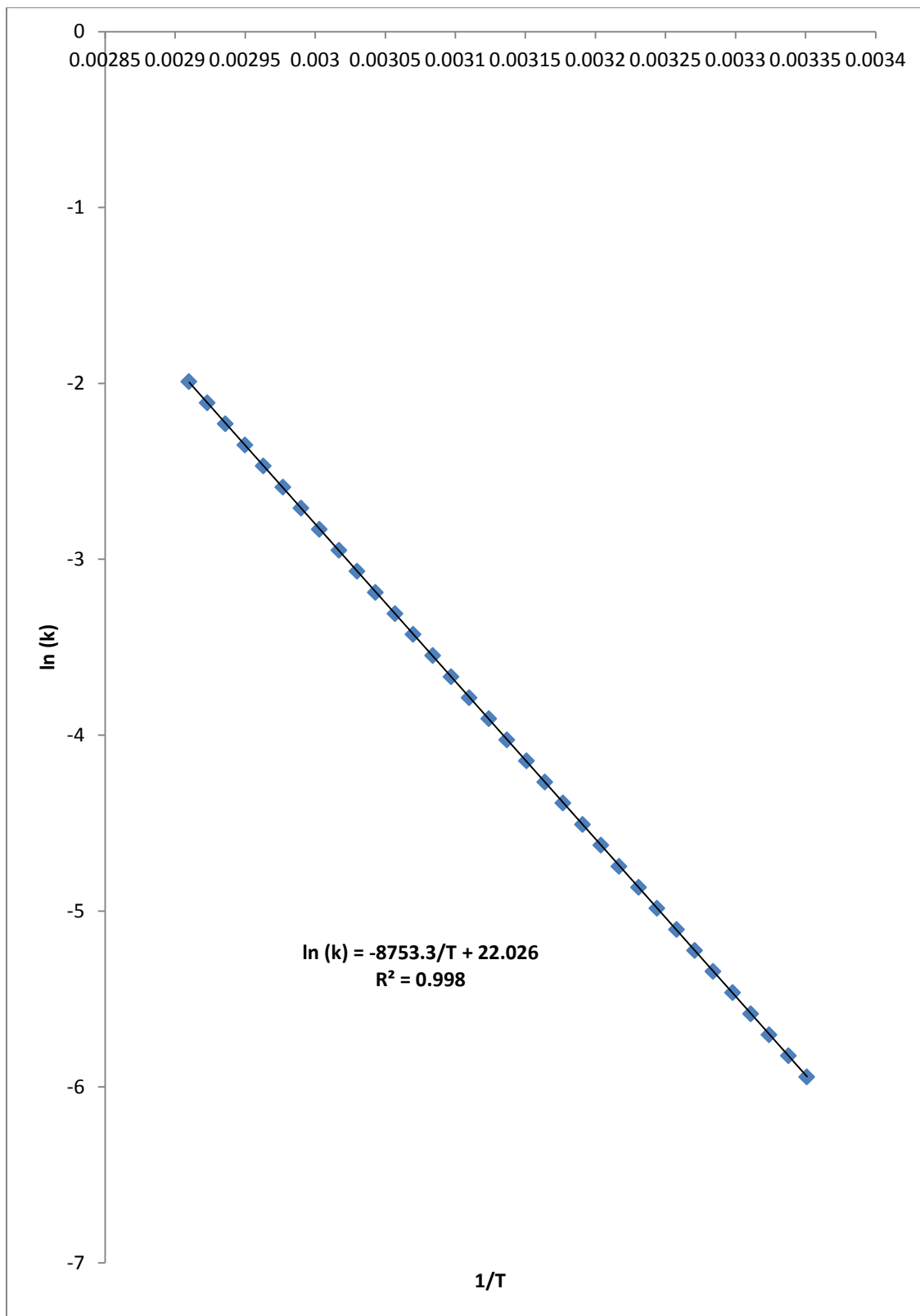


Figure (5.23): Arrhenius plot of experiment-3

The values obtained for the specific rate constants as a function of temperature are given in equations (26),(27) and (28) below:

$$k_1(T) = 1.24 * 10^9 \exp\left(-\frac{65.49}{RT}\right) \quad (24)$$

$$k_2(T) = 5.79 * 10^9 \exp\left(-\frac{69.78}{RT}\right) \quad (25)$$

$$k_3(T) = 3.68 * 10^9 \exp\left(-\frac{72.77}{RT}\right) \quad (26)$$

The thermodynamic information extracted from the experiments was the heat of the reaction ( $\Delta H_{rxn}$ ). This was assumed to be independent of temperature and was determined by using eq(8). Table(7) below shows  $\Delta H_r$  values of the various experiments.

Table (5.7): Thermodynamic information of the experiments :

Experiment	1	2	3
$\Delta H_{rxn}$ (kJ/mol)	61.59	61.58	61.58

## 5.9 MODELING APPROACH

The experimental work discussed has shown that the reactions between the acetic anhydride and methanol occurring in adiabatic batch reactor (thermos-flask) exhibit a first order reaction kinetics with respect to the acetic anhydride. This is discussed in the section 5.9 above. The kinetic parameters of the reactions are discussed in section 5.10 above. Thus for a first order adiabatic batch process, one can write design equation, rate law expression and stiochiometry equations describing the process are as follow:

a) Design Equation:

$$N_{A0} \frac{dX}{dt} = -r_A V \quad (27)$$

b) Rate law:

$$-r_A = k(T)C_A \quad (28)$$

c) Stoichiometry:

$$C_A = \left( \frac{N_{A0}}{V} \right) (1 - X) \quad (29)$$

It assumed that since there is negligible or no change in density during the course of the reaction, the total volume ( $V$ ) is considered to be constant. Combining equations (27) –(29), a differential equation describing the rate of change of conversion ( $X$ ) with respect to time can be written as:

$$\frac{dX}{dt} = k(T)(1 - X) \quad (30)$$

$$\text{where } k(T) = A * \exp\left(-\frac{E_A}{RT}\right) \quad (31)$$

The kinetic parameters, pre-exponential constant ( $A$ ) and the activation energy ( $E_A$ ) has been determined experimentally in all the three reactions as discussed in section above. The adiabat of the processes can be written as:

$$T = T_0 + \Delta T_a * X \quad (32)$$

Differentiating equation (32) with respect to time and plugging in equation (30) gives differential equation (33):

$$\frac{dT}{dt} = k(T) * \{[T_0 + \Delta T_a] - T\} \quad (33)$$

$$\text{where } k(T) = A * \exp\left(-\frac{E_A}{RT}\right) \quad (34)$$

For a given process, given  $T_0$ ,  $\Delta T_a$ ,  $A$  and  $E_a$  as initial starting points, simultaneous solution of equations (33) and (34) with the help of Matlab (R2010a) program was used in the simulations process.

## 5.10 MODEL VALIDATION

The formulated models were validated by direct analysis and comparison of the model – predicted temperature (T) and the values obtained from experimental measurements for equality. Analysis and the comparison between the model predicted temperature values and the experimentally measured temperature values show some amount of deviation of the model-predicted temperature values from the experimentally measured values. The deviation in model equations results may be due to non-incorporation of some practical conditions in the model equation and solution strategy. Also assumptions made in the model equation’s development may be responsible in the deviation of the model results. This can be improved by refining the model equation, and introduction of correction factor to the bring model- predicted temperature values to those of the experimental values. Percentage deviation (%  $D_{model}$ ) of model-predicted temperature from experimentally measured values is given by equation (35) below:

$$D_{model} (\alpha) = \left( \frac{M - E}{E} \right) * 100 \% \quad (35)$$

where the correction factor ( $\beta$ ) =  $-(D_{model})$  (36)

and (M)-model-predicted temperature, and (E)-experimentally measured temperature.

The model is also validated by considering the correlation coefficients ( $R^2$ ) of the model-predicted temperature and the experimentally measured temperature.

## 5.11 RESULTS AND DISCUSSIONS

Figure (5.21a) shows the profiles of the experimentally measured and model-predicted temperature below:

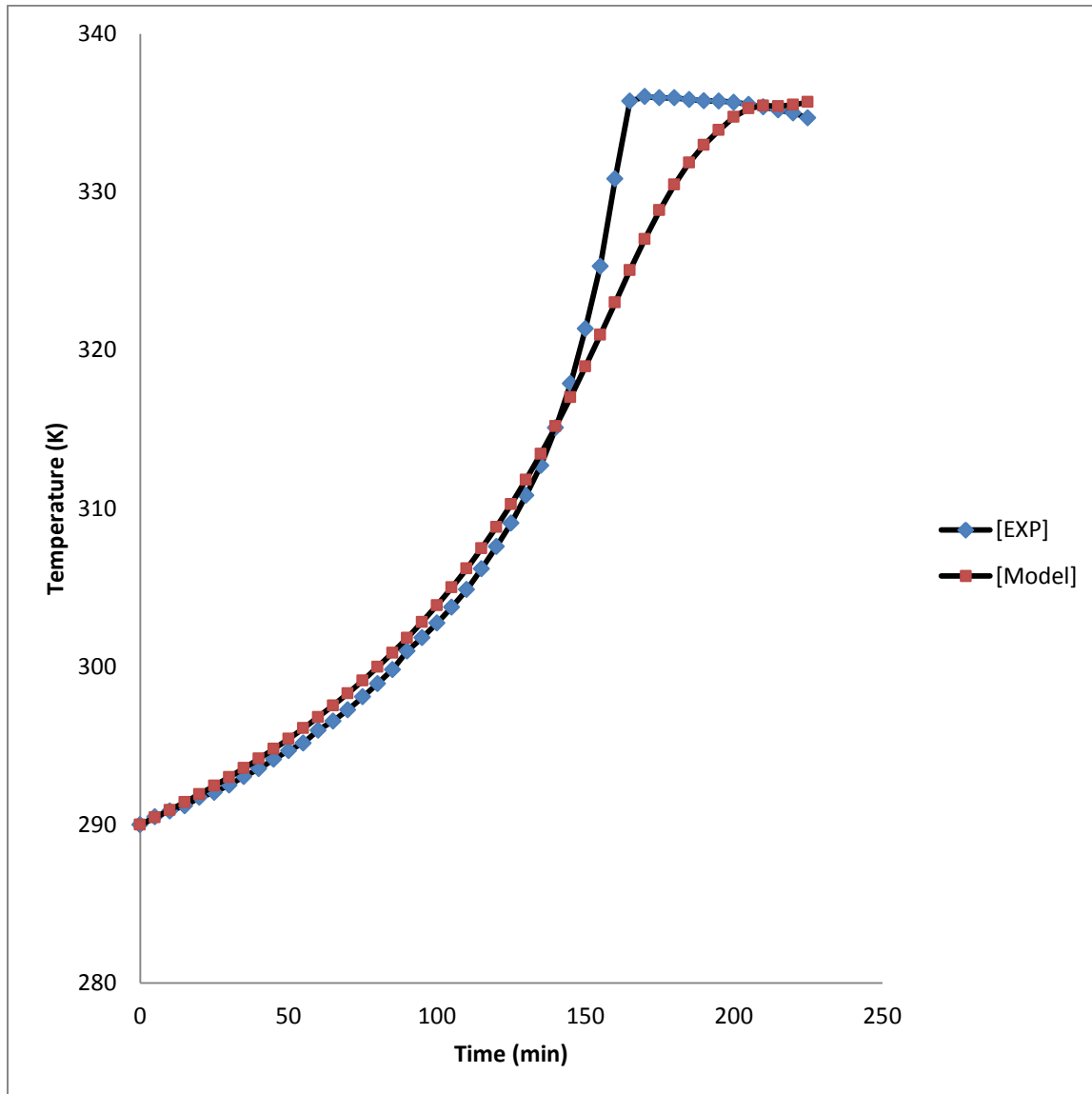


Figure (5.24a): Comparison of the model- predicted and experimentally measured temperature against time for experiment (1)

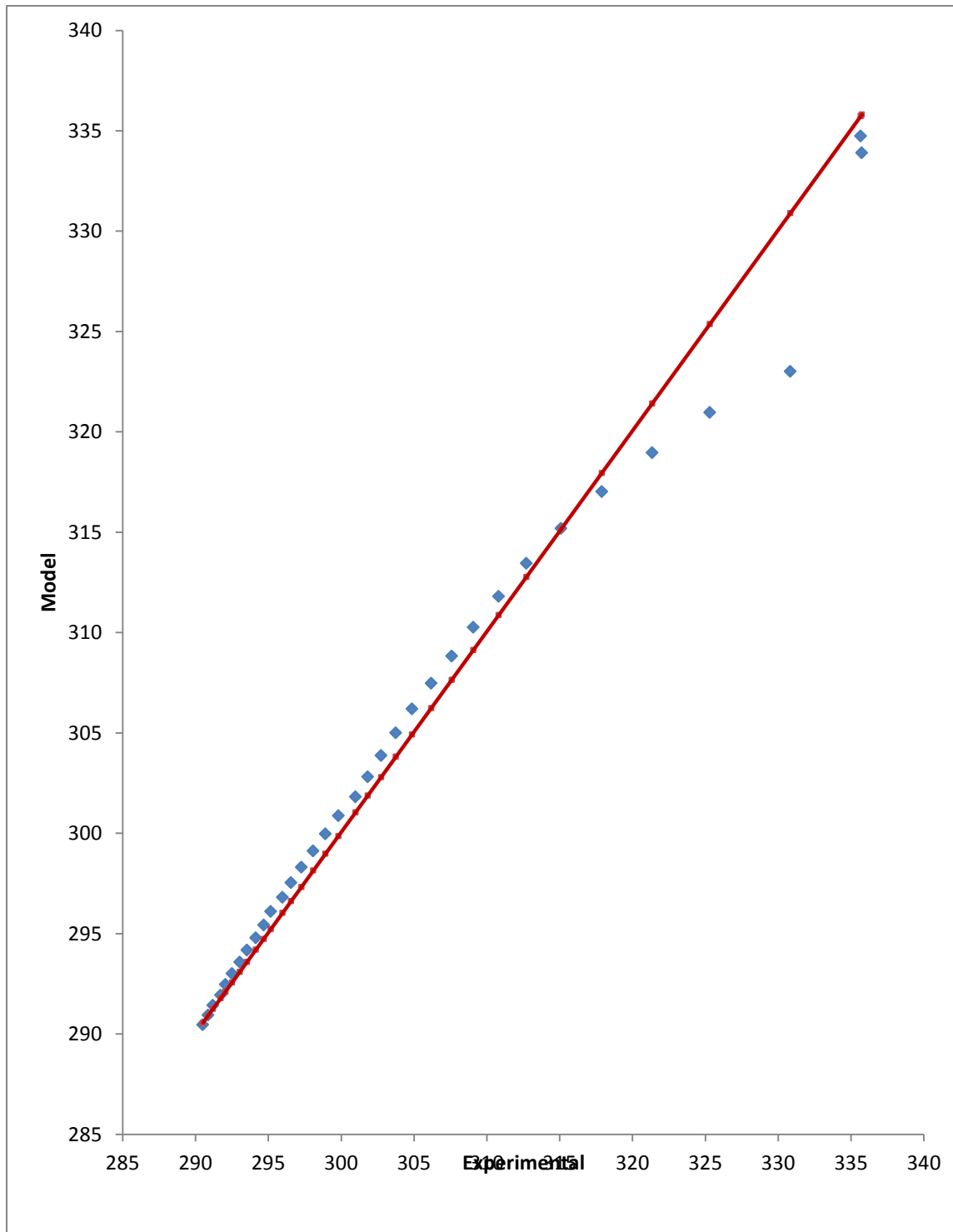


Figure (5.24b) show the parity plot of model-predicted and experimentally measured temperature of experiment (1):

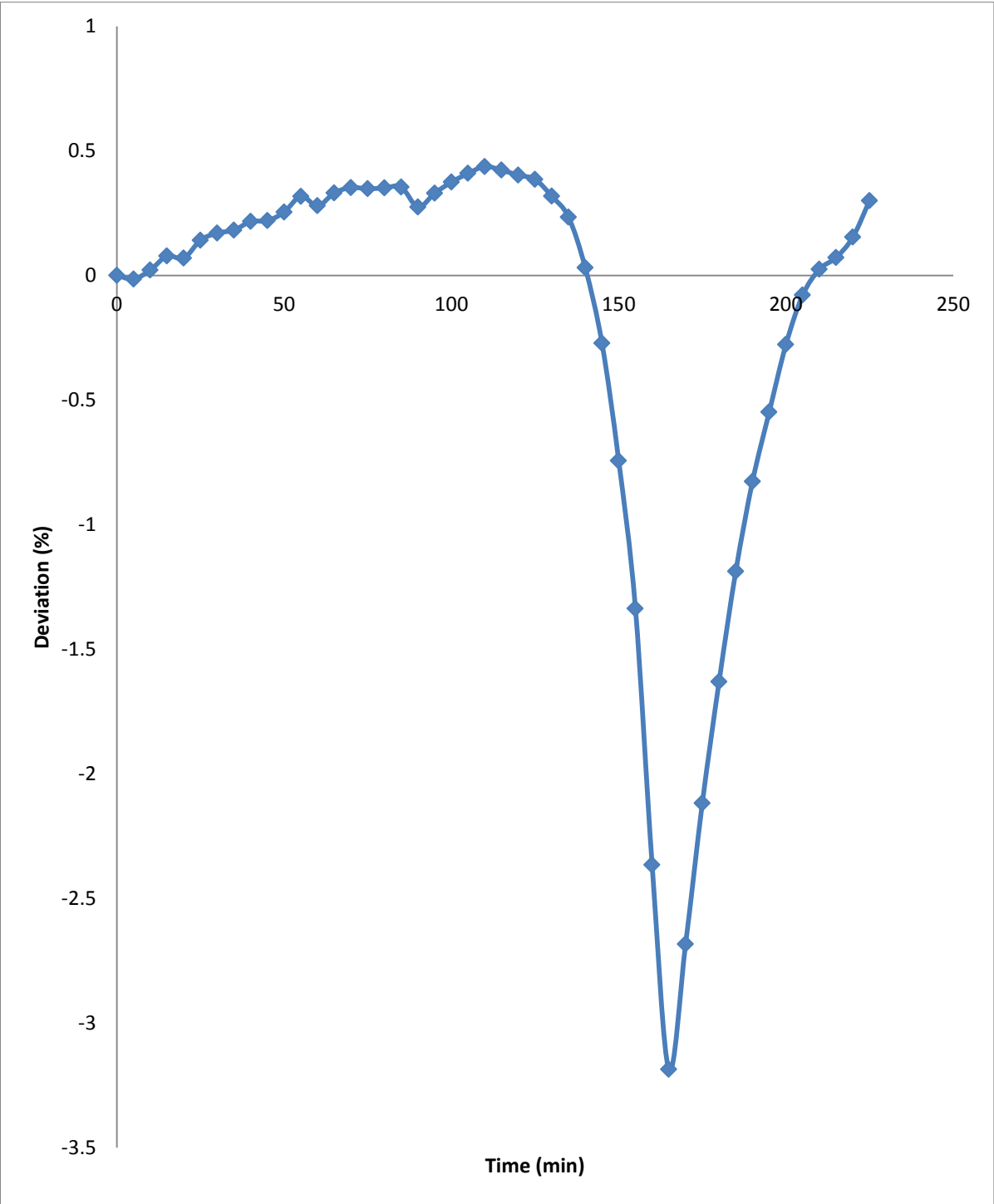


Figure (5.24c): Variation of model-predicted temperature with its associated deviation from experimental results-Experiment (1)

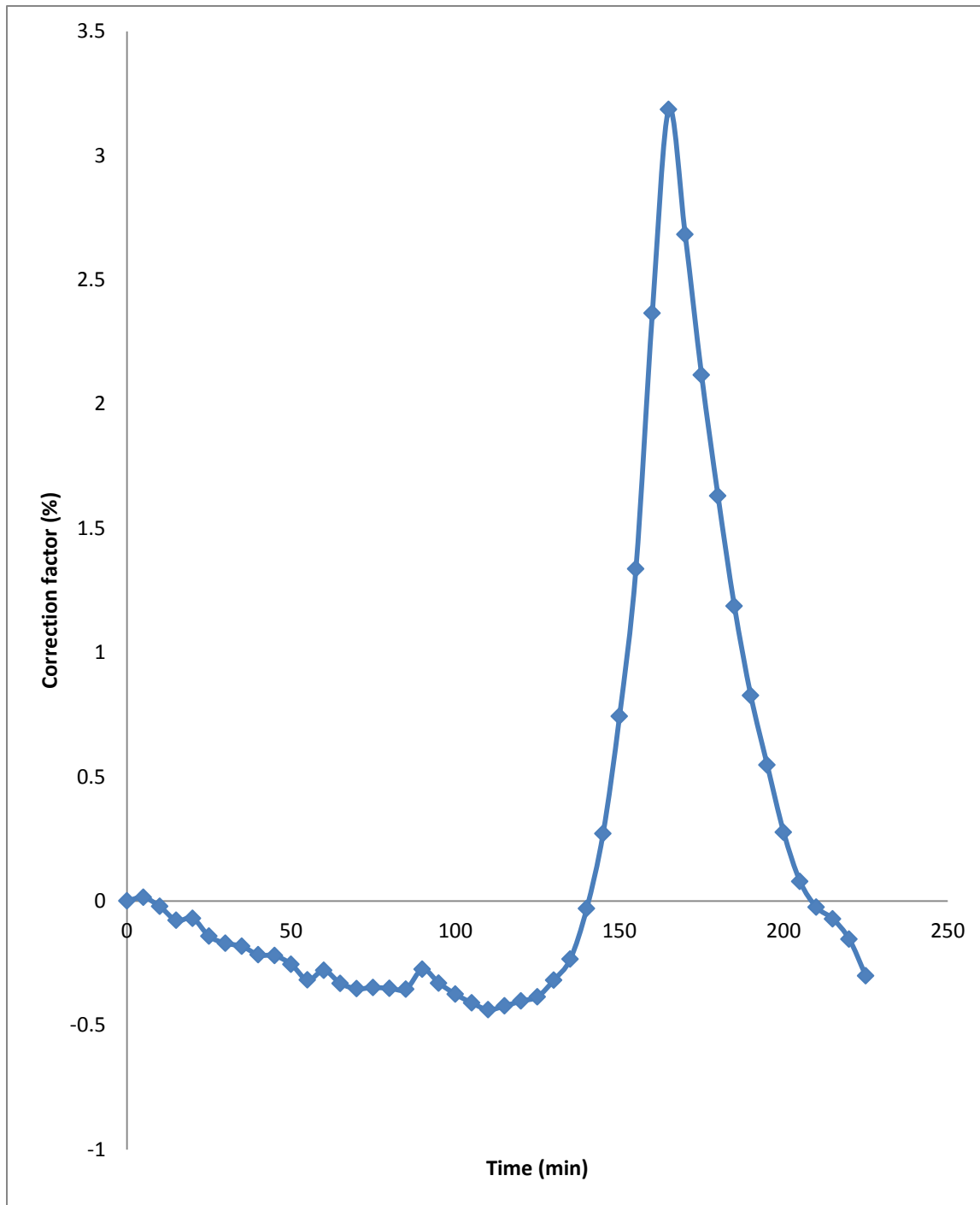


Figure (5.24d): Variation of model-predicted temperature with its associated correction factor- Experiment (1)

Figure (5.22a) shows the profiles of the experimentally measured and model-predicted temperature below:

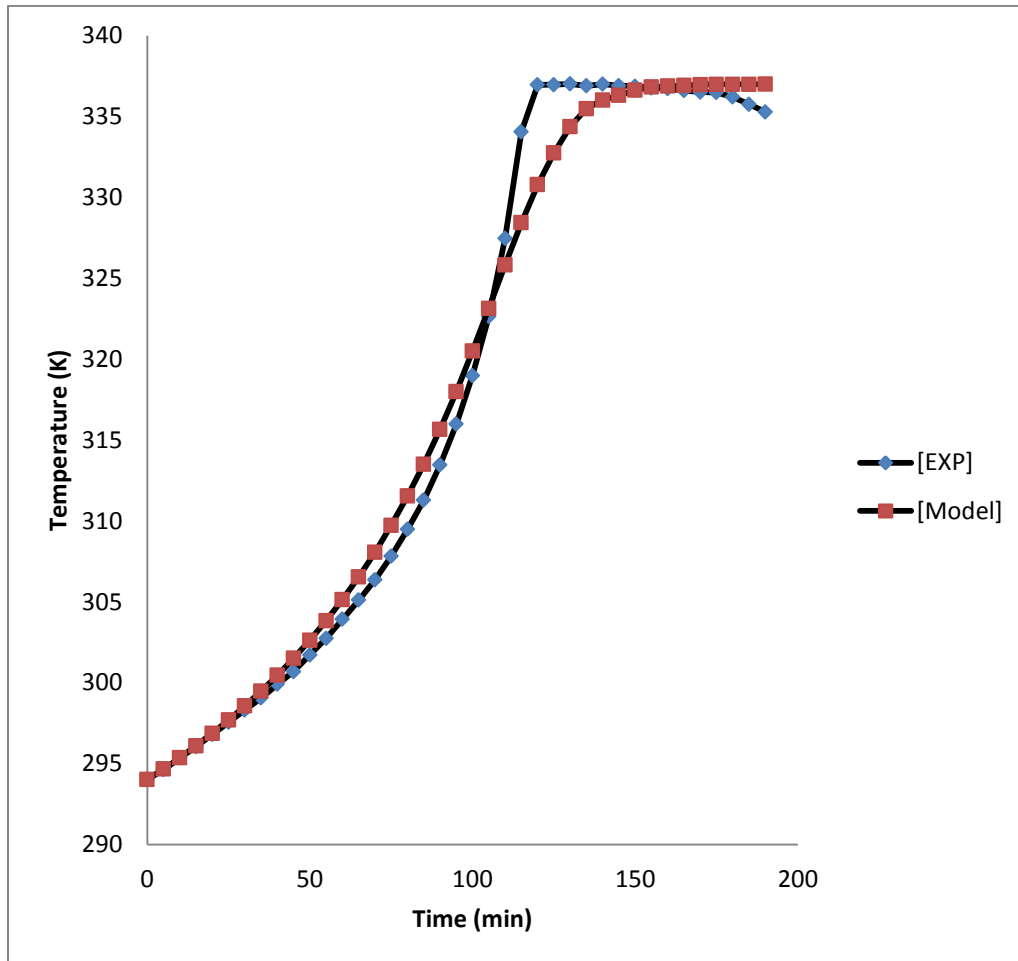


Figure (5.25a): Comparison of the model- predicted and experimentally measured temperature against time for experiment (2)

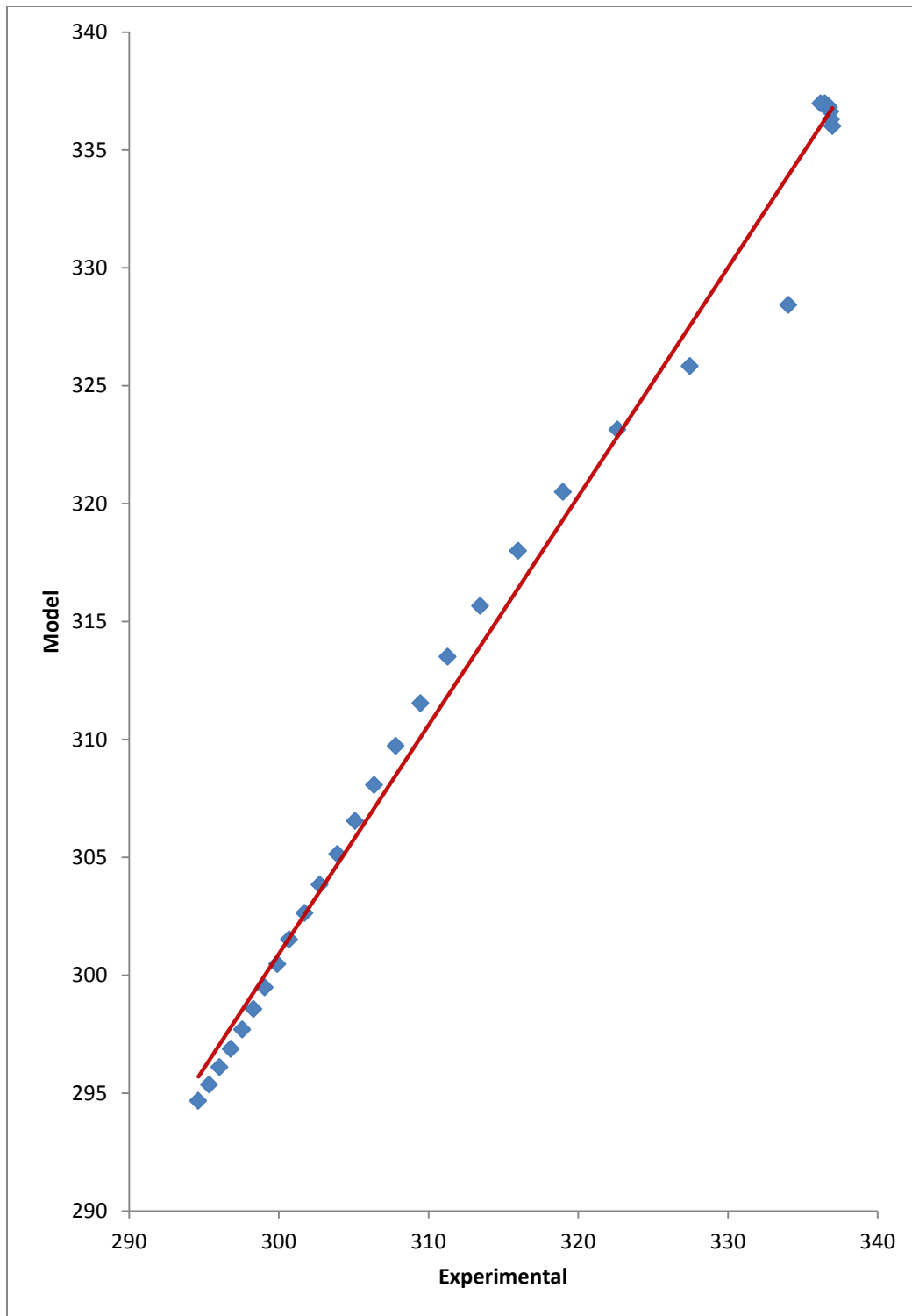


Figure (5.25b) show the parity plot of model-predicted and experimentally measured temperature of experiment (2):

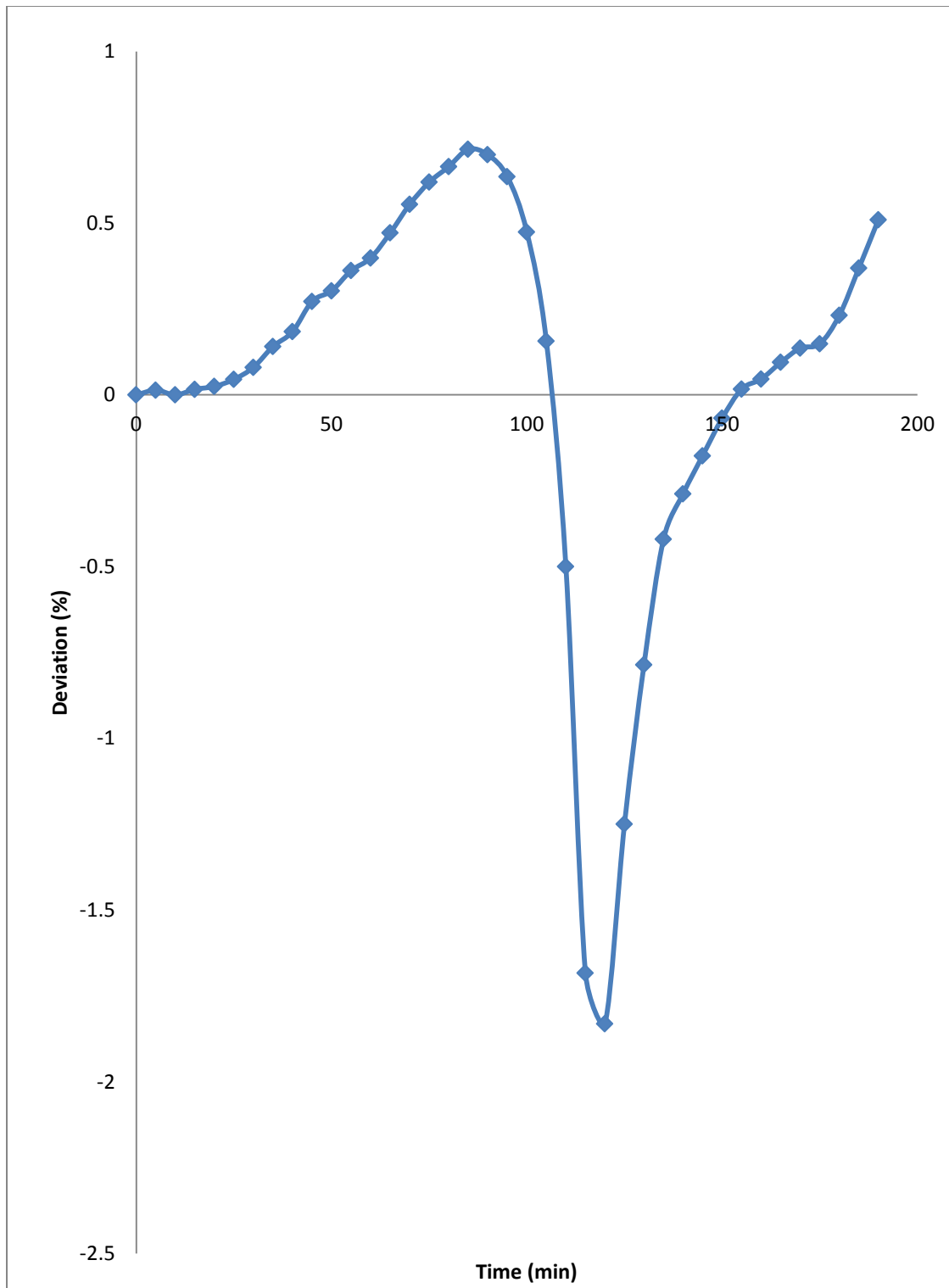


Figure (5.25c): Variation of model-predicted temperature with its associated deviation from experimental results-Experiment (2)

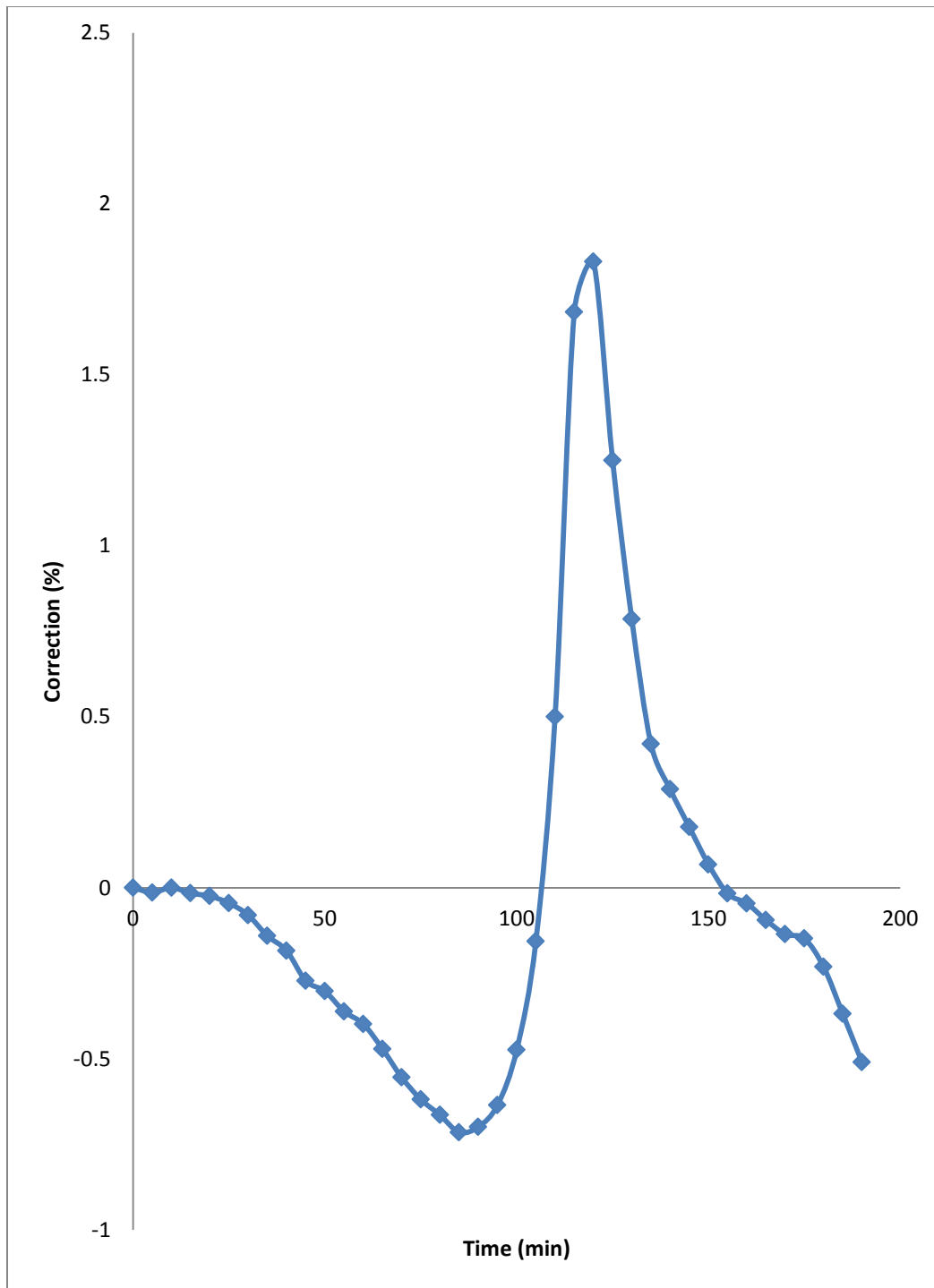


Figure (5.25d): Variation of model-predicted temperature with its associated correction factor- Experiment (2)

Figure (5.26a) shows the profiles of the experimentally measured and model-predicted temperature below:

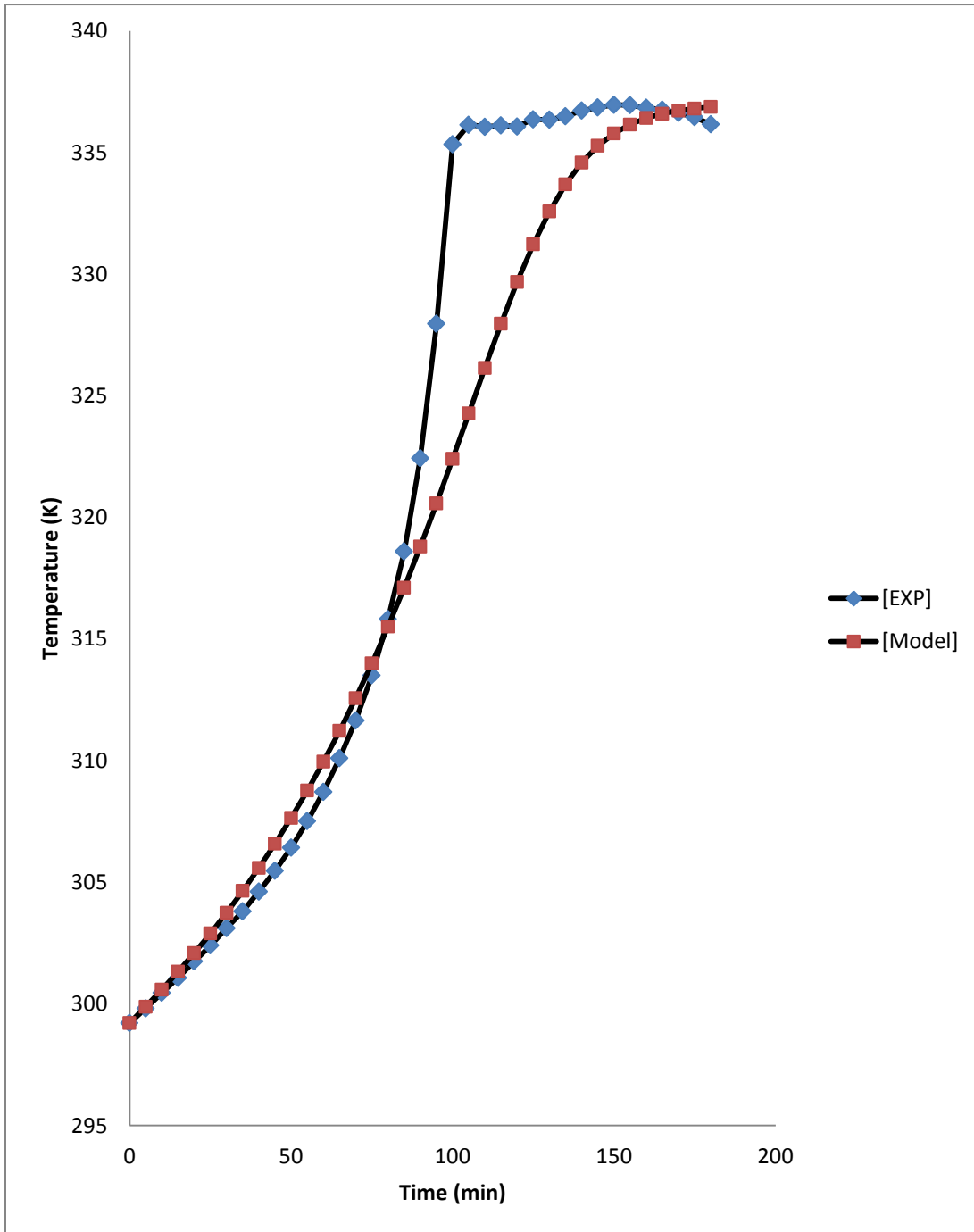


Figure (5.26a): Comparison of the model- predicted and experimentally measured temperature against time for experiment (3)

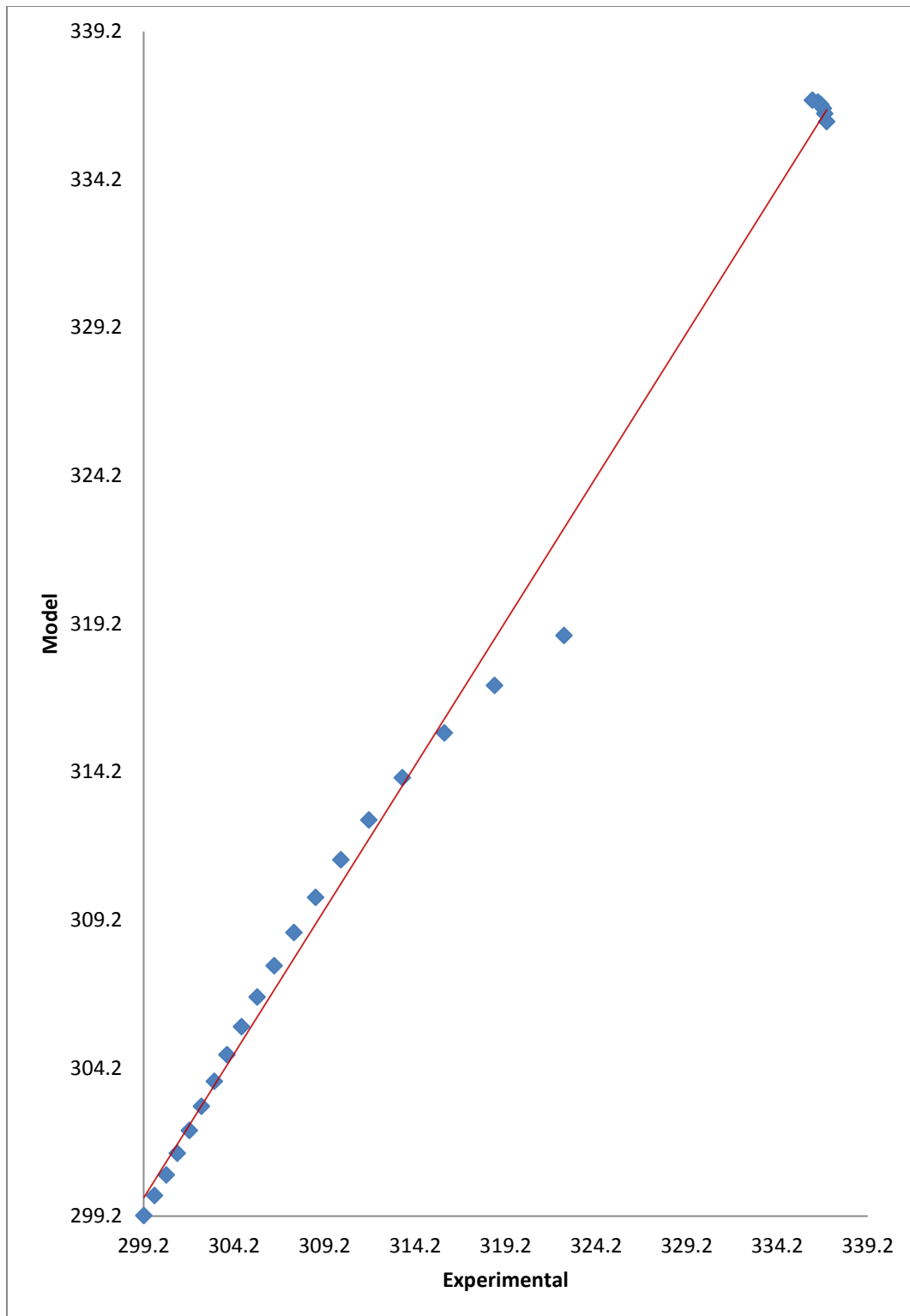


Figure (5.26b) show the parity plot of model-predicted and experimentally measured temperature of experiment (3)

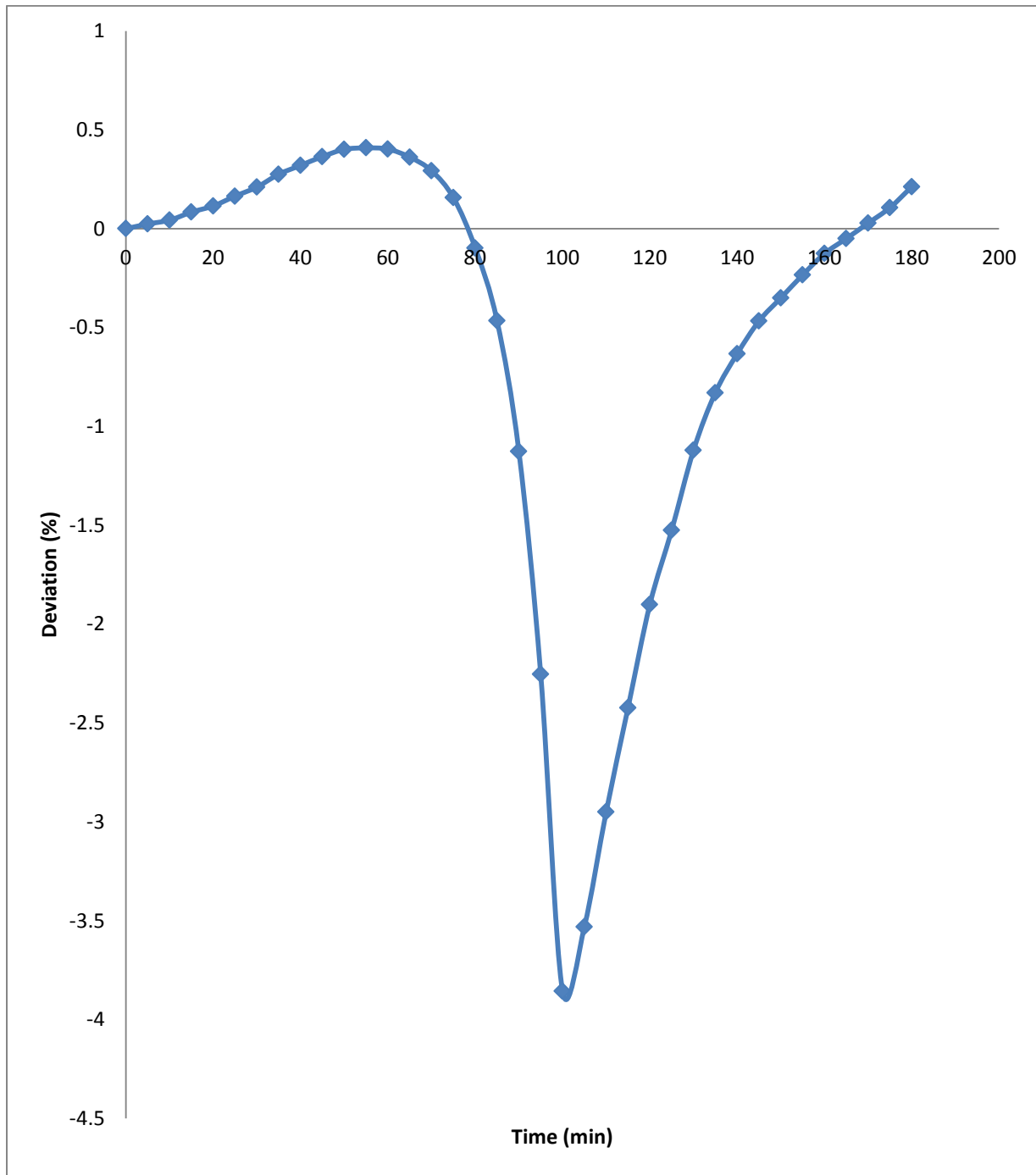


Figure (5.26c): Variation of model-predicted temperature with its associated deviation from experimental results-Experiment (3)

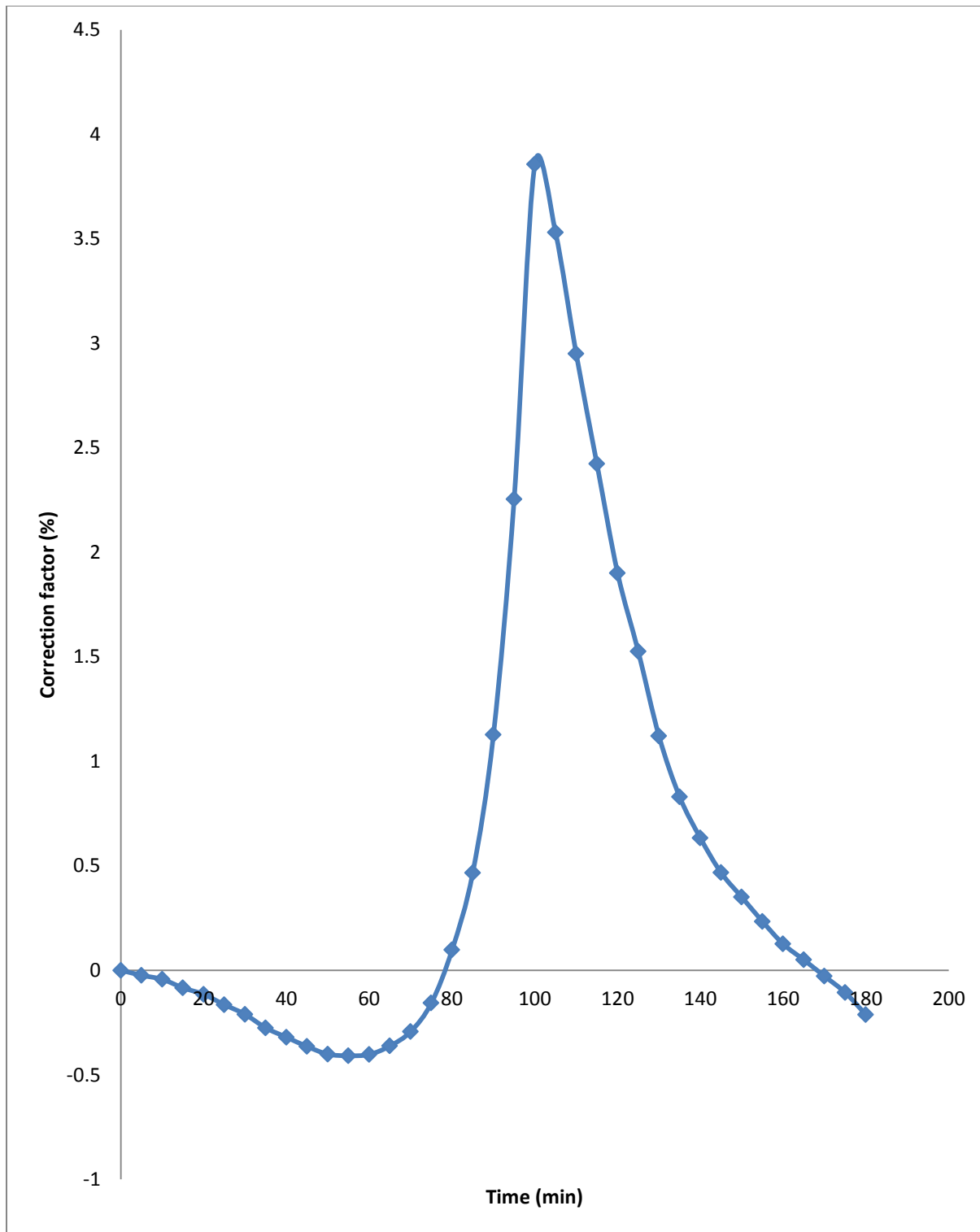


Figure (5.26d): Variation of model-predicted temperature with its associated correction factor- Experiment (3)

By direct comparison of model-predicted temperature profiles and experimentally measured temperature profiles it is seen in figures 5.21a, 5.22a and 5.23a the model proposed agrees quite well in predicting the experimentally measured temperatures. The parity plots shown in figures 5.21b, 5.22b and 5.23c are also used as a means of validation of the proposed model. It is seen from the plots that there is good agreement between model-predicted temperatures and experimentally measured temperatures. An ideal comparison testing validity of the model is achieved by considering the r-squared values (coefficient of determination). Comparing the data from both the model and the experiment it was noticed that the r-squared values were 0.980, 0.991 and 0.994 respectively for experiments 1, 2 and 3. This suggests proximate agreement between model-predicted temperatures and that of the experimentally measured temperatures. The maximum percentage deviations of the model-predicted temperatures, from the corresponding experimental values are 3.18%, 1.83% and 3.86% for experiments 1, 2 and 3. The deviations are depicted graphically in figures 5.21c, 5.22c and 5.23c. The deviation values are quite within the acceptable deviation range of experimental results and give an indication of the reliability and usefulness of the proposed model. The correction factors which were the negative form of the deviations are shown in figures 5.21d, 5.22d and 5.23d. The correction factors take care of the effects of all the issues that were not considered during the experiments and the assumptions which were not catered for during the model formulation. The model as it stands can be used to predict liquid-phase temperature of the esterification process of acetic anhydride and methanol. The predicted temperatures can then be used to predict the liquid phase composition with the help of equation (9) above during reactive distillation process until the reaction reaches the maximum steady boiling temperature of 335K. At this near boiling temperature one expects the vapor-phase of the system to consist of some reactants and products species and by thermodynamic considerations the vapor-phase compositions can be predicted. This then constitutes a step toward the preliminary design of reactive distillation system of the esterification process of acetic anhydride with methanol.

## 5.12 CONCLUSIONS

The mathematical models developed have shown satisfactory results in simulating the liquid-phase temperatures of the esterification of acetic anhydride with methanol. The results were found in good agreement with experimental results. The maximum deviation of the model-predicted temperatures was found to be not more than 4% in all cases which is quiet within acceptable range of experimental results. Nonetheless, further work should incorporate more process parameters into the model with the aim of reducing the deviations of the model-predicted temperature values from those of the experimentally measured observed values. The findings from the simulation results can be used to develop the technology (reactive distillation) to convert acetic anhydride-methanol system to methyl acetate and acetic acid.

## 5.13 ACKNOWLEDGEMENTS

N. A would like to thank the National Research Fund (NRF) of South Africa, Directors of Centre of Material Processing and Synthesis (COMPS), Prof. David Glasser and Prof Diane Hildebrandt, University of Witwatersrand, Johannesburg, South Africa for financial support of this work.

## 5.14 LIST OF SYMBOLS

$\Delta H_{rxn}$ -heat of reaction (KJ/mol)

H-Enthalpy

$H_0$ - Initial Enthalpy

$\Delta T$  (ad) –adiabatic temperature change (K)

$\Delta \epsilon$  –extent of reaction

A –preexponential factor

B,C – thermistor constants

$C_A$ -concentration of A (mol/L)

$C_p$  –specific heat capacity

$C_{P,AA}$  –specific heat capacity of acetic anhydride

$C_{P,m}$  –specific heat capacity of methanol

$C_{P,mix}$ -constant heat capacity of reaction mixture (kJ/mol.K)

$C_{P,W}$  –specific heat capacity of water

$E_a$  – activation energy

$I_{total}$  – total current of the circuit

$K_{eqm}^o$  –Equilibrium constant

$m$  –mass

$M_{AA}$  –Mass of acetic anhydride

$M_m$  –Mass of methanol

$M_{eqv}$  –Equivalent amount of water

$M_T$ -mass of reaction mixture(Kg)

$N_A$  –mole of A (mol)

$Q$ -heat produced by stirrer

$R$  – molar gas constant

$R_2$  – known resistance in the circuit

$-r_A$  –rate of reaction of (A)

$R_{TH}$  – Thermistor resistance

$t$  – time

$T_{amb}$  –ambient temperature

$T_{max}$  –maximum temperature (K)

$T_0$  –initial temperature

T-reactor temperature (K)

$T_S$  – steady state temperature (K)

U –heat transfer coefficient ( $J/m^2 \text{ s.K}$ )

v – total voltage of the circuit

V-Volume of vessel

$V_{out}$  – voltage measured by thermistor

$V_{TH}$  – voltage across thermistor resistance

X- conversion

$\beta$ - constant

## 5.15 REFERENCES

Mohl, K. D., Kienle, A., Gilles, E. D., Rapmund, P., Sundmacher, K., Hoffmann, U. (1997), “Nonlinear Dynamics of Reactive Distillation Processes for the Production of Fuel Ether”, *Comp. Chem. Eng.* Vol 21, S983-S994.

Kreul, U. L., Gorak, A., Dittrich, C., (1998), “Catalytic Distillation: Advanced Simulation and Experimental Validation”, *Comp. Chem. Eng.* Vol 22, 371 -373

Popken, T., Steinigeweg, S., Gmehling, J., (2001), “Synthesis and Hydrolysis of Methyl Acetate Reactive Distillation using Structured Catalytic Packing: Experiments and Simulation”, *Ind. Eng. Chem. Res.*, Vol. 40, 1566 -1574.

Bock, H., Jimoh, M., Wozny, G. (1997), “Analysis of Reactive Distillation using the Esterification of Acetic Acid as an example”, *Chem. Eng. Technol.* 20 182 -191.

Teo, H. T. R., Saha, B., (2004),” Heterogeneous Catalysed Esterification of Acetic Acid with Isoamyl Alcohol: Kinetic Studied”, *J. Catal.* 228 174 -182.

Agreda, V. H., Partin, L. R., Heise, L. R., (1990), "High-Purity Methyl Acetate via Reactive Distillation", Chem. Eng. Prog. Vol 86 No.2, 40-46.

Keys, D. B., (1932), " Esterification Processes and Equipment", Ind. Eng. Chem., Vol. 24, 1096 -1103.

Kenig, E. Y., Bäder, H., Górak, A., Beßling, B., Adrian, T., Schoenmakers, H., (2001), "Investigation of Ethyl Acetate Reactive Distillation Process", Chem. Eng. Sci.", 6185 - 6193.

## CHAPTER 6

*THIS PAPER HAS BEEN PUBLISHED IN THE JOURNAL OF CHEMICAL ENGINEERING AND PROCESS TECHNOLOGY (USA PUBLISHER) 2013,4:8.DOI:10.4172/2157-7048.1000176*

**KINETIC MODELLING OF THE HYDROLYSIS OF ACETIC ANHYDRIDE AT HIGHER TEMPERATURES USING ADIABATIC BATCH REACTOR**

**(THERMOS-FLASK)**

*N.Asiedu<sup>\*</sup>, D.Hildebrandt<sup>\*</sup>, D.Glasser<sup>\*</sup>*

Centre of Material and Process Synthesis, School of Chemical and Metallurgical Engineering, University of Witwatersrand, Private mail Bag X3, Wits 2050, Johannesburg, South Africa.

\*Authors to whom correspondence may be addressed:

Emails: [nasiedusoe@yahoo.co.uk](mailto:nasiedusoe@yahoo.co.uk)

: [Diane.Hildebrandt@wits.ac.za](mailto:Diane.Hildebrandt@wits.ac.za)

: [David.Glasser@wits.ac.za](mailto:David.Glasser@wits.ac.za)

## ABSTRACT

The kinetics of the reactions of acetic anhydride-excess water has been studied as a function of temperature under adiabatic conditions in a thermos-flask fitted with a negative coefficient thermistor and kinetic data obtained at higher temperatures. This method was used for the excess acetic anhydride-water reactions. The authenticity of the experimental adiabatic system was verified by determination of the kinetic parameters of the acetic anhydride-excess water reactions and compared with published kinetic parameters. The reaction kinetics of excess acetic anhydride-water reactions which has not been determined previously was modeled using the same adiabatic analysis and the average experimental activation energy, heat of reaction, pre-exponential factor and the order of reaction with respect to water determined. The kinetics of acetic anhydride-methanol process was also modeled under the same experimental conditions. The kinetics of this process has not been modeled using this method before. The results obtained agreed very with the published results which employed different techniques.

**Keywords:** Kinetic modeling, Thermos flask, hydrolysis, esterification, exothermic reactions, temperature.

## 6.1 INTRODUCTION

Classical techniques for modeling reaction kinetics have been depended on measuring or monitoring concentration-time profiles of liquid phase reactions. This method requires that at some time the researcher must have means of arresting the reaction and take measurement rapidly and continuo the process. With this approach some continuous measuring techniques are possible, pH, conductivity, (Kralj 2007), Fourier transfer infrared (Haji et al 2003). These methods actually require different approach when it comes to the analysis of the experimental results, and one is always at the disadvantage when reaction rates are extremely fast. Temperature-time profiles of exothermic reaction are used instead of concentration-time profiles for the determination of the kinetic parameters. This method is now used in modern laboratories and can be done with a high degree of accuracy.

Most reactions have reasonable amount of heat of reaction and measuring dices such as thermistor can be used to measure temperature changes up to accuracy on 0.0001 °C. It follows that in principle an adiabatic reaction covering only 10 °C should be measureable to one part in

$10^5$ , which compares very well with the accuracy of chemical titration used in isothermal experiments (Gordon, 1946). Thus reactions with very small heat of reactions could be handled easily. If one is to model an exothermic reaction by estimating the kinetic parameters of a process when concentration and temperature vary simultaneously, one need to perform regression analysis directly on the differential equations describing the process (King, 1967). Recently this regression analysis is easily performed by high speed digital computers. Previous researchers have been confined to the case where reactions occur under adiabatic conditions (Livingstone, 1961). Bell and Clunie (1952) used flow reactors and it has generally been used for fast reactions. The temperature-time profiles have been converted directly concentration-time profiles and then been analyzed by the classical methods. The method of Schmidt et al (1964) requires numerical evaluations of the first and second derivatives functions of concentration. The current technique applied for the analysis of the results in this paper is not subject to any limitations and does not require prior knowledge of the heat of reaction. Some studies have been reported in elsewhere in the literature on the kinetic parameters of acetic anhydride hydrolysis. Eldridge and Pirect (1950) obtained the pseudo-first order reaction rate constant using a batch reactor. It is well-known that the reaction rate increases with temperature increase. The rate of temperature rise can be represented as a slope of the temperature-time curve. Some studies has been reported in the past using temperature-time profiles to predict the kinetics of the hydrolysis of acetic anhydride in excess distilled water. Williams (1974) reported the kinetics and stoichiometry of the reaction between hydrogen peroxide and sodium thiosulphate. An adiabatic reactor was used with a thermocouple and a strip-chart recorder to determine the kinetic parameters of the hydrolysis of acetic anhydride in dilute aqueous solutions (Glasser and Williams, 1971). A vessel was placed in a constant temperature bath and the heat lost from the reactor was described mathematically. A thermistor was used for the temperature readings. King and Glasser (1965) studied the kinetic parameters of the hydrolysis of acetic anhydride in dilute solutions. An adiabatic reactor was used in the experiments.

The walls of the reactor were kept at the same temperature as the fluid by passing a high current through the reactor walls. Temperature readings were taken by the use of thermocouples. In this work hydrolysis of acetic anhydride in excess distilled water (dilute solution) was studied and compared with hydrolysis in excess anhydride solution in adiabatic conditions. It is known that not much work has been done on the case where hydrolysis is carried out in excess acetic

anhydride solution using adiabatic batch reactor. Moreover this work is also to test the current model of the hydrolysis of excess acetic anhydride under adiabatic conditions. It is claimed that the hydrolysis follows a first order kinetic model. The same method is also used to elucidate the kinetic parameters of the reaction between acetic anhydride and methanol. This process has not been studied in this manner as known to the authors.

## 6.2 THEORY OF HOMOGENEOUS REACTIONS

Given a constant volume, the rate at which homogeneous processes proceed can be expressed as the change in concentration of a given reactant per unit time. There are a lot of hypothesis attempting to explain how chemical reactions occur. King (1964) proposed that reacting molecules in the liquid solutions are in constant state of motion. He described the solutions as numerous cages composed of many solvent molecules and particular molecules of a reactant, 'hole' in the exist and are large enough to accommodated a molecule. As hole is filled by an adjacent molecule it is observed that both the molecule and the hole physically move. This type of random motion occurs throughout the batch and describes diffusion in liquids. The homogeneous reactions cannot proceed faster than the rate at which the rate reactant molecules diffuse into the same 'solvent cage'. In most cases the rate of reaction are considerable lower than the frequency of the reactant molecules diffusing into each other. The fact that not all collisions of reactants results I a reaction is explained by the insufficient activation energy that those reactants posses (Shatynski and Hanesian, 1993). Thus during chemical reaction the state in which reactant species are caged together, the interaction with solvent molecules against the trapped reactants may or may not provide activation energy for the reaction to occur.

In another theory Morrison and Boyd (1983), stated that for a reaction to occur the collision should be of enough energy that is activation energy ( $E_a$ ) and the molecules orientation should be in the right direction. The moving reacting species provides the activation energy in the form of kinetic energy. Thus the rate of reaction can be defined as:

$$\mathit{rate} = (Z)(P) \exp\left(-\frac{E_a}{RT}\right) \quad (1)$$

Z –collision frequency which depends on the concentration of the reacting species, the system pressure, the size of the particles and the speed they are moving.

P – probability factor, which depends on the geometry of the articles and orientation at collision.

The exponential term in eq(1) is the fraction of collision that has enough energy greater than  $E_a$  to enable reaction to occur. The energy factor has a great deal of influence on the rate of the reaction. It depends on the temperature and the activation energy. From eq(1) it can be seen that a small change in  $E_a$  will affect the rate of reaction or the fraction of collisions required for a reaction to occur. It is also seen that an increase in temperature will increase the kinetic energy of the reacting species and hence the number of the collisions.

### 6.3 THE MATHEMATICAL MODEL OF THE REACTING SYSTEM

Given an adiabatic batch reactor the mathematical model is made up of a set of differential equations resulting from the mass and energy balances referred only to the reaction mixture because there is no heat transfer. The stoichiometry of the reactions studied is given below:



For a constant –volume batch reactor one can write:

$$-r_A = \frac{1}{V} \frac{dN_A}{dt} = -\frac{dC_A}{dt} \quad (4)$$

The energy balance equation can be established as:

$$\text{Heat generated} = \text{Heat absorbed by reactor contents} +$$

$$\text{Heat transferred through reactor walls} \quad (5)$$

$$(-\Delta H)(-r_A)Vdt + Q_{stirrer}dt = mC_p dT + UA(\Delta T)dt \quad (6)$$

$$\text{Given } (-r_A) = \frac{d\varepsilon}{dt} \quad (7)$$

where ( $\epsilon$ ) is the extent of reaction, we can rearrange eq(6) to give eq(8) below:

$$UA (\Delta T)dt + mC_p = (-\Delta H) \frac{d\epsilon}{dt} \quad (8)$$

Assume that heat given by stirrer speed ( $Q_{\text{stirrer}}$ ) is negligible. Integrating eq(8) gives

$$(T - T_o) + \frac{UA}{mC_p} \int_0^\infty (T - T_o)dt = \frac{(-\Delta H)}{mC_p} \Delta\epsilon \quad (9)$$

The LSH of eq(9) can be used to correct experimental data to adiabatic conditions. It is assumed that the reaction is independent of temperature, hence correcting the experimental data the adiabatic temperature rise parameter ( $\Delta T_{ad}$ ) can be obtained from the experimental result for the process. This adiabatic temperature rise is equal to the RHS of eq(9) or we can write;

$$\Delta T_{ad} = \frac{(-\Delta H)\epsilon}{mC_p} \quad (10)$$

From eq(9) one can easily show that the energy balance equation of an adiabatic batch reactor reduces to a linear form given by eq(11) as:

$$T = T_o + \Delta T_{ad} \epsilon \quad (11)$$

Theoretically the adiabatic temperature rise is by definition obtained when extent of reaction ( $\epsilon$ ) =1 or conversion ( $x$ ) = 1, with respect to the reactant of interest and its value can be computed in advance from the initial conditions (temperature and heat capacities) of the reacting species. Equation (11) also allows one to find extent of reaction and or conversion at any instant under adiabatic conditions by using only one measure of temperature. Then from the initial concentrations of the reactants the concentrations products can be monitored at any instant in the reactor.

#### 6.4 THE EXPERIMENTAL SET-UP

The experimental set- up consist of adiabatic batch reactor (thermos-flask) made up of 18/8 stainless steel thermos-flask of total volume of 500mL equipped with a removable magnetic stirrer as shown in figure (5.1) The flask is provided with a negative temperature coefficient thermistor connected on-line with a data-logging system. The signal from the sensor (thermistor)

is fed to a measuring and a control unit amplifier and a power interface. The acquisition units are connected to a data processor. A process control engineering support data management. The data acquisition system called Clarity has the following part numbers: C50 Clarity Chromatography SW, single instrument, 3 x 55 Clarity Add-on instrument SW, 194 (INT9 quad channel A/D converter card). The hardware is INT9 PCI A/D 24 bit converter. The properties: Input signal range 100mV -10V. Acquisition frequency 10 -100Hz, Internal A/D converter ( INT9-1 to 4 channel PCI A/D converter). All physically available analog inputs and outputs as well as virtual channel are all automatically monitored and the process values are stored. The process values are transmitted in such a way that the computer screen displays profiles of voltage-time curves. Data acquisition software was used to convert the compressed data form of the history file on the hard disk into text file format. The text files are converted to excel spreadsheet and the data are then transported into matlab 2010a for analysis.

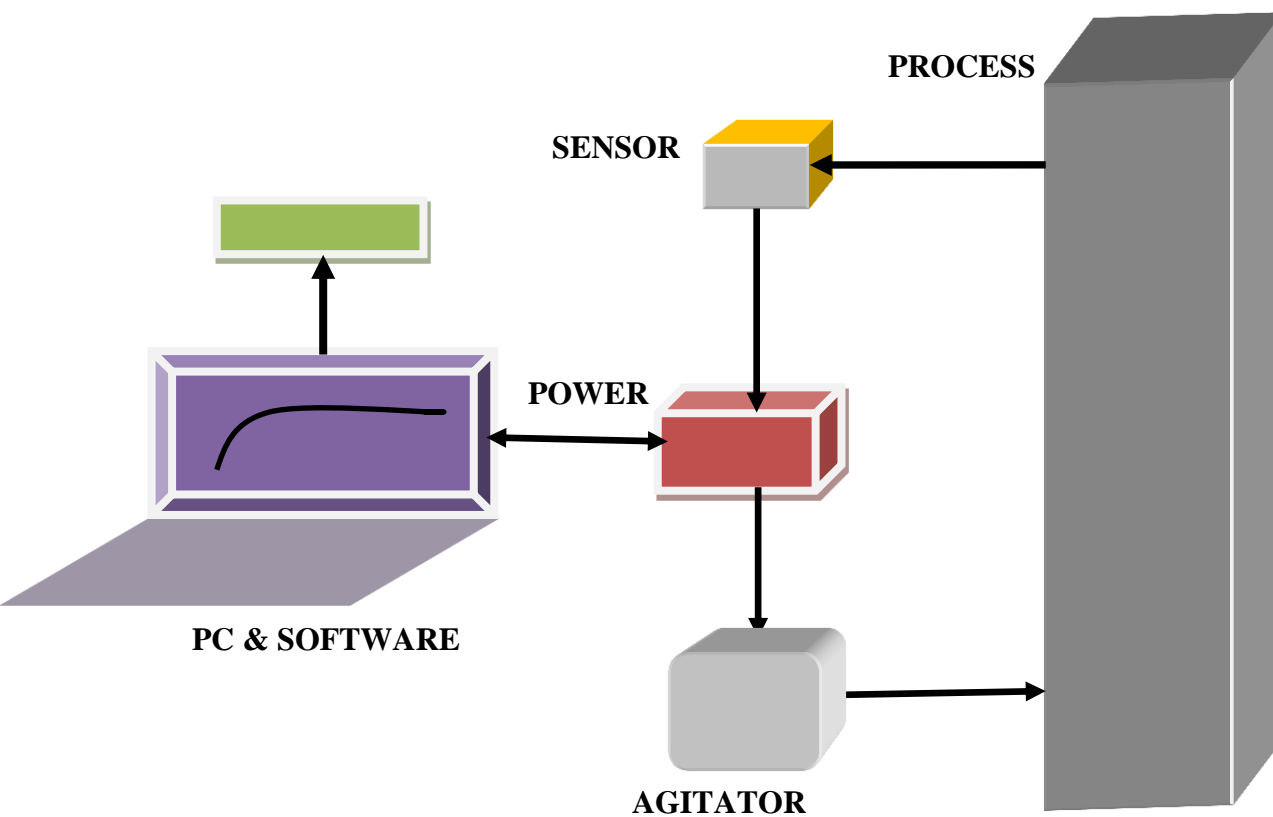
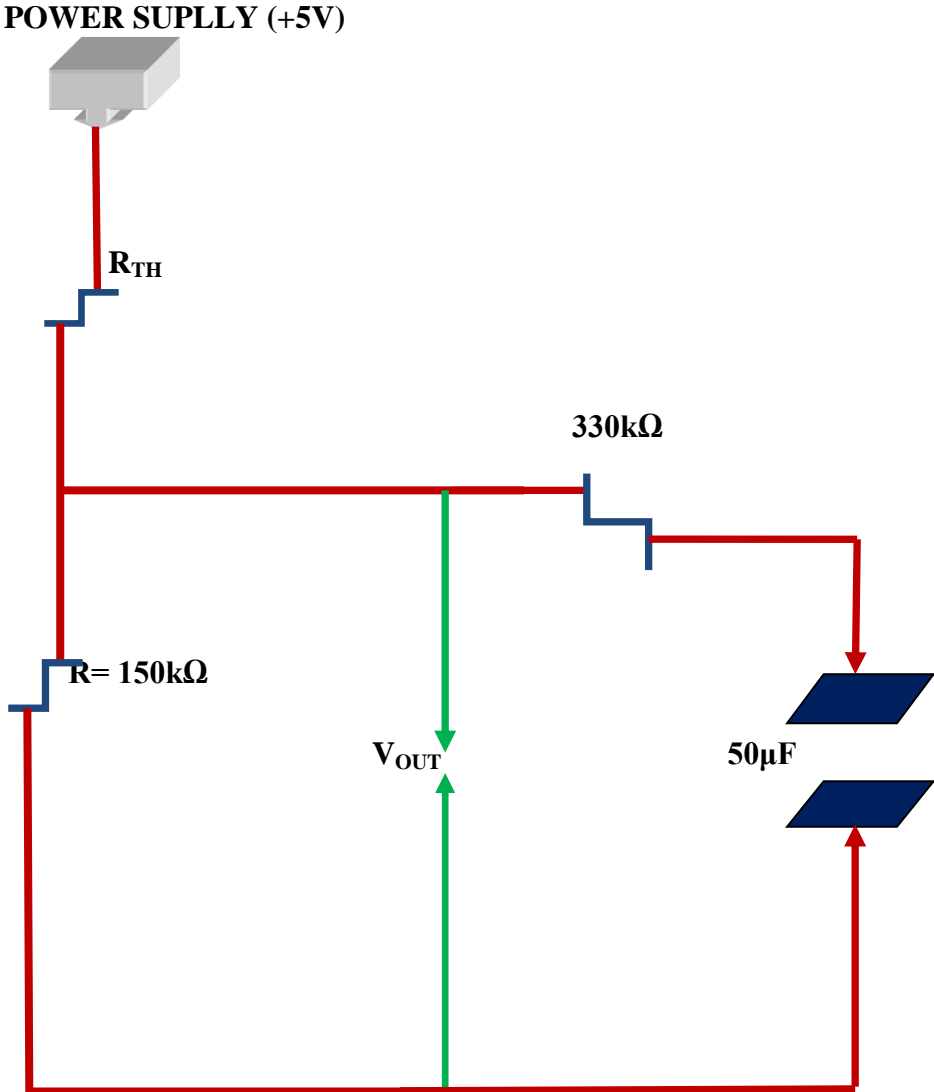


Figure (6.1): Block diagram of experimental set-up

## 6.5 THE THERMISTOR CALIBRATION

This section describes the experimental details concerning the measurements of liquid phase reactions by temperature-time techniques. Temperature changes are a common feature of almost all chemical reactions and can be easily measured by a variety of thermometric techniques. Following the temperature changes is useful especially for fast chemical reactions where the reacting species are not easily analyzed chemically. This section thus describes the theory and the calibration of the thermistor used in the experiments described in this paper.

6.5.1 THE ELECTRICAL CIRCUIT OF THE SYSTEM



Figure(6.2): The electrical circuit of the system

### 6.5.2 THE CIRCUIT THEORY

From Kirchhoff law's we can write:

$$V_{out} + V_{TH} = 5V \quad (12)$$

$V_{out}$  – Voltage measured by thermistor during the course of reaction.

$V_{TH}$  – Voltage across resistance ( $R_{TH}$ ).

From (12) one can write:

$$V_{TH} = 5V - V_{out} \quad (13)$$

$$R_{TH} = \frac{V_{TH}}{I_{total}} \quad (14)$$

From the circuit  $V_{TH}$  and  $I_{total}$  are unknowns.  $R_{TH}$  is resistance due to the thermistor, and  $I_{total}$  is the same through the circuit and can be determine as:

$$I_{total} = \frac{V_{out}}{R} \quad (15)$$

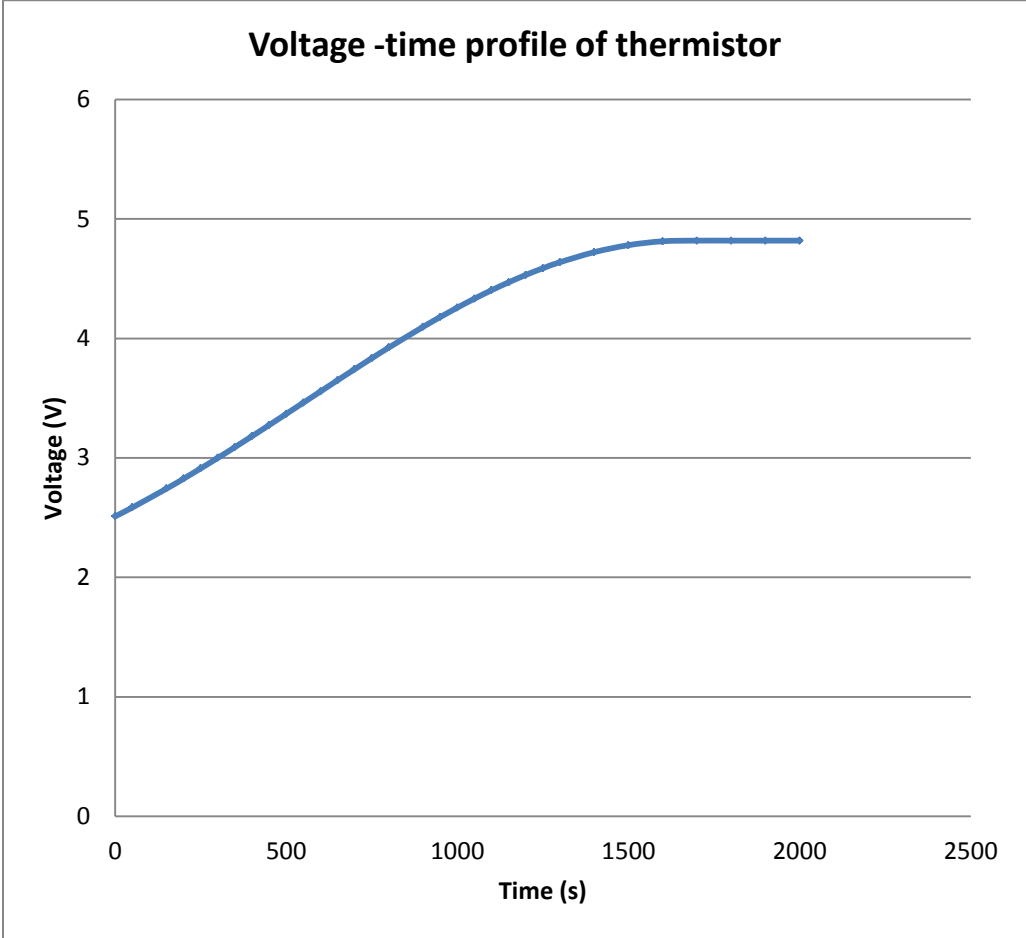
$V_{out}$  is known from experimental voltage –time profile and  $R$  (150k $\Omega$ ) is also known from the circuit. Thus when  $I_{total}$  is determined from eq(15),  $R_{TH}$  which is the thermistor's resistance and related to temperature at any time during the chemical reaction can be determine as:

$$R_{TH} = \frac{V_{out}}{I_{total}} \quad (16)$$

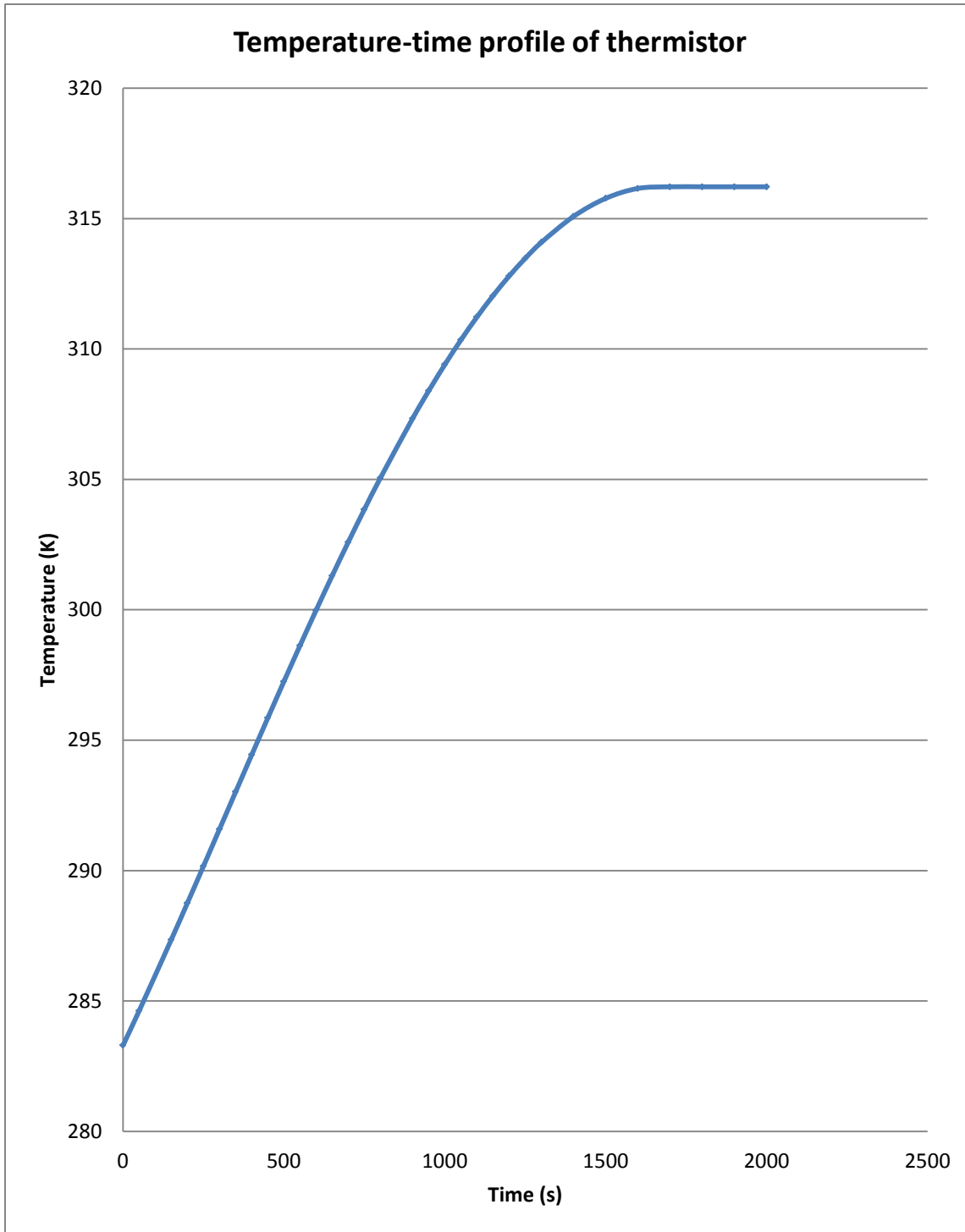
### 6.5.3 THE THERMISTOR CALIBRATION

The thermistor used in the experiments was negative temperature coefficient with unknown thermistor constants. The calibrations involve the determination of the thermistor constants and establish the relationship between the thermistor's resistance and temperature. This was done by fitting both the thermistor and an electronic digital temperature measuring device in a sealed vessel and the system was slowly warmed until the voltage reaches it asymptotic state.

The thermistor was connected to a computer with data acquisition software to provide data of voltage –time real-time plot as shown in figure (3) below. The voltage –time data was used to match the temperature-time data obtained from the electronic digital temperature device.



Figure(6.3): The thermistor voltage-time profile



Figure(6.4): The thermistor temperature-time profile

#### 6.5.4 RELATIONSHIP BETWEEN THERMISTOR RESISTANCE AND TEMPERATURE

Thermistor resistance ( $R_{TH}$ ) and Temperature (T) in Kelvin was modeled using the empirical equation given developed by Considine (1957)

$$R_{TH} = \exp \left( \frac{B}{T} + C \right) \quad (17)$$

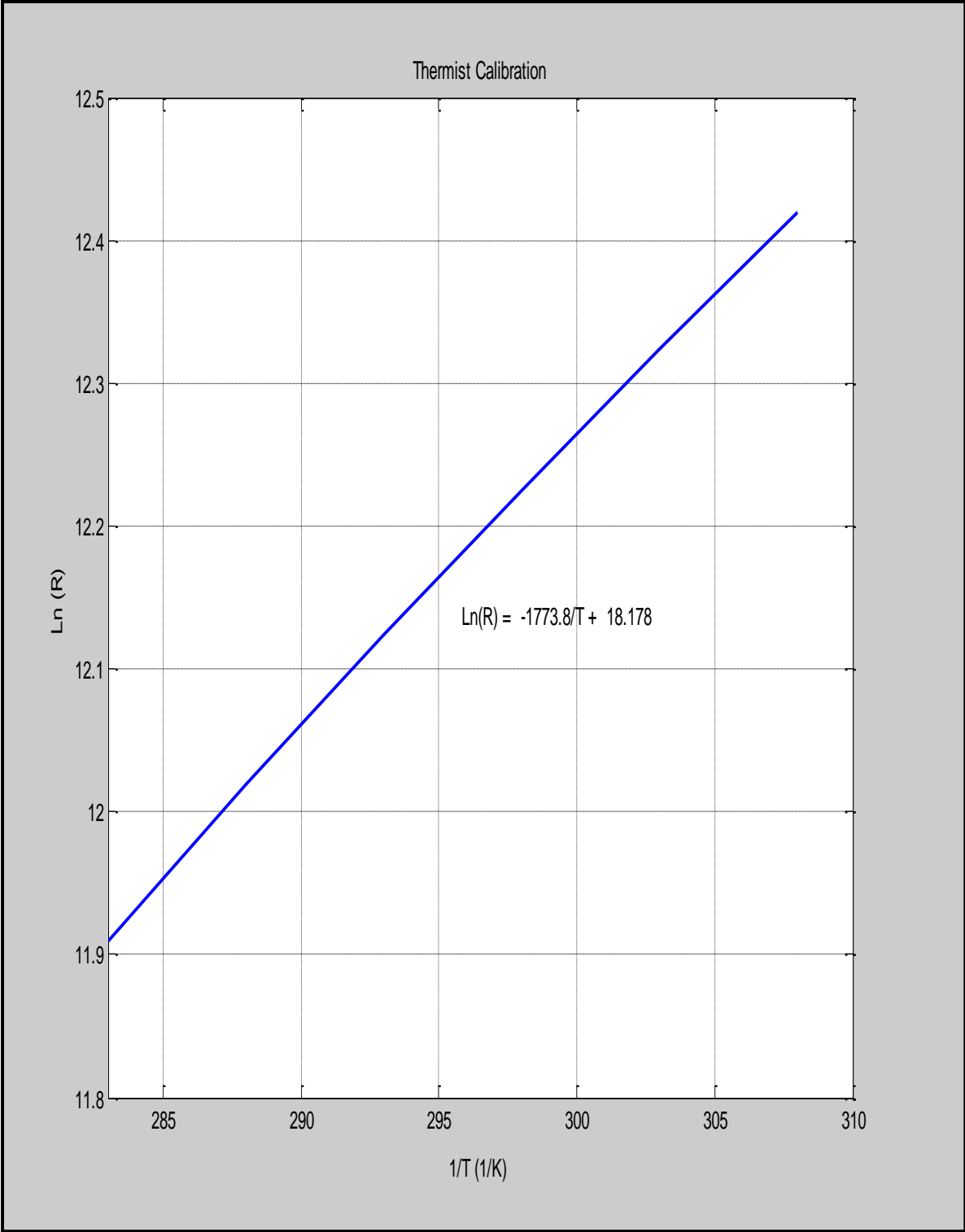
or

$$\ln(R_{TH}) = \frac{B}{T} + C \quad (18)$$

where the parameters (B) and (C) are the thermistor constants and were obtained from experimental calibration using warm water. The constants were determined by fitting the “best” least square straight line plot of  $\ln(R_{TH})$  against  $1/T$ , giving the thermistor equation as:

$$\ln(R_{TH}) = -\frac{1773.8}{T} + 18.178 \quad (19)$$

The calibration plot is shown in figure (6.5) below:



Figure(6.5): Regression line of  $\ln(R_{TH})$  against  $1/T$

## 6.6 THE REACTOR (THERMOS-FLASK) CALIBRATION

The reaction vessel used was an ordinary dewer thermos-flask with removable screw cap lid. The flask has a total volume of 500mL. The calibration involves the determination of the heat transfer coefficient of the flask and fitting the experimental data to the model described in eq(20) below:

$$T = T_s + (T_o - T_s) \exp\left(-\frac{UA}{mC_p} t\right) \quad (20)$$

In this experiment 400.00g of distilled water at 361K ( $T_o$ ) was injected into the reaction vessel and left the system temperature to fall over a period of time until the temperature-time profile reaches its asymptotic state or the steady-state temperature ( $T_s$ ). The figure (6.6) below shows the temperature-time profile of the cooling process.

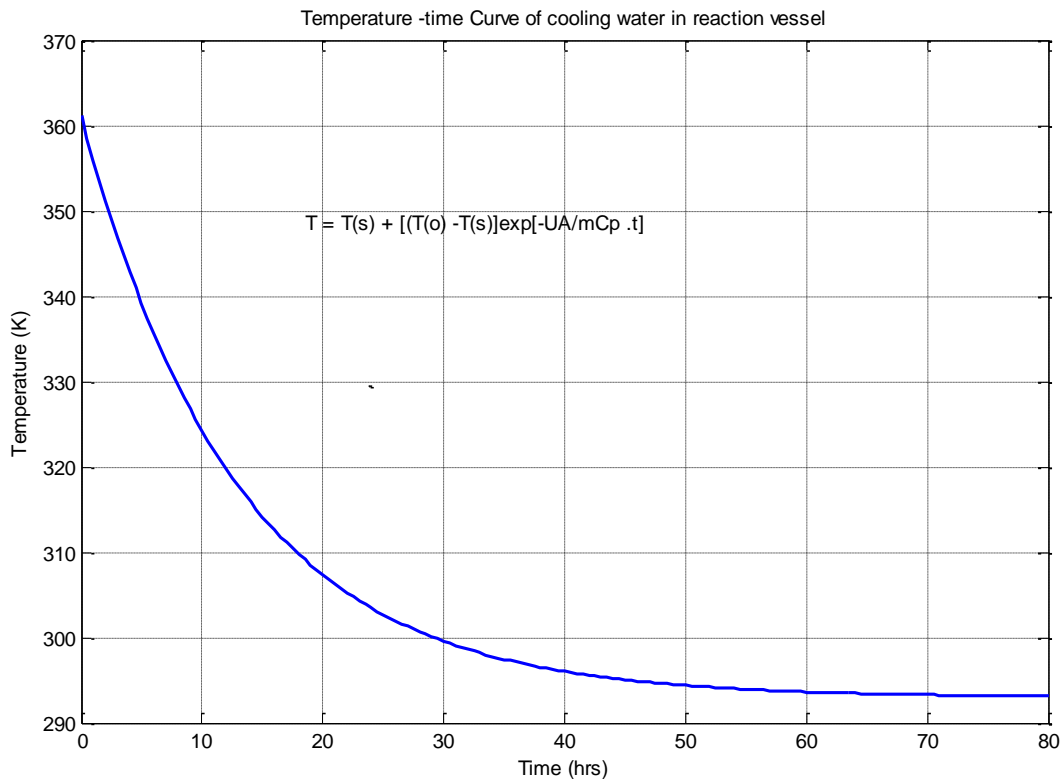


Fig (6.6) : Adiabatic Reactor (Thermos-flask) cooling curve@  $T(0) = 361K$

From eq(20) the values of  $T_o$  and  $T_s$  were obtained from fig(6). Rearrangement of eq(20) gives;

$$\ln\left(\frac{T - T_s}{T_o - T_s}\right) = \ln(Y) = \left(-\frac{UA}{mC_p}t\right) \quad (21)$$

Since T and t values are known least square regression analysis was performed and a straight plot of ln(Y) against time is shown in figure (6.7) below:

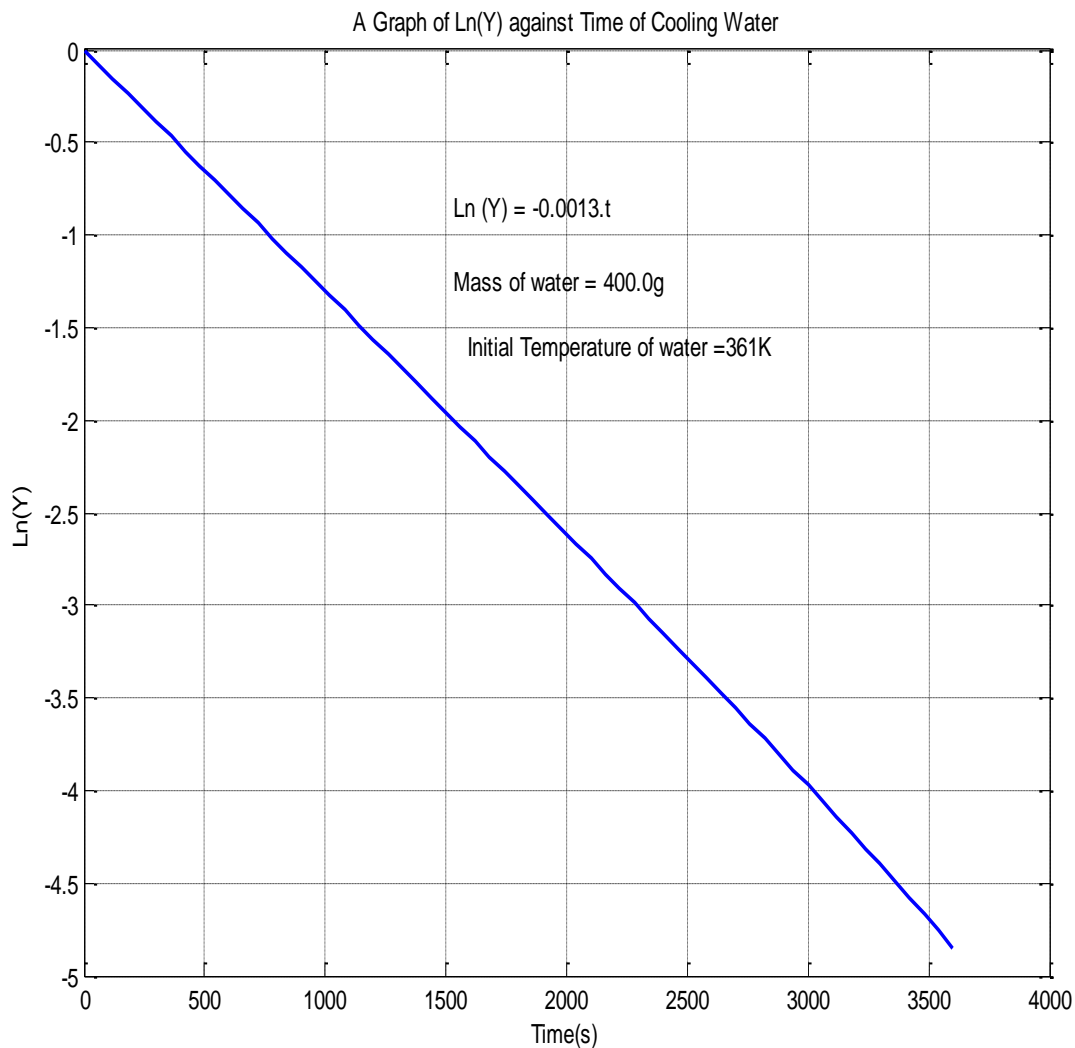


Fig (6.7) :Regression line of heat transfer coefficient of reactor

The slope of the straight line of fig(7) is given by  $0.0013s^{-1}(\text{min}^{-1})$  which corresponds to the value of the heat transfer coefficient of the flask.

## 6.7 EXPERIMENTAL PROCEDURES AND RESULTS

### 6.7.1 EXCESS WATER-ACETIC ANHYDRIDE REACTIONS

Analytical reagent grade acetic anhydride and distilled water was used in all experiments. In all experiments 1 mol of acetic anhydride was injected into the reaction vessel followed by 10 mols of distilled water. These quantities (volumes) were used so that at least 60% of the length of the sensor (thermistor) would be submerged in the resulting initial reacting mixture. Reactants were brought to a steady- state temperature before starting the stirrer to initiate the reaction. In course of the reaction, the stirrer speed was set at 1000 rev/min, the resulting voltage –time profiles were captured and the corresponding temperature-time curve was determined using the thermistor equation derived above. Runs were carried out adiabatically at the following initial temperatures: 305K, 310K and 328K.

### 6.7.2 EXPERIMENTAL DETERMINATION OF HEAT TRANSFER COEFFICIENT OF THE PROCESS

For a given system (reaction vessel and content) one can write:

$$\left(\frac{mC_p}{UA}\right)_{system} = \left(\frac{m C_p}{UA}\right)_{water} + \left(\frac{mC_p}{UA}\right)_{vessel} \quad (22)$$

In this experiment different amount of water ( $m_w$ ) (200g, 300g and 400g) was injected into the reaction flask at 343.08K, 347.77K and 347.85K and allowed to cool until the temperature reaches a steady-state temperature ( $T_s$ ). Figures (6.8a), (6.9a) and (6.10a) of the cooling processes are shown below. The cooling process thus follows equation (20) above. A nonlinear least-square regression analysis was performed on all the three experimental curves. Using eq(21), the value of  $UA/mC_p$  for each cooling curve was obtained. Figures (6.8b),(6.9b) and (6.10b) shows the regression lines.

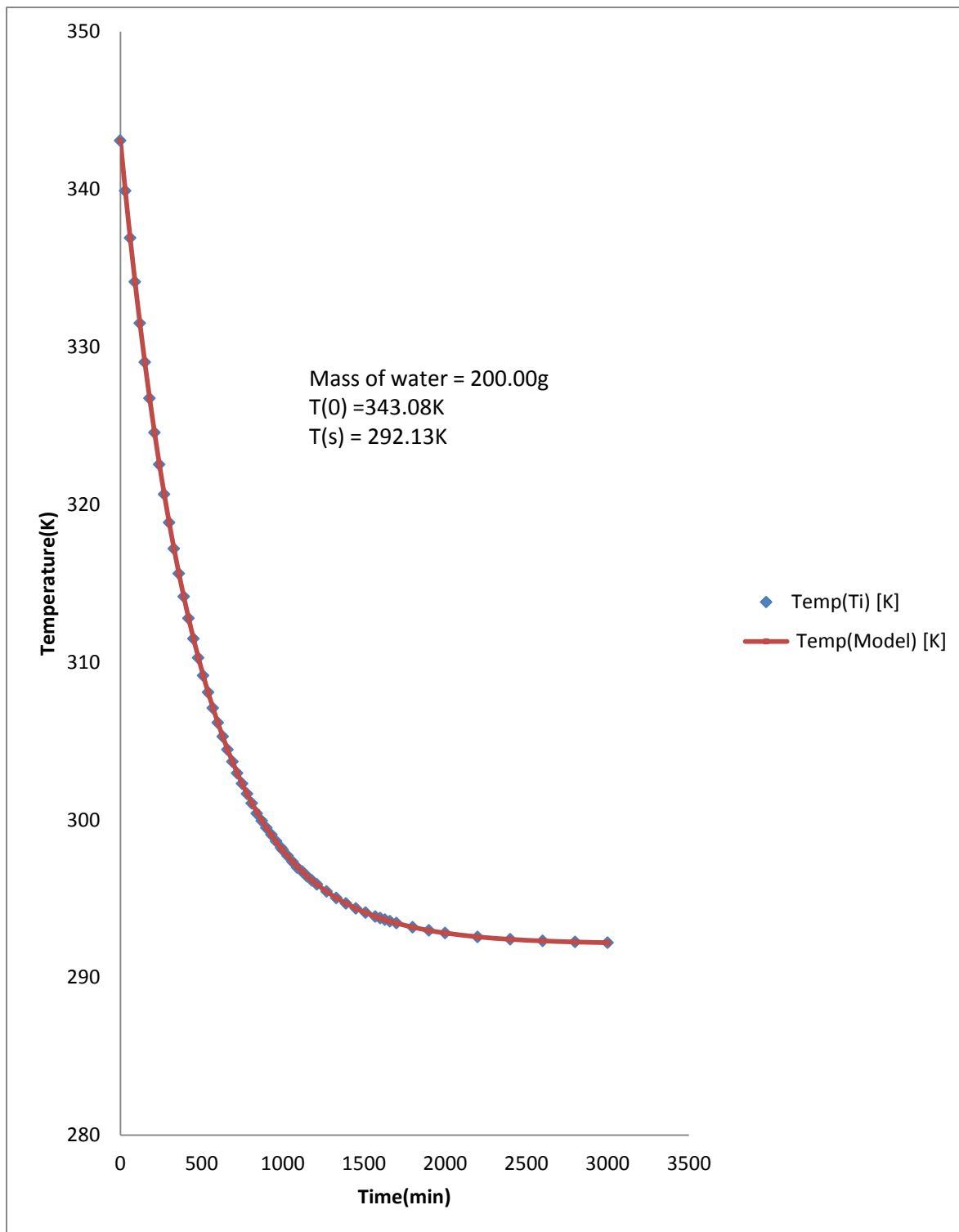


Fig (6.8a): Adiabatic Reactor (Thermos-flask) cooling curve @  $T(0) = 343.08\text{K}$

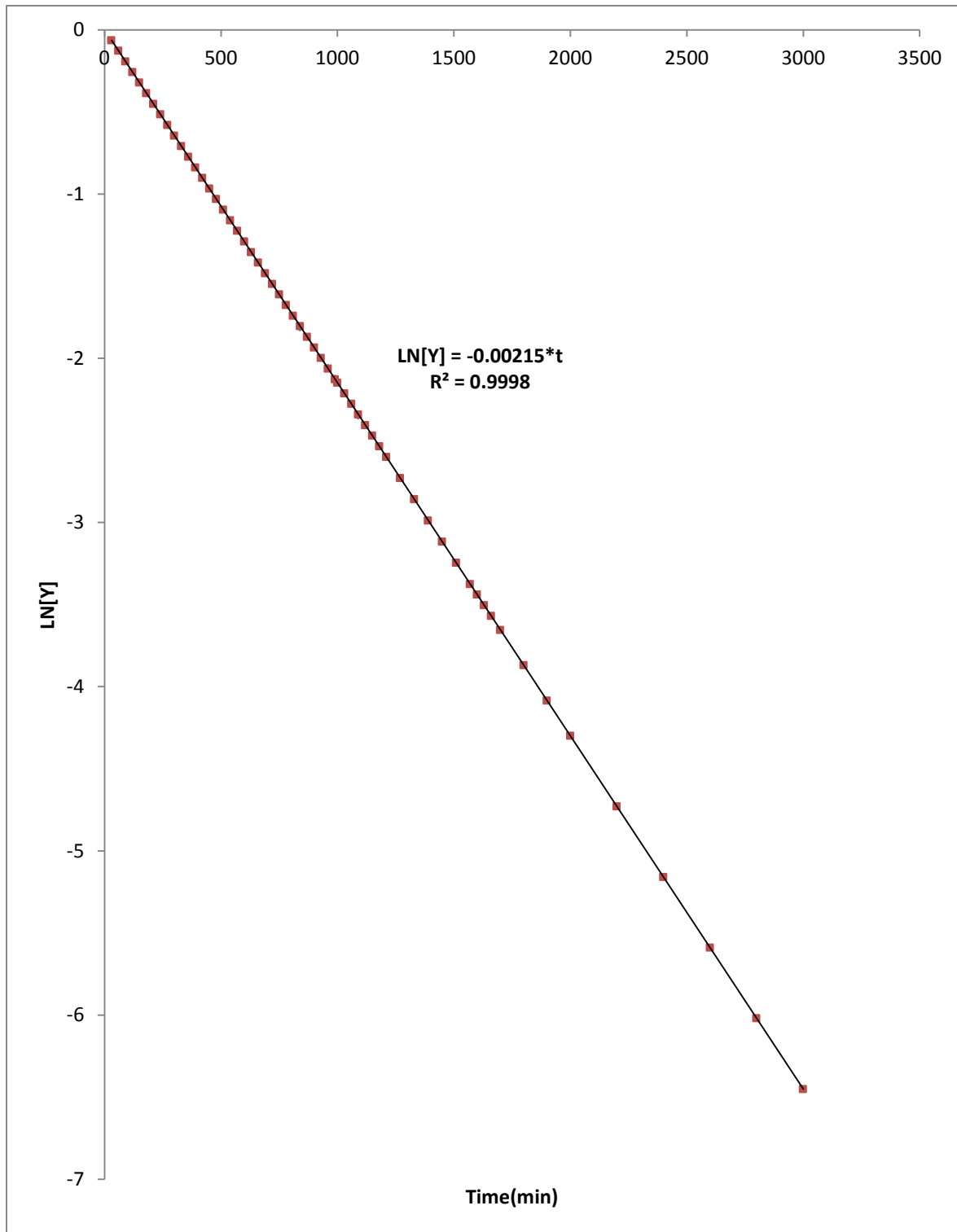


Fig (6.8b): Regression line of heat transfer coefficient of reactor

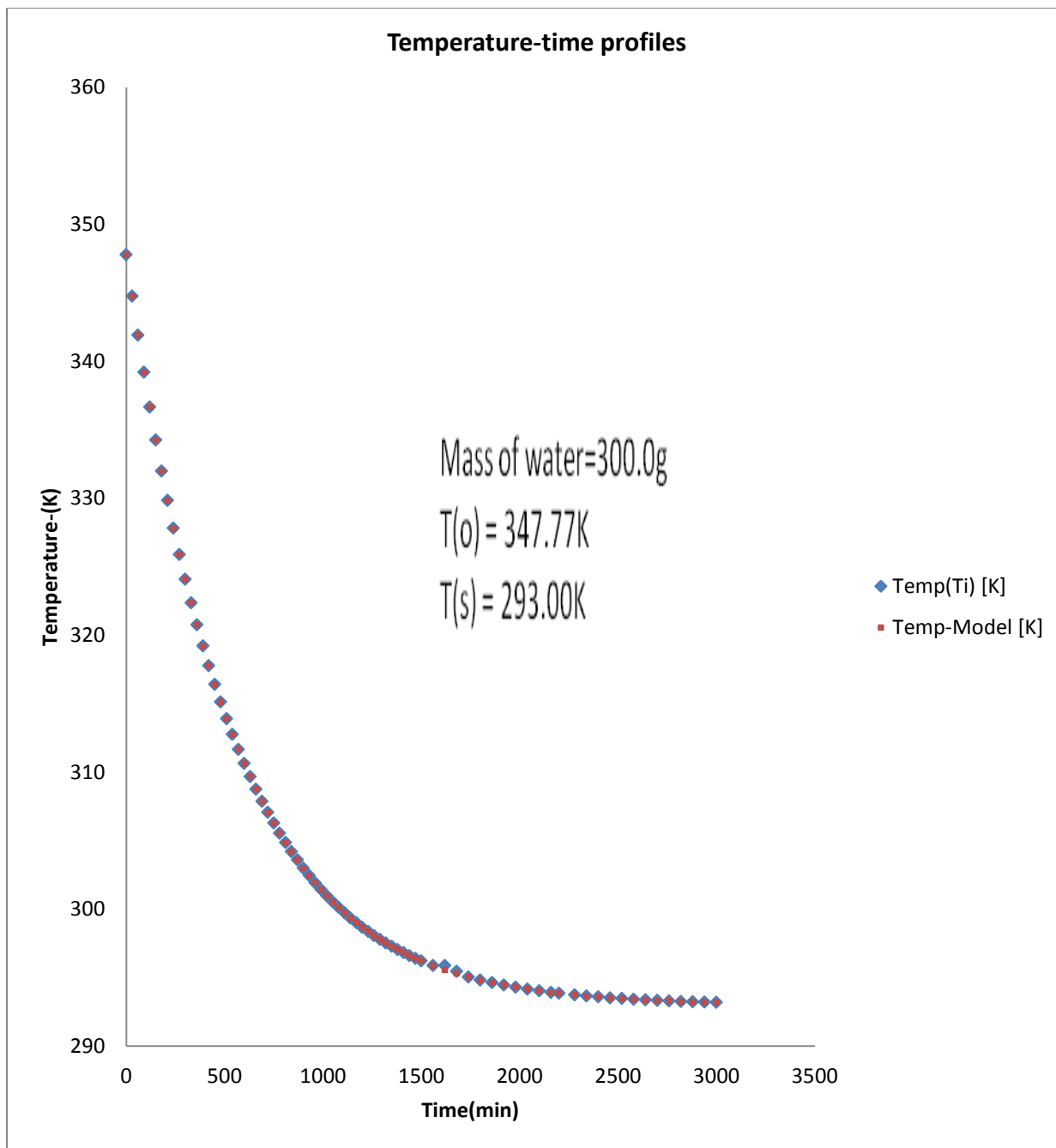


Fig (6.9a): Adiabatic Reactor (Thermos-flask) cooling curve @  $T(0) = 347.77\text{K}$

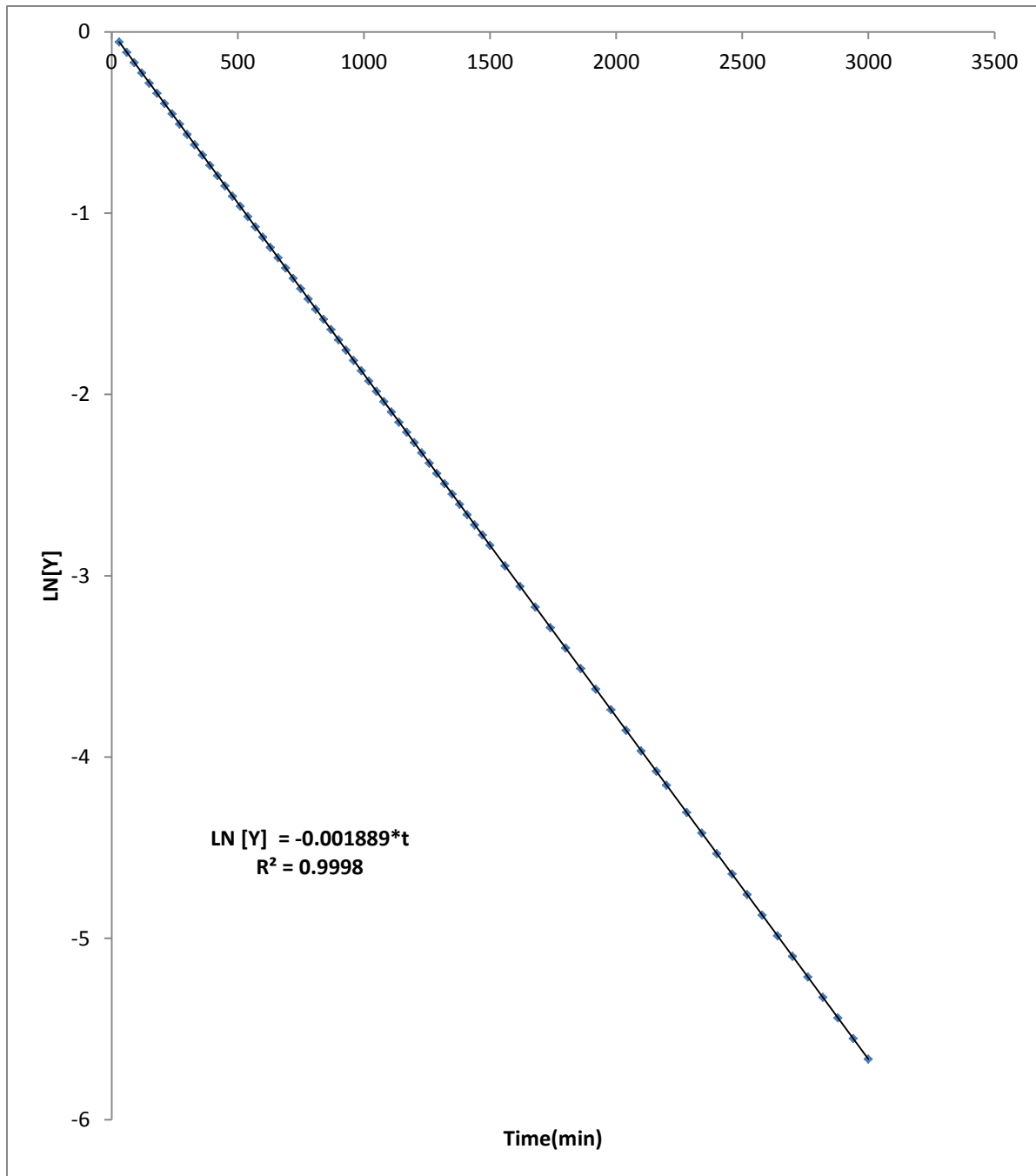


Fig (6.9b): Regression line of heat transfer coefficient of reactor

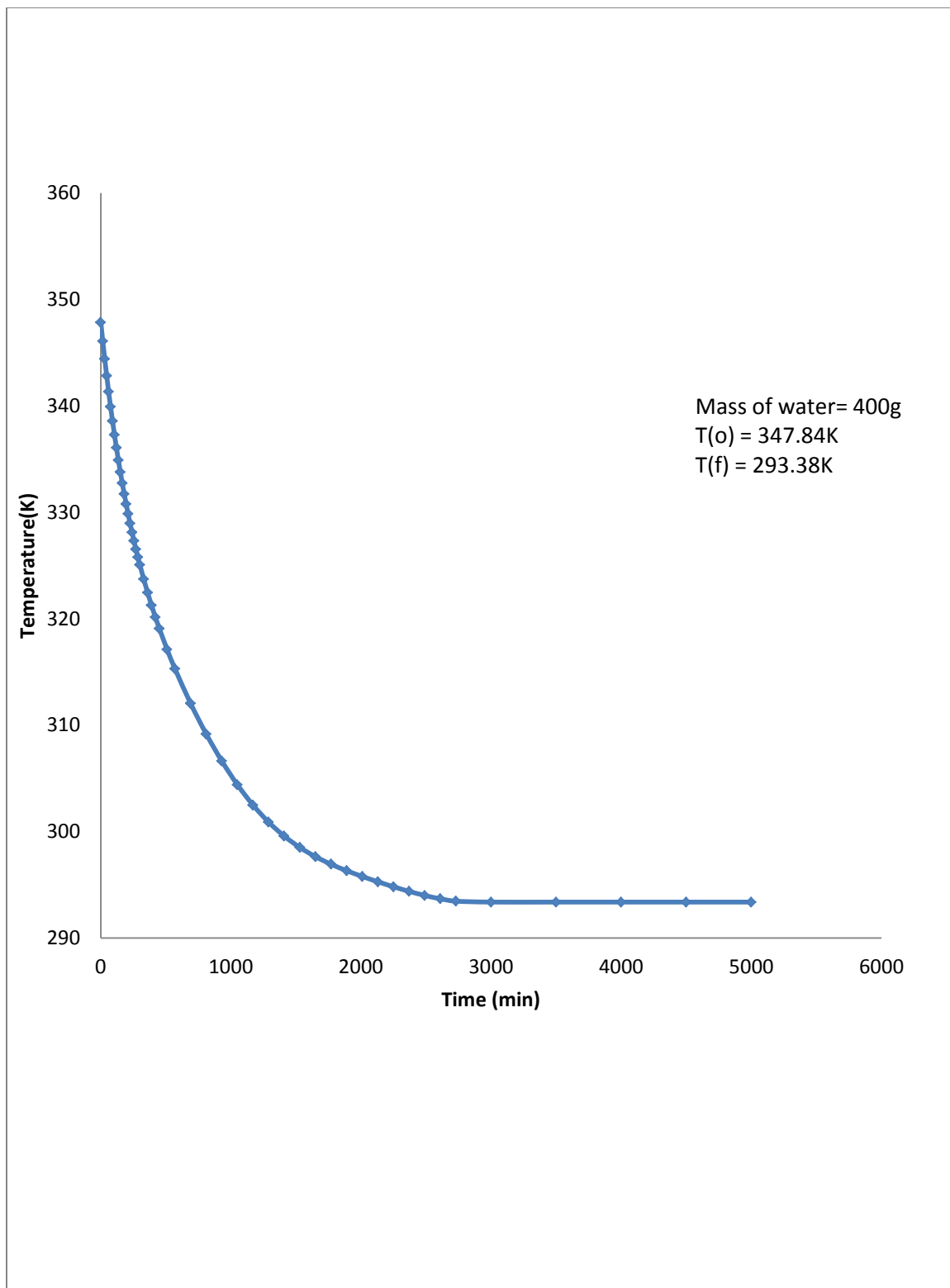


Fig (6.10a): Adiabatic Reactor (Thermos-flask) cooling curve @  $T(0) = 347.80\text{K}$

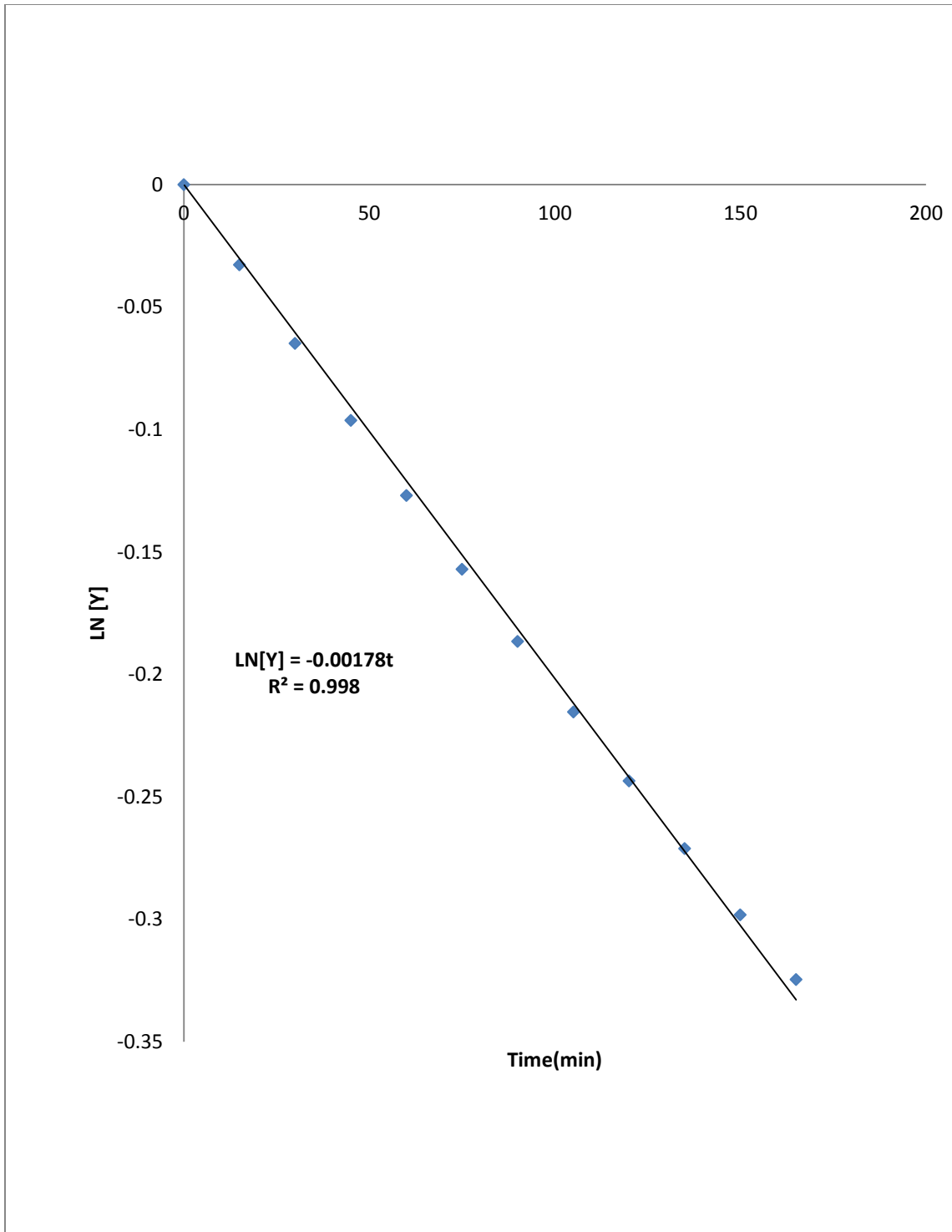


Fig (6.10b): Regression line of heat transfer coefficient of reactor

Table (6.1): Summary of characteristics of figures (6.8)-(6.10)

Mass of water(g)	Initial Temperature(K)	Final Temperature(K)	UA/mCp (min <sup>-1</sup> )
200	343.08	292.13	0.00215
300	347.77	293.00	0.00189
400	347.84	293.38	0.00178

From table (6.1) a plot of mass of water (m) against (mC<sub>p</sub>/UA) is shown in figure(6.11) below:

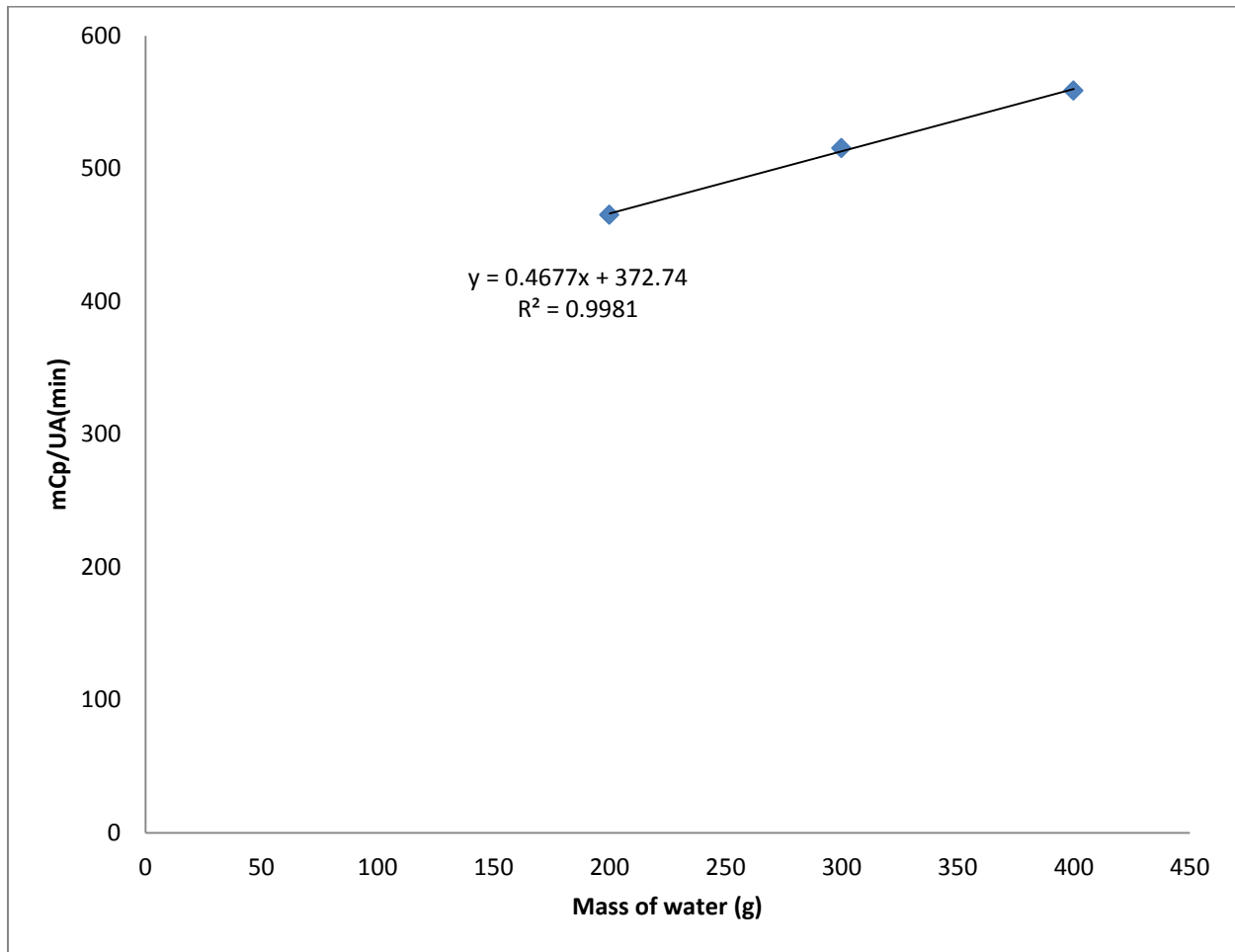


Fig (6.11): A plot of mass of water (m) against (mC<sub>p</sub>/UA)

### 6.7.3 DETERMINATION OF UA/mC<sub>p</sub> FOR THE REACTION MIXTURE

Table (6.2) below consist of some of the physical constants of the reacting species which was used in the determination of the quantity UA/mC<sub>p</sub>.

Table (6.2) : Some constants of reacting species:

Species	Moles	Molar mass(g/mol)	C <sub>p</sub> (J/mol.K)
Acetic anhydride	1.0	102.9	189.7
Water	10.0	18.01	75.4

Equation (23) was used to determine specific heat of the reacting mixture (C<sub>p,mix</sub>) and the quantity M<sub>T</sub>C<sub>p,mix</sub>.

$$C_{P,mix} = \frac{m_{AA}}{M_T} C_{P,AA} + \frac{m_W}{M_T} C_{P,W} \quad (23)$$

M<sub>T</sub>, is the total mass of the reacting mixture and M<sub>T</sub>C<sub>p,mix</sub> was calculated to be 943.64 J/K. Since the reaction is not pure water we therefore determined its equivalent mass of water by dividing 943.64J/K by the specific heat of water:

$$m_{eqv\ water} = \frac{(M_T C_P)_{mix}}{C_{P,water}} = 225.5g\ water \quad (24)$$

From figure (11) the value of the quantity (UA/mC<sub>p</sub>)<sub>mix</sub> was determined to be 0.00209/min. This value was plugged in eq(9) above and the corrections of the experimental results to adiabatic conditions was performed. The figures (6.12),(6.13) and (6.14) below shows the experimental and the corrected temperature profiles for all the three runs.

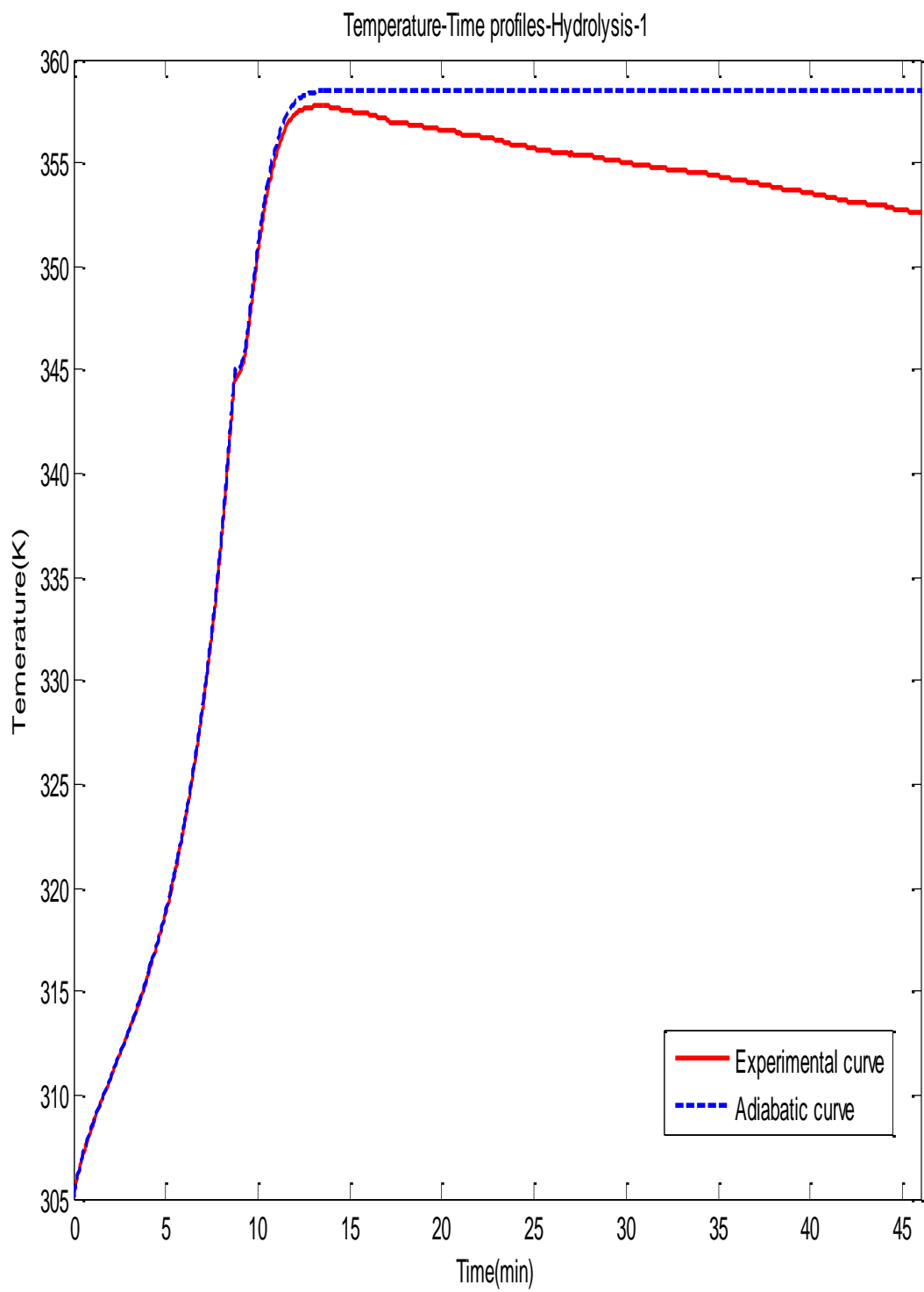


Fig (6.12): Temperature-time plots of acetic anhydride-excess water reaction at 305K

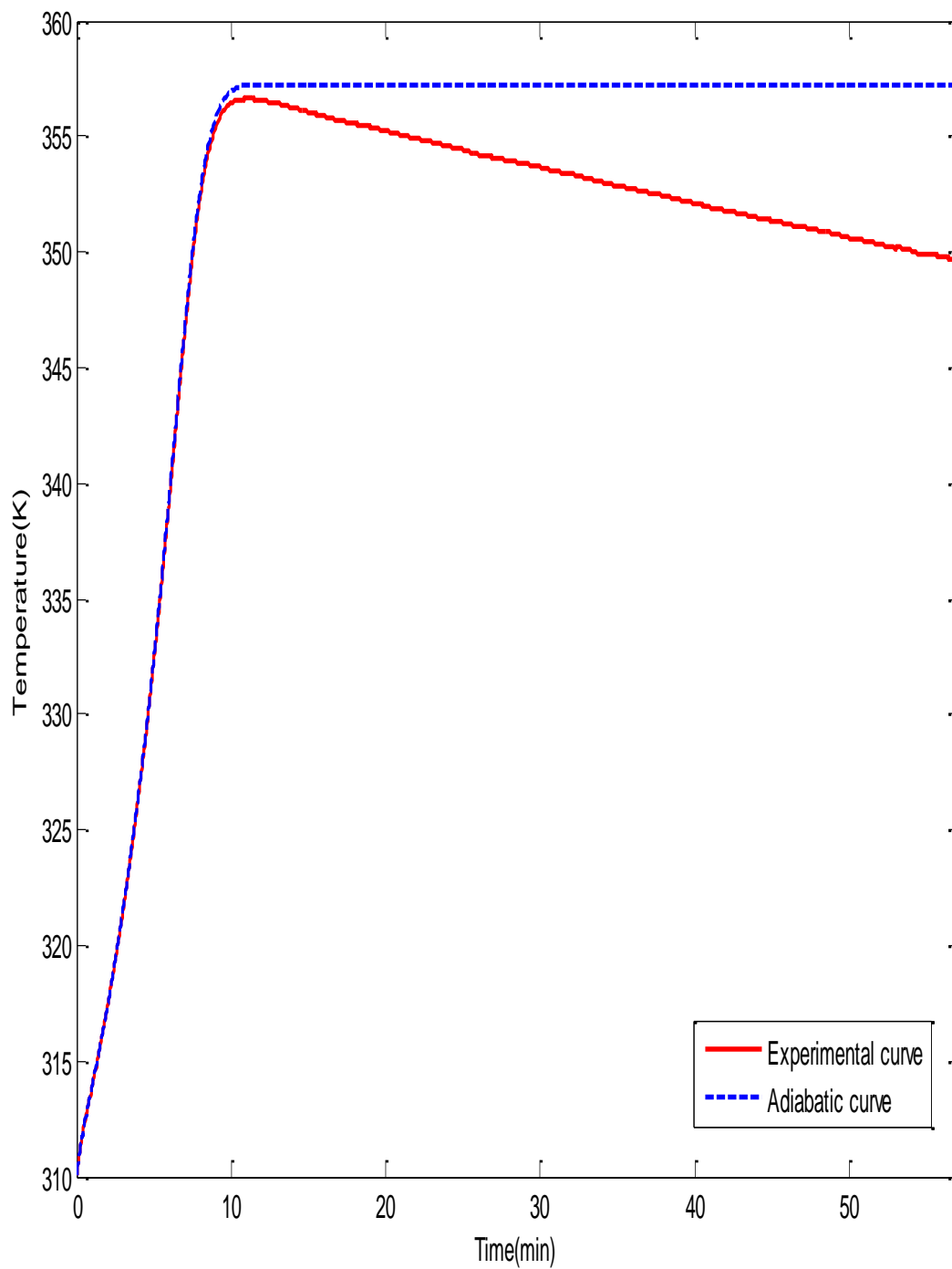


Fig (6.13): Temperature-time plots of acetic anhydride-excess water reaction at 310K

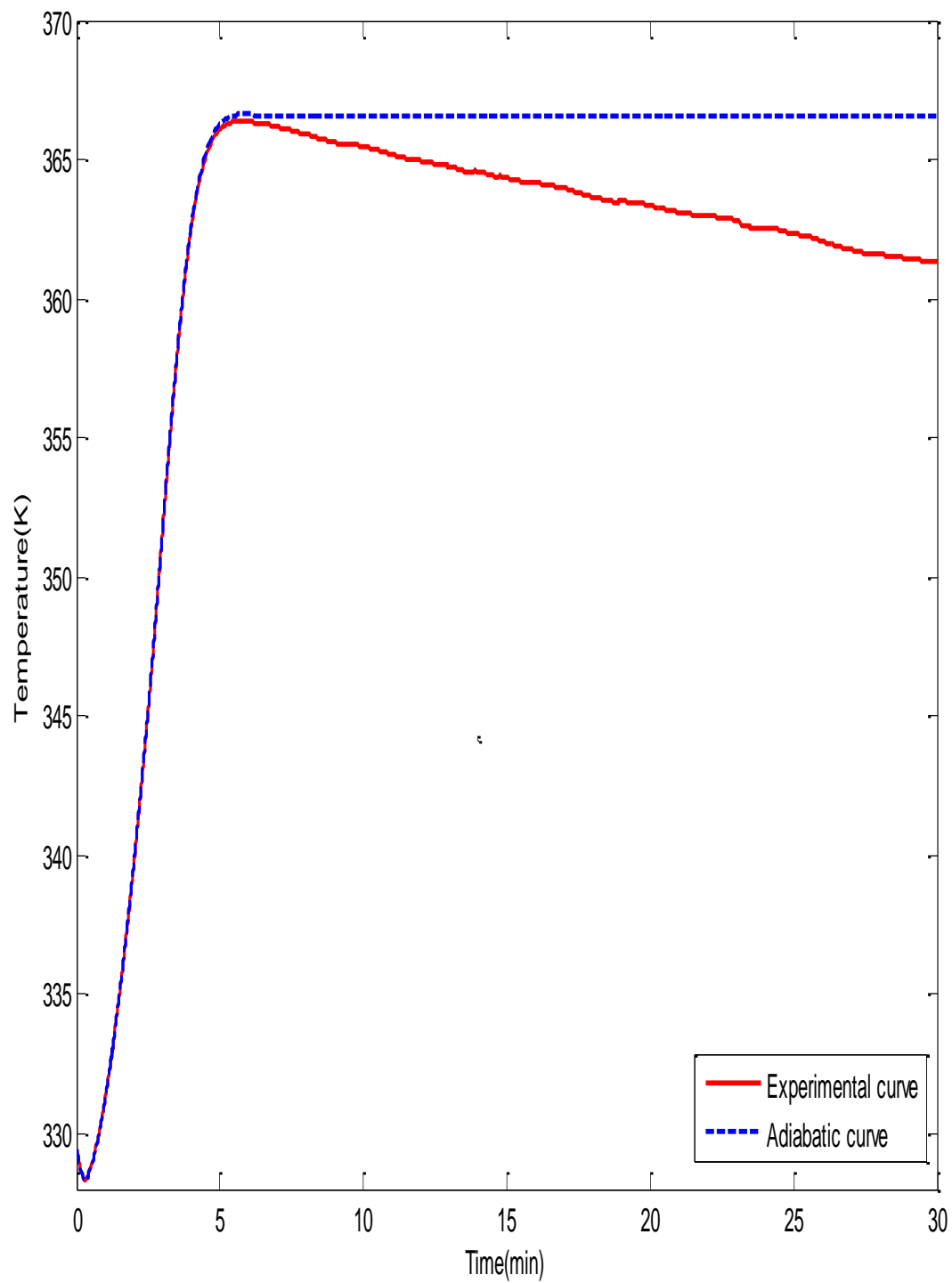


Fig (6.14): Temperature-time plots of acetic anhydride-excess water reaction at 328K

Table (6.3) : Summary of the characteristics of the above temperature-time plot

Experiment	T(o)(K)	T <sub>(max adiabatic)</sub> (K)	(ΔT) <sub>adiabatic</sub> (K)
1	305.10	358.50	52.67
2	310.10	358.70	56.40
3	328.40	366.40	38.00

From eq(11) the variation of acetic anhydride concentration with temperature/time was deduces as:

$$C_{AA} = 3.64 - \alpha (T - T_0) \quad (25)$$

The constant ( $\alpha$ ) in eq(25) was calculated using the initial concentration of the acetic anhydride, 3.64mol/L and the adiabatic temperature change ( $\Delta T$ )<sub>adiabatic</sub> values provided in table (3).The figures (6.15),(6.16) and (6.17) show how acetic anhydride concentrations varies with time for the three experiments.

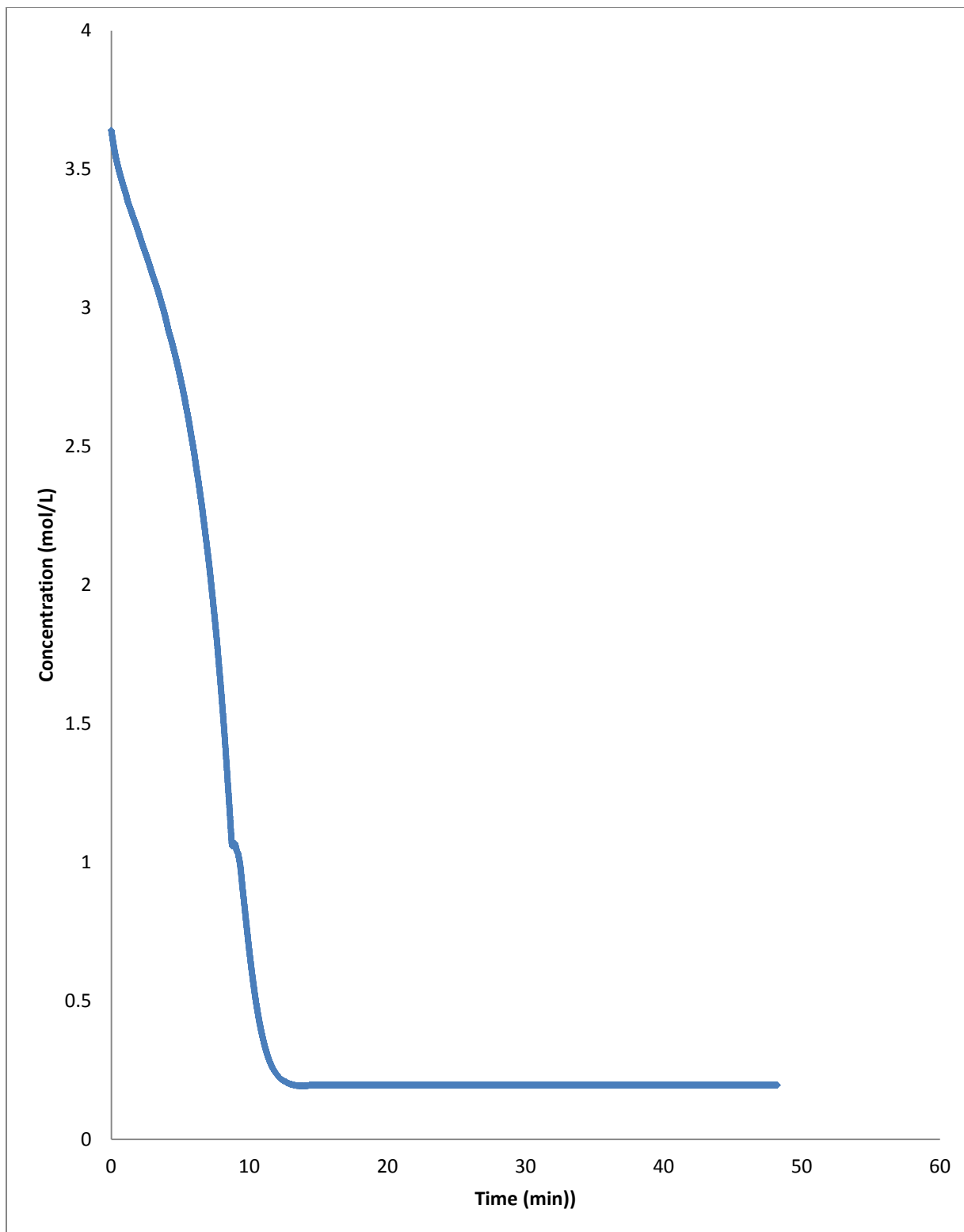


Fig (6.15): Concentration-time plots of acetic anhydride-excess water reaction at 305K

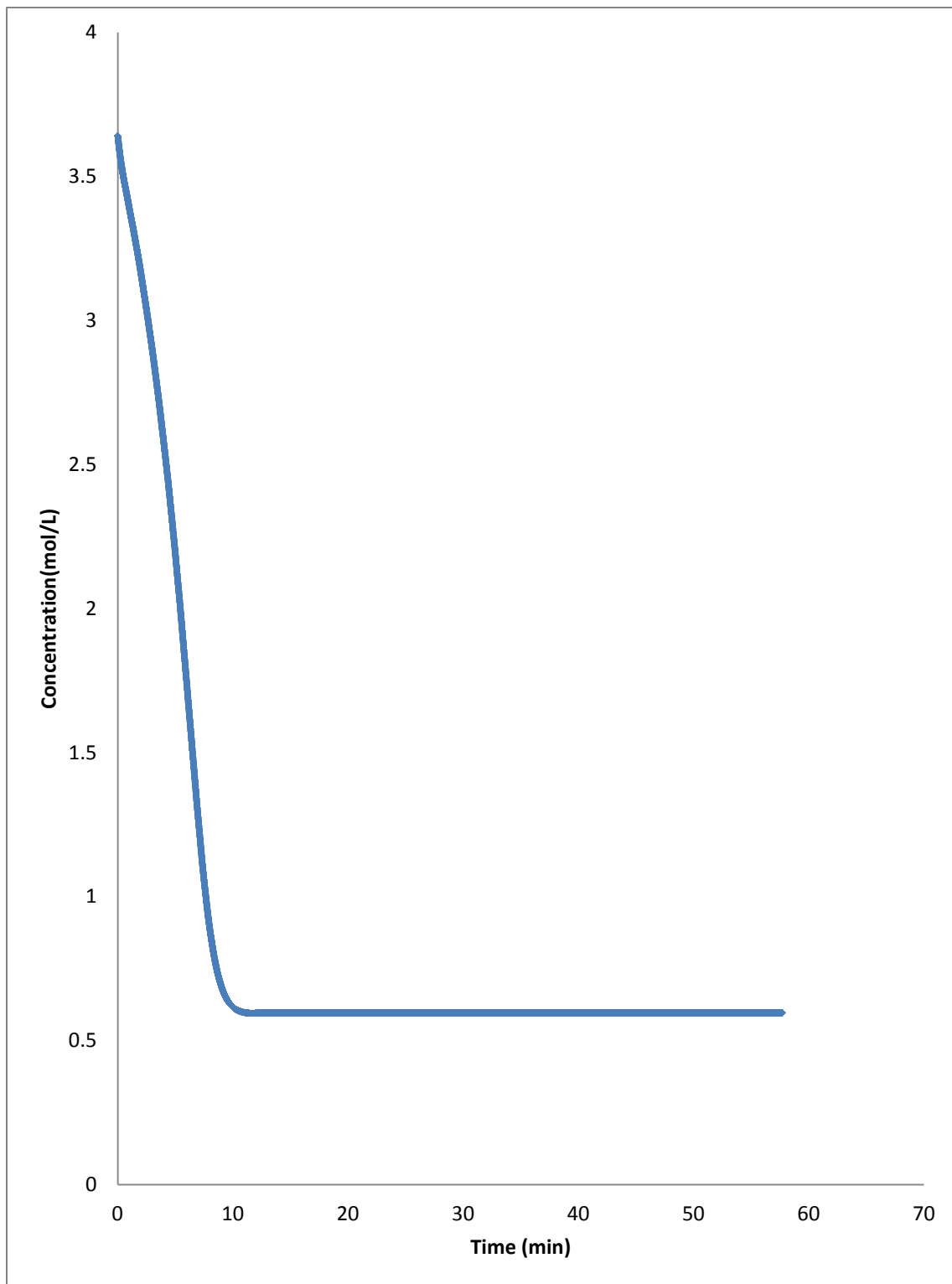


Fig (6.16): Concentration-time plots of acetic anhydride-excess water reaction at 310K

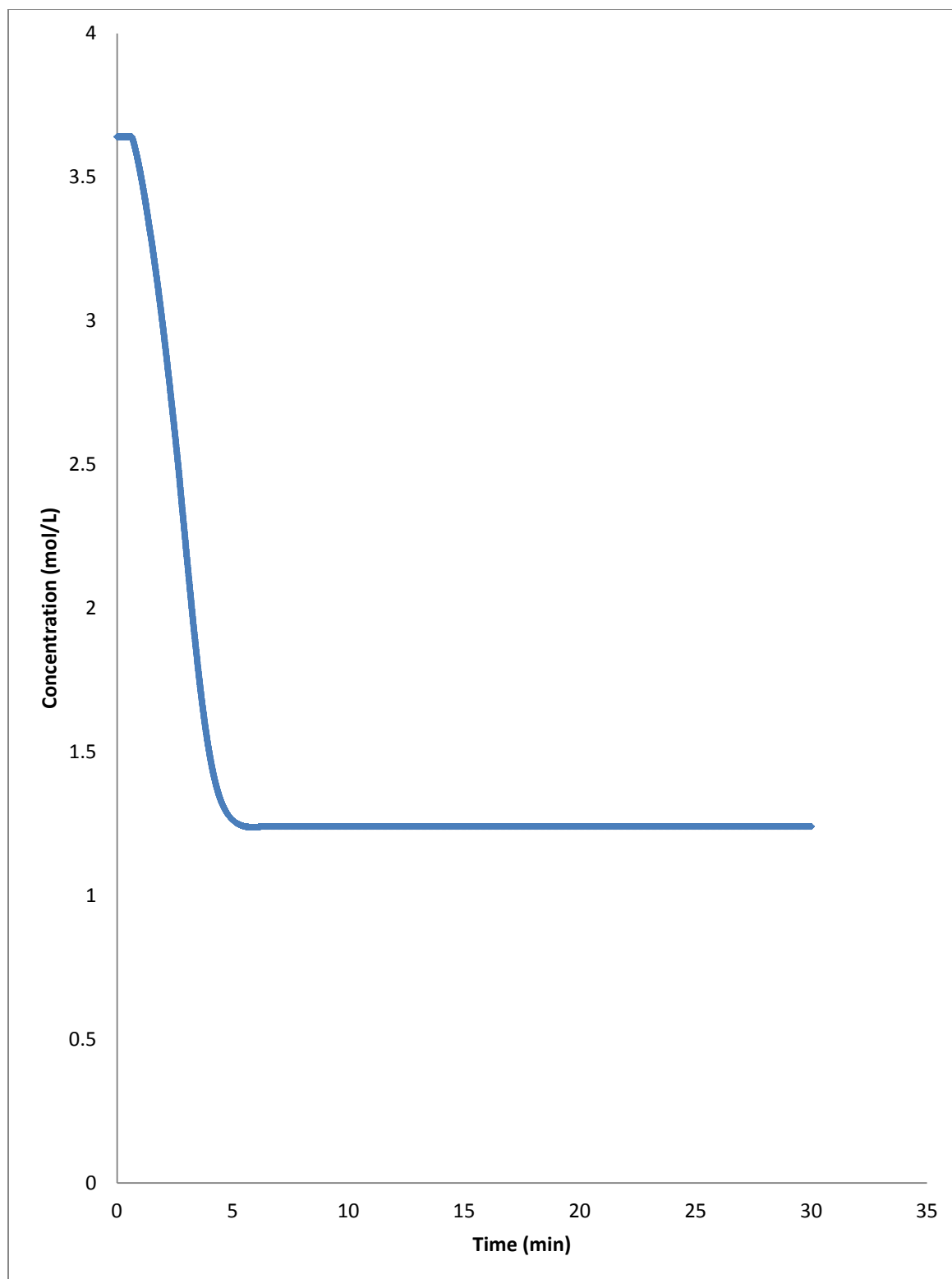


Fig (6.17): Concentration-time plots of acetic anhydride-excess water reaction at 328K

## 6.7.4 VARIATION OF RATE OF REACTION WITH CONCENTRATION

### CHANGE

The average rate of a reaction ( $-r_A$ ) which is a function of temperature and concentration and for a pseudo-first process such acetic anhydride reacting in excess water, at a particular temperature the specific rate constant value should be the same in all three cases of the processes considered.

$$\text{Recall that } k(T) = \frac{-r_A(T)}{C_A} \quad (26)$$

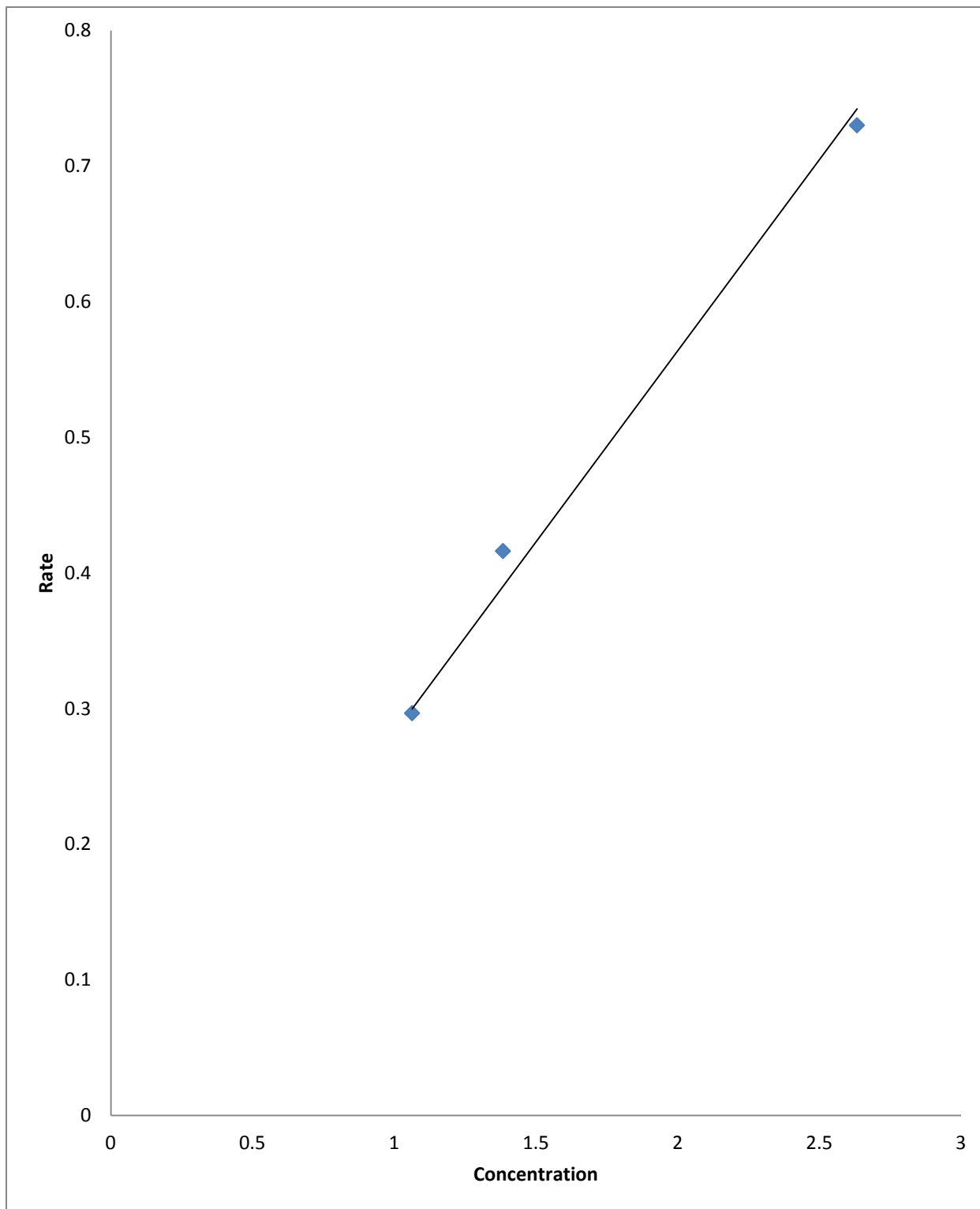
The average rate of reaction at a particular time was determined from the concentration time-time plots by determining the first derivatives at different time intervals numerically using the concentration-time data of the runs.

Table (6.4) : Variations of temperature, rate and concentration at T =345K

<b>T=345K</b>			
Experiment	Concentration	Rate	Rate constant (k)
1	1.0637	0.2965	0.2787
2	1.3848	0.4160	0.3004
3	2.633	0.7300	0.2772

Average (k) = 0.285

Standard deviation (k) = 0.0013



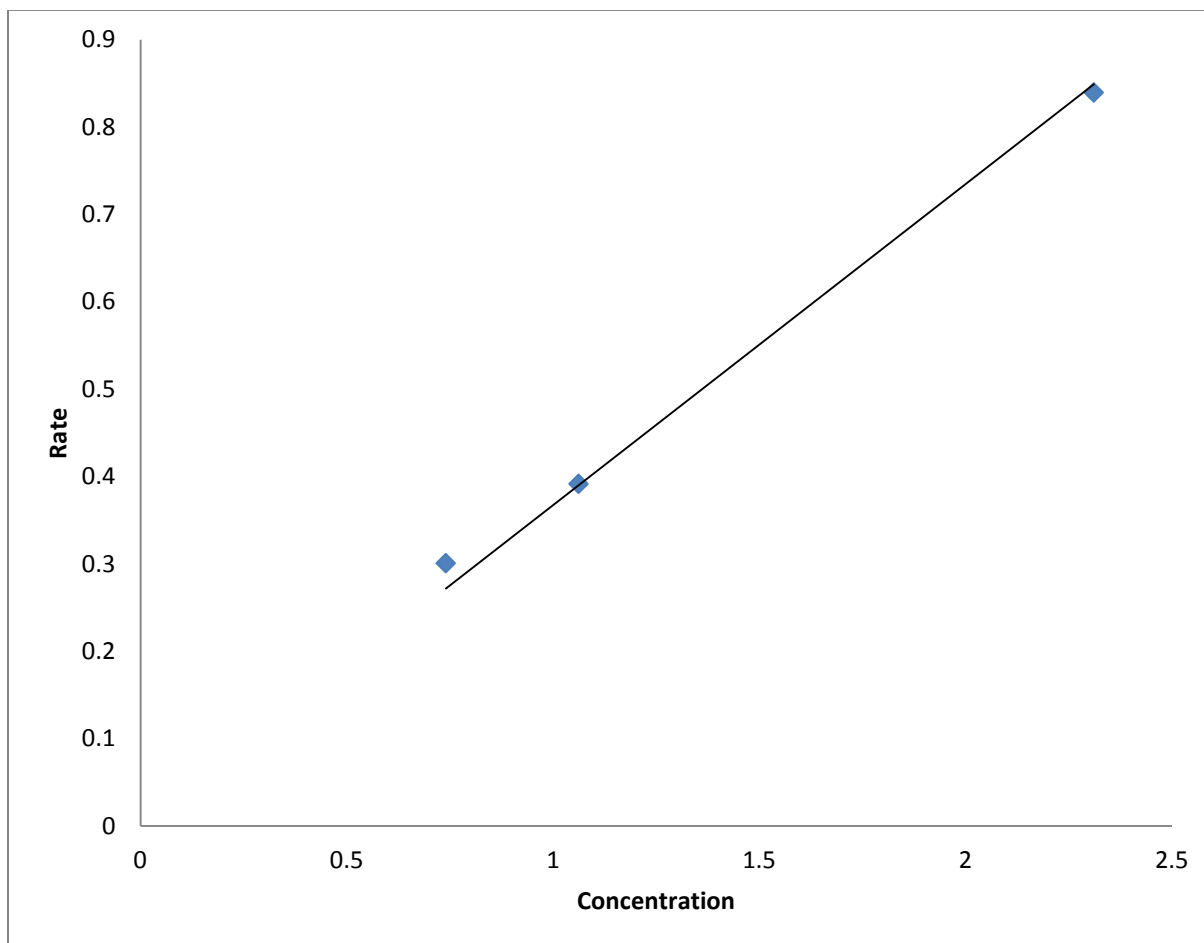
Figure(6.18): Concentration-rate plot @ 345K

Table (6.5) : Variations of temperature, rate and concentration at T =350K

<b>T=350K</b>			
Experiment	Concentration	Rate	Rate constant (k)
1	0.7403	0.3005	0.4059
2	1.0623	0.3913	0.3684
3	2.3109	0.8391	0.3613

Average (k) =0.3785

Standard deviation (k) =0.024



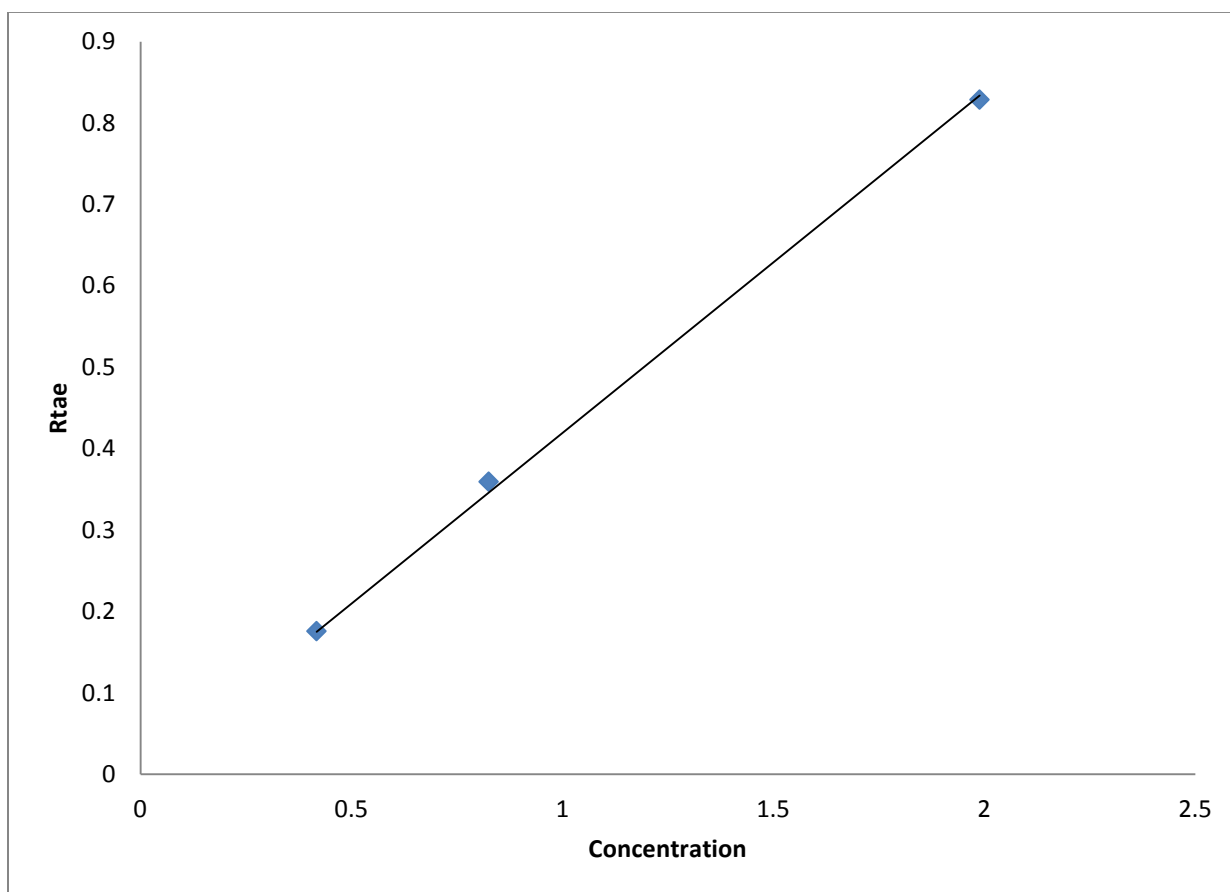
Figure(6.19): Concentration-rate plot @ 350K

Table (6.6) : Variations of temperature, rate and concentration at T =355K

<b>T=355K</b>			
Experiment	Concentration	Rate	Rate constant (k)
1	0.4177	0.1746	0.4199
2	0.8256	0.3590	0.4348
3	1.9893	0.8283	0.4164

Average (k) =0.4237

Standard deviation (k) = 0.0098



Figure(6.20): Concentration-rate plot @ 355K

### 6.7.5 KINETICS AND THERMODYNAMIC ANALYSIS OF THE EXPERIMENTS

The rate information obtained from the concentration-time plot enabled one to calculate specific rate constant  $k(T)$  of the processes at any time ( $t$ ) and temperature ( $T$ ). Arrhenius plots were thus generated from which kinetic parameters of runs were extracted.

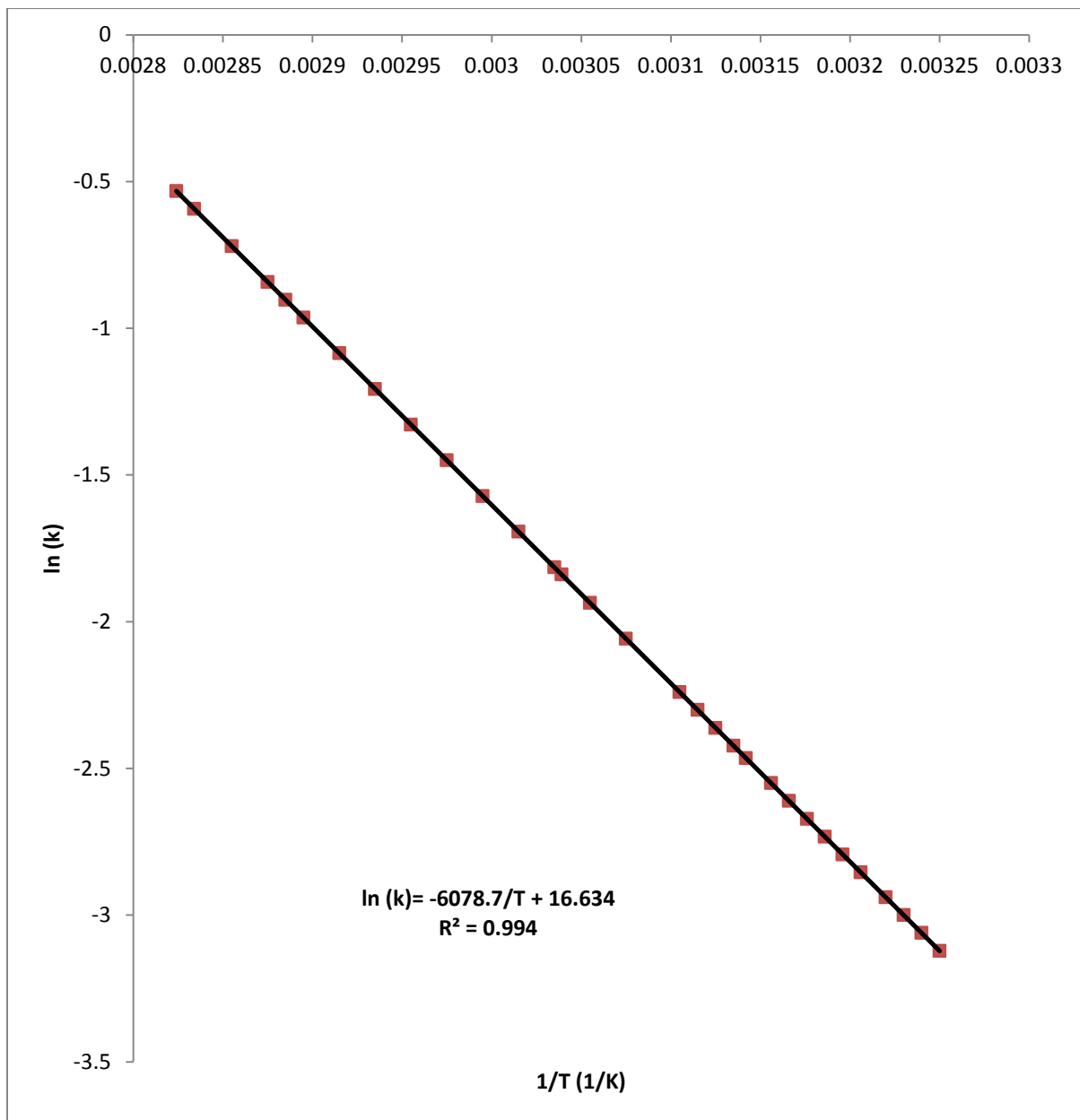


Figure (6.21): Arrhenius plot of experiment-1

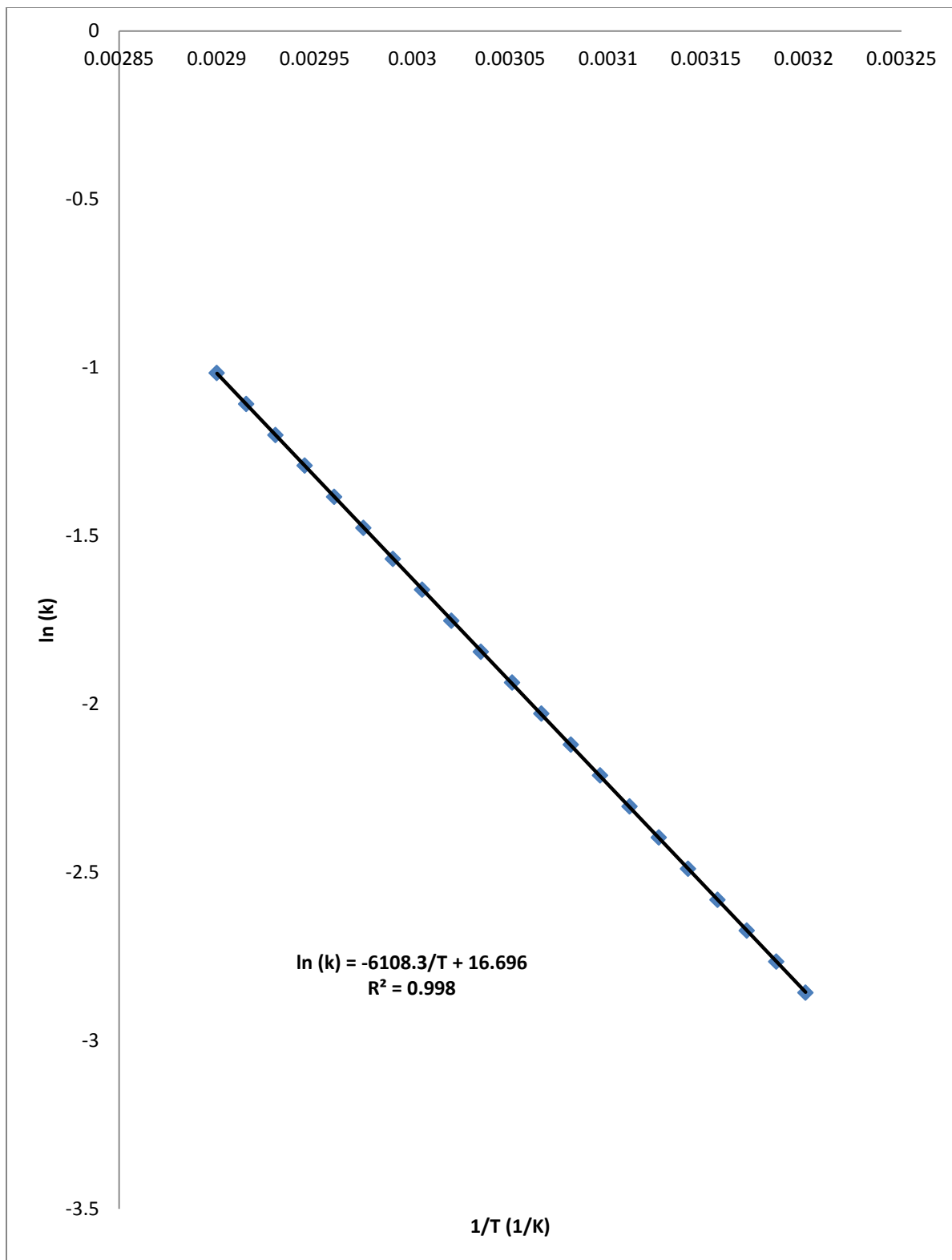


Figure (6.22): Arrhenius plot of experiment-2

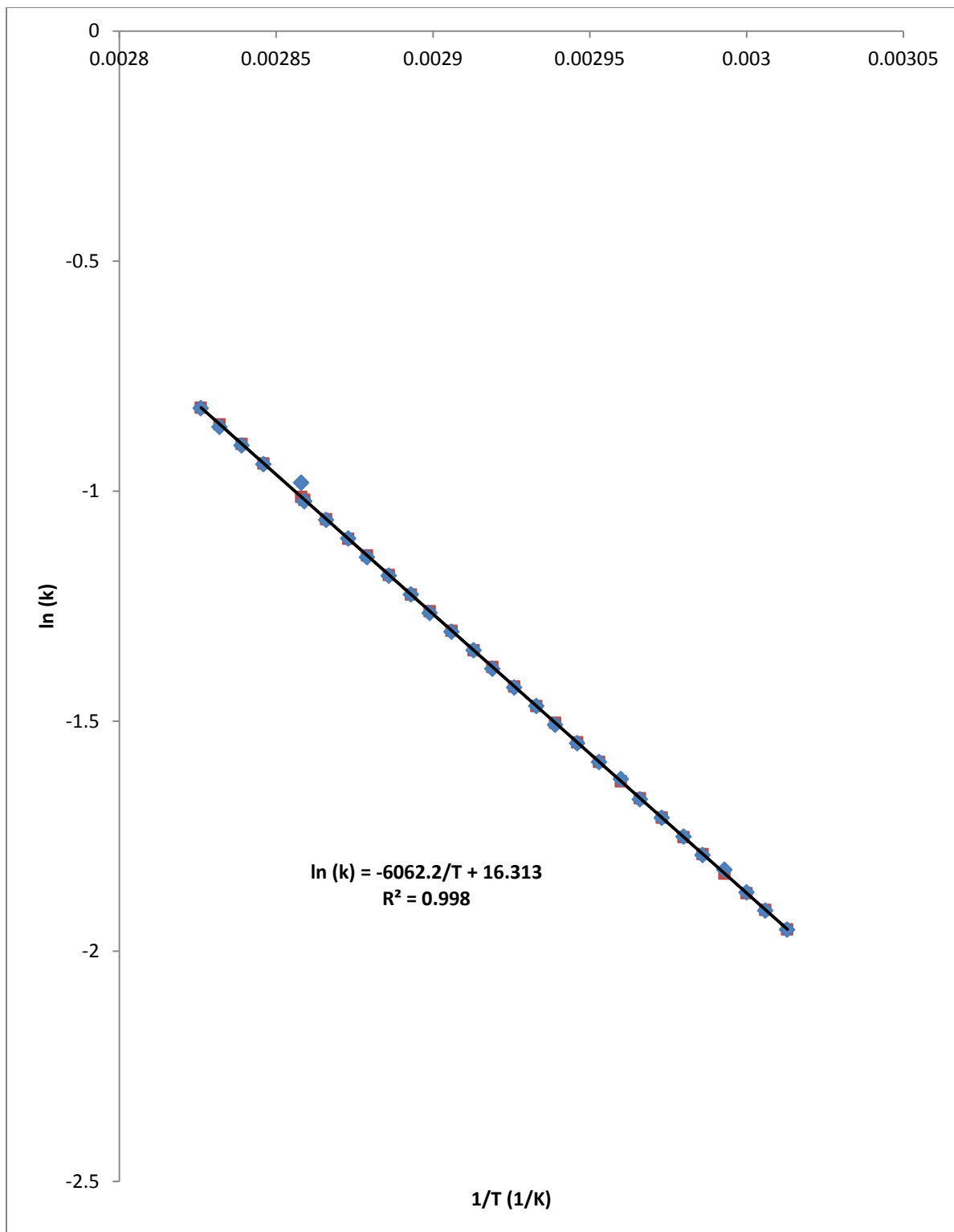


Figure (6.23): Arrhenius plot of experiment-3

The values obtained for the specific rate constants as a function of temperature are given in equations (27),(28) and (29) below:

$$k_1(T) = 1.68 * 10^7 \exp\left(-\frac{6078.7}{T}\right) \quad (27)$$

$$k_2(T) = 1.78 * 10^7 \exp\left(-\frac{6108.3}{T}\right) \quad (28)$$

$$k_3(T) = 1.22 * 10^7 \exp\left(-\frac{6062.2}{T}\right) \quad (29)$$

The thermodynamic information extracted from the experiments was the heat of the reaction ( $\Delta H_{rxn}$ ). This was assumed to be independent of temperature and was determined by using eq(10). Table(6.7) below shows  $\Delta H_r$  values of the various experiments.

Table (6.7) : Thermodynamic information of the experiments

Experiment	1	2	3
$\Delta H_{rxn}$ (kJ/mol)	-53.36	-53.44	-53.51

## 6.8 EXPERIMENTAL PROCEDURES AND RESULTS

### 6.8.1 EXCESS ACETIC ANHYDRIDE-WATER REACTIONS

Analytical reagent grade acetic anhydride and distilled water was used in all experiments. In these experiments 2.645mols of acetic anhydride was injected into the reaction vessel followed by 0.556mols of distilled water. These quantities (volumes) were used so that at least 60% of the length of the sensor (thermistor) would be submerged in the resulting initial reacting mixture. Reactants were brought to a steady- state temperature before starting the stirrer to initiate the reaction. The stirrer speed was set at 1000 rev/min, the resulting voltage –time profiles were captured and the corresponding temperature-time curve was determined using the thermistor equation derived above. Runs were carried out adiabatically at the following initial temperatures: 286.8K, 293.6K and 304.5K.

### 6.8.2 DETERMINATION OF $UA/mC_p$ FOR THE REACTION MIXTURE

The quantity  $UA/mC_p$  was determined for each of the runs using the cooling parts of the curves. It is noticed from the cooling parts of the runs were similar to the curve cooling water experiments described in section 4.8 above. It was an indication the cooling part of the experimental runs was real cooling process and no reaction took place during that process. The cooling parts thus follows eq(20) above. A nonlinear regression analysis was perform on all the cooling parts using eq(21) and the value of  $UA/mC_p$  was determined for all the experimental runs. The steady-state temperature ( $T_s$ ) for the experiments was 293K. Figures (6.23b), (6.24b) and (6.25b) show the regressed lines of the experiments cooling sections and their  $UA/mC_p$  was obtained and used for the corrections of the experimental curves, corresponding experimental and adiabatic curves are shown below. The adiabatic curves was determined using eq(9) above.

Table (6.8): Initial temperatures and the corresponding values of the  $UA/mC_p$  of the runs.

Experiment	Initial Temperature(K)	UA/mC <sub>p</sub> (min <sup>-1</sup> )
4	286.8	0.002030
5	293.6	0.002698
6	304.5	0.002795

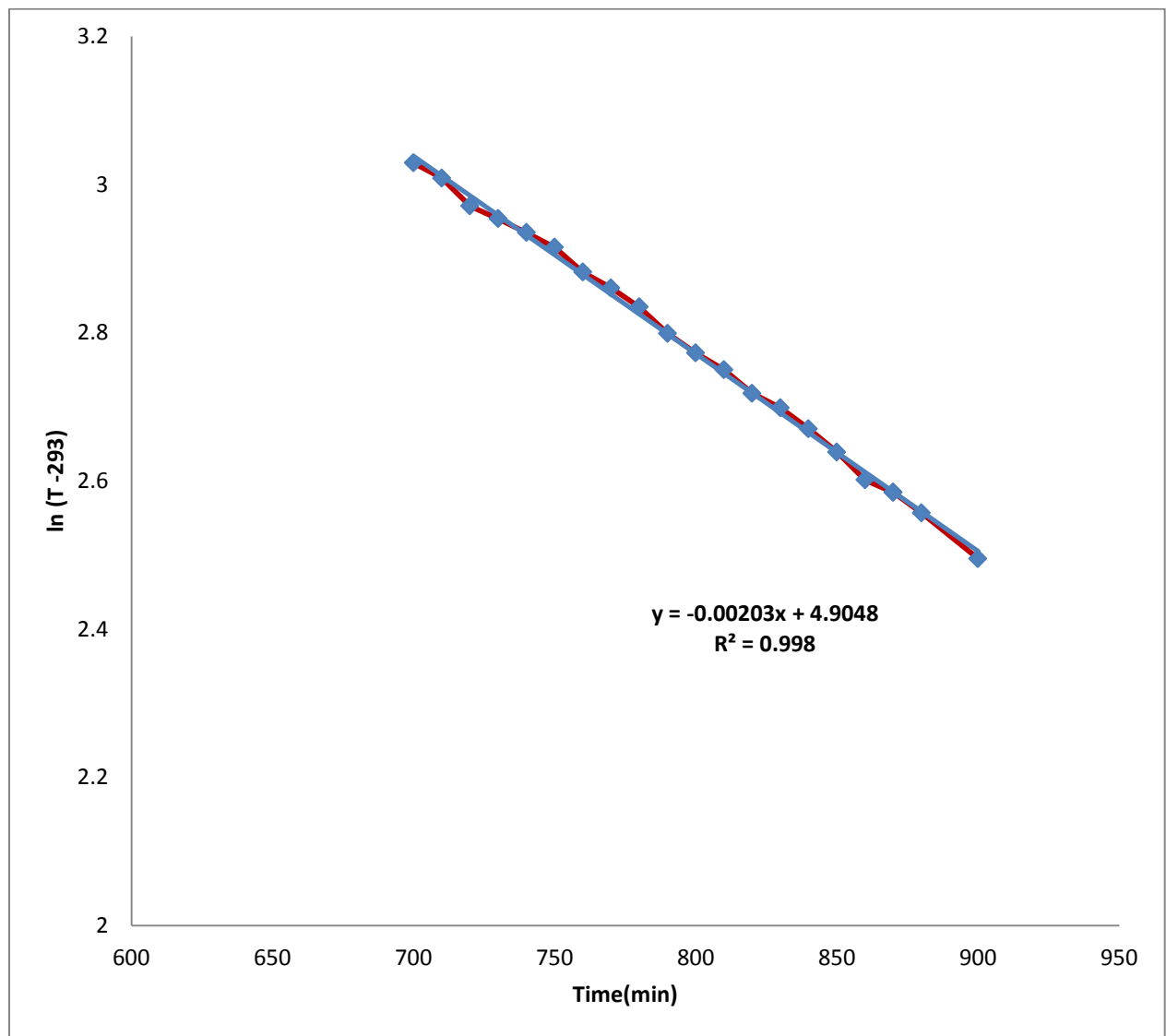


Fig (6.24a): Regression line for the UA/mc<sub>p</sub> of experiment-4

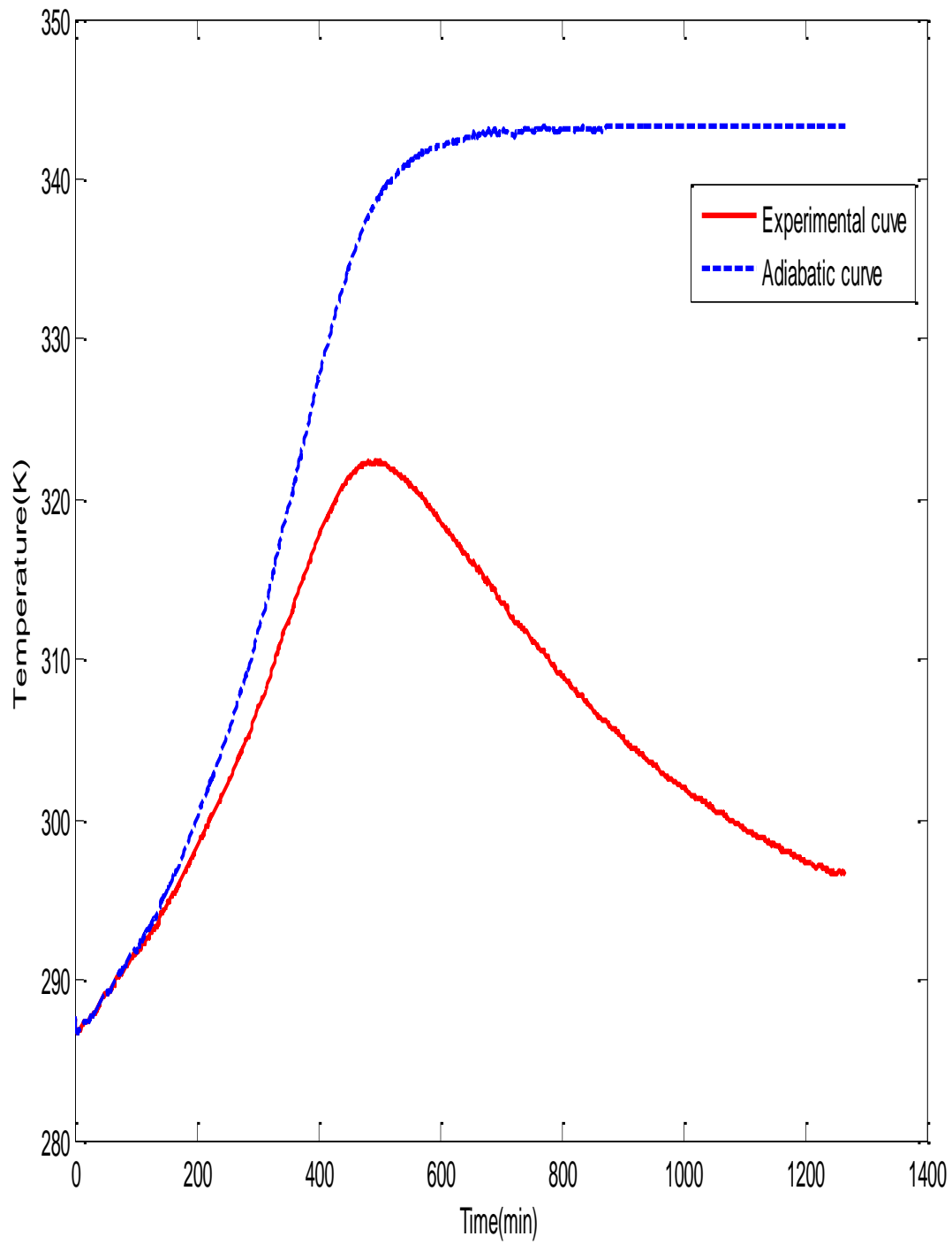


Fig (6.24b): Experimental and Adiabatic curves of experiment-4

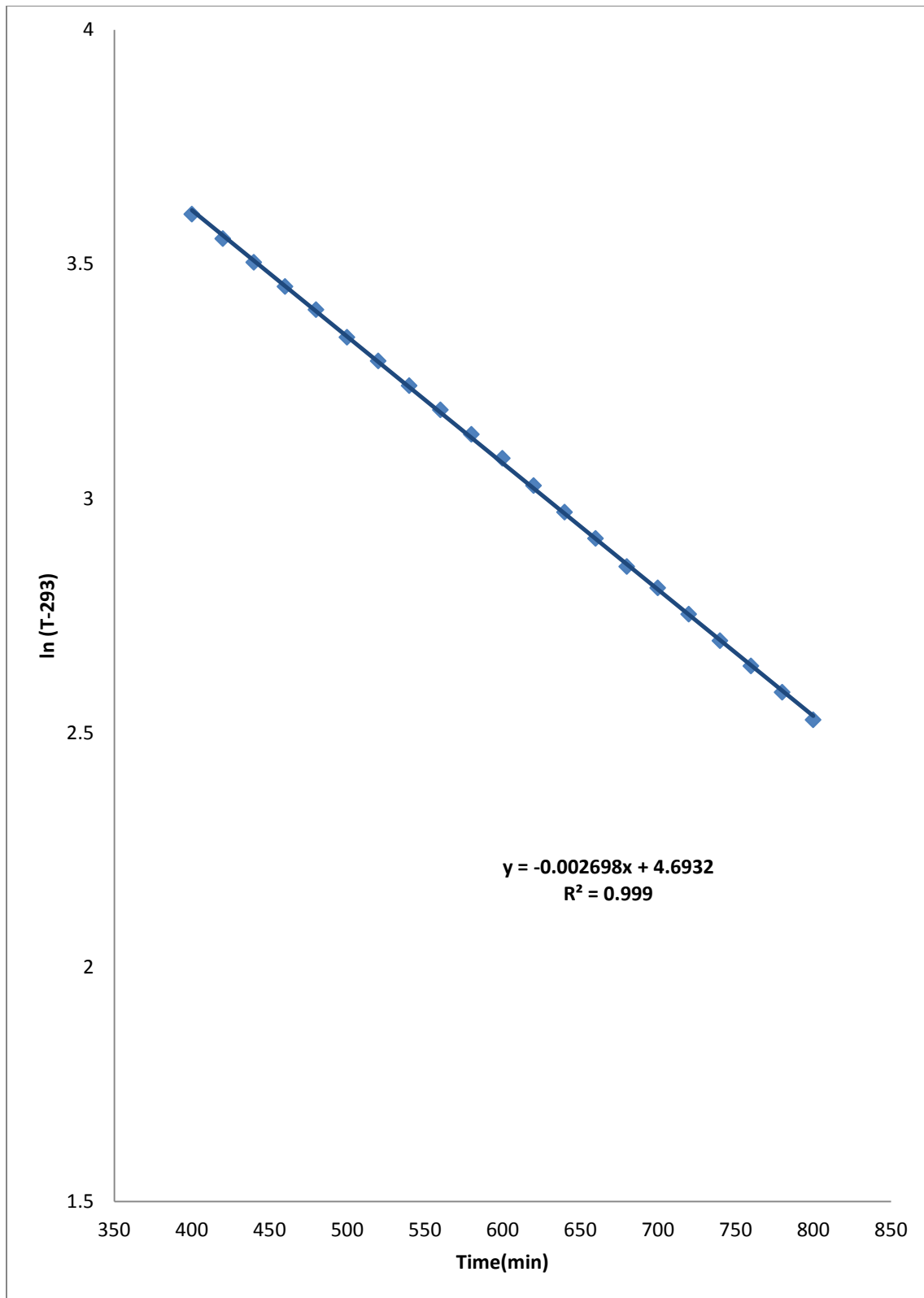


Fig (6.25a): Regression line for the UA/mc<sub>p</sub> of experiment-5

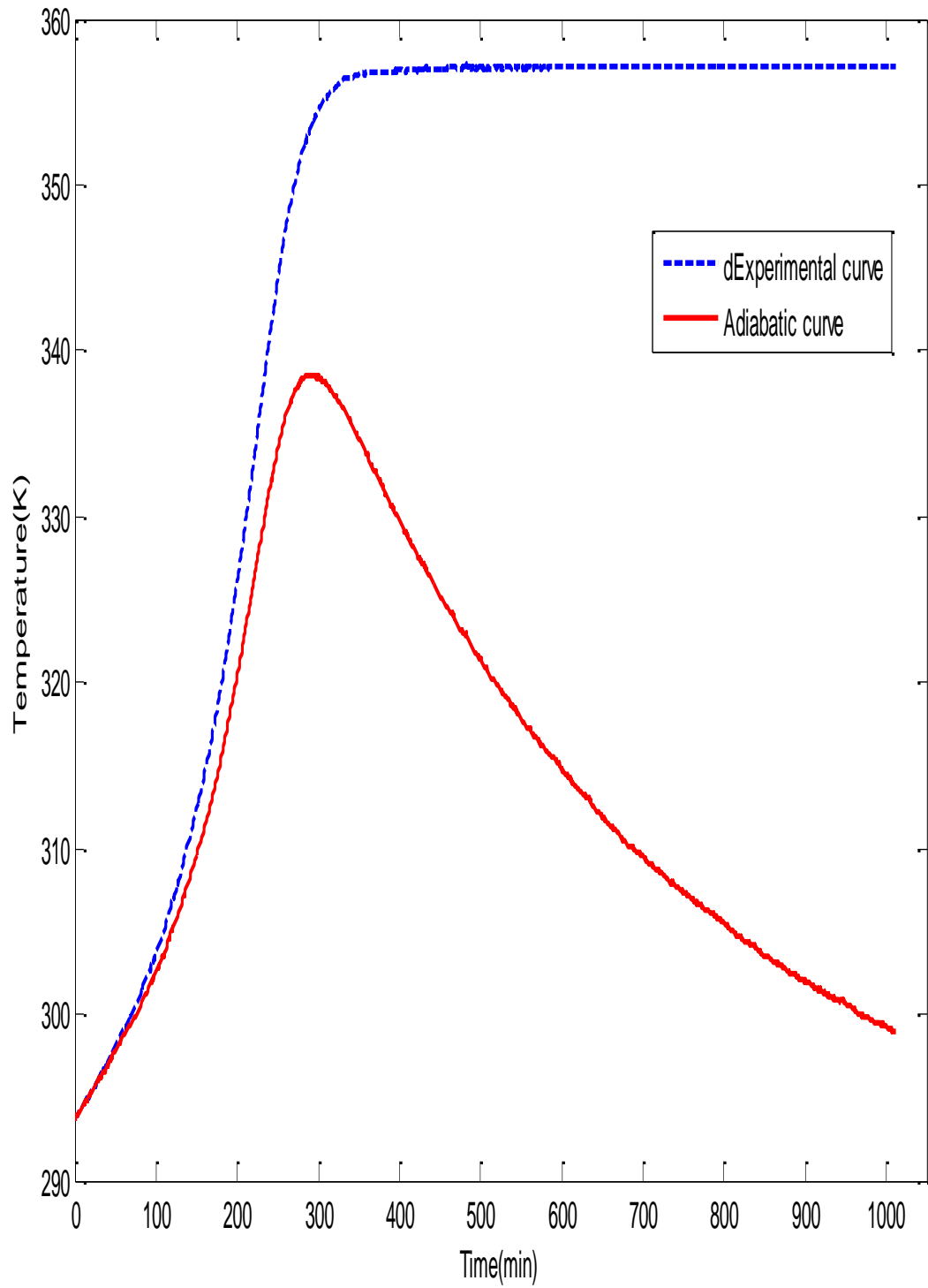


Fig (6.25b): Experimental and Adiabatic curves of experiment-5

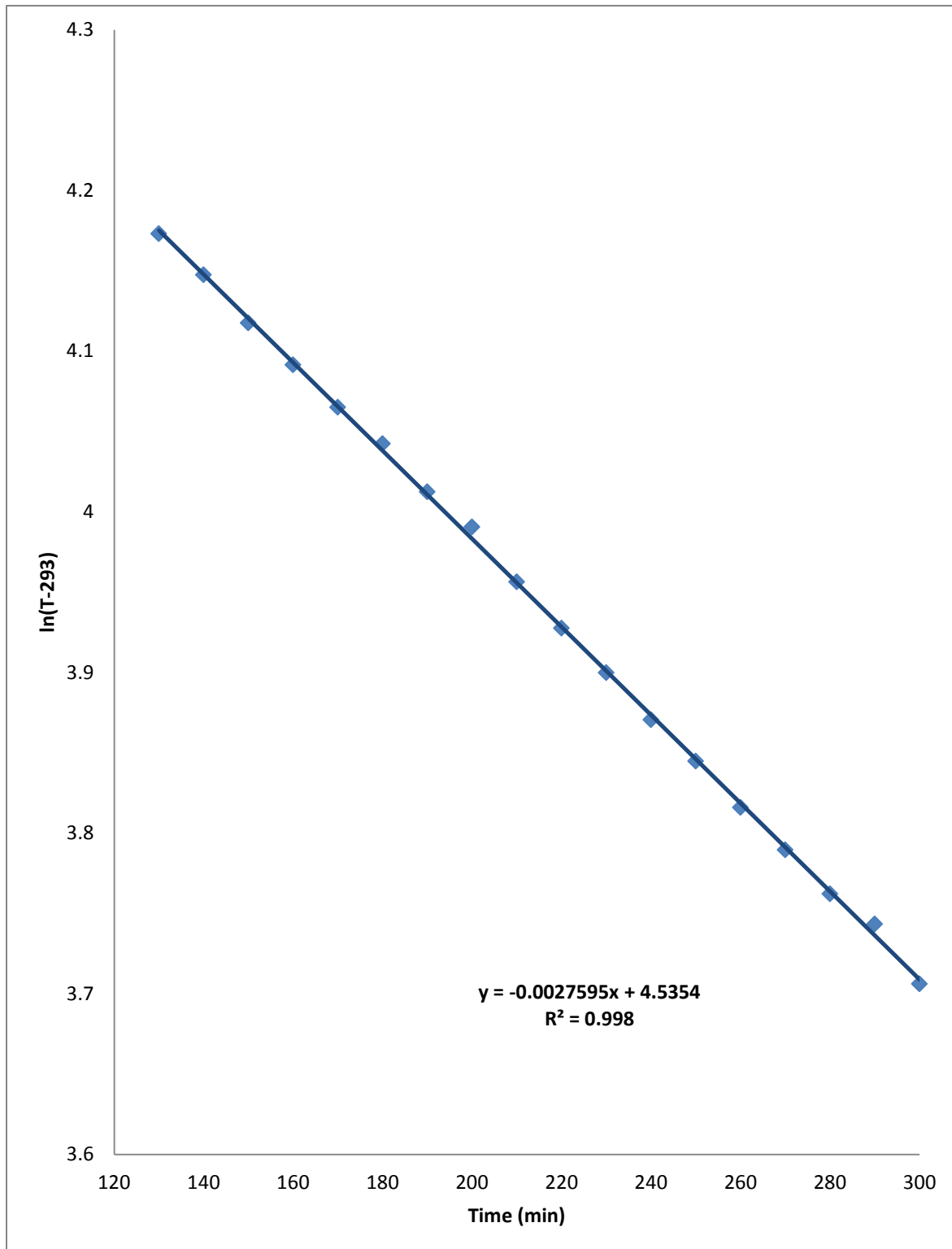


Fig (6.26a): Regression line for the UA/mc<sub>P</sub> of experiment-6

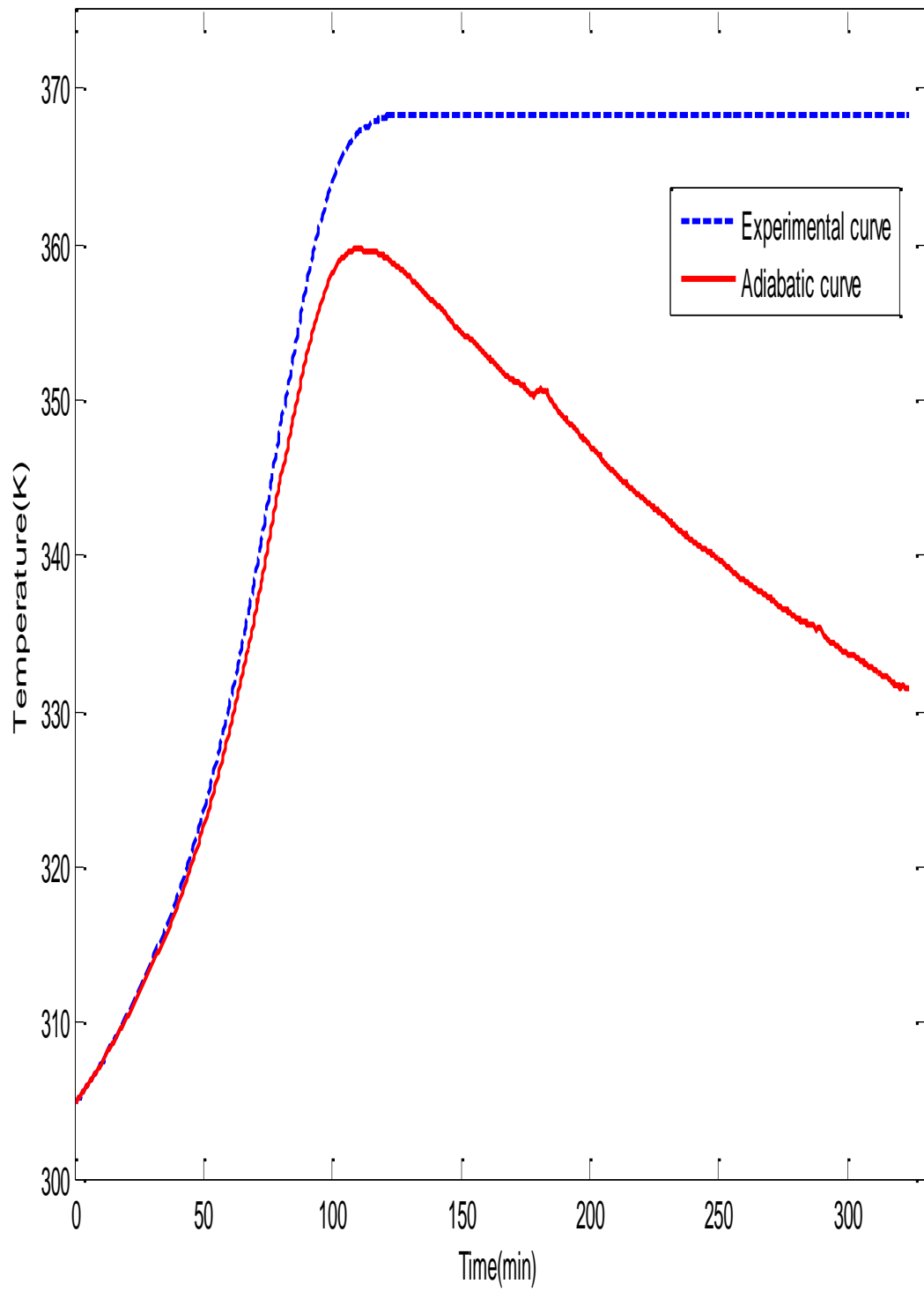


Fig (6.26b): Experimental and Adiabatic curves of experiment-6

Table (6.9) : Summary of the characteristics of the above temperature-time plot

Experiment	T <sub>0</sub> (K)	T <sub>max(adiabatic)</sub> (K)	ΔT <sub>exp(adiabatic)</sub> (K)
4	286.8	343.2	56.4
5	293.6	357.1	63.5
6	304.5	368.3	63.8

From eq(11) the variation of water concentration with temperature/time was deduces as:

$$C_{H_{20}} = 2.13 - \alpha (T - T_0) \quad (30)$$

The constant ( $\alpha$ ) in eq(29) was calculated using the initial concentration of the water 2.13mol/L and the adiabatic theoretical temperature change ( $\Delta T$ )<sub>adiabatic</sub>. The figures (6.26),(6.27) and (6.28) show how water concentration varies with time for the three experiments.

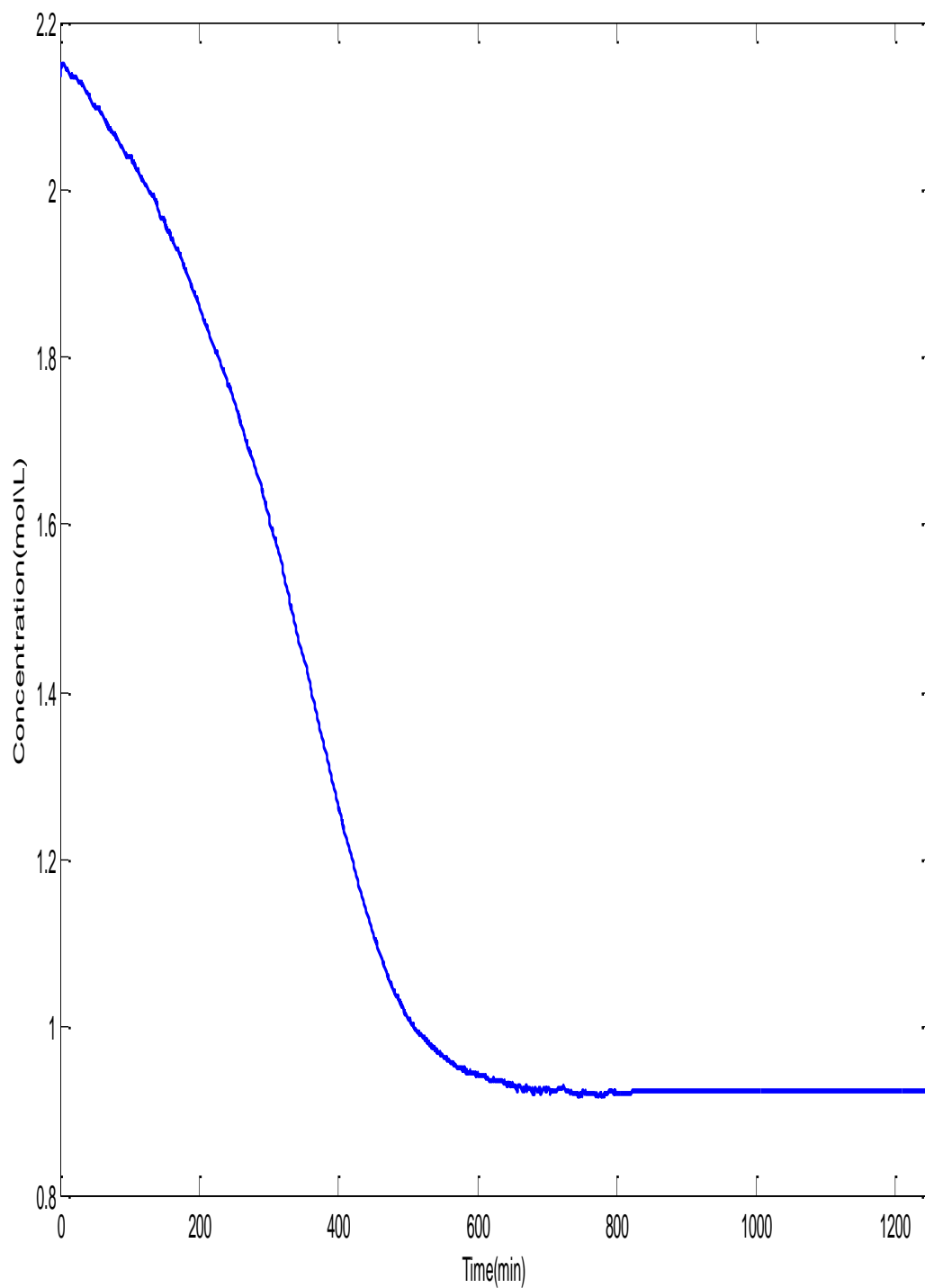


Fig (6.27): Concentration-time plots of excess acetic anhydride-water reaction at 286K

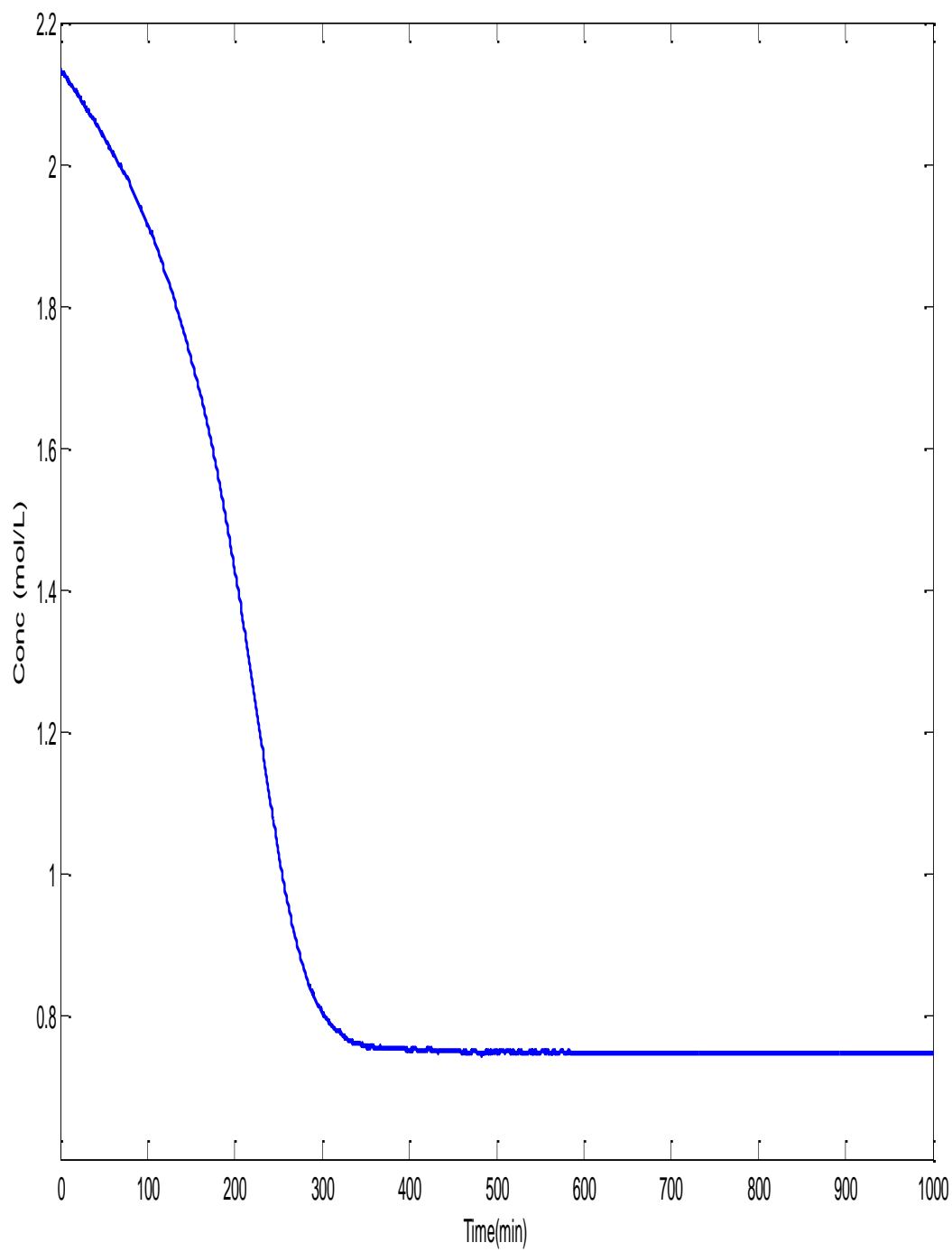


Fig (6.28): Concentration-time plots of excess acetic anhydride-water reaction at 293K

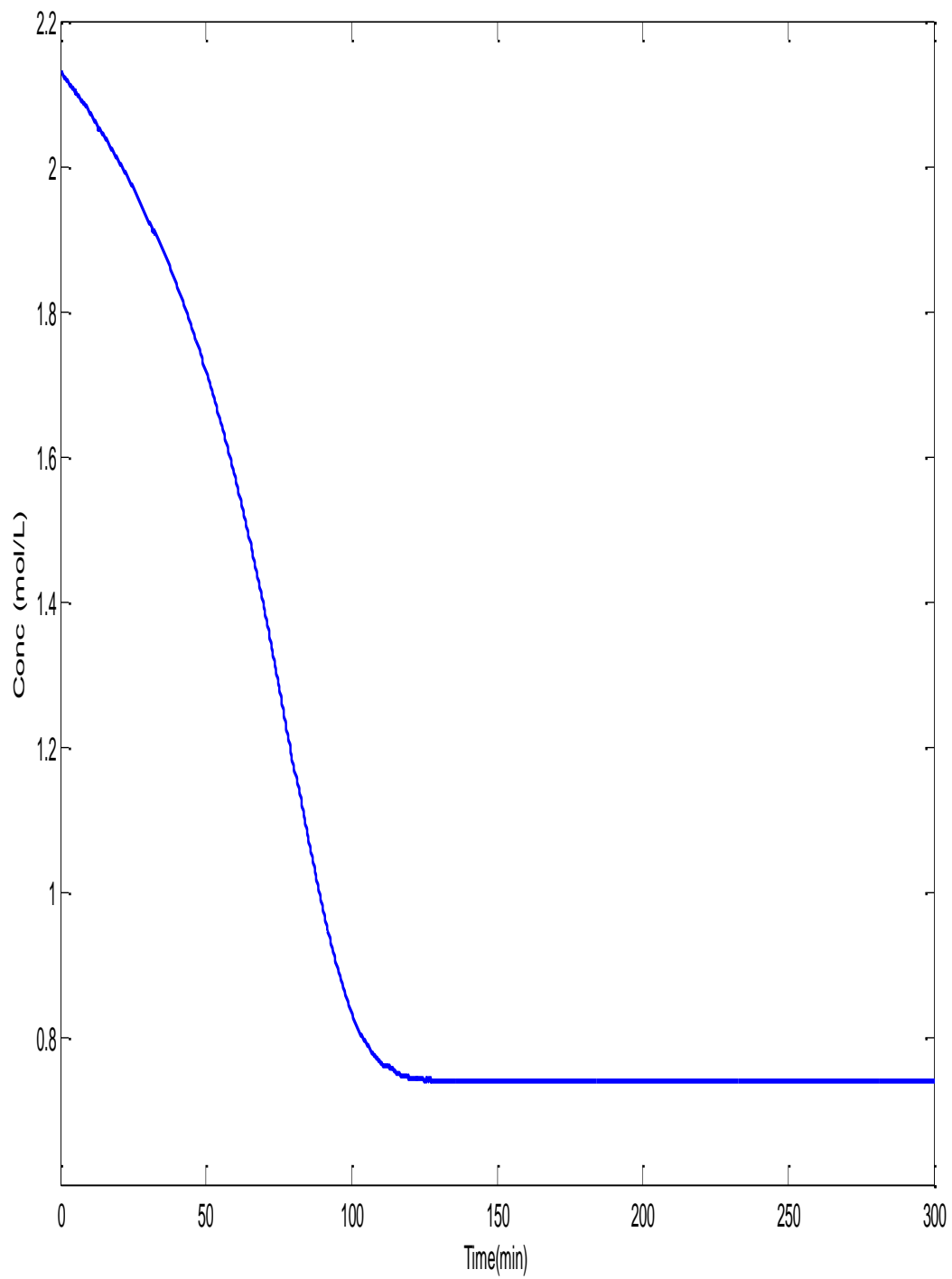


Fig (6.29): Concentration-time plots of excess acetic anhydride-water reaction at 304K

### 6.8.3 VARIATION OF RATE OF REACTION WITH CONCENTRATION

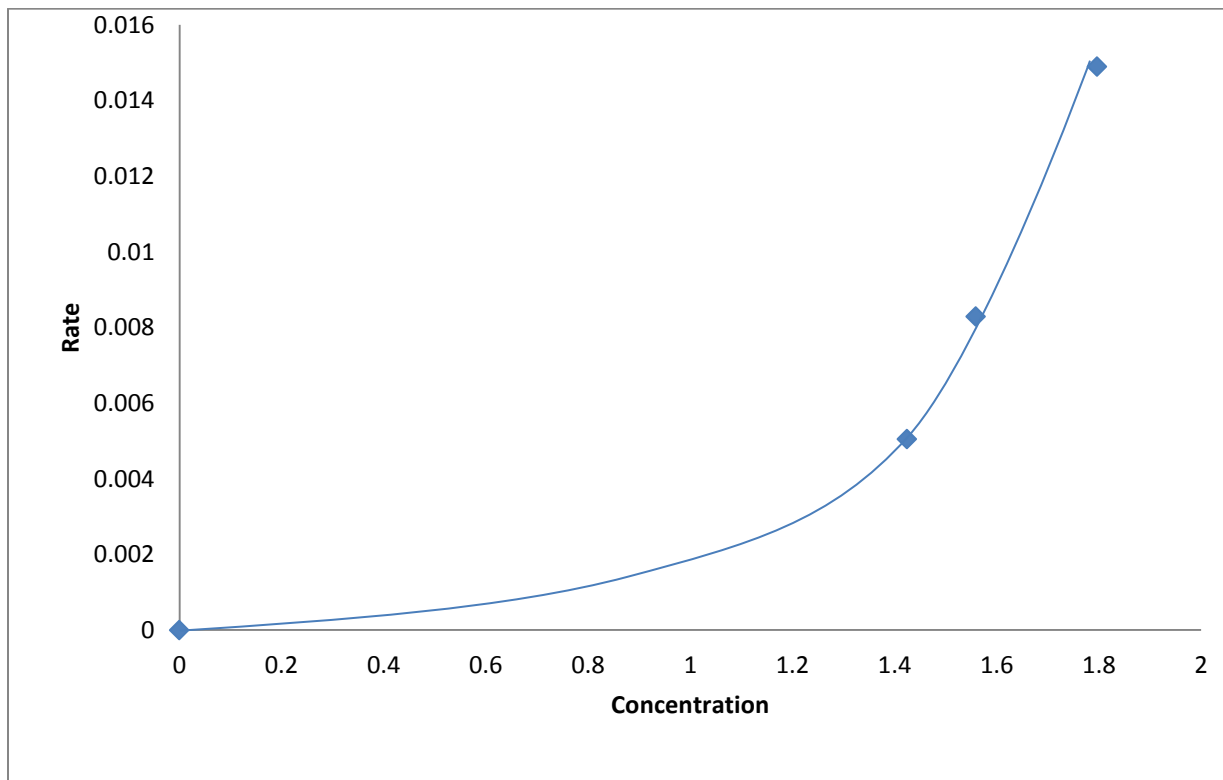
#### CHANGE

Table (6.10) :Variations of temperature, rate and concentration at T =320K

<b>T=320K</b>			
Experiment	Concentration	Rate	Rate constant (k)
4	1.42458	0.0050506	0.0003545
5	1.55912	0.008286	0.0053150
6	1.79670	0.014893	0.0082890

Average (k) = 0.00572

Standard deviation (k) = 0.0024



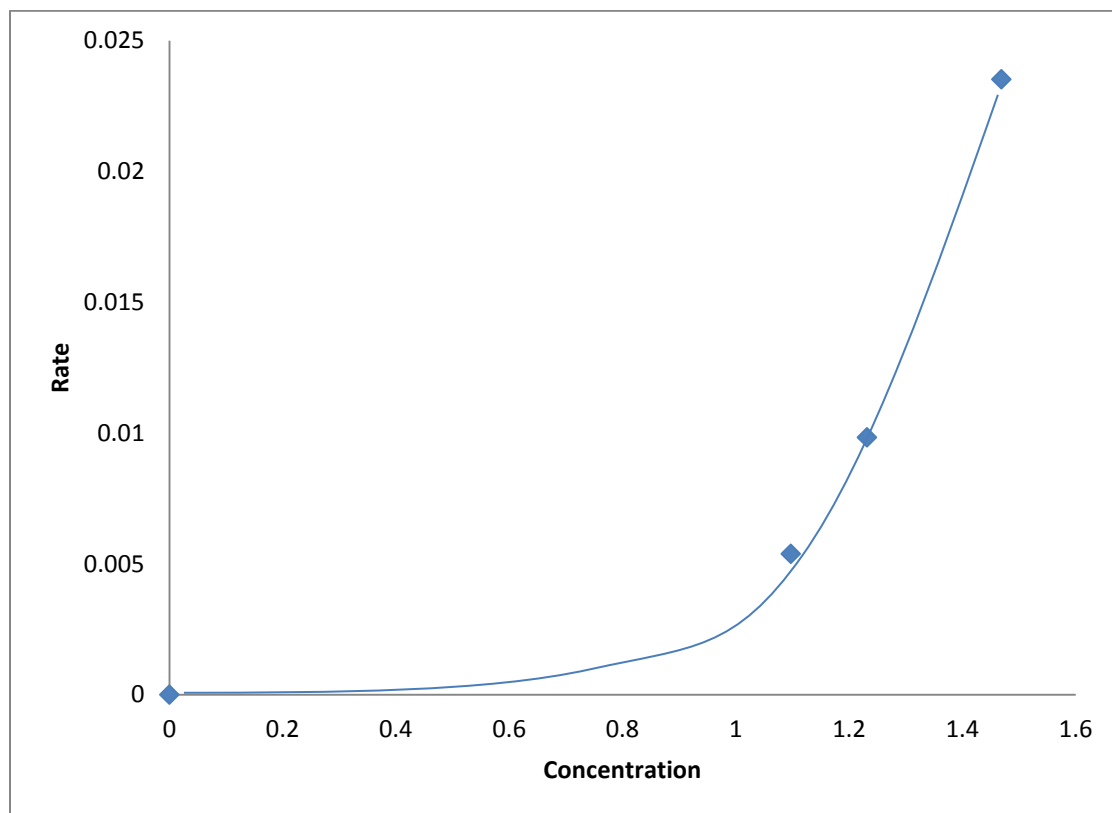
Figure(6.30): Concentration-rate plot @ 320K

Table (6.11) : Variations of temperature, rate and concentration at T =335K

<b>T=335K</b>			
Experiment	Concentration	Rate	Rate constant (k)
4	1.0972539	0.0053749	0.0048985
5	1.2317951	0.0098262	0.0079771
6	1.4693163	0.0235028	0.0159953

Average (k) = 0.009624

Standard deviation (k) = 0.00573



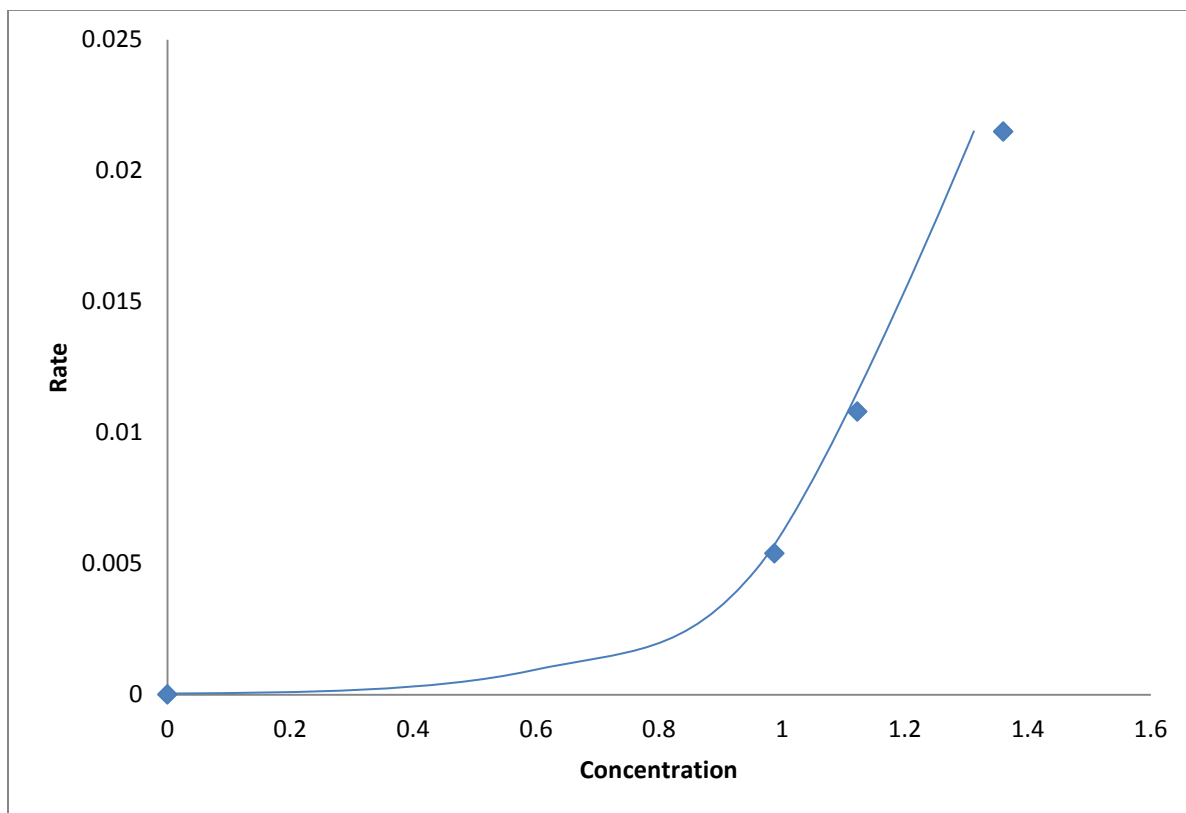
Figure(6.31): Concentration-rate plot @ 335K

Table (6.12) : Variations of temperature, rate and concentration at T =340K

<b>T=340K</b>			
Experiment	Concentration	Rate	Rate constant (k)
4	0.9881278	0.0053892	0.0054539
5	1.1226940	0.01079109	0.0096116
6	1.3602177	0.0214770	0.0157889

Average (k) = 0.0126

Standard deviation (k) = 0.00819



Figure(6.32): Concentration-rate plot @ 340K

#### 6.8.4 KINETICS AND THERMODYNAMIC ANALYSIS OF THE EXPERIMENT

The rate information obtained from the concentration-time was to calculated specific rate constant  $k(T)$  of the processes at any time ( $t$ ) and temperature ( $T$ ). Arrhenius plots was thus generated from which kinetic parameters of runs was determined. The figure (6.32), (6.33) and (6.34) shows the Arrhenius plots for all the three experiments.

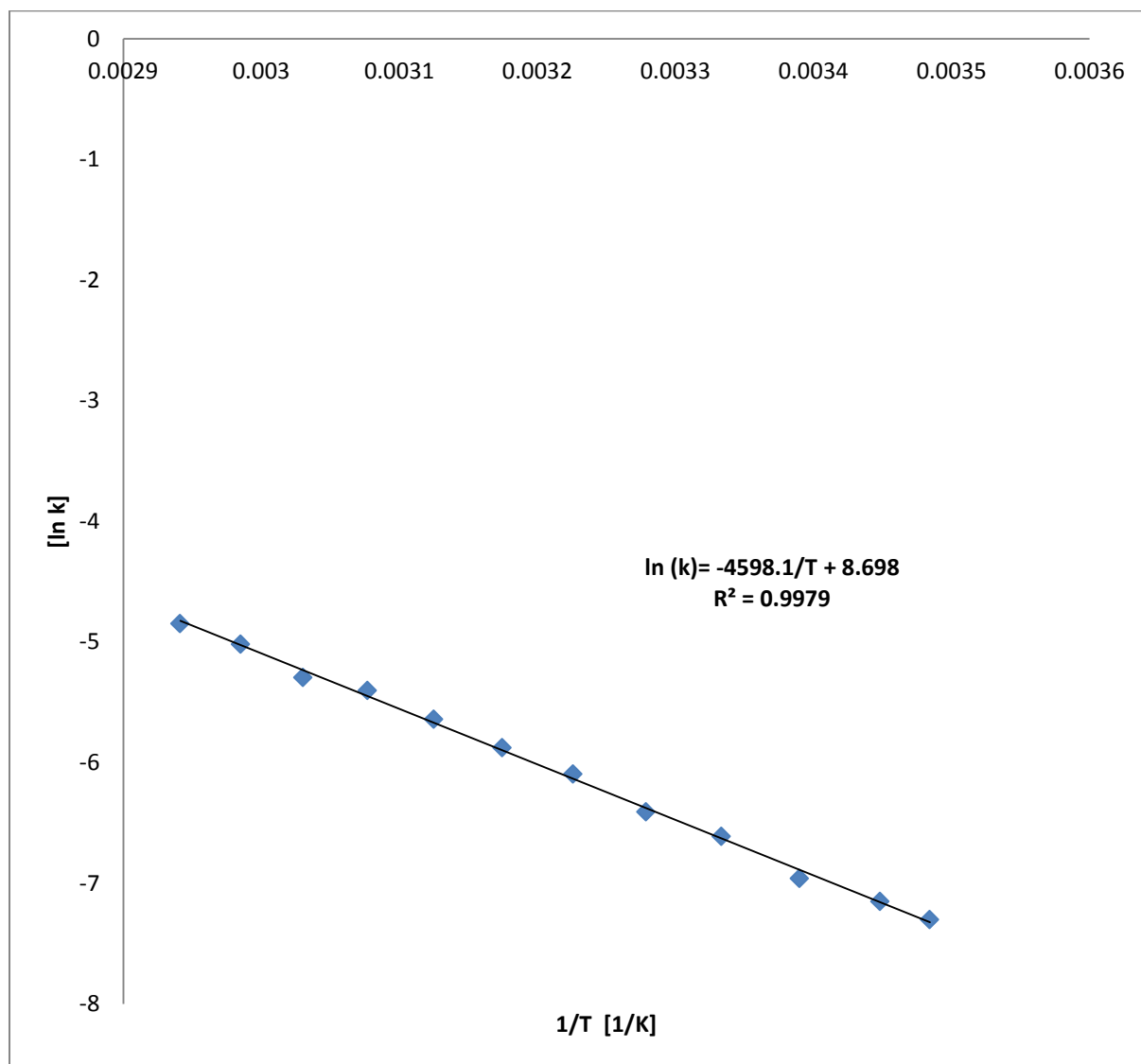


Figure (6.33): Arrhenius plot of experiment-4

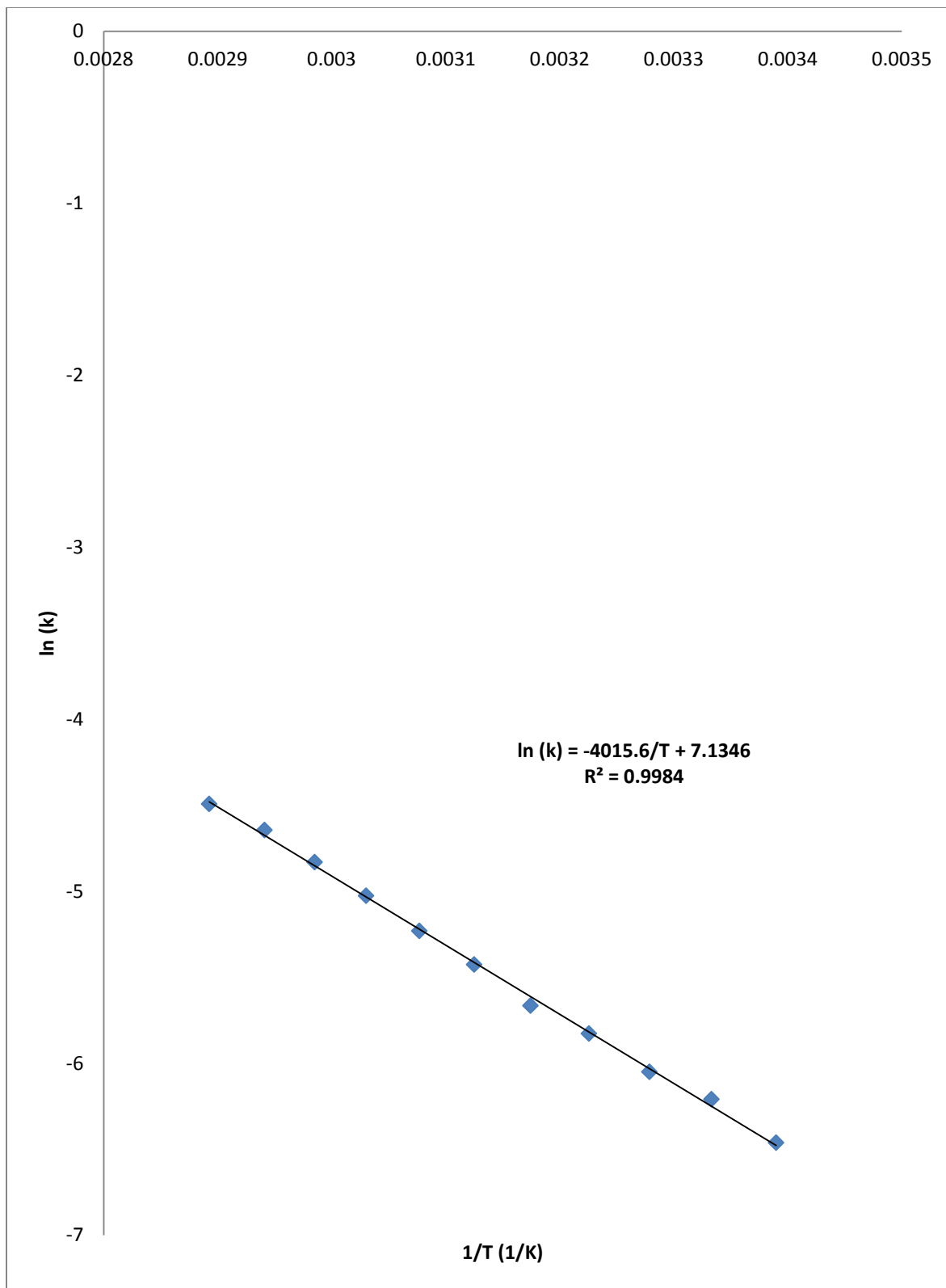


Figure (6.34): Arrhenius plot of experiment-5

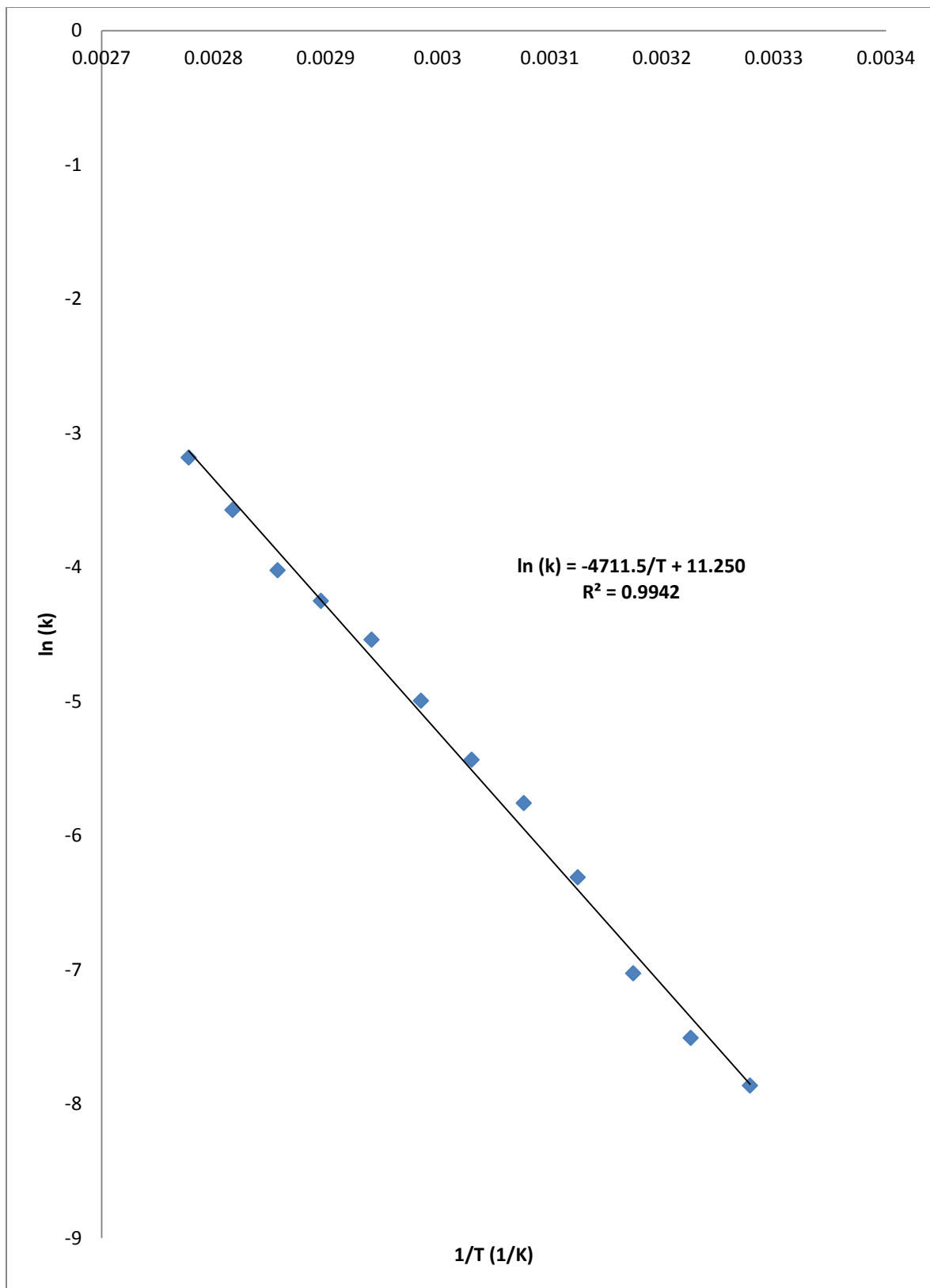


Figure (6.35): Arrhenius plot of experiment-6

The values obtained for the specific rate constants as a function of temperature are given in equations (6.32),(6.33) and (6.34) below:

$$k_1(T) = 5.99 * 10^3 \exp\left(-\frac{4598.1}{T}\right) \quad (31)$$

$$k_2(T) = 1.25 * 10^3 \exp\left(-\frac{4015.6}{T}\right) \quad (32)$$

$$k_3(T) = 7.69 * 10^7 \exp\left(-\frac{4711.5}{T}\right) \quad (33)$$

The thermodynamic information extracted from the experiments was the heat of the reaction ( $\Delta H_{rxn}$ ). This was assumed to be independent of temperature and was determined by using eq(10). Table(6.13) below shows  $\Delta H_r$  values of the various experiments.

Table (6.13) : Thermodynamic information of the experiments

Experiment	4	5	6
$\Delta H_{rxn}$ (kJ/mol)	-53.92	-60.71	-60.99

## 6.9 EXPERIMENTAL PROCEDURES AND RESULTS

### 6.9.1 ACETIC ANHYDRIDE-METHANOL REACTIONS

Analytical reagent grade acetic anhydride and methanol was used in all experiments. In these experiments 1mol of acetic anhydride was injected into the reaction vessel followed by 3 mols of methanol. The experimental procedures were the same as those described in section above. The Runs were carried out adiabatically at the following initial temperatures: 290K, 294K and 299K.

### 6.9.2 DETERMINATION OF UA/mC<sub>p</sub> FOR THE REACTION MIXTURE

Table (6.14) below consist of some of the physical constants of the reacting species which was used in the determination of the quantity UA/mC<sub>p</sub>.

Table (6.14) : Some constants of reacting species

Species	Moles	Molar mass(g/mol)	C <sub>p</sub> (J/mol.K)
Acetic anhydride	1.0	102.9	189.7
methanol	3.0	32.04	79.5

Equation (23) was used to determine specific heat of the mixture (C<sub>p,mix</sub>) and the quantity M<sub>T</sub>C<sub>p,mix</sub>.

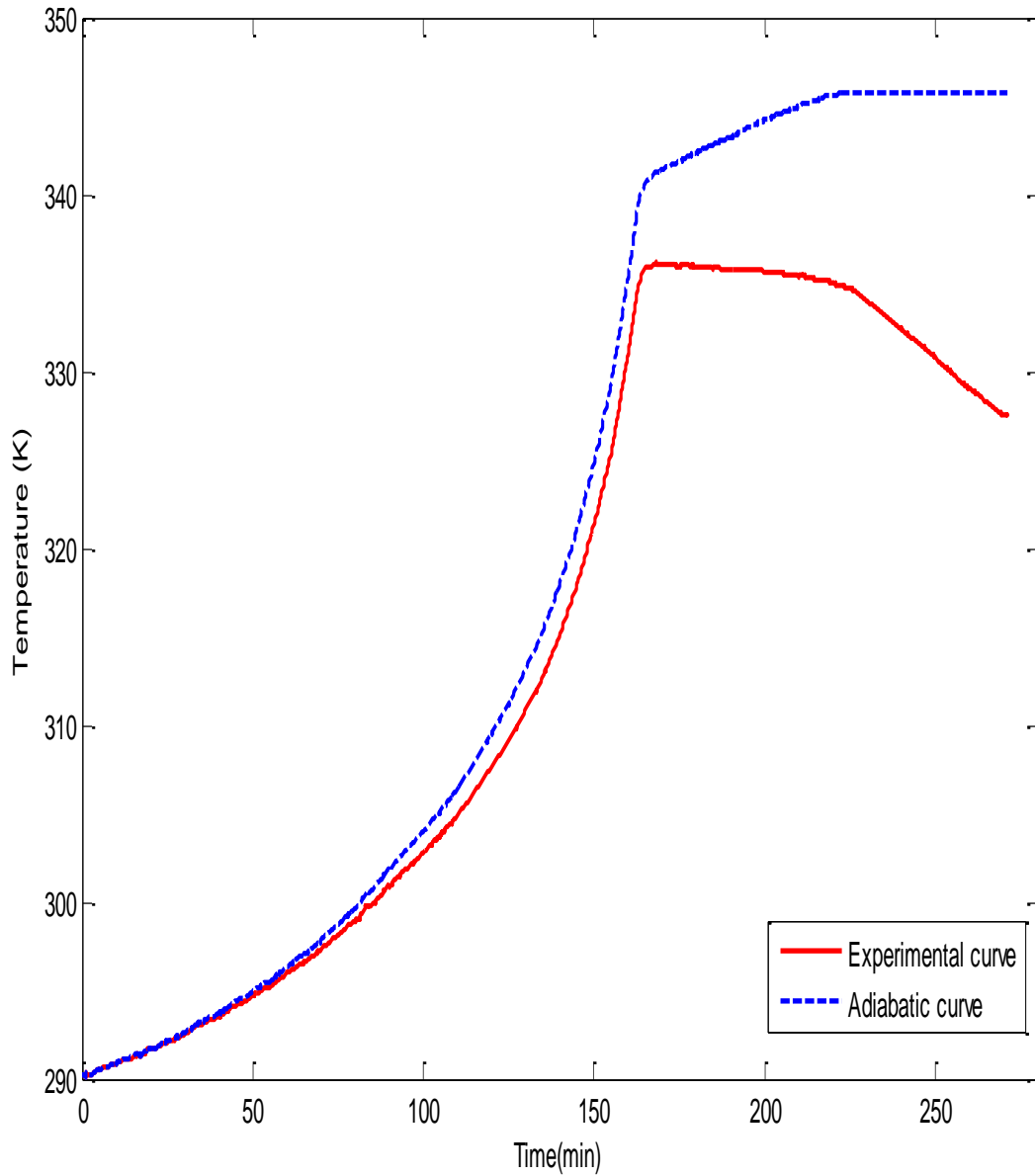
$$C_{P,mix} = \frac{m_{AA}}{M_T} C_{P,AA} + \frac{m_m}{M_T} C_{P,m} \quad (34)$$

M<sub>T</sub>C<sub>p,mix</sub> was calculated to be 545.19 J/mol. K Since the reaction is not pure water we therefore determined its equivalent mass of water by dividing 545.19 J/mol. K by the specific heat of water;

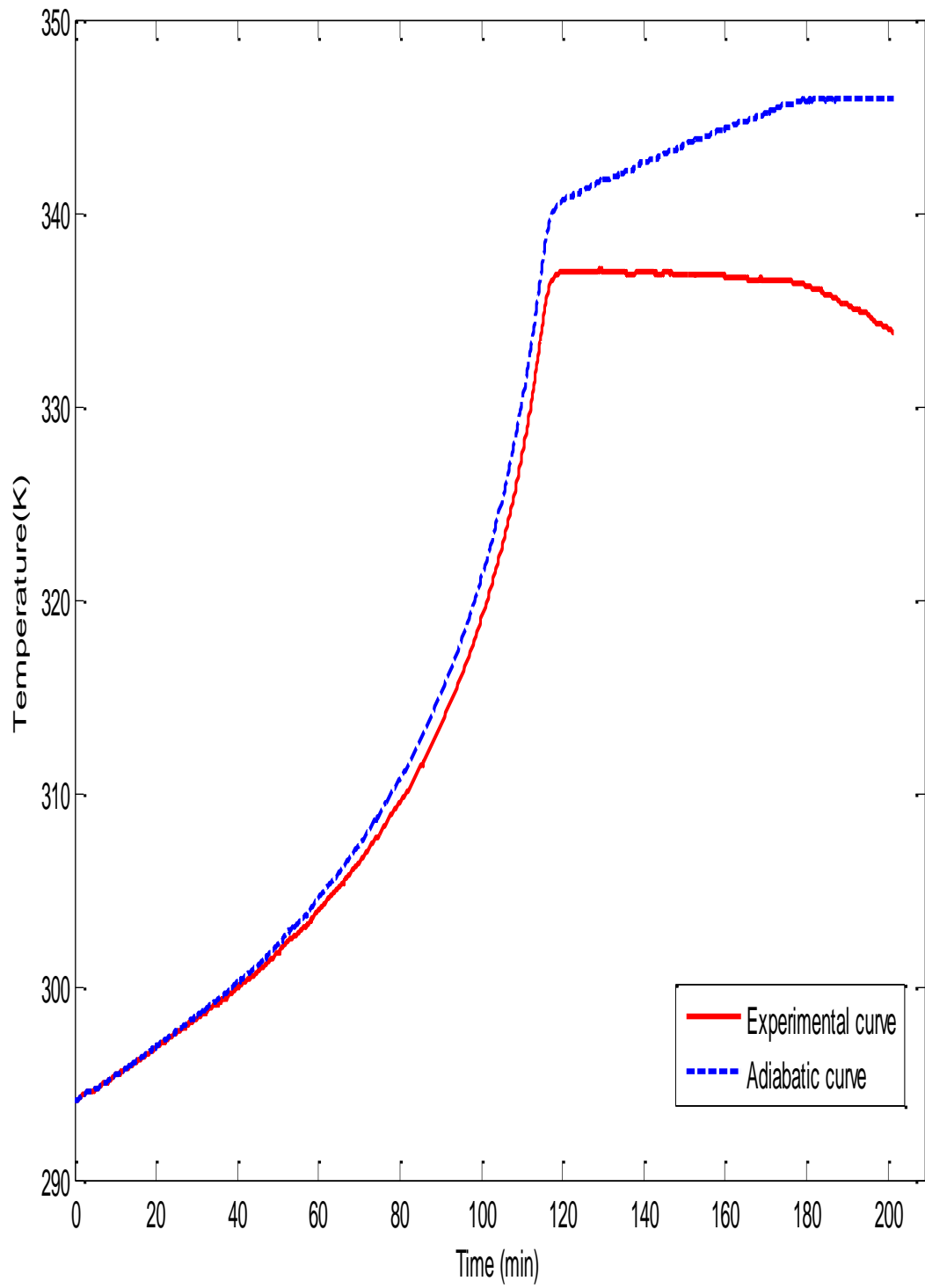
$$m_{eqv \text{ water}} = \frac{(M_T C_P)_{mix}}{C_{P,water}} = 130.38 \text{ g water} \quad (35)$$

From the equation of the line in figure (14) the value of the quantity (UA/mC<sub>p</sub>)<sub>mix</sub> was determined to be 0.002307/min.

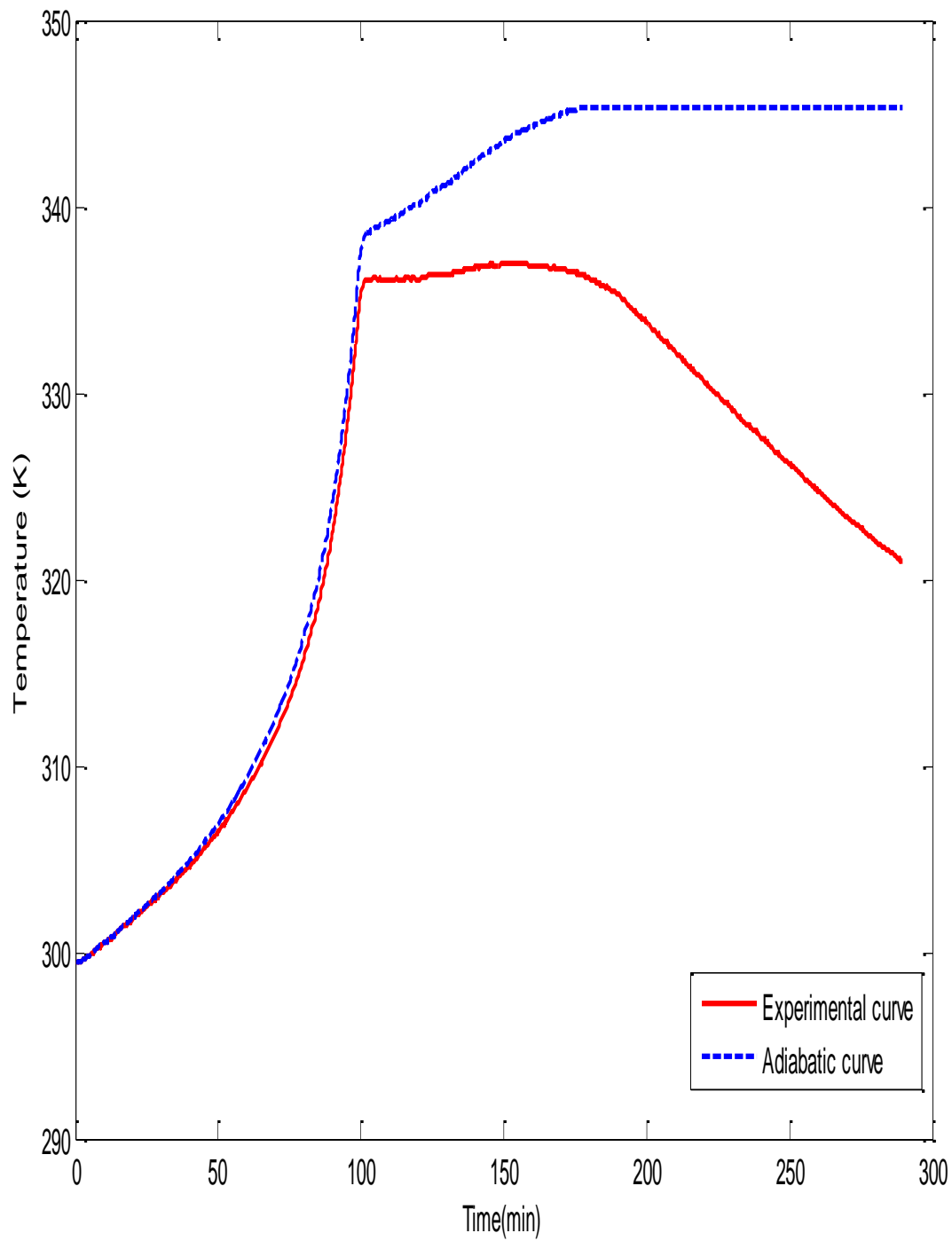
This value was plugged in eq(9) above and the corrections of the experimental results to adiabatic conditions was performed. The figures (6.34),(6.35) and (6.36) below shows the experimental and the corrected temperature profiles for all the three experiments.



Fig(6.36): Experimental and Adiabatic curves of experiment-7



Fig(6.37): Experimental and Adiabatic curves of experiment-8



Fig(6.38): Experimental and Adiabatic curves of experiment-9

Table (6.15) : Summary of the characteristics of the above temperature-time plot

Experiment	T(0)(K)	T <sub>max(adiabatic)</sub> (K)	ΔT <sub>exp(adiabatic)</sub> (K)
7	290.01	345.80	55.69
8	294.00	345.60	51.9
9	299.20	345.30	46.13

From eq(11) the variation of acetic anhydride concentration with temperature/time and was deduces as:

$$C_{AA} = C_{AO} - \beta (T - T_0) \quad (36)$$

The constant (β) in eq(36) was calculated using the initial concentration of the acetic anhydride 4.364 mol/L and the adiabatic theoretical temperature change (ΔT)<sub>adiabatic</sub>. The figures (6.39),(6.40) and (6.41) show how acetic anhydride concentration varies with time for the three experiments.

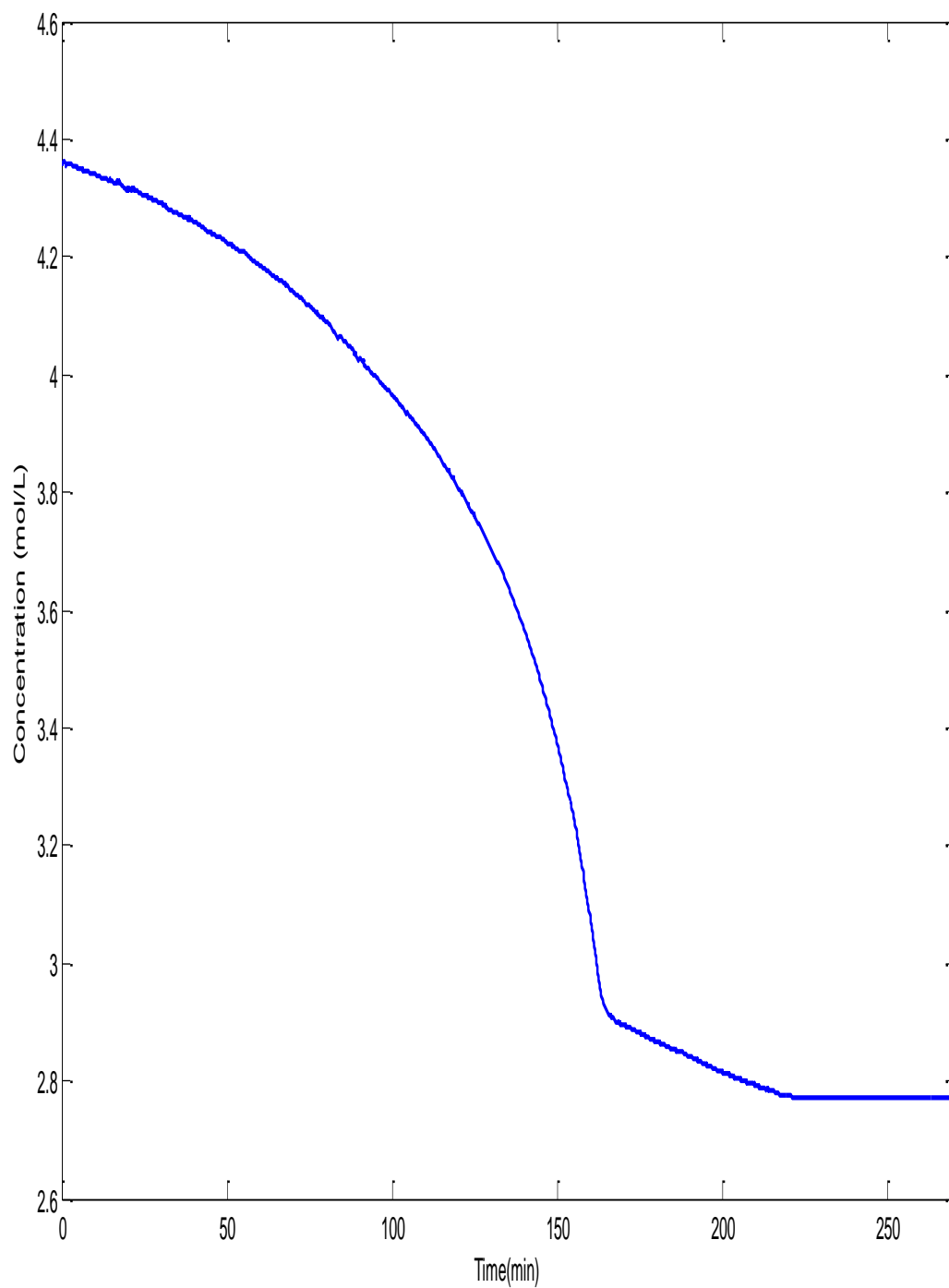


Fig (6.39): Concentration-time plot of acetic anhydride-reaction reaction-Experiment (7)

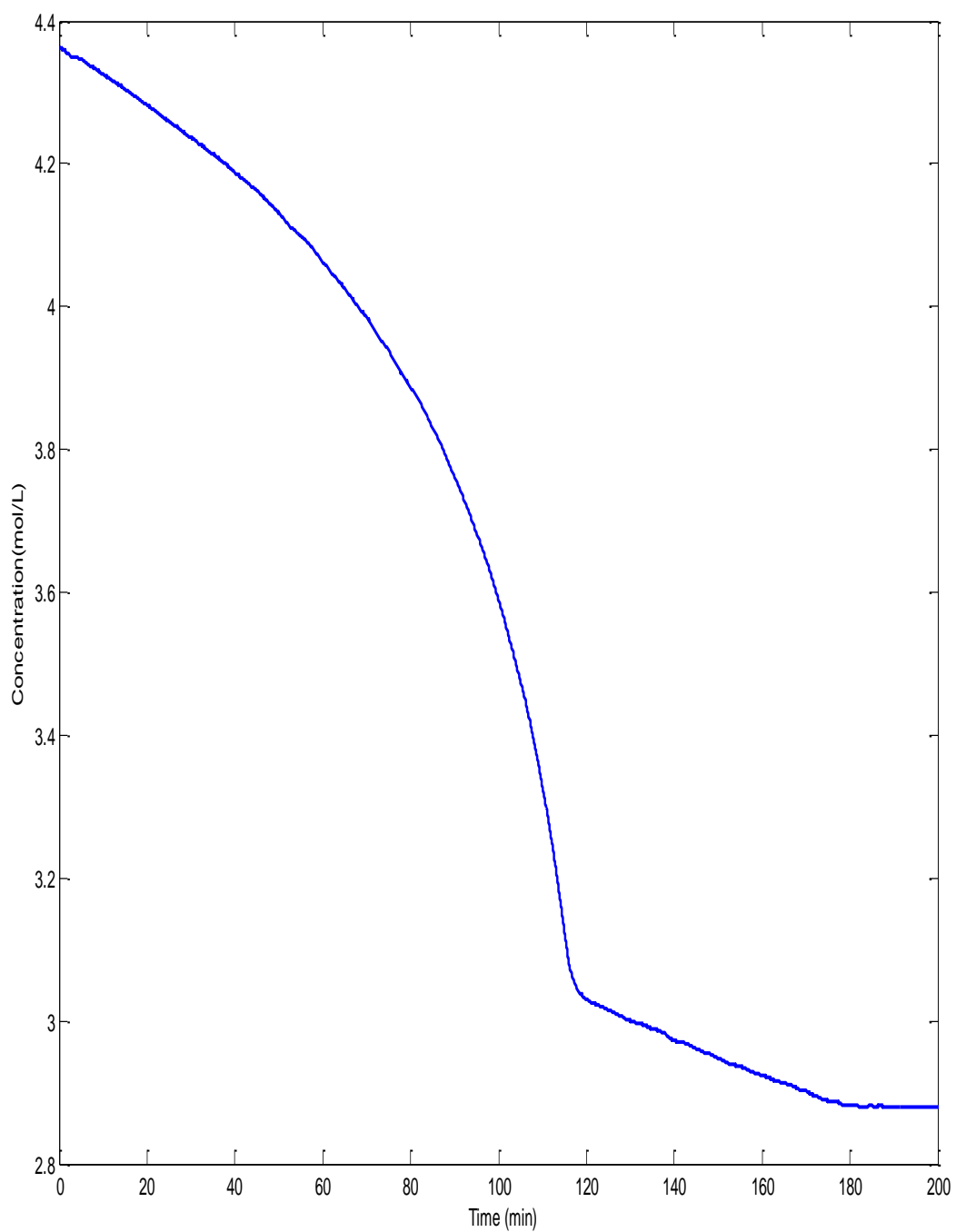


Fig (6.40): Concentration-time plot of acetic anhydride-reaction reaction-Experiment (8)

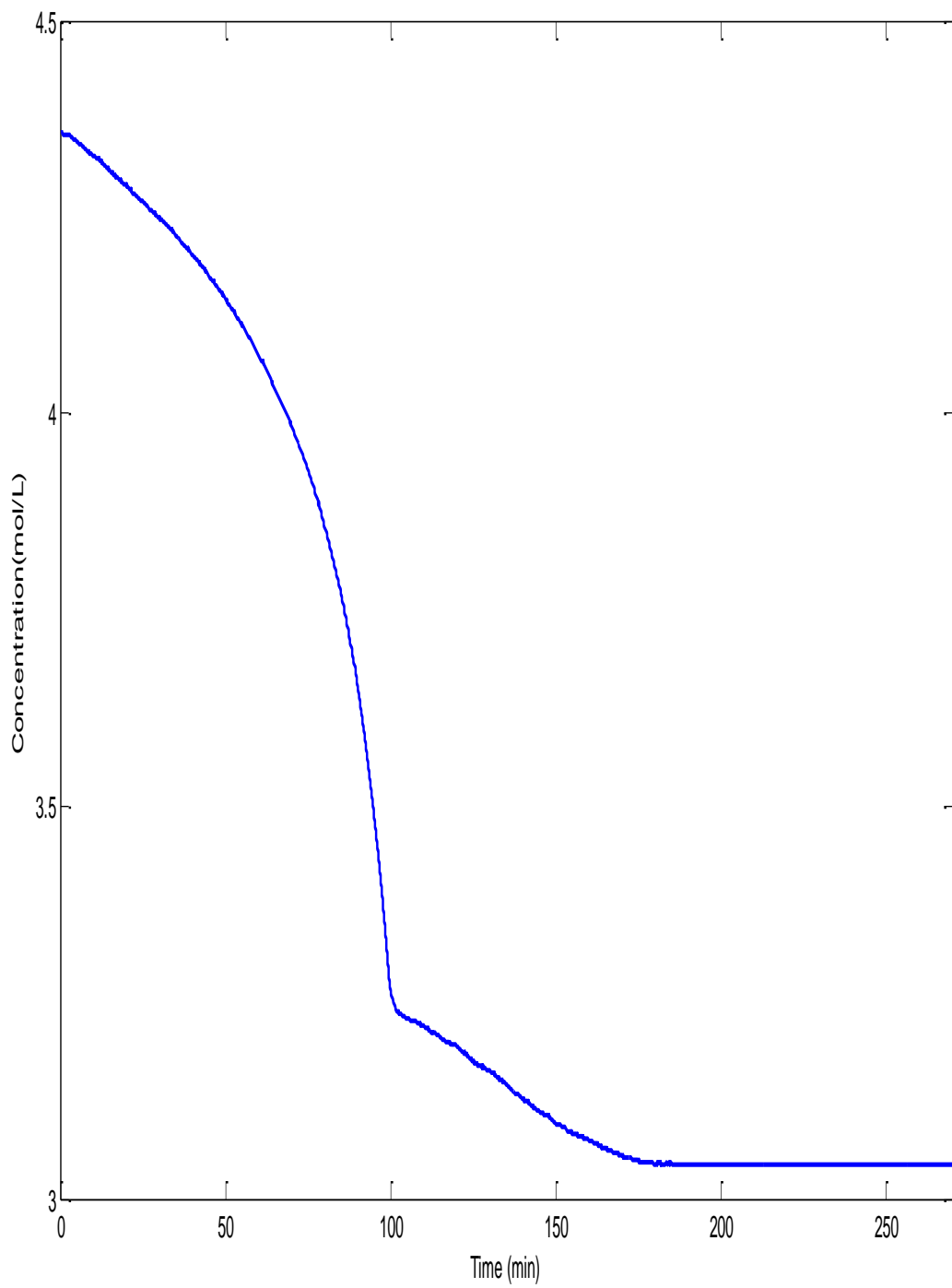


Fig (6.41): Concentration-time plot of acetic anhydride-reaction reaction-Experiment (9)

### 6.9.3 VARIATION OF RATE OF REACTION WITH CONCENTRATION

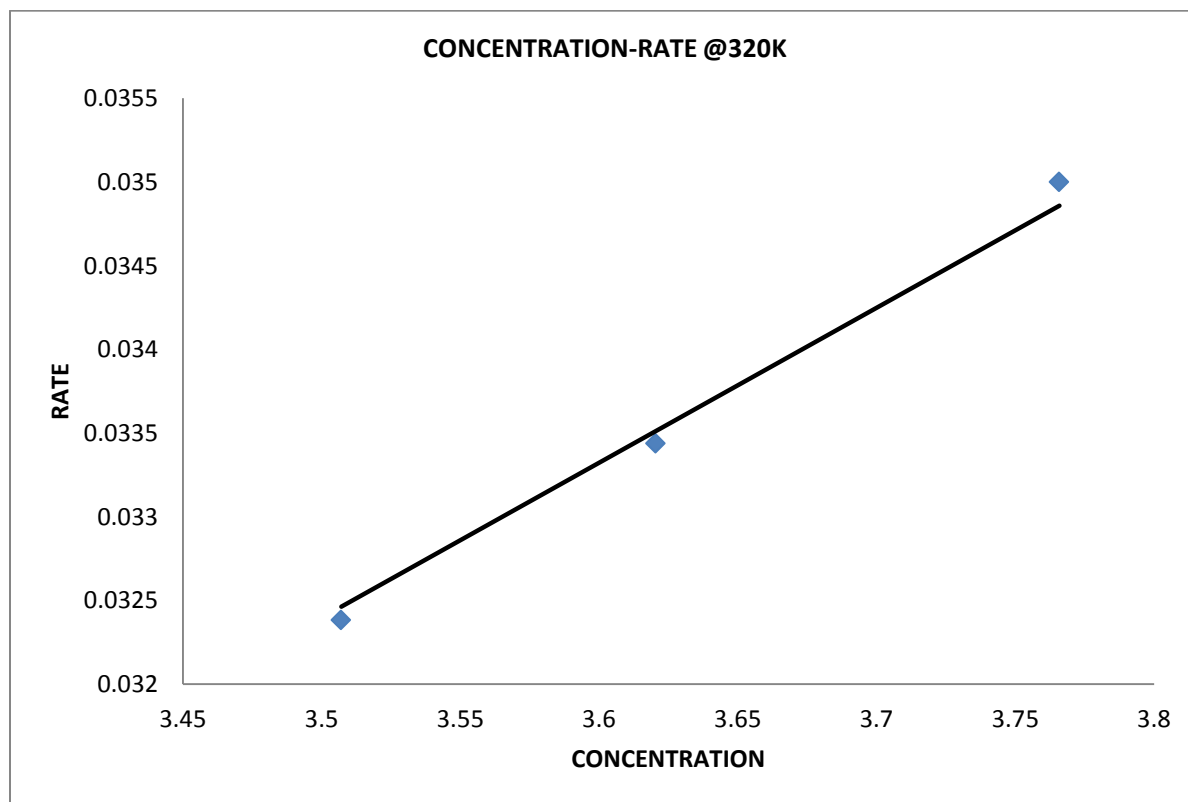
#### CHANGE

Table (6.16) : Variations of temperature, rate and concentration at T =320K

<b>T=320K</b>			
Experiment	Concentration	Rate	Rate constant (k)
7	3.507025023	0.03238313	0.00936158
8	3.620338071	0.033438511	0.00923629
9	3.765872632	0.03500009	0.00929425

Average (k) =0.00936

Standard deviation (k) =  $6.27 \times 10^{-5}$



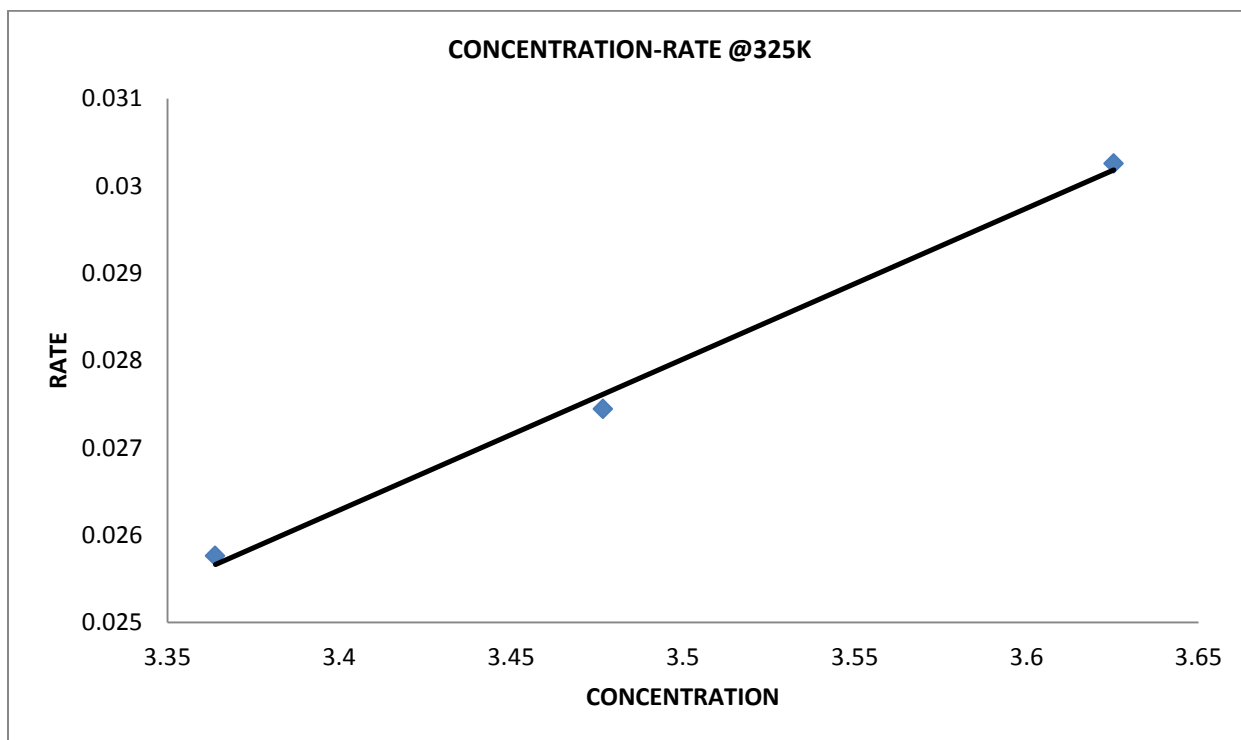
Figure(6.42): Concentration-rate plot @ 320K

Table (6.17) : Variations of temperature, rate and concentration at T =335K

<b>T=335K</b>			
Experiment	Concentration	Rate	Rate constant (k)
4	3.363932095	0.025762791	0.007658535
5	3.476755343	0.027443908	0.00789354
6	3.625365284	0.030256856	0.008345878

Average (k) = 0.007965

Standard deviation (k) = 0.000349



Figure(6.43): Concentration-rate plot @ 335K

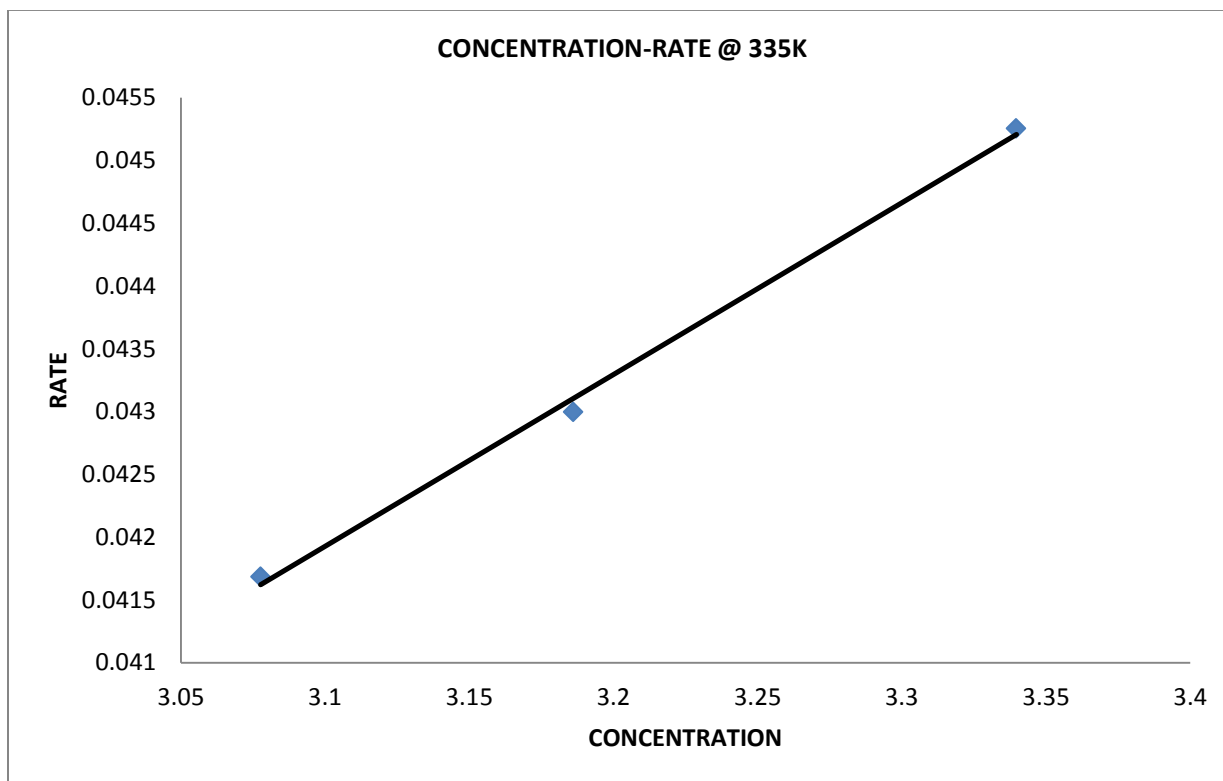
Table (6.18) : Variations of temperature, rate and concentration at T =340K

**T=340K**

Experiment	Concentration	Rate	Rate constant (k)
4	3.077605537	0.041685326	0.013544727
5	3.186062023	0.04299617	0.013495082
6	3.339671258	0.045253824	0.013550382

Average (k) = 0.013530064

Standard deviation (k) = 3.04267E-05



Figure(6.44): Concentration-rate plot @ 340K

#### **6.9.4 KINETICS AND THERMODYNAMIC ANALYSIS**

The rate information obtained from the concentration-time plot enabled one to calculate specific rate constant  $k(T)$  of the processes at any time ( $t$ ) and temperature ( $T$ ). Arrhenius plots were thus generated from which kinetic parameters of the runs were extracted. The figures (6.45), (6.46) and (6.47) below show the Arrhenius plots for all the three experiments.

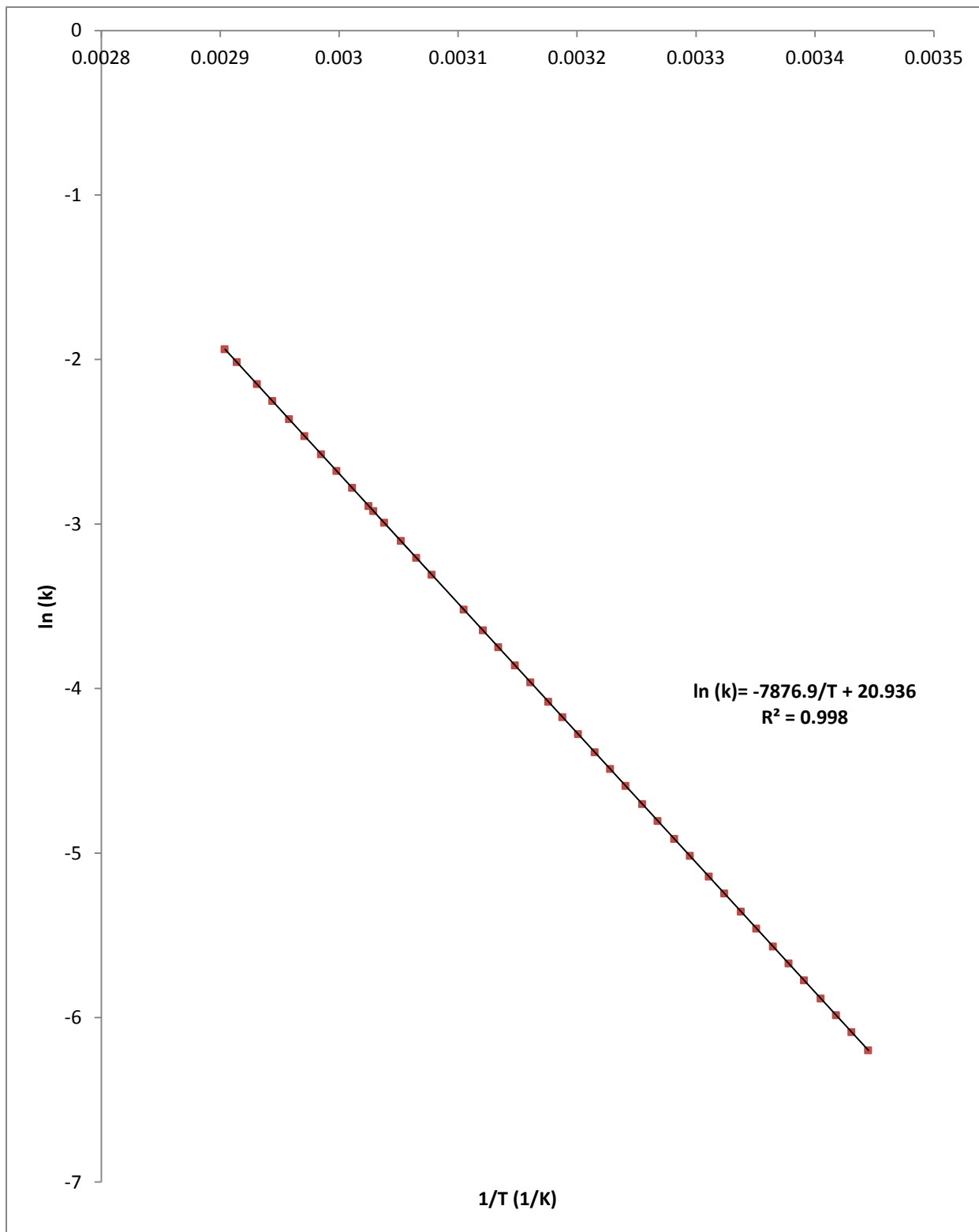


Figure (6.45): Arrhenius plot of experiment-7

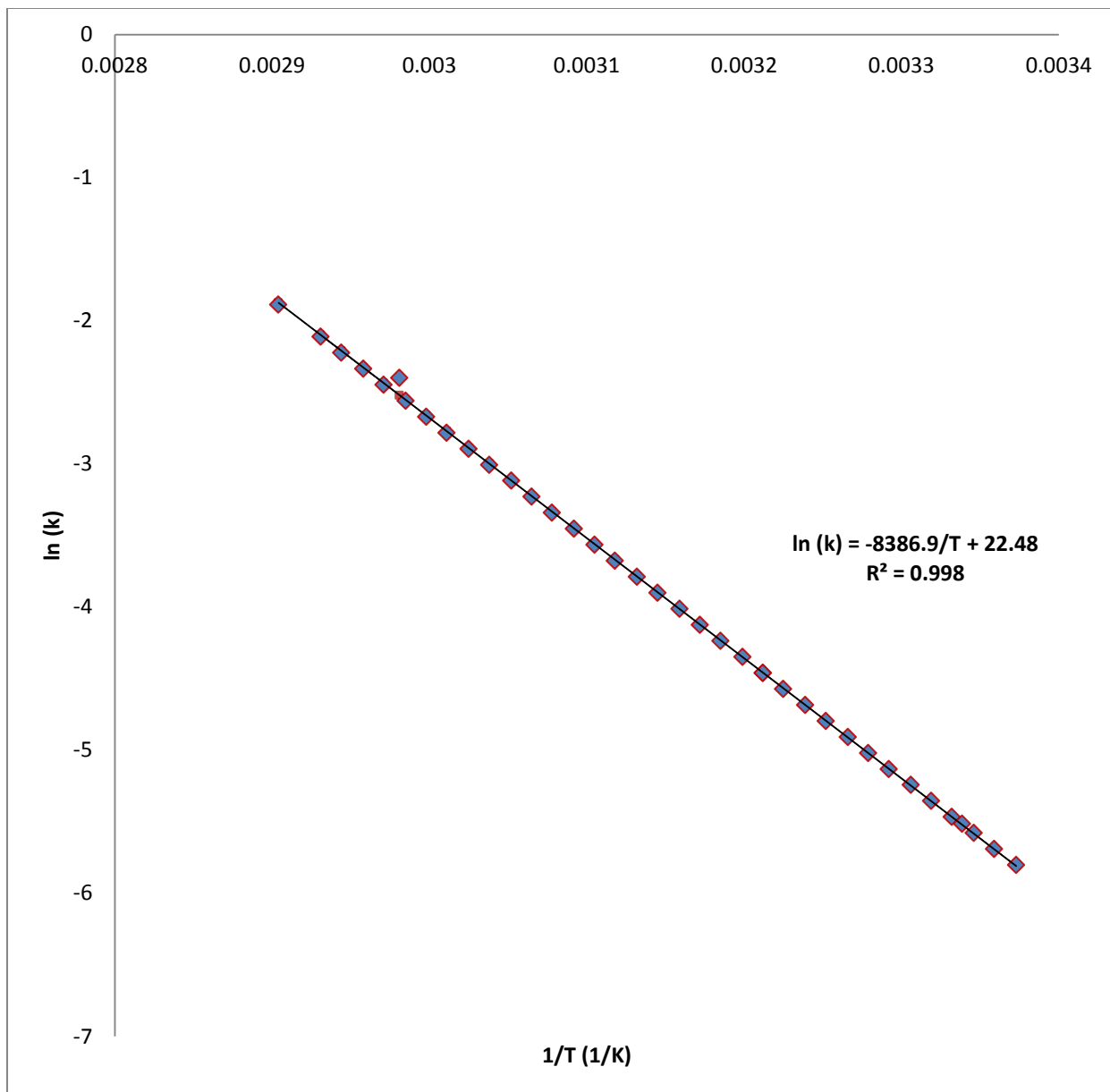


Figure (6.46): Arrhenius plot of experiment-8

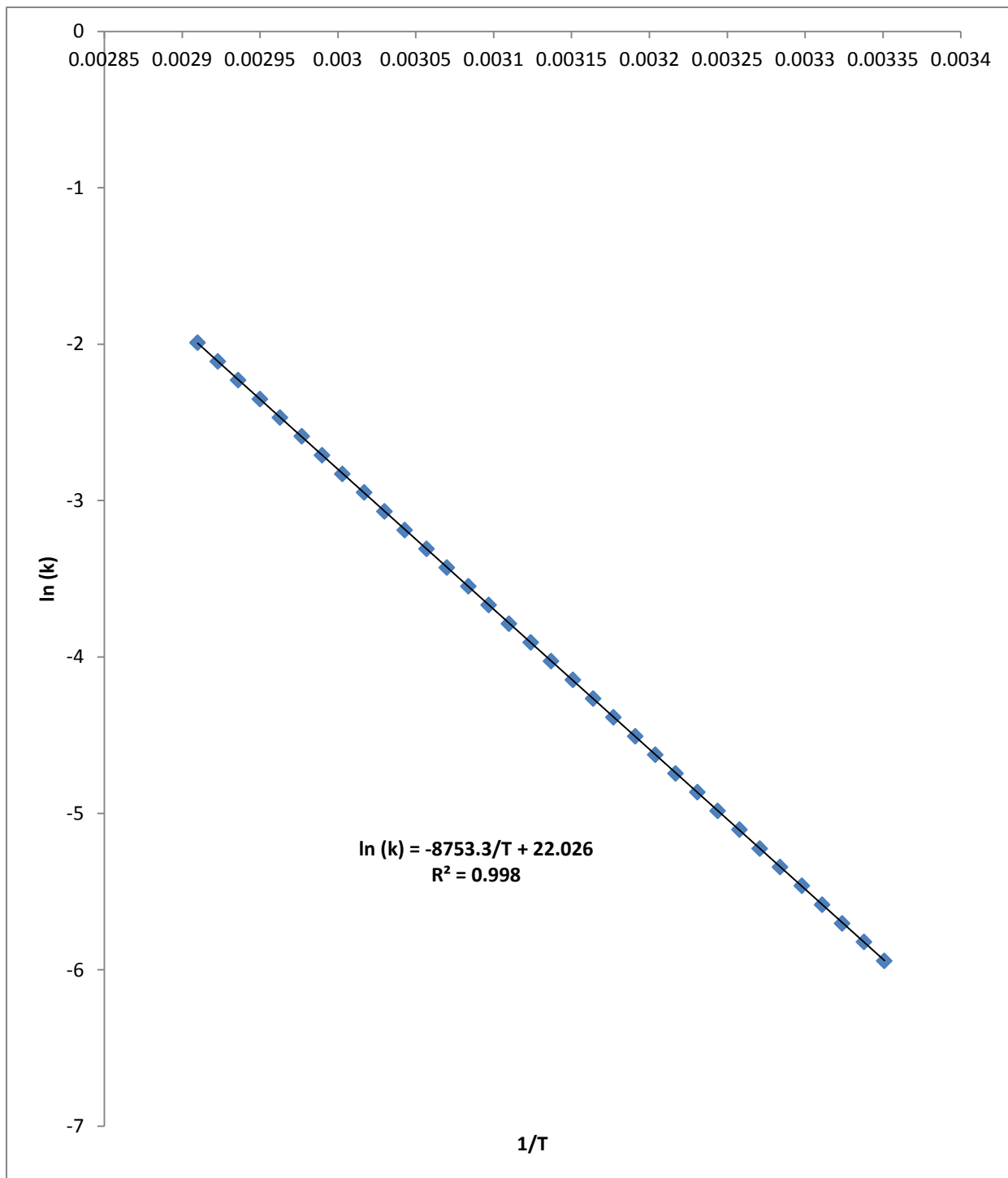


Figure (6.47): Arrhenius plot of experiment-9

The values obtained for the specific rate constants as a function of temperature are given in equations (26),(27) and (28) below:

$$k_1(T) = 1.24 * 10^9 \exp\left(-\frac{7876.9}{T}\right) \quad (36)$$

$$k_2(T) = 5.79 * 10^9 \exp\left(-\frac{8386.9}{T}\right) \quad (37)$$

$$k_3(T) = 3.68 * 10^9 \exp\left(-\frac{8785.3}{T}\right) \quad (38)$$

The thermodynamic information extracted from the experiments was the heat of the reaction ( $\Delta H_{rxn}$ ). This was assumed to be independent of temperature and was determined by using eq(10). Table(6.16) below shows  $\Delta H_r$  values of the various experiments.

Table (6.19): Thermodynamic information of the experiments

Experiment	7	8	9
$\Delta H_{rxn}$ (kJ/mol)	61.59	61.58	61.58

## 6.10 DISCUSSION OF RESULTS.

The experimental results in all the processes studied showed that a strong relationship exists between reaction rates and changes in temperature for exothermic reactions as stated in the literature. The reactions between excess water (10 mols) and acetic anhydride (1 mol) thus hydrolysis reactions-(A) were carried out at 305K-358K, 310K-358K and 328K-366K. The extent of the reactions was followed by monitoring the changes in temperature in the reaction vessel. The experimental and the adiabatic curves are shown in figures (6.18) – (6.20). The reactions between excess acetic anhydride (2.65 mols) and water (0.55 mol) thus hydrolysis reactions-(B) were carried out at 286K-343K, 293K-257K and 304K-368K. The profiles of experimental and adiabatic curves are shown in figures (6.29)-(6.31) respectively. The experimental reaction profiles (Hydrolysis process –A and Hydrolysis process –B) of this study shows that hydrolysis process –A and hydrolysis process-B are completely two different processes. One unanticipated finding was the pronounced nature of the s-shape of the hydrolysis-B profiles compared with the hydrolysis-A profiles. On the other hand, another interesting finding was the cooling parts of the processes. Hydrolysis-A, showed very gradual cooling process as compared with Hydrolysis-B which showed a cooling process similar to the cooling process of figures (A)-(B) of the experimental determination of heat transfer coefficient of the of the reaction vessel (thermos-flask). There may be several possible explanations to these observations. A possible explanation for this might be that the rate of heat loss during the cooling processes is higher for hydrolysis-B than that of hydrolysis-A. These parts thus suggest real cooling process. On the other hand, the rate of cooling of the hydrolysis-A processes, although very slow there might be some amount of reactions taking place. It is also interesting to note that, the processes (hydrolysis-A and –B) showed different reaction times for the processes to reach their maximum temperatures during their reactions. This finding was somewhat not surprising. The observed differences discussed is however very significant. The experimental profiles of the esterification reactions, acetic anhydride (1 mol)-methanol (3 mols) showed very similar reaction profiles. They were carried out at 290K-345K, 294K-345 and 299K-345K.

The experimental and the adiabatic curves are shown in figures (6.34) – (6.36). Surprisingly all the experimental profiles reached an approximate maximum temperature of 345K. This finding is due to the fact that methanol which has a boiling point of about 342K might have acquired

enough energy generated from the exothermic reaction and started boiling in the reaction vessel. The reaction order for all the hydrolysis-A experiments were first order with respect to the acetic anhydride. This is shown in the rate – concentration plots in the figures (6.18)-(6.20). This result is consistent with other researchers, Kralj (2007), Haji et al (2005). However, contrary to our expectations the rate –concentration plots of the hydrolysis-B was very surprising as the profiles appeared to be part of a parabola suggesting a second order process. This finding is unexpected and has not previously been reported. The rate law temperature dependence were satisfactorily correlated by means of the Arrhenius function from [307K-354K], [312K-345K] and [332K-354K] for the hydrolysis-A. Figures (6.21) –(6.23) shows the Arrhenius plots of the hydrolysis-A. From the plots the values of the activation energies and pre-exponential factors were determined as shown in the equations (27)-(28). Similarities of the activation energies (50.54 kJ/mol, 50.78 kJ/mol, 50.40 kJ/mol) which agrees very well with what is reported by Haji (2005) and Kralj (2007). The average activation energy reported in the literature is 50.24kJ/mol, Haji (2005) which differs by +0.65% from the value reported in this work. For the hydrolysis-B processes, Arrhenius functions from [287K-340K], [295K-345K] and [305K-360K] for the hydrolysis-B are shown in Figures (4.32) –(4.34) . From the plots, the values of the activation energies and pre-exponential factors were determined as shown in the equations (31)-(33). The activation energies (38.23 kJ/mol, 33.89 kJ/mol, 39.19 kJ/mol) are however smaller than that of the hydrolysis-A, this is not surprising since the studies has shown that the kinetics of the hydrolysis-A and hydrolysis-B appears very different processes. These activation energies of the hydrolysis-B reactions have not been reported in the literature. The Arrhenius functions from [290K-344K], [296K-344K] and [298K-344K] for the acetic anhydride-methanol processes are shown in figures (4.43) –(4.45). From the plots the values of the activation energies and pre-exponential factors were determined as shown in the equations (36)-(38).

The activation energies determined (65.49 kJ/mol, 69.72 kJ/mol, 72.77 kJ/mol) agree well with what is reported by Yih-Shing Duh et al (1996). The heat of the reactions determined from the experiments was assumed to be independent of temperature. The values obtained for hydrolysis-A are shown in table (6.7). The average value compared well with what was obtained by Glasser and Williams (1971). The values determined for the hydrolysis-B are shown in the table (4.13), these have not yet been reported. The values for the esterification processes agree well with what is reported by Yih-Shing Dul et al (1996) and they are shown in table 6.16.

## 6.11 CONCLUSIONS

The kinetics of the reactions acetic anhydride/excess water, excess acetic anhydride-water and acetic anhydride/ methanol has been modeled as a function of temperature in an adiabatic batch reactor (thermos-flask) using a negative coefficient thermistor as a measuring device. The validity of the procedure used was proven by comparing the experimental kinetic results of the acetic anhydride/excess water reactions to published results. Thus the technique could be applied with confidence to systems with no kinetic information. Excess acetic anhydride/water reactions which have no literature information on it kinetics were shown to follow a second order kinetics with respect to the water. The activation energy is approximately  $37.1 \pm 2.8$  kJ/mol. The heat of reaction which was assumed to be independent of temperature for the excess acetic anhydride/water is approximately  $58.5 \pm 4.0$  kJ/mol. The heat of mixing was assumed negligible and was not considered in the heat of reaction calculations. The kinetic model of the esterification reaction between acetic anhydride/methanol reactions which has not been previously determined by this technique showed results which compares very well with published results. It is seen that the apparatus used in this work is sufficiently simple and sufficiently inexpensive. In spite of this we have been able to measure effective first and second order constants without any special precautions. Hence the method applied in these studied can be recommended for kinetic and thermodynamic studies of unknown systems.

## 6.12 ACKNOWLEDGEMENTS

N. A would like to thank the National Research Fund (NRF) of South Africa, Directors of Centre of Material Processing and Synthesis (COMPS), Prof. David Glasser and Prof Diane Hildebrandt, University of Witwatersrand, Johannesburg, South Africa for financial support of this work.

## 6.13 LIST OF SYMBOLS

$\Delta H_{\text{rxn}}$ -heat of reaction (KJ/mol)

$\Delta T$  (ad) –adiabatic temperature change (K)

$\Delta\varepsilon$  –extent of reaction

A –preexponential factor

B,C – thermistor constants

$C_A$ -concentration of A (mol/L)

$C_p$  –specific heat capacity

$C_{p,AA}$  –specific heat capacity of acetic anhydride

$C_{p,mix}$ -constant heat capacity of reaction mixture (kJ/mol.K)

$C_{p,W}$  –specific heat capacity of water

$E_a$  – activation energy

$I_{total}$  – total current of the circuit

$k_1, k_2, k_3$ -specific rate constant

m –mass

$M_{AA}$  –Mass of acetic anhydride

$M_{AA}$  –Mass of water

$M_{eqv}$  –Equivalent amount of water

$M_T$ -mass of reaction mixture(Kg)

$N_A$  –mole of A (mol)

p-probability factor

Q-heat produced by stirrer

R – molar gas constant

$R_2$  – known resistance in the circuit

$r_A$  –rate of reaction of (A)

$R_{TH}$  – Thermistor resistance

$t$  – time

$T$  –absolute temperature

$T_{max}$  –maximum temperature (K)

$T_o$  –initial temperature

$T$ -reactor temperature (K)

$T_S$  – steady state temperature (K)

$T_s$  –steady-state temperature

$U$  –heat transfer coefficient

$U$  –heat transfer coefficient ( $J/m^2 \text{ s.K}$ )

$v$  – total voltage of the circuit

$V$  -volume

$V_{out}$  – voltage measured by thermistor

$V_{TH}$  – voltage across thermistor resistance

$Z$ -collision frequency

$\alpha, \beta$ - constants

## **6.14 REFERENCES**

Bell, R. P. and Clunie, J. C. (1952). "Proc. Roy. Soc." A212, 16

Considine, D. M., (1957) "Process Instruments and Controls Hand book", MCgraw-Hill Book Co., Inc., New York, pp. 2 -60.

Eldridge, J. W., Piret, E. L. (1950), "Continuous-flow stirred-tank reactor system I, Design equations for homogeneous liquid phase reactions, Experimental data", Chem Eng. Prog., 46, 290.

Glasser, D. and Williams, D. F. (1971). "I & E. C. Fundam" 10, 516

Glasser, D., Williams, D. F. (1971). "The study of liquid-phase kinetics using temperature as a measured variable", Ind. Eng. Chem, Fundam., vol 10, No. 3.

Haji, S., Erhey, C. (2005) "Kinetics of hydrolysis of acetic anhydride by in situ FTIR spectroscopy", Chemical Engineering Education, 56-61.

King, E. L. (1964) "How Chemical Reactions Occur", W. A. Benjamin: New York, pp 5- 70

King, R. P. (1967), "Estimation of parameters in systems Defined by Differential Equations", S.Afr. J. Sci, 91- 96.

King, R. P., Glasser, D. (1967) "The use of Adiabatic Calorimeter for Reaction Rate Studies", S. Afr. Ind. Chem. 12-15.

Kraji, A. K. (2007), "Checking the Kinetics of Acetic Acid production by Measuring the Conductivity", J. Ind. Eng. Chem., Vol 13, No. 4, 631 -636.

Livingstone, R., (1961) "Technique of organic chemistry", Weissberger, Ed., VII, 2<sup>nd</sup> ed, Pt 1, p 75, Interscience, N. Y.

Morrisson, R., Boyd, R. "Organic Chemistry", 4<sup>th</sup> ed. Allyn and Bocon. Boston (1983)

Schmidt, J. P., Mickley, H. S. and Grotch, S. L. (1964). "A.I. Ch.E. J." 10, 149

Shatyski, J. J., Hanesian, D. (1993) "Adiabatic Kinetics Studies of the Cytidine/Acetic Anhydride reaction by Utilizing Temperature Versus Time Data", Ind. Eng. Chem. Res. 32, 594.

Williams, R. D. (1974) "Indirect Measurement of Reaction Rate", Chem. Eng. Educ. Winter, 23 -30.

Yih-Shing Dul et al (1996), "Applications of reaction calorimetry in reaction kinetics and thermal hazard evaluation" Thermochemica Acta 285 67-79

## CHAPTER 7

### OVERALL CONCLUSIONS AND PROSPECTS

The thesis has demonstrated that valuable information could be obtained from temperature-time measurements (history) of exothermic chemical reactions (processes). The experimental set-up used in the experiments was sufficiently simple and inexpensive so as to be able to implement and use in any laboratory. In spite of this simplicity, measurements were accurate enough in order to be able to use the data to determine reaction rates and thermodynamic data such as heats of reaction.

This thesis for the first time has modelled the reaction kinetics of the hydrolysis reaction between excess acetic anhydride and limited amounts of water and reported all the kinetic parameters associated with the reaction at higher temperatures. The reaction kinetics of the esterification reaction of acetic anhydride with methanol was also measured and modelled. Although the reaction kinetics for this reaction appears in the literature it has not been measured and analysed previously by the techniques described in this thesis.

This work has developed and demonstrated a new methodology using the energy balance for adiabatic batch reactor systems in combination with the Gibbs-Helmholtz equation to extract important thermodynamic parameters (heat of reaction and equilibrium constant) from the temperature-time history of exothermic reversible esterification processes. Moreover, this work has also developed a simulation model using temperature-time information for the esterification reaction between acetic anhydride and methanol. This simulation model can be applied to model liquid phase temperature and compositions. With the help of thermodynamics and in particular VLE information, the vapour phase composition can be inferred. This simulation model is therefore a step towards the design of a reactive distillation system for the acetic anhydride-methanol process. In conclusion, it is claimed that the reaction kinetic modelling of the excess acetic anhydride-water reactions, the new methodology developed for the determination of thermodynamic parameters (heat of reaction and equilibrium constant) and the simulation model developed for the acetic anhydride-methanol process are all significant contributions in the field

of chemical reaction kinetics, applied thermodynamics and reactive distillation preliminary design. This research has led to some questions which need further investigation. Suggested future work includes using the newly developed technique at higher temperature. This will enable one to understand what happens to the solution of the non-linear equations that need to solve. Moreover, further work should incorporate parameters into the model developed for the acetic anhydride-methanol process with the aim of reducing the deviations of the model-predicted temperature values from the experimentally observed values. By improving the model, more accurate determination of liquid and vapor phase temperatures and compositions could be predicted during the operations of such systems.